UNIVERSITÉ DE TOULON

for the degree of
DOCTOR OF INFORMATICS
École Doctorale 548

METHODS FOR THE JOINT ANALYSIS OF SPECIES PRESENCE, BASED ON ACOUSTIC MONITORING, AND THEIR ENVIRONMENT

- A large-scale, multi-year study of birds in Québec, Humpback whale in the Caribbean and Sperm whale in the Mediterranean Sea -

Presented by STÉPHANE CHAVIN

Laboratoire d'Informatique des Systèmes
University of Toulon

Jury composition :

ELENA PAPALE : Reporter
MARC MAZEROLLE : Reporter
HERVÉ GLOTIN : Director
YANN OURMIÈRES : Director
THOMAS PELLEGRINI : Reviewer
PAUL BEST : Supervisor
PASCALE GIRAUDET : Supervisor
FRANÇOIS SARANO : Supervisor

September 2026

Stéphane CHAVIN: *Methods for the joint analysis of species presence, based on acoustic monitoring, and their environment* © September 2026

ABSTRACT

Abstract : Monitoring biodiversity, as well as modelling the preferred habitats of certain species and their responses to specific changes, requires accurate environmental models and reliable observations. As bioacoustics is commonly used in biodiversity monitoring, we propose using detections from automatic detection systems powered by artificial neural networks, alongside various methods for mapping species distribution, to identify the preferred environmental parameters of different species. A YOLO model was trained to detect and classify humpback whales units as well as certain bird species, yielding satisfactory results. Visual observations of sperm whales in the Mediterranean have enabled the creation of maps to illustrate their habitats and highlight areas where collisions with boats are most likely to occur. The analysis of static and dynamic parameters highlights the complexity of environmental studies and the challenges that artificial neural networks may face when tackling this task.

Résumé : Le suivi de la biodiversité, ainsi que la modélisation des habitats de prédilection de certaines espèces, ainsi leurs réactions à certains changements, nécessite des modèles environnementaux précis et des observations fiables. La bioacoustique étant couramment utilisée dans le suivi de la biodiversité, nous proposons d'utiliser les détections issues de la détection automatique obtenues à l'aide de réseaux de neurones artificiels, ainsi que diverses méthodes de cartographie de la répartition des espèces, afin de mettre en évidence les paramètres environnementaux préférés de différentes espèces. Un modèle YOLO a été entrainé pour détecter et classifier les unités des baleines à bosse ainsi que certaines espèces d'oiseaux, donnant des résultats satisfaisants. Les observations visuelles des cachalots en Méditerranée ont permis d'élaborer des cartes pour expliquer leur habitats et mettre en évidence les zones où les collisions avec des bateaux sont plus susceptibles de se produire. L'analyse des paramètres fixes et dynamiques montre la complexité des études environnementales et les difficultés rencontrées par les réseaux de neurones artificiels dans cette tâche.

PUBLICATIONS

The following list enumerates the various works on which research has been conducted and which have been published or presented to the public during the course of this thesis :

[1] **Stéphane Chavin**, Hervé Glotin, Paul Best, and Yann Ourmières. "Repertoire usage similarity increases before decreasing during the breeding season: an Automatic Analysis of a Complete Breeding Season Throughout the Caribbean". working paper or preprint. Aug. 2026. URL: https://hal.science/hal-05723162.

[2] **Stéphane Chavin**, Anouk Simard, Jean-François Jetté, Marc-André Villard, Yann Ourmières, and Hervé Glotin. "Scalable Bird Diversity: Mastering High-Chorus Soundscape and Species Richness with Time-frequency YOLOv5". working paper or preprint. Aug. 2026. URL: https://hal.science/hal-05723151.

[3] Justine Girardet, Hervé Glotin, **Stéphane Chavin**, Marion Poupard, Julie Guiderdoni, and Véronique Sarano. "Arctic diel and circadian acoustic pattern of Orcas, Fin, and Humpback whales revealed by deep learning from two months of continuous recordings". In: *Ecological Informatics* 93 (Feb. 2026), p. 103564. ISSN: 1574-9541. DOI: 10.1016/j.ecoinf.2025.103564.

[4] **Stéphane Chavin**, Yann Ourmières, and Hervé Glotin. "Physeter and oceanography conditions in high maritime traffic areas". In: (2025). DOI: 10.5194/oos2025-1109.

[5] Philémon Prevot, Lisa Ferre, Tristan Villepreux, **Stéphane Chavin**, and Hervé Glotin. *PSIBIOM Technical Report LIS CNRS UTLN - 2024-11*. Tech. rep. Université de Toulon ; CIAN ; Laboratoire d'informatique et des Systèmes - LIS (UMR 7020), Nov. 2024. URL: https://hal.science/hal-04918712v1/file/PSIBIOM_202411_Rapport_Rech_CIAN.pdf.

[6] Lisa Ferré, **Stéphane Chavin**, Tristan Villepreux, and Hervé Glotin. *Rapport de recherche sur le suivi des Sotalies (Sotalia guianensis) en Guyane*. Tech. rep. Université de Toulon ; GEPOG-Université des Antilles et de la Guyane ; CIAN ; Laboratoire d'informatique et des Systèmes - LIS (UMR 7020), July 2024. URL: https://hal.science/hal-04918738v1/file/GEPOG_SOTALIE_RR_2024071_CIAN5.pdf.

[7] Tristan Villepreux, Philémon Prevot, Lisa Ferre, **Stéphane Chavin**, and Hervé Glotin. *PSIBIOM Technical Report LIS CNRS UTLN CIAN - 2024-07*. Tech. rep. Université de toulon ; CIAN ; Laboratoire d'informatique et des Systèmes - LIS (UMR 7020), July 2024. URL: https://hal.science/hal-04918690v1/file/PSIBIOM_202407_Rapport_Rech_CIAN.pdf.

[8] **Stéphane Chavin**, Jérôme Couvat, Paul Best, Laurent Bouveret, Julien Chalifour, Tacumba Duncan, Sébastien Gréaux, Cathy Lacourbas, Sarah Manuel, Benjamin de Montgolfier, Marit Pistor, and Hervé Glotin. "Exploration temps-fréquence du répertoire et évolution des chants des baleines à bosse de l'Atlantique Nord". In: *SERENADE*. Toulon, France, June 2024. URL: https://hal.science/hal-04918598.

[9] Justine Girardet, Véronique Sarano, Agnese Marchini, **Stéphane Chavin**, Julie Guiderdoni, and Hervé Glotin. *Circadian rhythms of cetaceans from Arctic and Mediterranean seas with controled anthropophony*. DCLDE. Poster. June 2024. URL: https://univ-tln.hal.science/hal-04945810.

[10] **Stéphane Chavin**, Jérôme Couvat, Paul Best, Laurent Bouveret, Julien Chalifour, Tacumba Duncan, Sébastien Gréaux, Cathy Lacourbas, Sarah Manuel, Benjamin de Montgolfier, Marit Pistor, and Hervé Glotin. *Time-Frequency Exploration of the Repertoire and Evolution of Humpback Whale Songs in the Caribbean Sea*. DCLDE. Poster. June 2024. URL: https://hal.science/hal-04917511.

[11] Lisa Ferre, Philémon Prevot, Tristan Villepreux, **Stéphane Chavin**, and Hervé Glotin. *PSIBIOM Technical Report LIS CNRS UTLN CIAN - 2024-05*. Tech. rep. Université Toulon ; CIAN ; Laboratoire d'informatique et des Systèmes - LIS (UMR 7020), May 2024. URL: https://hal.science/hal-04918661.

[12] **Stéphane Chavin**, Pierre Mahé, and Hervé Glotin. *Rapport intermédiaire sur l'étude Sotalie (Sotalia guianensis)*. Tech. rep. Université de toulon, Mar. 2024. URL: https://hal.science/hal-04918478.

[13] Hervé Glotin, Justine Girardet, Jean-Marc Prévot, François Sarano, Véronique Sarano, Pascale Giraudet, Valentin Gies, Nathalie Prévot d'Alvise, Maxence Ferrari, Marion Poupard, Kathie Dunning, Gaetan Patenotre, **Stéphane Chavin**, Pierre Priou, Julie Guiderdoni, Rodolphe Tanneau, Lionel Camus, and Malik Chami. *Seconde exploration bioacoustique en fjord arctique: mise en évidence de chorus inédits de quatre superprédateurs & étude de leurs interactions*. Tech. rep. University of toulon, CIAN ; Laboratoire d'informatique et des Systèmes - LIS (UMR 7020), Feb. 2024. URL: https://mnhn.hal.science/mnhn-04785408.

[14] Hervé Glotin, **Stéphane Chavin**, Justine Girardet, Pascale Giraudet, Paul Best, Maxence Ferrari, Véronique Sarano, François Sarano, Pierre Mahé, Valentin Barchasz, Valentin Gies, Nicolas Deloustal, Fabien de Varenne, Julie Patris, Jean-Marc Prévot, Olivier Philippe, Franck Hieramente, Vincent Bertin, Paschal Coyle, and Sébastien Paris. *Bilan d'une décennie d'observations des grands cétacés en milieu anthropisé Nord Pelagos: BOMBYX, KM3NeT, et antennes mobiles Sphyrna et WhaleWay.* Tech. rep. Université de toulon, Oct. 2023. URL: https://univ-tln.hal.science/hal-04939839.

[15] **Stéphane Chavin**, Pierre Mahé, and Hervé Glotin. *Avancement des IA Audio et Vision*. Tech. rep. University of toulon, CIAN, Aug. 2023. URL: https://mnhn.hal.science/mnhn-04918362.

[16] **Stéphane Chavin**, Pierre Mahé, Thomas Hermet, Nicolas Deloustal, and Hervé Glotin. *Analyse automatisée de la diversité acoustique, de la détection d'espèces aux indices bioacoustique - Rapport de recherche*. Tech. rep. toulon, Mar. 2023. URL: https://mnhn.hal.science/mnhn-04918405.

—

"I only went out for a walk and finally concluded to stay out till sundown,
for going out, I found, was really going in."
John Muir

—

ACKNOWLEDGEMENTS

Although a doctoral thesis can be seen as a personal project, it is the result of numerous collaborations, and for this reason I would like to thank everyone who contributed to it, whether directly or indirectly.

First and foremost, I would like to thank my co-directors, **Hervé Glotin** and **Yann Ourmières**, who guided me through my research and offered me valuable advice. I would also like to thank my supervisors, **Paul Best**, **Pascale Giraudet**, and **François Sarano**. Their advice and numerous reviews have helped me improve throughout my years at the lab. A special mention goes to Paul, who, ever since I arrived at the lab as an internship student, has always taken the time to help me move in the right direction.

I would also like to thank the people with whom I had the opportunity to work, notably **Véronique Sarano** for the analysis of Mediterranean sperm whales, **Anouk Simard**, **Jean-François Jetté**, and **Marc-André Villard** for the study of the Québec recordings, as well as **Jérôme Couvat** for the CARI'MAM data.

Next, my thanks go to the members of the LIS, especially my colleagues and former office colleagues **Adam**, **Adrien**, **Corentin**, **Gaëtan**, **Justine**, **Lara**, **Lelïo**, **Lilou**, **Loïs**, **Marie-Lou**, **Marion**, **Maxence**, **Maxime**, **Nicolas**, **Pierre**, **Philémon**, **Renaud**, **Sébastien V.**, **Séverin**, **Tristan** and **Vivien**, as well as those who have temporarily joined us **Benjamin**, **Félix**, **Gaspard**, **Maha**, **Matthias**, **Matthieu**, **Nina**, **Opalin**, **Stelios**, **Thomas**, **Tohi**, **Valentin** and **Yaël**. Thank you also to the permanent and researchers, **Adoration**, **Franck**, **Julie**, **Sébastien P.**, **Sébastien B.**, **Sylvain** and **Vincente**. Discussions in the corridors and during coffee breaks in Room X134 have always been enriching.

Thank you to the whales and birds for their songs, to the sperm whales for simply being there, to the forests on land and in the sea for the oxygen they provide us with, and to all living things for simply living.

Finally, I would like to thank my family, who have stood by me all this time and have been so supportive of my many passions.

Last but not least, I'd like to sincerely thank **Lisa**, who reassured me throughout this thesis —especially during times of doubt— and who always managed to plan a new trip, a dive, or a hike to take my mind away from my worries and help me refocus on what really matters.

1 INTRODUCTION 1
1.1 Environment . . . 1
1.1.1 Abiotic components . . . 1
1.1.2 Biotic components . . . 2
1.1.3 Human and its activities . . . 2
1.1.4 Environment assessment . . . 3
1.2 Bioacoustics . . . 4
1.2.1 Communication oriented . . . 4
1.2.2 Foraging oriented . . . 5
1.3 Passive Acoustic Monitoring (PAM) . . . 5
1.3.1 Operated recorders . . . 5
1.3.2 Autonomous Recording Unit (ARU) . . . 6
1.4 Recording Analysis . . . 6
1.4.1 Signal processing . . . 7
1.4.2 Artificial Neural Networks . . . 8
1.4.3 Environmental influences on acoustic recordings 8
1.5 Context for each species . . . 9
1.5.1 Humpback whale . . . 9
1.5.2 Sperm whale . . . 10
1.5.3 Birds in Northern America . . . 11
1.6 Thesis objectives and plan . . . 12
2 STATE OF THE ART AND CONTEXT 15
2.1 Artificial Neural Network (ANN) . . . 15
2.1.1 Mono class detector and classifier . . . 17
2.1.2 Object Detection . . . 18
2.2 The use of ANNs in bioacoustics . . . 19
2.3 Impact of fixed parameters on species distribution . . . 21
2.4 Impact of long term dynamic parameters on species distribution . . . 23
2.5 Impact of short term dynamic parameters on species distribution . . . 25
3 MATERIALS 27
3.1 Multi year survey in the breeding ground of the Humpback whale, across the Caribbean . . . 27
3.2 On site Sperm whale observations in the Mediterranean Sea . . . 29
3.3 Terrestrial dataset from the temperate regions of Québec to the Arctic . . . 32
3.4 Access to the environmental variables . . . 33
3.4.1 Marine variables . . . 33
3.4.2 Terrestrial variables . . . 35
4 METHODS 37
4.1 Training and optimising a YOLOv5 model . . . 38
4.1.1 Workflow . . . 38
4.1.2 Annotation . . . 40
4.1.3 Training . . . 47

4.1.4 Active learning . . . 48
4.2 BirdNET analysis . . . 49
4.3 Transformer model . . . 49
4.4 Maximising the scores by adjusting the detection threshold . . . 50
4.4.1 Bird model . . . 50
4.4.2 Humpback whale model . . . 51
4.5 Post-processing the detections . . . 51
4.5.1 Filtering and call density estimation . . . 51
4.5.2 Humpback whale phrases reconstruction . . . 52
4.6 Species Distribution Modelling (SDM) . . . 52
4.6.1 Presence-only model . . . 53
4.6.2 Presence-absence model . . . 56
4.7 Cumulative Utilisation Impact (CUI) . . . 59
4.8 Acoustic indices . . . 60
4.9 Estimation of the Repertoire Sharing (RS) value for the Humpback whale . . . 60
4.10 Statistical analysis . . . 62
5 DETECTION AND CLASSIFICATION 63
5.1 A YOLOv5 model on 23 different units for Humpback whale . . . 64
5.1.1 Generalisation of the model . . . 67
5.1.2 Comparison to another architecture . . . 68
5.2 A YOLOv5 model on 27 bird species . . . 71
5.2.1 Bird model evaluation . . . 71
5.2.2 Comparision to BirdNET . . . 75
5.3 Comparing the box detection to nROI index for bird species richness estimation . . . 78
5.4 Discussion . . . 80
5.4.1 Humpback whale model scores . . . 80
5.4.2 Birds model scores and comparison with BirdNET 81
5.4.3 Importance of the confidence threshold adjustment . . . 82
5.4.4 Improvement in detection in high chorus level . 83
5.4.5 Box detection for analysis . . . 84
5.4.6 Difficulties and bias . . . 85
6 RELATIONS BETWEEN DETECTION AND FIXED ENVIRONMENT 87
6.1 Coastal parameters for the humpback whale . . . 88
6.2 Habitat composition for birds in Québec . . . 92
6.3 Importance of bathymetric characteristics for the sperm whale in the Mediterranean . . . 95
6.4 Discussion . . . 100
6.4.1 Habitat preferences . . . 100
6.4.2 Detecting only songs can reduce the predicted densities . . . 104

6.4.3 Sperm whale sampling bias 105
7 RELATIONS BETWEEN DETECTION AND LONG TERMS DYNAMIC PARAMETERS 107
7.1 Humpback whale presence 108
7.2 Seasonal variation of humpback whale vocal repertoire 114
7.3 Sperm whale suitable habitat 117
7.3.1 Importance of surface and deep parameters . . 117
7.3.2 Increasing human pressure 121
7.4 Seasonal changes for birds migration in Québec 123
8 RELATIONS BETWEEN DETECTION AND SHORT TERMS DYNAMIC PARAMETERS 133
8.1 Brief evolution of the oceanic conditions in the Stoechades canyon 134
8.2 Response to higher temperatures for the bird detection rates 141
8.3 Discussion on dynamic parameters 143
8.3.1 Sperm whale preferences on habitat and dynamic parameters 143
8.3.2 Habitat suitability is not abundance or density estimation 144
8.3.3 Bird preferences and habitat 145
8.3.4 GAM and MaxENT model bias 146
8.3.5 Human pressure 148
9 GENERAL DISCUSSION 153
9.0.1 The growing impact of human activity on natural habitats 153
9.0.2 Defining the objective of the research 154
9.0.3 Choosing the best methods 155
10 CONCLUSION 159
11 CONTRIBUTIONS 161

BIBLIOGRAPHY 163

LIST OF FIGURES

Figure 1 **Humpback whale Distribution Map across the world (in blue)** 9
Figure 2 ***Megaptera novaeangliae* North Atlantic Population Migration Map** 10
Figure 3 **Sperm Whale Distribution Map (in blue)** . . 11
Figure 4 **Northern America Birds' Flyways** 12
Figure 5 **Main part of a convolutional neural network, with the example of a humpback whale song spectrogram.** 15
Figure 6 **Representation of how the Intersection over Union (IoU) is measured and is evaluated** . . 19
Figure 7 **Mediterranean Sea global current** 24
Figure 8 **Map of the different ARU positions in the Caribbean region, from Bermuda to Aruba** . 28
Figure 9 **Map of the sperm whale observations from the different Longitude 181 missions in the Mediterranean Sea** 31
Figure 10 **Geographical sub areas and subunits with the sampled area during Longitude 181 missions** 32
Figure 11 **OBIS dataset observation densities across the Mediterranean Sea** 33
Figure 12 **Map of the different positions of the Autonomous Recording Unit (ARU) in Québec.** 34
Figure 13 **Vegetation Zones of Canada in 2020 from [125]** 36
Figure 14 **Example of a Raven annotation file with bounding box in red and relative information in the bottom table.** 39
Figure 15 **Workflow of the RAVEN2YOLO method** . . . 39
Figure 16 **Spectrogram for each unit of the North Atlantic humpback whale's vocal repertoire on breeding grounds** 41
Figure 17 **Representation of the humpback whale vocal repertoire categories using 2 dimension UMAP** 42
Figure 18 **Random Forest confusion matrix over the 23 units of the humpback whale vocal repertoire.** 44
Figure 19 **Representation of the humpback whale's vocal repertoire using two-dimensional UMAP** 45
Figure 20 **27 bird species repertoire** 47
Figure 21 **Representation of the different levels of Chorus** 48
Figure 22 **Transformer Encoder-Only Architecture** . . . 50

Figure 23 **Representation of the splines that make up the Generalised Additive Model (GAM) (top), and the fitted model representation (bottom)** 56
Figure 24 **Example of the labels given to our model and the resulting predictions with their associated confidence score on bird chorus.** 64
Figure 25 **Confusion matrix of YOLO model over humpback whale units** 65
Figure 26 **Original spectrogram (a) with the attention map extracted from the model, at the layer 0 (b), layer 1 (c) and -1 (d)** 66
Figure 27 **Original spectrogram of noise (a) with the attention map extracted from the model, at the layer 0 (b), layer 1 (c) and -1 (d)** 67
Figure 28 **Post hoc analysis of the missed detection per file over 11 files** 68
Figure 29 **Detection of our YOLO model for humpback whale units over a Antigua recordings in 2025.** 68
Figure 30 **Detection of our YOLO model for humpback whale units over a Moorea recordings in 2025.** 69
Figure 31 **F1 score for the YOLO model compared to the transformer** 70
Figure 32 **Confusion matrix on the test set of the annotations from the Québec, Canada database, with a total of 27 species** 73
Figure 33 **Receiver Operating Characteristic (ROC) curve of the 27 species for our model compared to BirdNET on the soundscape dataset from Québec, Canada database** 77
Figure 34 **Evaluation of our model and BirdNET over the three different scenarios on the soundscape final validation dataset** 78
Figure 35 **F0.5-score for BirdNET at a true positive rate scenario of 0.1 and our model at a true positive rate scenario of 0.5 for the 27 species on the soundscape dataset from Québec, Canada database** 79
Figure 36 **Number of detected boxes with the nROI index compared to the number of boxes from YOLO on the soundscape dataset from Québec, Canada database** 79
Figure 37 **Example of the time annotations, the BirdNET predictions and our model boxes over three examples of the chorus levels.** 84

Figure 38 **Weekly mean detection per recording hour during the breeding season and over the 14 considered stations** 89
Figure 39 **Bathymetric and slope map of the Caribbean region** 90
Figure 40 **Detection Rate of humpback whale unit in 2021 as a function of the distance to 5,000 m depth.** 90
Figure 41 **Predicted habitat suitability using the combination of the distance to the 5000 meter depth and the distance to the shore.** 91
Figure 42 **Distribution of the total recording time in hours for each year, depending on the latitude of the station** 92
Figure 43 **Linear regression between the detection rate and the latitudes (a.) and altitudes (b.).** 93
Figure 44 **Evolution of detection density per hour of recording across Québec between weeks 18 and 33 of 2022, 2023 and 2024.** 93
Figure 45 **Preferences for latitude, altitude and habitat of the three sample species (OVEN, WCSP and RCKI) between 2020 and 2024.** 94
Figure 46 **Number of sperm whale observations inside a canyon (with a 1.5km range around) compared outside (left) and the details of the canyon' surfaces (right)** 95
Figure 47 **Fixed parameter maps with slope (a) depth (b) rugosity (c) and distance to canyons (d) in the western basin of the Mediterranean** . . . 96
Figure 48 **MaxENT model projection using the bathymetry, with the response curve and its ROC AUC over the test set OBIS.** 96
Figure 49 **MaxENT model projection using the rugosity, with the response curve and its ROC AUC over the test set OBIS.** 97
Figure 50 **MaxENT model projection using only the distance to canyons, with the response curve and its ROC AUC over the test set OBIS.** 98
Figure 51 **MaxENT model projection using the slope, with the response curve and its ROC AUC over the test set OBIS.** 99
Figure 52 **MaxENT model projection using all four fixed parameters, with the jackknife representation of the AUC and gain of each parameters.** . . . 100
Figure 53 **Three-dimensional representation of the Caribbean region incorporating bathymetric information.** 102

Figure 54 **Comparison between a MaxENT model without bias layer (left) and with (right) using only fixed parameters.** 105
Figure 55 **Results of the humpback whale GAM with the response curves of its components.** 109
Figure 56 **Chlorophyll-a concentration over 3 periods of time in the Northern Atlantic (top) and the Caribbean (bottom).** 110
Figure 57 **Surface salinity evolution over 3 periods of time in the Caribbean.** 111
Figure 58 **Mixed layer depth over 3 periods of time in the Caribbean.** 111
Figure 59 **Temperatures over 3 periods of time in the Caribbean.** 112
Figure 60 **Results of the prediction of humpback whale distribution on December 12th 2021 (a), April 7th (b) and June 20th (c), using the Generalised Additive Model (GAM)** 112
Figure 61 **GAM estimated call rates of humpback whales throughout the entire breeding ground during the 2021 breeding season and until the end of September.** 113
Figure 62 **Spatial repertoire sharing as a function of time (top), and temporal repertoire sharing for each station (bottom)** 115
Figure 63 **Example of the succession of different units and clear phrases from a humpback whale's song, as recorded in the Caribbean** 117
Figure 64 **Mediterranean dynamic parameters averaged between May and October.** 119
Figure 65 **Result of the MaxENT model using all fixed and variable parameters averaged between May and October.** 120
Figure 66 **Response curve of some of the parameters that composes the MaxENT model.** 121
Figure 67 **Proportion of OBIS observations that fall within the areas predicted by our model, at different confidence levels.** 122
Figure 68 **Result of the Cumulative Utilisation Impact (CUI) for each boat categories.** 123
Figure 69 **Result of the Cumulative Utilisation Impact of all boat categories summed together.** . . . 124
Figure 70 **Zoom on the Pelagos Sanctuary for the different boat categories Cumulative Utilisation Impact.** 125

Figure 71 **Mean detection per hour of recording for the 3 different areas for the top 5 detected species in 2023** 126
Figure 72 **Results of the bird GAM with the response curves of temperature, total precipitation and wind intensity.** 127
Figure 73 **Results of the bird GAM with the response curves of temperature, latitude and week number** 128
Figure 74 **Prediction of the potential birds distribution across Québec at different times of 2021 based on the GAM.** 130
Figure 75 **The evolution of sunset and sunrise times for a station located at 46° (a) and a station located at 58° (b), in relation to the call rate of birds in the same station.** 131
Figure 76 **Stoechades canyon 3D representation** 134
Figure 77 **Current intensity following a latitudinal cut above the Stoechades canyon between August and December 2023** 135
Figure 78 **Different sea surface current conditions with different event types** 136
Figure 79 **Chlorophyll-a concentration during different days for a depth latitudinal cut** 137
Figure 80 **Current eastward component evolution during different days for a depth latitudinal cut** 138
Figure 81 **Current northward component evolution during different days for a depth latitudinal cut** 139
Figure 82 **Sea surface current orientation on September 28th and October 2nd with a front off-shore the islands of Hyères.** 140
Figure 83 **Daily temperature and detection rate with total recording time for 2022 season in the Côte-Nord regions.** 142
Figure 84 **Daily temperature and detection rate with total recording time for 2023 season in the Abitibi Témiscamingue region.** 142
Figure 85 **Daily and hourly evolution of the decibel levels for (a.) Guadeloupe Anse Bertrand and (b.) Guadeloupe Deshaies between 6500 and 12,500 Hz** 149
Figure 86 **Evolution of the NSDI value across days and hours in the ZEC Onatchiway station** 150

LIST OF TABLES

Table 1 **Some of the Human activities and their impacts on the environment from [13–15]** 3
Table 2 **Confusion matrix for model prediction and score evaluation.** 17
Table 3 **Summary of the mission, date and location associated with the number of positive points apart of the 318 (acoustic or visual confirmation)** 30
Table 4 **Boat categories an macrocategories from EMODnet, associated to their average speed and sizes** 35
Table 5 **Mean lower, higher and centre frequency and duration of annotation in bold and their std** . 43
Table 6 **Bird Species used in the model with their four-letters codes** 46
Table 7 **Environmental variables and their interest for the model of the sperm whale in the Mediterranean** 54
Table 8 **Environmental variables and their interest for humpback whale** 57
Table 9 **Environmental variables and their interest for birds** 58
Table 10 **Boat categories and their associated impact values on the sperm whale population, along with the final CUI impact.** 59
Table 11 **Units number of annotation, split train, validation and test with associated Precision, Recall map@50 scores on the test set for YOLOv5** 69
Table 12 **Metrics comparison between YOLO and a simple transformer** 70
Table 13 **Model performance with different parameters for 30 epochs on the annotations from the Québec, Canada database** 74
Table 14 **Area Under the ROC Curve of each species for our model and BirdNET with the different TPR scenarios associated with the positive threshold to set for the detections on the soundscape dataset from Québec, Canada database** 76
Table 15 **Average Precision score for both models** . . . 76
Table 16 **Bird Species GAM model and response to each parameters** 129

ACRONYMS

ACCOMBAMS Agreement on the Conservation of Cetaceans of the Black Sea, Mediterranean Sea and Contiguous Atlantic Area

ACI Acoustic Complexity Index

ADAM Adaptive Moment Estimation

AI Artificial Intelligence

AIC Akaike's Information Criterion

AIS Automatic Identification System

ANN Artificial Neural Network

ARU Autonomous Recording Unit

AUC Area Under the Curve

BRC Balearic Return Current

CAMS Copernicus Atmosphere Monitoring Service

CARI'MAM Caribbean Marine Mammals Preservation Network

CNN Convolutional Neural Network

CUI Cumulative Utilisation Impact

DCM Deep Chlorophyll Maximum

EMODnet European Marine Observation and Data Network

FAO Food and Agricultural Organisation

FPR False Positive Rate

GAM Generalised Additive Model

GEBCO General Bathymetric Chart of the Oceans

GPU Graphical Processing Unit

IUCN International Union for Conservation of Nature

IoU Interval over Union

mAP mean Average Precision

MPA Marine Protected AreaNCNorthern Current

OBIS Ocean Biodiversity Information System

PAM Passive Acoustic Monitoring

PSD Power Spectral Density

ROC Receiver Operating Characteristics

ROI Region Of Interest

RS Repertoire Sharing

SDM Species Distribution Map

SGD Stochastic Gradient Descent

SNR Signal to Noise Ratio

SSH Sea Surface Height

SST Sea Surface Temperature

STFT Short Time Fourier Transform

TPR True Positive Rate

UMAP Uniform Manifold Approximation and Projection

YOLO You Only Look Once

ZEC Zone d'exploitation contrôlée

1 INTRODUCTION

1.1 Environment 1
1.1.1 Abiotic components 1
1.1.2 Biotic components 2
1.1.3 Human and its activities 2
1.1.4 Environment assessment 3
1.2 Bioacoustics 4
1.2.1 Communication oriented 4
1.2.2 Foraging oriented 5
1.3 Passive Acoustic Monitoring (PAM) 5
1.3.1 Operated recorders 5
1.3.2 Autonomous Recording Unit (ARU) 6
1.4 Recording Analysis 6
1.4.1 Signal processing 7
1.4.2 Artificial Neural Networks 8
1.4.3 Environmental influences on acoustic recordings 8
1.5 Context for each species 9
1.5.1 Humpback whale 9
1.5.2 Sperm whale 10
1.5.3 Birds in Northern America 11
1.6 Thesis objectives and plan 12

1.1 ENVIRONMENT

The environment, or natural environment, can be defined as *"something that means everything to everything"* as it *"influence living organisms and gets influenced by them"* [1]. In a more direct definition, the environment is the surroundings, and is composed of two components which are the biotic component and the abiotic one [1]. The biotic component comprises all living organisms, from the most primitive to the most complex, whereas the abiotic component encompasses all chemical and physical factors that exert an influence on living organisms. While the environment is the "everything", an ecosystem is defined as the interaction between all living and non-living components of it and can be characterised for example as aquatic ecosystem or terrestrial ecosystem due to their different abiotic components.

1.1.1 *Abiotic components*

The abiotic component comprises a multitude of non-living parameters, including soil, light, temperature, mineral elements or water [1].

These parameters are capable of being both independent and directly linked to another parameter. In a similar fashion, an abiotic parameter in one ecosystem has the capacity to exert an effect on those in another. In terrestrial environments, wind has been shown to exert an influence on temperature or humidity. In coastal environments, however, it has also been demonstrated to affect sea currents, sea temperature and salinity.

1.1.2 *Biotic components*

The biotic component of the environment comprises all living organisms, ranging from bacteria to the largest marine mammals, such as blue whales, and the largest trees, such as giant sequoias [2], which can reach heights of up to 80 metres. The organisms under consideration are dependent on both the abiotic and biotic components of their environment. The vast majority of plant species are dependent on sunlight for photosynthesis, atmosphere for oxygen and carbon and soil as a source of nitrogen which is essential for their survival [3, 4], and conversely, the majority of animal species are dependent on these same plants for their own survival. It is evident that other animals, such as predators, are dependent on those that are predominantly herbivorous. Two distinct groups are then identifiable: the producers and the consumers. In the field of ecology, producers are defined as autotrophic organisms, analogous to plants that engage in photosynthesis. Consumers, on the other hand, are defined as organisms that consume producers and are predominantly animals [1]. Nevertheless, an additional group manifests itself: the decomposers. These comprise fungi, bacteria and others, which subsist on the organic matter or detritus of other groups. The presence of these decomposers has been demonstrated to have a positive effect on the quality of soil [3, 5], which is considered to be an essential abiotic component. The organisation of this entire cycle is then established between producers, consumers and decomposers, who thus depend on the abiotic components to which they contribute.

1.1.3 *Human and its activities*

Human is part of the environment, and is part of many ecosystems as humans are ubiquitous on earth. Like other species, humans are remodelling their own ecosystem by consuming resources. Recent studies however suggest that human consumption is too high for their ecosystem to regenerate [6] and also that the modifications on the structure of their ecosystems is too important. Deforestation, agriculture, habitat modification and overconsumption are now a threat to many ecosystems on earth [7] and therefore a threat for human. All these parameters put together lead to an increase of biodiversity

loss [8–10] and increase of greenhouse gases which results in climate changes [11] around the globe. These rapid changes are set to have a profound impact on the existing composition of various ecosystems. The escalating practices of intensive agriculture and forestry, for instance, are contributing to substantial deforestation, which in turn is resulting in significant concerns regarding soil erosion, habitat fragmentation, and, consequently, biodiversity loss [12]. As described in Table 1, human pressure can be characterised in a number of ways, including direct pressures such as habitat destruction and indirect pressures such as environmental disturbance, resource regulation, chemical release, gas emission and noise production. Subsequently, the contribution of these impacts can be categorised into distinct levels of environmental pressure.

Table 1: Some of the Human activities and their impacts on the environment from [13–15]

Human Activities	Sub Activities	Impacts on Environments
Agriculture and Forestry	Deforestation , Nutrient Input	Affecting air quality and climate, eutrophication and dead zones, algal blooms and aquatic ecosystem disruption, biodiversity loss, soil erosion, Habitat fragmentation
Manufacturing	Plastics industry, Pharmaceuticals	Plastic pollution, altering surface and groundwater flows, increased evaporation, drug pollution
Aquaculture and Fishing	Pelagic Fishing, Bottom Trawling	Sea floor destruction, by-catch
Extraction of materials	Mining	Release heavy metals into the environment, deforestation
Fossil fuel	Extraction, Combustion	Altered the global carbon cycle and accelerated climate change, decrease soil quality, decrease air quality, oil spills
Species invasion	Human introduced	Biodiversity loss, human disease spread
Transport	Shipping, mobility	Air pollution, noise pollution, habitat fragmentation, collision

Nevertheless, to analyse how different species respond to environmental impacts in areas where they coexist with humans, it could be effective to monitor how that environment evolves.

1.1.4 *Environment assessment*

Since the advent of intensive agriculture and other human activities that have had an impact on the environment, there has been a corresponding development of knowledge about the latter. Nonetheless, the practice of monitoring the progression of this phenomenon through the use of metrics and precise instruments was initiated in the mid-twentieth century. For instance, this was when societal concerns regarding the impact of chemicals and pesticides on soil began to manifest [16]. In the contemporary era, the use of spatial technologies has led to a significant advancement in environmental monitoring. For example, the use of buoy, linked to satellites, to monitor the

velocity of the surface water of the ocean, or the tracking of atmospheric conditions with the objective of predicting weather patterns in a specific location using satellites, demonstrate the application of technology in environmental research. In contrast to the abiotic component, for which we have a lot of information, tracking the biotic component becomes a more challenging task. Certain locations are difficult to access and have scarce documentation, resulting in a lack of research and limited available information. For instance, some species habits are not documented. Nevertheless, the advent of new technologies continues to engender novel perspectives within this domain. For example, bioacoustics is becoming an important tool for biotic monitoring, and particularly, soniferous animals.

1.2 BIOACOUSTICS

Bioacoustics is a transdisciplinary science that combines the biological and acoustic domains. Typically, the term refers to the investigation of sound production, dispersion and reception from animals (including humans). This looks at how sound is produced and detected, at how it is also received at neurophysiological and anatomical level, and the relationship between acoustic signals and the environment they are transmitted through. In the animal kingdom, sound plays a pivotal role in a variety of functions, including communication and foraging for food.

1.2.1 *Communication oriented*

In the domain of acoustics, communication can be categorised into two distinct classifications: intraspecific communication, which occurs between multiple individuals of the same species, and interspecific communication, which occurs between individuals of different species. The definition of communication can be delineated as the emission of a sound from one animal to another, and the subsequent behaviour in response of the latter. This behaviour may manifest as the production of a new acoustic signal produced by the receptor, or it may be defined as a behavioural response that could be for example an escape (for territorial call) or an approach (for mating call) [17]. In the context of intraspecific communication, two distinct groups can be identified. The first of these is social communication, defined as a mechanism through which a species establishes and maintains social connections [18]. For instance, when two individuals communicate with sound, they emit vocalisations and responses that provide information about their position, food or danger for example. The second is song. Indeed, as demonstrated by research findings [19–21], certain species have been observed to use an alternative form of communication, such as the vocalisations and songs exhibited by birds, marine

mammals and primates. These species have the capacity to generate intricate vocalisations and melodious songs. The link between these songs and mating has been demonstrated [22], with the former being found to be associated with the latter in terms of female attraction. However, sound production can be used, for some species, without any receiver objective.

1.2.2 *Foraging oriented*

In order to find prey in an environment, some species use sound. By emitting short but precise sounds, these animals are using what is called echolocation, which helps them to map their environment. When the sound is emitted, in the water or in the air, it reach a surface, or a prey, and then is reflected to the emitter which will be able to localise it based on parameters that are still difficult to analyse. This mechanism is, for example, used by *Chiroptera*, and sperm whale *(Physeter macrocephalus)*, and it requires specific sound production and perception mechanism. Since it is used almost at anytime when the animal is moving, it can then be used to monitor its presence via acoustic sensing.

1.3 PASSIVE ACOUSTIC MONITORING (PAM)

It is in that general context that bioacoustic surveys are used. However, there are different methodology for bioacoustics and they are used in different purposes. First, the active acoustic is a type of survey that consists in emitting sound and then study its propagation or species responses to it. It is used in playback experiments, that are made in order to understand the response of a species to a specific noise, or it can be used in order to improve the knowledge in acoustics physics. The second, and the one that is used for this thesis, is the passive acoustic monitoring (PAM). This method can be define as the study of the sounds that are received from an emitter without emitting any. There are two main ways to do this: either place recorders in an area and wait for the animals to come, or go out into the field near the animals and record their sounds.

1.3.1 *Operated recorders*

The use of operated recorders in passive acoustic involves the deployment of a recording device in a designated location to document a particular species or environmental feature with someone to monitor the recorders. The implementation of this process may be accomplished through the use of a simple mono recorder or a more sophisticated antenna configuration. The use of this protocol is predominantly contingent upon the confirmation of the target species'

presence within a designated location, or when visual information is deemed pertinent to the analysis in question. For instance, in the context of marine mammal monitoring, operated recorders can entail the use of a multi-hydrophone antenna, which is linked to cameras, with the objective of facilitating ethological analysis. This may include the association of a particular sound to a specific behaviour, or the identification of individual signatures [23, 24]. In the context of bird monitoring, this method is employed to verify the species of bird observed through visual confirmation.

1.3.2 *Autonomous Recording Unit (ARU)*

In circumstances where the species' habitat usage remains to be fully characterised, it is proposed that a recording instrument be deployed in a designated location, programmed to undertake daily recordings for a duration commensurate with the operational lifespan of the battery or the storage capacity. This practice is designated as the duty cycle. The recorders in question are known as Autonomous Recording Units (ARUs), and they have been extensively used in the context of bird monitoring and marine mammal surveys. As demonstrated in numerous studies, ARUs offer the advantage of scalable monitoring due to their capacity to be deployed in multiple locations concurrently [25]. Furthermore, they do not impact the behaviour of the animals being recorded, which prevents any alteration to the results. ARUs also offer an excellent reproducibility as they are standardised, hence avoiding human bias. However, ARUs can be expensive as the price for a recorder vary between 150€ (for a terrestrial Song Meter Micro 2 for example) and more than 5,000€ for some underwater ARUs. The complexity of the location, the number of ARUs and the duty cycle can be problematic. Recent advances in the field of bird monitoring have indicated that a reduction in the duty cycle, defined as the recording of less audio with a single automatic recording unit (ARU), results in lesser impact in the estimation of species richness within the designated area rather than a reduction of the number of AURs [**Bernard_etal2026**]. It can thus be concluded that it is preferable to have a greater quantity of ARU in a variety of locations, whilst simultaneously maintaining a reduced data duty cycle. What's more, this amount of data has to be analysed to extract the information, and this can be a time-consuming and meticulous process.

1.4 RECORDING ANALYSIS

There are various ways to approach the analysis of acoustic monitoring recordings. For example, the aim could be to identify the species recorded or to gather information about the surrounding environment. The following sections will detail the most basic approach first,

then move on to the automatic analysis of the signal, and finally cover the use of artificial neural networks.

1.4.1 *Signal processing*

1.4.1.1 *Manual analysis and Automatic detection based on signal features*

For species detection, analysing the recording manually can be a solution when the quantity of data is small. With operated recorders, the interesting parts of the data are usually annotated from the field notes and enable to only listen and verify these parts of the signal on spectrograms for example. This method can be time consuming, however, when done by experts it can be more precise and valuable. Analysing some files in order to find interesting part can also be done using automatic analysis of the signal. For example, to automatically detect sperm whale clicks, research already used the intensity of the signal with a fixed threshold using a method called Teager–Kaiser (TK) energy operator [26, 27]. When the energy at a frequency is higher than the fixed threshold, the algorithm considers that the acoustic event can be a detection and then requires manual verification. However, these methods can be less precise and are species dependent as they require to know the specific frequencies corresponding to the species.

1.4.1.2 *Acoustic indices/ecoacoustic*

When species detection is not the purpose of the experiment, acoustic indices can be a proxy of the soundscape and therefore the species composition. In this context, many indices were developed for different purposes using mathematical computation based on signal descriptions. Analysing the complexity of an environment can then be used by computing the Acoustic Complexity Index (ACI), which measure multiple frequency bands, in order to extract differences in the acoustic energy along temporal steps. Other indices measure the soundscape components and express the ratio of the anthropic sound over the biotic ones, by computing biophony (living organisms sound) measures between 1 and 2 kHz and the anthropophony measures (human noise) between 2 and 8 kHz. The ratio of the results gives an idea of how much the signal contains anthropogenic sound and therefore perturbation [28]. Other indices are used like the Biodiversity Index (BI), the Acoustic Diversity Index (ADI) or the Entropy (H). In addition, other indices were developed using the automatic detection of Region of Interest (RoI) by measuring the decibel ratio, and then counting the number of RoI as a proxy of the species richness [29]. But the precision of all these methods, as well as automatic detection using machine learning, are subject to precision variation due to background noises or the complexity of the environment and its variations.

1.4.2 *Artificial Neural Networks*

Defined as a computational model inspired by the structure and functions of biological neural networks, Artificial Neural Networks (ANN) were imagined during the mid 20th century [30] and are now being used in bioacoustics and many other research fields. In bioacoustics, it can be used to detect species or specific events. In the case of passive bioacoustic monitoring, as the recorders do not only contain interesting acoustics features, it is necessary to have a look at the data in order to filter it and extract the salient parts. However, as said before, this process can be difficult and time consuming. Recent research focused on developing ANN that are trained for a specific task like detecting a species in a recording. The use of these tools rapidly gained popularity and yielded promising results, which were comparable to those of human performance. One of the main examples on the use of ANN is the plant identifier application Pl@ntNET [31], able to detect with high accuracy thousands of plant species based on images or the bird classifier BirdNET [32] that has become a reference for bird monitoring around the world with over 8,000 species in its dataset. Nowadays, multiple architectures exist for these ANN but one of the most commonly used for bioacoustics is the Convolutional Neural Network (CNN).

1.4.3 *Environmental influences on acoustic recordings*

In the field of bioacoustics, it is important to consider the environmental factors that influence animal vocalisations. It is important to note that the environment is subject to constant change due to factors such as temperature and humidity, which must be considered when conducting a survey. Indeed, given that sound propagates at a rate five times faster in an aquatic environment than in air, the outcomes are not comparable. Also, in shallow water, sound propagation is reduced, and the physics of the ocean also affects this process. As warmer temperatures result in more carbon dioxide being pumped into the ocean [33], this leads to a decrease in pH, which in turn decreases the propagation of sound underwater [34]. In bird monitoring experiment, when conducted in a wetland, which is characterised by a scarcity of trees, sound has been observed to propagate over greater distances when compared to the conditions present in a forest. This is attributed to the fact that trees and leaves in a forest act as reflectors and absorbers of sound, thereby modifying its propagation dynamics. In a densely wooded environment, the propagation of sound within the 1-4 kHz range is found to be significantly limited [35]. In light of the numerous potential variations, it is imperative to establish a comprehensive monitoring protocol, with particular attention to the location and any anticipated obstacles to sound propagation. In the

context of evolving environmental factors, the species composition undergoes modifications, influenced by factors such as migration patterns or daily activity cycles. This underscores the necessity for PAM to consider these parameters in order to ensure optimal positioning and record at the designated time, taking into account the environmental context [36].

1.5 CONTEXT FOR EACH SPECIES

The following section provides a contextual overview of the studied species in this work. This thesis is focused on three distinct taxa: the humpback whale *(Megaptera novaeangliae)*, the sperm whale *(Physeter macrocephalus)* and birds (*Aves*). The first two species are aquatic, whilst the remaining species are predominantly aerial. However, despite their apparent differences at first, they have numerous features in common. For instance, they are all capable of emitting sound for the purpose of socialisation, and they are also all dependent on their environment, whether it is the abiotic or biotic kind.

1.5.1 *Humpback whale*

Humpback whale, *Megaptera novaeangliae* are *Mysticeti*, which correspond to baleen whale. Protected since 1982, it is present over all the world's oceans (Figure 1).

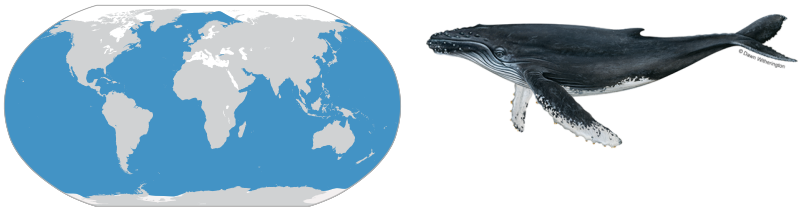


Figure 1: Humpback whale Distribution Map across the world (in blue) : Map and illustration from : fisheries.noaa.gov

Humpback whales are also known for their long migrations between the poles – which are rich in krill and are feeding ground – and the equator, where they breed. There are several populations of humpback whales, and every year, the North Atlantic population migrates from the North Pole (Svalbard/Norway, Newfoundland/Labrador) to breed in the Caribbean or Cape Verde between December and May (Figure. 2).

While males and females of all age classes, including calves, produce non-song calls on breeding and feeding grounds [37, 38], only mature males (or close-to-mature males) are known to produce a complex and organised song during the breeding period [39]. It is

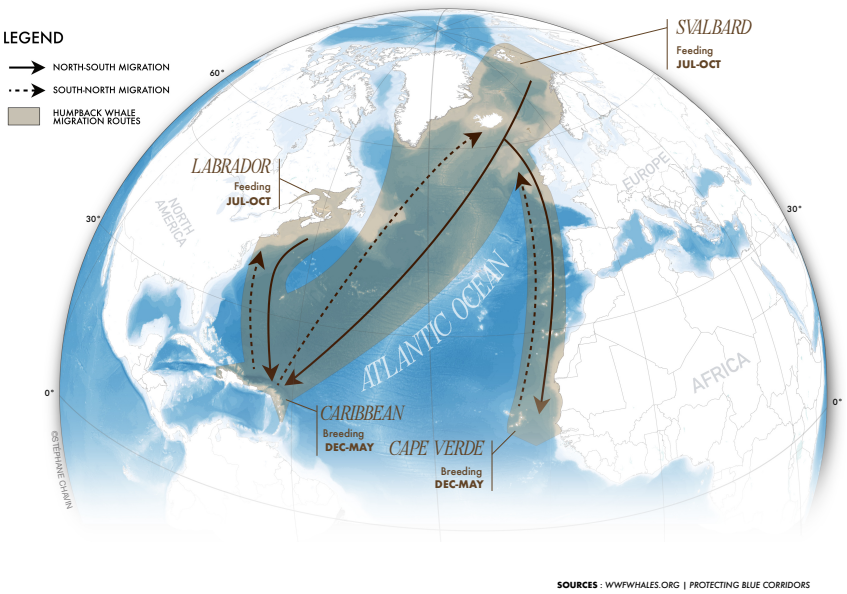


Figure 2: ***Megaptera novaeangliae*** **North Atlantic Population Migration Map**

hypothesised that the purpose of these complex songs, performed by males, is to showcase their fitness levels, thus increasing their chances of reproduction [22]. However, it has also been observed that these songs are also mediating male-male interactions [18]. The structure of these songs has been extensively studied [19, 40], often focusing on their repetitive patterns. The basic elements taken into account when analysing these songs are vocalisations. Each being separated by silences, they are typically attributed to distinct categories that we will call units. Units typically last between 1 to 3 seconds, with a frequency range of 20 Hz to 24,000 Hz [41]. When arranged in sequences with a specific order, they form phrases [19]. A phrase consists of at least two vocalisations, organised in a rhythmic pattern [42], and lasts an average of 15 seconds. The repetition of phrases forms themes, which can last up to two minutes [43]. These themes are then repeated multiple times to create a song, which is itself repeated several times during a singing session, lasting from 30 minutes to several hours [19, 43].

1.5.2 *Sperm whale*

Sperm whale (*Physeter macrocephalus*) are toothed whale. Present from the high to the low latitudes, they are also present in the Mediterranean Sea (Figure 3). Around the world, male sperm whale are known to migrate from the pole to warmer water, as seen with the Mauritius group [44] that migrate from the subantarctic waters to the Mauritius waters to breed. On the contrary, females and calves are

known to stay in the tropical waters, all year round as they can find enough food in these latitudes [45].

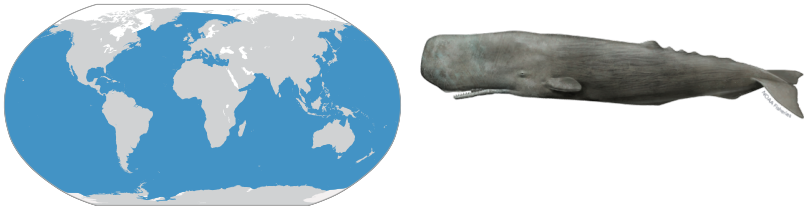


Figure 3: Sperm Whale Distribution Map (in blue) : Map and illustration from : fisheries.noaa.gov

The social structure of the species is matriarchal, with males typically departing from the pod at sexual maturity and leading more solitary lives [46]. The social groups have been observed to remain at the surface for extended periods, yet they possess the capability to undertake deep dives in order to feed on species inhabiting the deep sea. In the course of these dives, individuals emit echolocation clicks for the purpose of locating their prey and subsequently hunting it. These extended dives, which can persist for a duration of up to an hour [47], pose a significant challenge in terms of observation and study, as it makes sperm whales visible only for less than 10 minutes every hour. Nevertheless, they constitute an interesting case study for passive acoustic monitoring, as they can be detected more than a kilometre away and emit sound for the entire foraging period. It is finally important to note that the species has been classified as 'Vulnerable' on the IUCN Red List [48], thus indicating that it is a species of concern.

1.5.3 *Birds in Northern America*

Within terrestrial biophony, diverse taxa contribute to the soundscape. Birds, for example, use song for communication and in particular for mate attraction and territory defence [20, 49]. However, they can also use other sounds like specific calls during migration called flying call [50].

Comparable to humpback whale, many bird species are migrating during the year. Between birds, different groups can then be dissociated, the permanent residents, who do not migrate, the short-distance migrants, who move in short distance during special weather event and the long-distance migrants who migrates long distance, across continents [52, 53]. However, other categories can be observe as some bird population undertake migration while another population from the same species does not, called partial migrants or some species are migrating some years and do not some other years, which are called

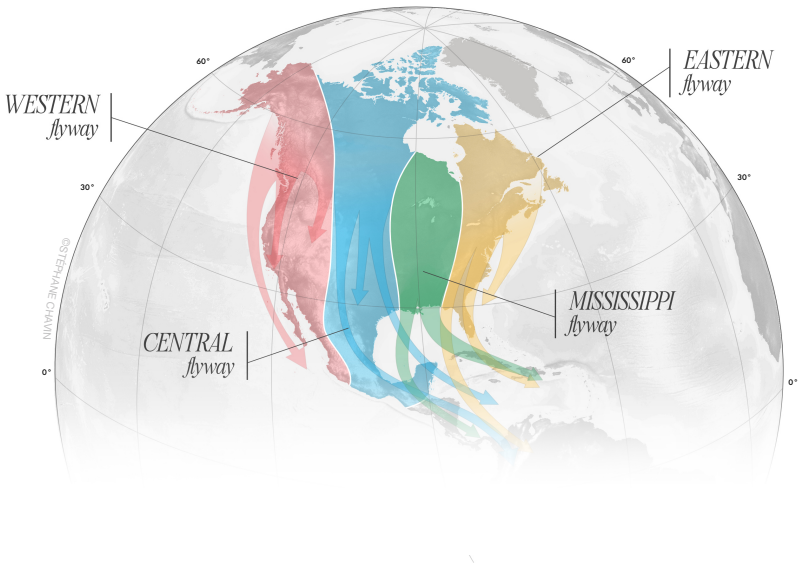


Figure 4: Northern America Birds' Flyways : Adapted from [51] and "The Boreal Songbird Initiative"

the irruptive migrants. Many studies focus on bird migrations and it has been observe that the migrations are usually performed primarily in order to leave areas with decreasing food resources, due to seasonal variations, to more favourable regions but also because of endogenous annual rhythm [54] compared to a clock that would give the individual the instinct to migrate [55]. In the Northern hemisphere and particularly in North America, birds are migrating for the spring season, from the lower latitudes to the higher. Based on many observations, different flyways were extracted, considering at first four different flyways [51]. Different studies however suggest that some of the flyways were mixing and were not perfectly defined as some bird can go from one to another [56, 57]. A proposition of these flyways is given on the Figure 4. The migration path from the breeding ground to the wintering ground is presented, as is the migration from south to north. The western flyway, which traverses California for example, is visible on the map and follow the Pacific coast. The eastern flyway follows the Atlantic Ocean, and the central flyway is more of a continental flyway across North America. The Mississippi flyway is located between the central and Atlantic pathways.

1.6 THESIS OBJECTIVES AND PLAN

As previously outlined, the study of the environment is a complex process, with its components exhibiting even greater levels of complexity. However, the objective of this thesis is to present a methodology that enables the monitoring of species using various criteria, including location and period for example, to assess their presence,

and subsequently use diverse techniques to characterise their habitat preferences. The structure of this thesis is as follows: firstly, it will present all the data that were used for the work; secondly, it will present all the methods that were developed and used; thirdly, it will comprise three chapters of results. The first of these will present the results of the artificial neural network and provide a comparison with the literature and other architectures. The second will consider the effect of fixed parameters on the presence of each species studied, taking into account the geomorphological part of the environment (the abiotic component for example). The third will consider the effect of dynamic parameters associated with fixed ones, in order to add more complexity and highlight the importance of each parameter. The decision to initiate the study with fixed environments was made with the objective of establishing a baseline for the analysis. This approach was adopted to facilitate an initial assessment of the significance of these parameters. The objective of this is to ascertain the geographical distribution of the species in question and to subsequently investigate the reasons why these models are not sufficient to predict their habitats. Nevertheless, the significance of the fixed environment is diminished in the absence of the dynamic ones. These will be incorporated into the final chapter as the concluding results of the species distribution analysis. In light of these findings, it will then be possible to hypothesise about the movement patterns of these species in the context of environmental modification, such as climate change, extreme events, or human activity.

2

STATE OF THE ART AND CONTEXT

2.1 Artificial Neural Network (ANN) 15
2.1.1 Mono class detector and classifier 17
2.1.2 Object Detection 18
2.2 The use of ANNs in bioacoustics 19
2.3 Impact of fixed parameters on species distribution . . . 21
2.4 Impact of long term dynamic parameters on species distribution 23
2.5 Impact of short term dynamic parameters on species distribution 25

2.1 ARTIFICIAL NEURAL NETWORK (ANN)

Given the present contribution of ANN to a number of PAM studies, there is a clear necessity to understand some of the mechanisms involved. For most ANN architectures, the model is composed of three types of layers - Input Layer, Hidden Layers and Output Layer as presented in the Figure 5.

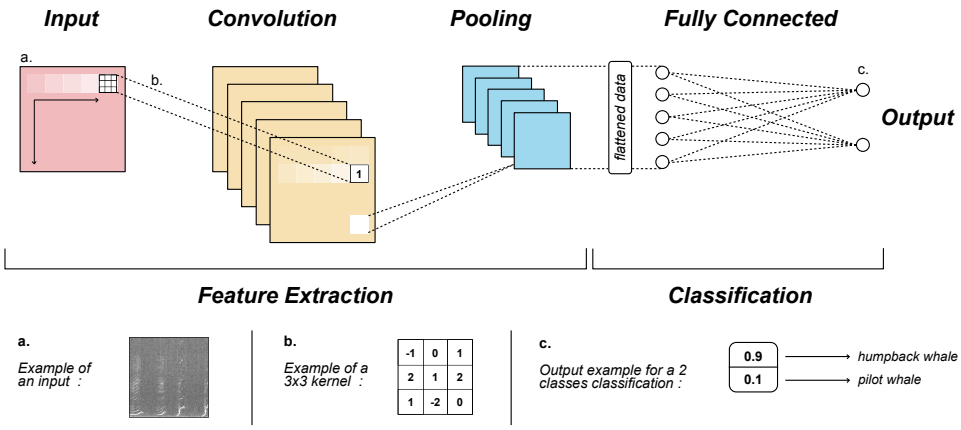


Figure 5: Main part of a convolutional neural network, with the example of a humpback whale song spectrogram.

The input layer, when working with a supervised ANN, which means that data are annotated, is the first layer where data enters the model. In bioacoustics, data can be the signal represented as a spectrogram after a Fourier Transform for example Figure 5.a.

The hidden layer is the part of the ANN that analyses and transforms the input layer to process it and extract different features. With a Convolutional Neural Networks (CNN), for example, hidden layers

are composed with various layer and particularly convolution layers. A convolution is a mathematical computation which consist of convolving an input (here, a spectrogram) while performing different calculations for each kernel (see Figure 5.b) across the input. This process extracts a reduced output based on the convolution. There are multiple type of convolution layer - 1 dimension or multiple dimensions -. The 1D convolution layer is used when the input is a vector. It convolves the input in one simple way. The second convolution layer is the multiple dimension layer, for example 2D convolution. While working on the same input, the kernel convolve over the spectrogram horizontally and then vertically which results in an abstract and equal or smaller input data. The values that compose the kernel are considered to be the weights of the layer in question. The initial kernels are created at the onset of the training process, and a gradient is also initialised, which is known as the loss function. The loss function is characterised by an equation in which the model evolves through a series of steps, each of a specific size known as the learning rate. The objective of the model during the training process is to achieve the minimum of the aforementioned equation, thereby attaining optimal performance levels and optimal feature extraction. During the training process, the kernels are adjusted using backpropagation, which is an algorithm that uses the predictions of the model to modify the previous steps, with the objective of minimising the loss. Additionally, an optimiser is employed, such as the Stochastic Gradient Descent (SGD) [58] or the Adaptive Moment Estimation (ADAM) [59] optimiser. The objective of both optimisers is to modify the model's characteristics during the training process, with the aim of converging towards a local minimum. Nevertheless, it is important to note that the model does not modify its weights at the level of individual training sample; rather, it typically does so at the level of batches. A batch is defined as a set of n training sample, which can be adapted, on which the model will operate. It is notable that upon the model's computation of all input data from a given batch, predictions are made, and the backpropagation process is subsequently initiated in order to adapt the weighting based on the errors and the evolution of the learning rate over the loss function. It has been hypothesised that an increase in batch size will yield superior results, as the model adapts its weights to the entire dataset. Nonetheless, in certain architectural frameworks and with limited datasets, an augmented batch size appears to diminish model accuracies, as observed in previous research [60]. Conversely, diminished batch sizes facilitate a more profound exploration of the gradient, thereby identifying better local minimum.

The final layer of the model is the output layer (Figure 5.c). It consist of n neurons, based on the number of classes (*e.g.* species) to predict. In the case of a model that aims to detect one species among two, if the model predict the correct species, the value for this species

should be close to 1 while the others near 0. When the model yields a true annotation, here the correct species, it is considered as a True Positive (TP) Table 2. When the model predicts a species, yet is not present, it is considered as a False Positive (FP). FP may also be attributed to the model's inability to differentiate between classes, resulting in confusion. The outcome of this can be measured and assessed using a confusion matrix. When the model does not predict the species, yet is present, it is considered as False Negative (FN) and a True Negative (TN) is when the model did not predict anything and it is true, or the model only predict one species and it is the only one to predict so the first species is a TP and the second one is a TN as the model predict its absence, as presented in Table 2. Based on this, we can evaluate metrics in order to verify if the model is accurate or not.

Table 2: Confusion matrix for model prediction and score evaluation.

pred \ *true*	Positive	Negative
Positive	TP	FP
Negative	FN	TN

2.1.1 *Mono class detector and classifier*

In machine learning, and in particular in bioacoustics, classification is widely used in order to know what is in a signal. However, some models are also used as detectors, when we only search for one species. Both models require annotations in time with an associated size in duration. By training a model with labelled data, for example humpback whale units, we associate a class to a representation of the last layer of the model, and by seeing all the annotations, the model optimises and then is able to predict the classes in a signal, associated with a confidence score. When working on mono class detector, the response of the model would be `humpback_whale` while for a multi class classifier it would be the unit corresponding to the vocalisation. For both tasks, the metrics to analyse are mostly the accuracy eq.1, the precision eq.2, and the recall eq.3, as well as the Area Under the Receiver Operating Curve (ROC AUC), which is the True Positive Rate eq.4 as a function of the False Positive Rate eq.5. For accuracy, precision, recall and TPR, the closer to 1, the better the model, however, for the FPR, the lower it is the better. As a result, for the final metric, the closer to 1 for the ROC AUC, the better.

$$\text{Accuracy} = \frac{TP + TN}{TP + TN + FP + FN} \tag{1}$$

$$\text{Precision} = \frac{TP}{TP + FP} \tag{2}$$

$$\text{Recall} = \frac{TP}{TP + FN} \tag{3}$$

$$TPR = \frac{TP}{TP + FP} \tag{4}$$

$$FPR = \frac{FP}{FP + FN} \tag{5}$$

2.1.2 *Object Detection*

Object detection in machine learning is used majorly in image analysis. It requires boxed or segmented annotations, which is more time consuming than time annotations only. While training, the model learns the annotated boxes as positive, and all the non-annotated part as a negatives (that can also be background). The output of the model is different detections, each associated to a class, with a confidence score. In this scenario, the main metric to consider is the mAP eq.6, which requires to first analyse the Intersection over Union (IoU) of the detection. The IoU is computed by measuring the area of overlap between the predicted box and the annotated one as presented in Figure 6. In the model architecture YOLO and more precisely the YOLOv5 for example, the prediction is removed if the IoU is under a value of 0.5. The mAP metrics considers the value of the average precision for each species, which is named AP and corresponds to the area under the precision-recall curve which is done by evaluating the resulting precision and recall to each threshold eq.7. This AP can be computed using different methods which will give different results. It can be measured using micro, macro or weighted average. The first one refer to the aggregation of the contributions of the different classes to compute the average metric while the macro average will compute the metric independently for each class and then take the average. Finally, the weighted average will compute each species independently and will then average using the contribution part of each class (which correspond to the number of annotation of one class over the total annotation). For object detection evaluation, the F-score eq.8, which combines Precision and Recall metrics at the same time with a specific threshold value. The most common F-score is the F1, with a β value of 1, but it can also be derived to F05 score or F2 score as it offers a different analysis. For example, F05 score can be computed when the model need to focus more on the precision than the recall.

$$mAP = \frac{1}{N}\sum_{i=1}^{N} AP_i \tag{6}$$

As the AP is measured as

$$AP_{IoU} = \sum_{i=1}^{n-1} (r_{i+1} - r_i) * p_{interp}(r_{i+1}) \tag{7}$$

where r1, r2, r3, ..., r_n are the recall levels in ascending order at which the AP is interpolated and p_interp is the interpolated precision value at this specific recall threshold.

$$F_\beta score = \frac{(1+\beta^2) * Precision * Recall}{(\beta^2 * Precision) + Recall} \tag{8}$$

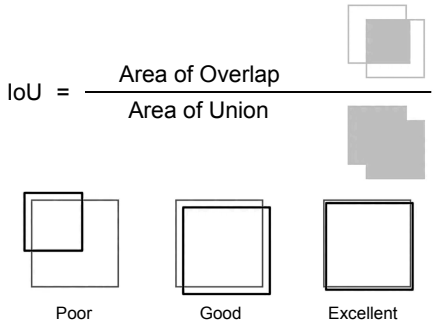


Figure 6: Representation of how the Intersection over Union (IoU) is measured and is evaluated

In bioacoustics, object detection is not as common due to its objective to locate objects, like signalisation signs, animals into images of camera trap [61, 62]. However, recent advances shows that these models perform well [63] on acoustic detection and classification task but can remain limited as they do not generalise easily.

2.2 THE USE OF ANNS IN BIOACOUSTICS

A multitude of research has been conducted on the development of precise models for bioacoustics, leading to the creation of sophisticated tools capable of predicting over 8,000 species with the BirdNET and Perch 2.0 models [32, 64]. Many of the models are focusing on avian monitoring as it is used in land ecosystem monitoring. The latest Perch 2.0 however is able to detect terrestrial animals, and marine mammals using the same architecture. Also, the BirdNET architecture can be fine-tuned for other species than the ones that was originally trained for. Some of the published models are able to predict with good accuracy the species in different recordings and can also be implemented inside an ARU which offer real time detection [65]. In

marine environment, PAMguard [66] is a widely used software which allows multiple tasks but also to use a neural network model to detect different species in underwater recordings. It can be used for baleen whale vocalisations, or even transient sounds like porpoise echolocation clicks [67].

The development of these models required large database which contains recordings and manual annotations. For birds and terrestrial ecosystem, models are usually relying on the XenoCanto dataset, which contains over 900,000 recordings of birds, 36,000 of grasshopper, 8,600 of bats, 5,500 of frogs and around 3,400 of land mammals, with each files associated to different species. About the marine mammals, the DCLDE (Detection Classification, Localisation and Density Estimation) workshop offers multiple datasets of annotations for different challenges [68, 69] as well as DOCC10 which focus more on *Odontoceti* clicks [70]. These datasets offer researchers confirmed annotations from different projects in order to develop more accurate models. More recently, the Global Library of Underwater Biological Sounds was created aiming to offer a new database for models [71] and will focus on all underwater species, from shrimp to marine mammals.

In a multitude of studies, the use of a pre-existing neural network has become a common practice, instead of the development of a fully personalised model. In fact, it is recommanded not to start from scratch but rather to use already trained models and using fine-tuning [72] on a self-made dataset. For example, BirdNET allows users to create a one species detector for birds or mammals [73] as well as DeepSqueak has already shown to be used for primates vocalisations [74]. These models can be interesting for some case studies, but can add some constraints as for example when birds are singing together, which create choruses, the task is more difficult and some models are less performant [75]. However, self-made dataset are less representative than official dataset and enable less comparison to other models. Also, self-made dataset can lead to over-fitting of the model for the given data and will then lead to a specific model, which reach high performances but is not able to generalise over new datasets. The decision of whether to develop a model that is specifically adapted to the given data or one that is applicable worldwide, albeit with reduced accuracy, is therefore a decision that depends on the researcher and its objectives.

Taking a more detailed look into the performances, the PAMguard model was evaluated on North Atlantic right whales *(Eubalaena glacialis)* and reach an average precision of 90.4% on the DCLDE 2013 dataset [76]. Also, when analysing at different false positive rate per hour, researchers found a recall of 88.3% at a rate of 5 false positive per hour and a recall of 96.6% at 20 false positive per hour. For the bird detectors, they perform well with a mean average precision of 79.1%

for BirdNET on audio recordings involving a single species and 50% on the BEANS dataset [77] for Perch 2.0. Recently, using boxed annotations and YOLO models, some studies were able to present results reaching high precision, with F1 score of 89% on Svalbard fin whale call, also established to 80% for another dataset without fine-tuning [78], or a precision of 84% and a recall of 70% on dolphin whistles [79].

The "You Only Look Once" (YOLO) model architecture is specifically designed for object detection. The structure of this model is composed of three distinct phases [80]: firstly, the backbone; then, the neck; and finally, the head. The initial process entails the organisation of convolutions, with the purpose of extracting the features of the input images and reducing the number of dimensions. The reduced input is then processed by the neck, the function of which is to integrate and refine feature representations. The resulting data is then transmitted to the head, where the model generates predictions and bounding boxes for each class label. The number of parameters in a neural network is frequently employed as a metric to denote the model's size and complexity. In the context of YOLO, the parameter count ranges from 1.9 million for the nano pretrained model to 86.7 million for the extra large model. In comparison, the BirdNET model contains approximately 12 million parameters. This is positioned between a small version of YOLOv5 (7 million) and a medium version (21 million). Nonetheless, the preceding version of BirdNET incorporated approximately 27 million parameters [32].

2.3 IMPACT OF FIXED PARAMETERS ON SPECIES DISTRIBUTION

In order to predict the presence of a particular species within a given environment, it is first required to ascertain the preferences of that species. However, it is important to note that this approach needs to differentiate the species that are resident throughout the year, as opposed to those that migrate. As previously outlined in this manuscript, the different species that are the focus of this study exhibit distinct behavioural patterns. Firstly, humpback whales (*Megaptera novaeangliae*) migrate from polar to equatorial regions in order to breed, and it is hypothesised that they do not consume food during their stay in the breeding grounds [81]. This suggests that food resources may not be the most significant predictor, despite the occurrence of feeding events [82]. However, avian species occurring in Canada are also migrating, motivated by two factors. Firstly, there is a decline in the availability of resources in their feeding grounds [83]. Secondly, the conditions in higher latitudes are more favourable to their survival and reproduction. The ability to predict the abundance of their prey would be a valuable asset. The final species of interest, the sperm whale *(Physeter macrocephalus)*, has been observed to be pre-

dominantly comprised of adult males in the northern part of the Western basin of the Mediterranean Sea, in proximity to the French coastline [84]. These cetaceans primarily forage in deep waters. In the context of deep-diving marine mammals, such as sperm whales, whose primary dietary sources comprise mesopelagic and bathypelagic prey, the most effective parameter for prediction would be the abundance of these prey species [85]. Nonetheless, monitoring the prey of certain species can be challenging. Consequently, the evaluation of the parameters that should impact the lower part of the food chain constitutes a more straightforward method of predicting the presence of these species in a given area [86]. For fin whales, for example, the MaxENT presence-only model revealed that current and chlorophyll-a were the main parameters for predicting habitat suitability [87].

The correlation between depth and the presence of sperm whales in the area has been well-established [85]. However, it should be noted that this is also linked to high slope values, which reveal a steep and rough underwater floor. This has been shown to contribute to an increase in prey richness [85]. Canyons have been identified as a geomorphic feature of significant importance [88, 89]. The formation of these structures by erosion leads to their distinct functions in the transportation of sediment to deeper environments, as well as its subsequent return through upwelling and mixing during periods of current change. This process has been observed to enhance local primary productivity, thereby potentially contributing to an increase in prey populations within the specific area.

The environmental composition preferences of the humpback whale are distinct. It has been observed that, during the breeding period, female specimens tend to demonstrate a preference for shallow waters in the early stages of their calves, in close proximity to the shoreline [81]. This behaviour could be indicative of a preference for areas that offer enhanced protection from the potentially adverse effects of oceanic conditions and predatory threats, such as orcas [90]. The habitat prefered during the breeding season is observed to be in proximity to the coast [91]. However, during the feeding period, when the whales are located in high latitudes, they have been observed to be found in deeper water, far from the coast [92, 93]. It has been observed that the habitat, stable and shallow, exerts a greater influence on preferences during the breeding period. Conversely, food resources and dynamic parameters during the feeding period appear to have a more significant impact. However, given that the fundamental purpose of migration for males is to reproduce, it is pertinent to investigate the potential of oceanic environments to enhance sound propagation, with consideration given to the depth of the ocean as a possible determining factor [94].

In the context of avian migration, with particular reference to species endemic to the North American continent, the prediction of their

presence in specific areas during the migration period could be informed by their latitudinal preferences and habitat requirements. It is acknowledged that higher latitudes are associated with longer migratory routes. Nonetheless, the prediction of the migration dates is influenced by dynamic parameters, such as the photoperiod, as evidenced by previous research [55]. Consequently, it will not be possible to predict the migration dates using fixed environmental parameters. Furthermore, it is important to acknowledge that migratory patterns exhibit notable variation among different bird species. It is acknowledged that certain species manifest a distinct predilection for specific habitats, such as wetlands or boreal forests. In contrast, others are classified as generalists, a designation attributable to their capacity to adapt to diverse environmental conditions [95].

2.4 IMPACT OF LONG TERM DYNAMIC PARAMETERS ON SPECIES DISTRIBUTION

Research conducted on humpback whales has already established a correlation between variations in parameters across different breeding areas. It is important to note that the temperature is a key factor, as no breeding areas were identified where the temperature exceeded 28°C [96]. In the context of climate change, insights into the North Atlantic population could facilitate comprehension of potential changes due to ocean temperature increases in the Caribbean. The observed arrival time in the Caribbean Sea is typically concomitant with lower sea temperatures in this region, corresponding to the transition from winter to early spring. As previously mentioned, the period of peak detection occurs between March and April, with the precise timing varying according to the island in question [97, 98]. However, the distribution of humpback whales in that region suggests that their presence under Martinique is quite rare, which indicates a potential change in the environment.

A correlation between dynamic variables in sperm whales and phytoplankton blooms has been indicated in previous studies [99, 100].or instance, the presence of sperm whales has been documented to be associated with such blooms, exhibiting a temporal lag ranging from four weeks to several months. In addition, given the difficulties inherent in determining the abundance of prey as they forage for food, it is possible to investigate dynamic parameters that can affect their prey [85]. Observations of the diet of sperm whales in the Mediterranean revealed that the majority of their consumption consisted of large meso-bathypelagic squid species, including *Histioteuthis bonnellii* and *Octopoteuthis sicula* [101]. In the global ocean, the current is one of the parameters that impacts all life, by moving animals and plants, as well as redistributing heat and nutrients [102, 103]. Indeed, the movement of heat from one location to another exerts an influence even

on meteorological phenomena. The Gulf Stream, is a major example of this phenomenon [104], and its impact is also evident during the summer months in Europe [105].

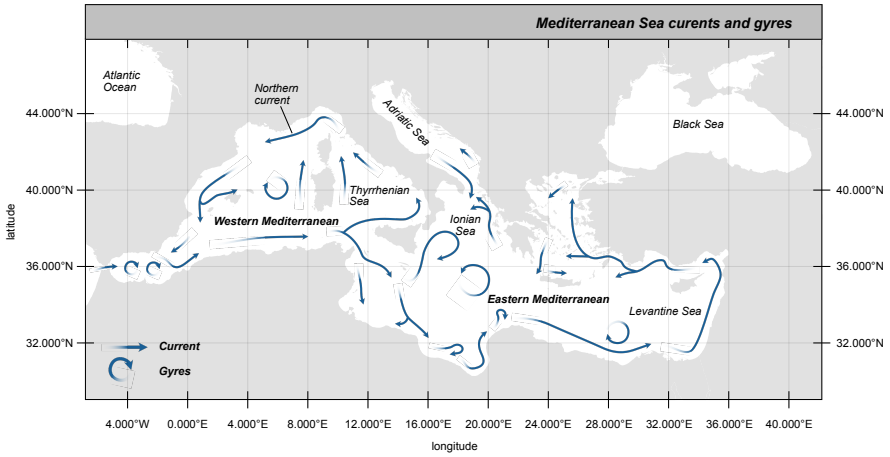


Figure 7: Mediterranean Sea global current : This map, adapted from [106], shows the different currents and gyres inside the Mediterranean Sea's various regions.

The Mediterranean Sea, and more specifically its western basin, is characterised by the presence of multiple currents. Among these, the North Current (NC) (Figure 7) is of particular significance. This current, which is strong in its movement, follows the 300-metre isobathic line that extends from Italy and France, terminating in Spain [107, 108]. The current exhibits seasonal variation in its characteristics. Its width ranges from approximately 35 km in the summer months to around 200 m in the winter months, with a maximum speed of approximately 40 to 0.5 m/s. In contrast, during the winter months, the width of the current extends to 28 km, with a depth ranging from 250 to 500 m, and its maximum speed increases to between 70 to 0.9 m/s. This variation in the width and depth is attributed to seasonal changes in the surrounding environment, as reported in previous study [109]. The Balearic Islands are characterised by a higher mean temperature than the Ligurian area, with a mean difference of approximately 1°C [110]. It has been determined that a secondary current is formed from the warmer water, exhibiting a directional difference from the prevailing NC. The northern part of the Mediterranean Sea has been identified as a significant contributor of nutrients, ranking among the most substantial sources within this region. The influx of nutrients is further augmented by the presence of the Rhône River, which has been shown to enhance the concentration of nutrients in the water, thereby stimulating primary production and phytoplankton growth in the surrounding area [111]. It is evident that the variations under scrutiny, when examined at the season level, have the capacity to exert influence over the presence of the sperm

whale's prey. This, in turn, may have a bearing on the abundance of the aforementioned species within specific geographical areas.

In the Canadian province of Québec, the seasons are characterised by significant variations in temperature, with extreme cold in winter and high temperatures in summer. However, these variations are not consistent across regions, with higher latitudes experiencing colder winters and lower latitudes experiencing warmer summers. As previously stated, the higher density of birds in the southern region can be attributed to the more challenging conditions experienced in the northern area. It was also stated that certain preferences were held with regard to specific habitat types, including deciduous and coniferous forests. The impact of changing climate patterns on the distribution of these habitats is well-documented, and it is widely accepted that the potential for these habitats to thrive is significantly diminished [112]. It is an established fact that previous observations on bird migrations have already led to the establishment of various parameters that impact the period of migration. For instance, the photoperiod is among the factors that induce migration [55]. The temperature is also a pertinent factor, as evidenced by observations which indicate its influence on both the length of stay and the arrival date [83]. The study of avian predators, with a particular focus on insects, is a crucial aspect of understanding the migratory patterns of birds. This is due to the fact that birds are more likely to consume insects during the migration period. Indeed, the data used in this thesis has also been employed for the monitoring of *Orthopera* peak occupancy, as referenced in previous study [113]. The findings of this study demonstrated a direct correlation between the variables under investigation and climate gradient, thereby indicating that peak activity occurred at a later stage in warmer climates than in cooler climates [113]. From an ornithological perspective, this phenomenon can be attributed to a comparatively shorter period in higher latitudes, which may occur at an earlier point in the season than in lower latitudes.

2.5 IMPACT OF SHORT TERM DYNAMIC PARAMETERS ON SPECIES DISTRIBUTION

Dynamic parameters are subject to considerable variation, with seasonal variation but sometimes daily fluctuations. For instance, in the Mediterranean Sea, the Northern Current (NC) is known to exhibit significant variations on a daily basis. At times, it approaches the coastline, at other times it is found at greater depths, and on occasion it is entirely absent, at least at the surface. As demonstrated in the preceding section, the presence of sperm whales has been observed to be correlated with variations in chlorophyll-a concentration. These variations in chlorophyll-a concentration are seasonal in nature; however, under the influence of strong wind events or specific oceanic condi-

tions, they can manifest as sporadic fluctuations, leading to blooms that are associated with the presence of sperm whales after a temporal lag of four weeks [100]. When considering brief meteorological phenomena, a noteworthy event is the heatwave, characterised by a period of elevated temperature. For various species, it is notable that they can demonstrate a degree of sensitivity to variations in temperature. This is evidenced by the documented optimum temperature for the humpback whale, the impact of the temperature gradient on the sperm whale, and the correlation with the temperature for the birds. Consequently, the impact of marine or terrestrial heatwaves can be substantial. As has been previously documented, the population of humpback whales has been subject to a substantial decline in the Gulf of Alaska following a series of heatwaves [114]. This study is concerned with the consequences of the marine heatwave that occurred in the north-eastern Pacific region between the years 2014 and 2016 on humpback whales. It was observed that there was a 50% decline in abundance, and this decline persisted for several years. Furthermore, there was a decrease in the number of calves. It has been observed by researchers that the abundance of herring in the area has been strongly affected by the heatwave, and that this decline may be correlate to the diminution of whales in this feeding area. Also, it has been established that elevated ambient temperatures can result in a significant decline in avian activity. This phenomenon has been documented in various studies [115, 116]. The preceding studies established that elevated ambient temperatures, typified by heatwaves, induce alterations in avian activity patterns, whereby birds transition from a state of active defence to a less pronounced response [116]. Consequently, avian populations will remain within the area, albeit with diminished levels of activity.

3

MATERIALS

3.1 Multi year survey in the breeding ground of the Humpback whale, across the Caribbean 27
3.2 On site Sperm whale observations in the Mediterranean Sea 29
3.3 Terrestrial dataset from the temperate regions of Québec to the Arctic 32
3.4 Access to the environmental variables 33
3.4.1 Marine variables 33
3.4.2 Terrestrial variables 35

Key points

A total of three different datasets were used:

- One was from the **Caribbean Sea** and included over 9,000 hours of recordings from 2021 to 2022, some of which contains **humpback whales**;
- One based on 318 observations of **sperm whales in the Mediterranean Sea** between 2022 and 2025;
- One from **Québec** containing around 340,000 files from 2016 to 2025 during the bird migration.

Environmental variables were downloaded from public data providers such as **GEBCO**, **Copernicus** and **EMODnet**.

To study biophonic changes in different ecosystems, this thesis relied on multiple datasets, ranging from multi-year, large-scale monitoring with monophonic microphone to opportunistic area sampling and visual observations, as different biodiversity monitoring projects have been used.

3.1 MULTI YEAR SURVEY IN THE BREEDING GROUND OF THE HUMPBACK WHALE, ACROSS THE CARIBBEAN

In order to improve knowledge and protection of marine mammals in the wider Caribbean region, a network of 19 acoustic recorders was deployed (Figure 8). Stations from Guadeloupe and Martinique were placed in the Agoa marine mammal sanctuary, covering 143,256 km² around the islands of Martinique, Guadeloupe, Saint-Barthélemy and Saint-Martin. Each of the 19 stations was positioned according to

previous observations, bathymetry, and constraints of local partners on site. Immersed at a depth of approximately 20 m and anchored by a weight of 20 kg, acoustic recorders were connected to a surface buoy, ensuring they remain approximately vertical in the water column.

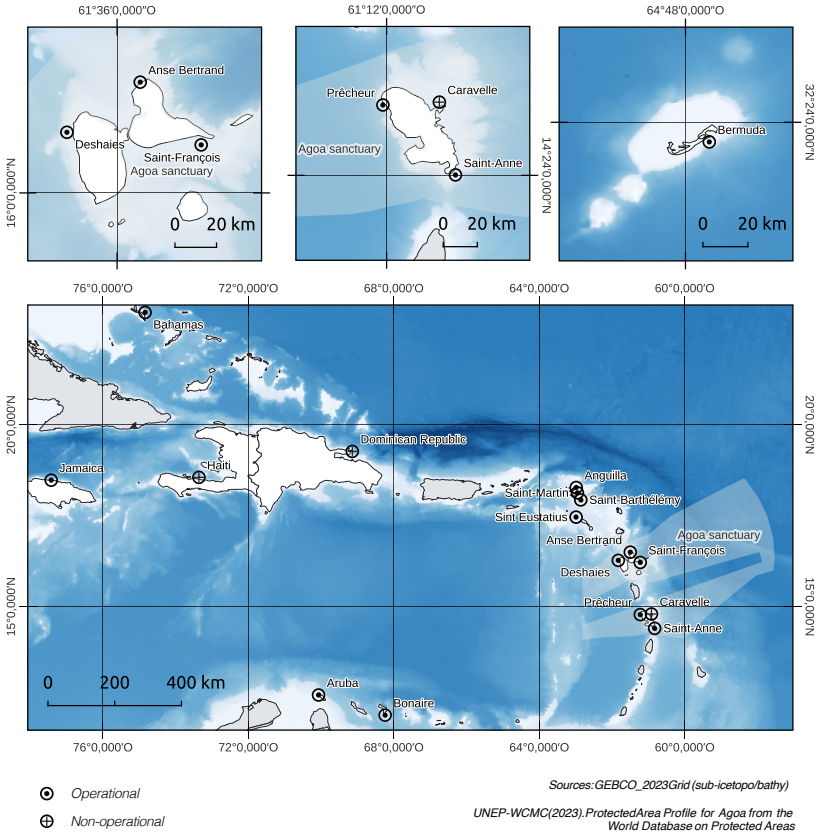


Figure 8: Map of the different ARU positions in the Caribbean region, from Bermuda to Aruba

Each station is equipped with a Cetacean Research C75 omnidirectional high-frequency hydrophone (usable freq. range 0.010 to 170 kHz, -180 dB Re / µPa), connected to the HighBlue mono recorder designed by the Scientific Microsystems for the Internet of Things (SMIoT) and CNRS LIS in CIAN [117]. The sampling frequency was either 256 kHz or 512 kHz. With 21 D 1.5 V batteries, 512 GB µSD storage and a duty cycle of 1 min of recording followed by a 5 min pause. This system has an autonomy of around 30 days, originally designed and implemented as a survey methodology for marine mammal populations [118]. With the different installations between December 2020 and December 2022, around 10,000 hours of recordings were collected. Periods during which humpback whales were potentially present, *i.e.* from January to the end of June, represented more than 4,000 hours of recordings across 14 operational stations (Figure 8).

3.2 ON SITE SPERM WHALE OBSERVATIONS IN THE MEDITERRANEAN SEA

Between 2022 and 2025, Longitude 181 conducted numerous missions in the Western Mediterranean basin, between Marseille and Imperia, in Italy, inside the Pelagos Sanctuary, a Marine Protected Area (MPA) aimed at the protection of marine mammals. These missions aimed to collect information on sperm whale habits, as well as information relative to particular individual such as its diving habits (e.g. surface duration, foraging duration and potential number of prey). This area of the Mediterranean comprises various canyons and is influenced by the Northern current, the major currents flowing from the Italian coast to the Gulf of Lion. The coast is mostly urban, with densely populated harbours such as those in Toulon, Nice and Marseille. As presented in Table 3, we consider observations from the Western Mediterranean and more particularly into the area GSA07, GSA08 and GSA09 from the Food and Agriculture Organisation (FAO) sub area system presented in Figure 10. A total of 318 observations, whether acoustic presence when hunting or surface observations were collected.

Table 3: Summary of the mission, date and location associated with the number of positive points apart of the 318 (acoustic or visual confirmation)

Mission	Year Month	Duration (days)	Number of Positive Points	Geographical Sub area	Grid Subunit
Whale Way 2	September 2022	14	35	**GSA07** and **GAS08** (Western Mediterranean)	M22C9, M23C9, M23C8, M24C7, M24C8, M24C9, M25C5, M25C5, M25C6, M25C9, M25D0, M26D0, M26C4, M26C5, M26C6, M26C9, M27C6, M27C7, M27C8, M27C9
Whale Way 3	April 2023	7	15	**GSA07** (Western Mediterranean)	M25C2, M25C3, M25C4, M26C2, M26C3
Whale Way 4	September to October 2023	14	93	**GSA07** (Western Mediterranean)	M25C4, M25C5, M26C4, M26C5, M26C6, M27C6, M27C7
Whale Way 5	September 2024 10	14	19	**GSA07** and **GAS09** (Western Mediterranean)	M25C2, M25C3, M25C4, M26C2, M26C4, M26C5, M26C6, M26C7, M27C6, M27C7
Whale Way 6	September to October 2025	14	89	**GSA07** (Western Mediterranean)	M25C2, M25C3, M25C4, M25C5, M26C2, M26C3, M26C4, M26C5, M26C6, M27C6, M27C7
Voile Ocean 1	May 2023	7	28	**GSA07** (Western Mediterranean)	M25C2, M25C3, M25C4, M26C2, M26C3, M26C4, M26C5
Voile Ocean 5	September 2024	7	25	**GSA07** (Western Mediterranean)	M26C4, M26C5, M26C6
Voile Ocean 7	September 2024	7	14	**GSA07** (Western Mediterranean)	M25C2, M25C3, M25C4, M26C2, M26C3, M26C4, M26C5, M26C6, M27C6

The protocol for the missions is opportunistic and does not follow any transect. The team undertake passive listening at intervals of 30-minute, using a SQ26 hydrophone connected to a Zoom H1N recorder, while maintaining a course along the bathymetric chart of 1,500 metres. Upon acoustic confirmation, the team first focused on locating a blow at the surface, before approaching in order to photograph the fluke and identify the individual. Acoustic monitoring was then undertaken during the dive, with some individuals observed over the course of several dives. The GPS positions obtained correspond to the diving footprint, within a radius of 1 km. The acoustic survey was also conducted during the night, while no visual observations were recorded.

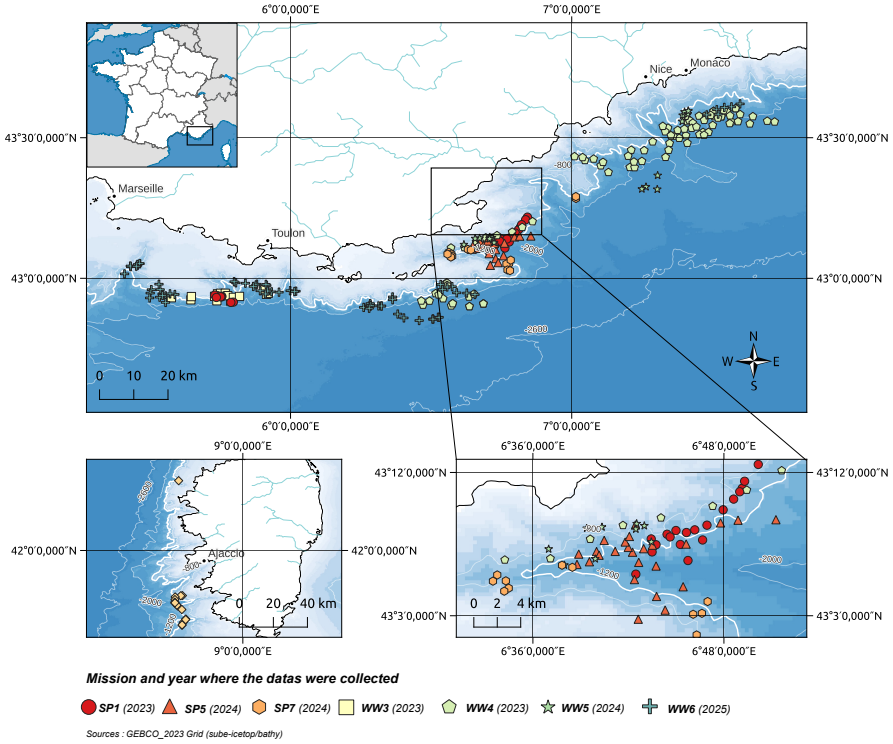


Figure 9: Map of the sperm whale observations from the different Longitude 181 missions in the Mediterranean Sea

For the purposes of this thesis, the data that were retained for analysis were exclusively those derived from visual observations of the animals' dives, in association with the GPS points corresponding to the footprints left behind. This subset of the global dataset comprises a total of 232 observations, as illustrated in Figure 9. Given the existence of both a photographic record of the fluke and the GPS location of the whale, the observations are then deemed to be positive. Nonetheless, in the absence of observations in certain areas, it is complex to certify the absence of sperm whale, given that the absence of activity in the recording does not equate to absence in the area, as the sperm whale is most of the time silent during surface or sleep.

As illustrated in Figure 10, the subunits are not sampled with equal frequency. Of the 25 sampled subunits, some were entered only once, while others, such as M26C6 (around Cannes) or M26C5 (between Le Levant and Fréjus), were sampled 12 and 13 times each.

To compare our observations to another database, we used the Ocean Biodiversity Information System (OBIS) database which is composed of over 112,000 record over the Ocean for more than 50 years. It is the results of 398 datasets, such as the long-term cetacean monitoring in the Azores based on whale watching observations that was performed between 2009 and 2020 [119] and is composed of 18,534 sperm whale records as presented in Figure 11 .

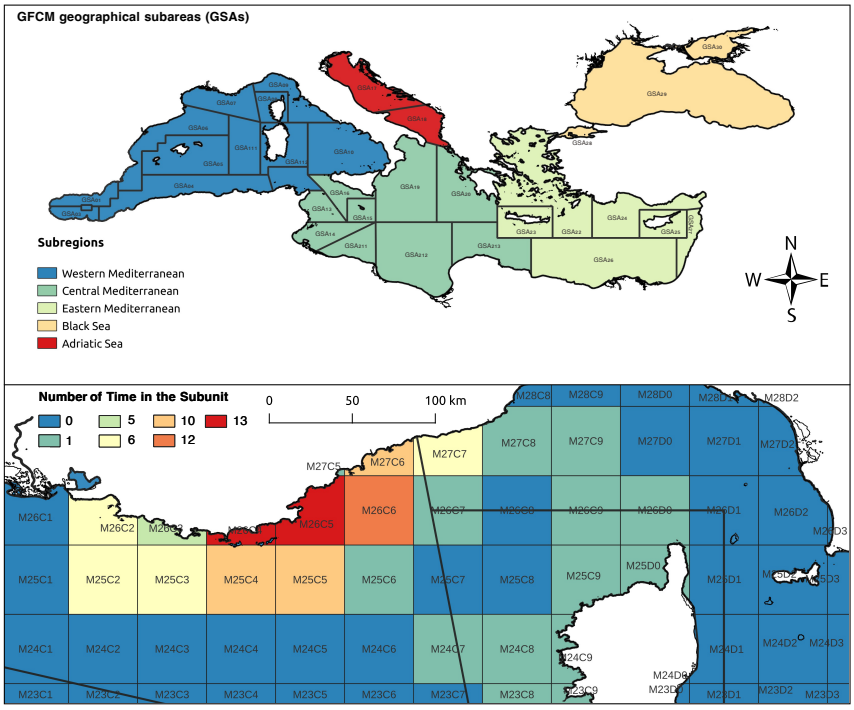


Figure 10: Geographical sub areas and subunits with the sampled area during Longitude 181 missions

3.3 TERRESTRIAL DATASET FROM THE TEMPERATE REGIONS OF QUÉBEC TO THE ARCTIC

As part of the Biodiversity Monitoring Network of the Québec provincial Government, Canada, ARUs have been deployed to cover the latitudinal breadth of Québec, ranging from 45° N to 61° N Figure 12.

Acoustic sampling was undertaken in 2016 until now (2026) and recordings were collected over four to six-month periods annually from April to October. The dataset thus available represents approximately 340,000 recordings. The long recording period allows for analyses of seasonal variations in species detections. Wildlife acoustics

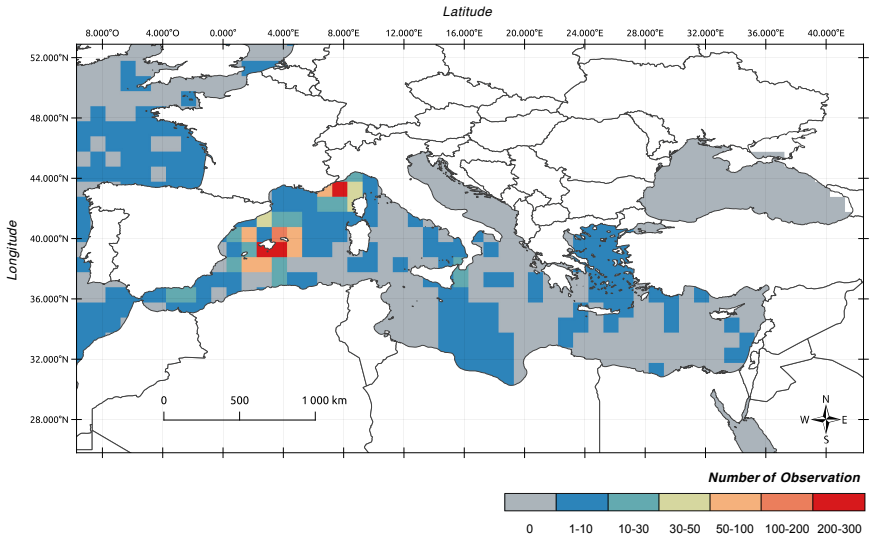


Figure 11: OBIS dataset observation densities across the Mediterranean Sea : The map highlights the two main areas where observations are concentrated: the Ligurian and Balearic regions.

SM3 were used before 2021 and were replaced by SMBAt mini with acoustic microphone in 2021 (half) and 2022 (all) and the PAM units were programmed to systematically record 15-minutes sessions at specific hours of the day corresponding to high songbird vocal activity. Some recordings are 30-minutes long and others (in 2022) are 1-hour long. Most audio data are sampled at 24,000 Hz to ensure high fidelity and capture intricate details of bird calls.

3.4 ACCESS TO THE ENVIRONMENTAL VARIABLES

3.4.1 *Marine variables*

The public dataset General Bathymetric Chart of the Oceans (GEBCO) sub_ice_topo from the 2023 [120] release has been downloaded to obtain the bathymetric informations. This dataset gives access to all the altimetric and bathymetric information in any place of the globe with a 15 arc-second interval grid which is approximately 500 x 500 m pixel size at the equator. Informations about the ocean rugosity and the slope were extracted from this dataset using the Geospatial Data Abstraction Library (GDAL) tools from QGIS [121]. Based on the GEBCO dataset, the distance to shore was computed by extracting the 0 metre line same as the distance to 5,000 bathymetric line, and the distance to that line to each pixels was computed with the measure of the nearest point calculator from QGIS.

The geomorphology informations, such as canyons, were extracted from the Harris et al. dataset [122]. It contains informations about all canyons in the Ocean with their associated surface in km². From the

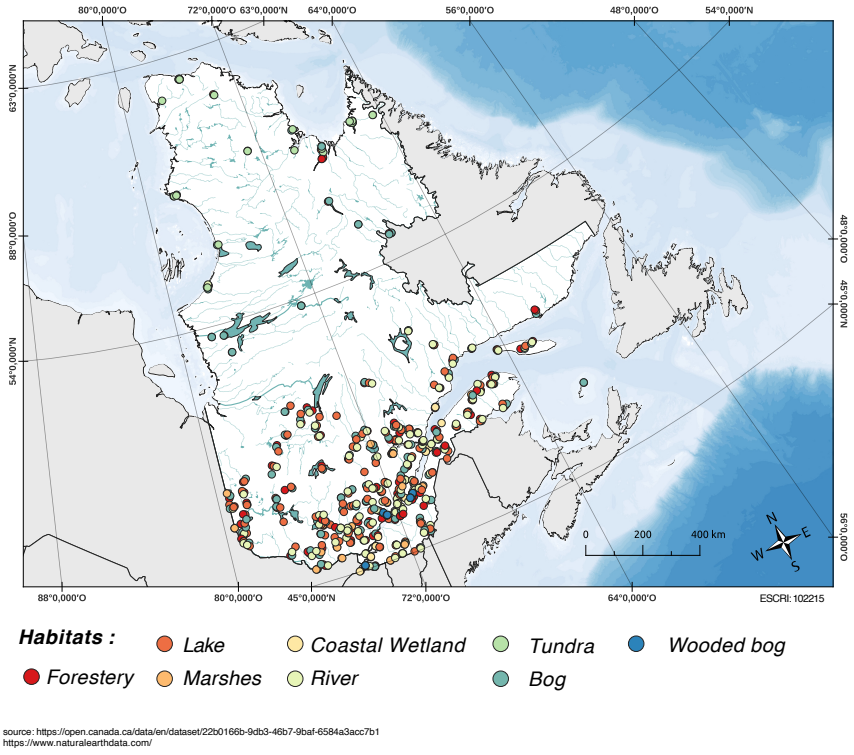


Figure 12: Map of the different positions of the Autonomous Recording Unit (ARU) in Québec.

canyon informations, the inter-canyon distance were computed using the QGIS tools.

The ocean variables, such as temperature of the sea surface in the Caribbean, were also downloaded from a public dataset called Copernicus [123] which offers an application programming interface (API) that allows registered users to download any data from their databases. Copernicus offer a total of 306 products that can be specified to an area, like Arctic Ocean, Baltic Sea or Mediterranean Sea. Their main products can be divided into two main parts, the *Analysis and Forecast* and the *Reanalysis*. The first one is based on model predictions and gives access to marine prevision up to 10 days, while the second integrates some observations, from satellite data or active buoys such as the buoys from the Argo program.

The Global Ocean Physics Analysis and Forecast has a grid of 0.083 degree, which correspond to approximately 8 kilometres and 50 vertical levels ranging from 0 to 5,500 metres. It covers the whole ocean and provides informations on daily sea water velocity (orientation and intensity using the Northward and Eastward components), the ocean mixed layer thickness, the sea water potential temperature as well as the sea water salinity and other parameters.

The Global Ocean Biogeochemistry Analysis and Forecast in another hand has a grid of 0.25 degree, which is less precise, but pro-

vide all the informations related to chlorophyll, like the mass concentration of chlorophyll-a in sea water or the net primary production of biomass expressed as carbon per unit volume in sea water.

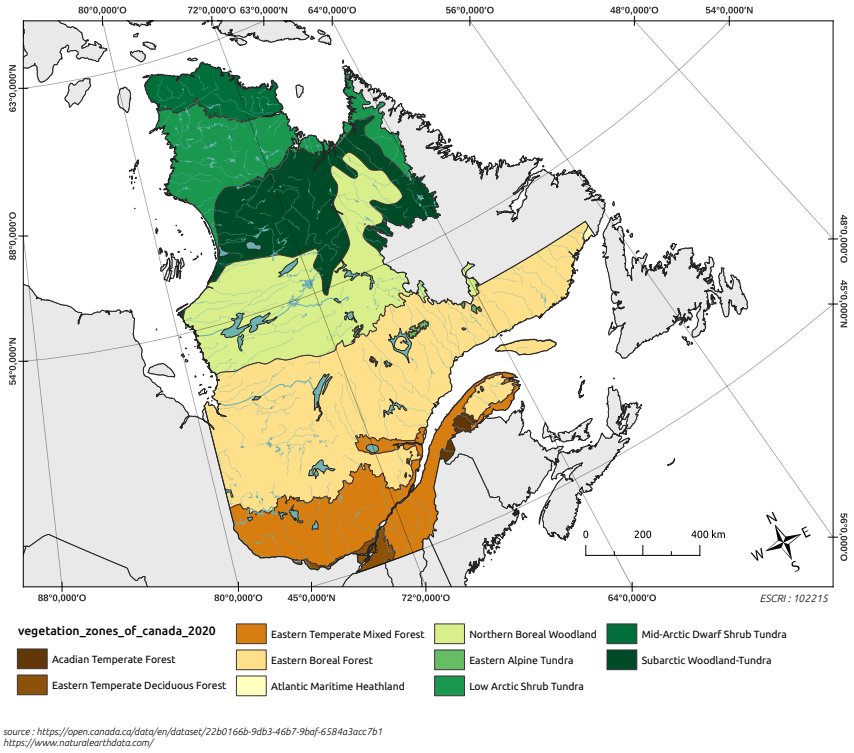
In order to analyse the anthropic impact, the boat density was extracted from the EMODnet Human Activities dataset [124] computed by the European services from 2018 and 2022. This dataset contains vessels density of twelve different macro categories of ship containing fishing, pleasure craft, passenger, cargo or tanker. These densities were calculated based on the Automatic Identification System (AIS) data available. These AIS data were collected for a total of 370,779 boats, and are downsample to 3 minutes and the resulted densities are split into twelve different files. Data from August 2022 were used in this work. As the purpose of the data in this thesis is to give an idea on the impact of the traffic density in term of collision risk, three different categories were created based on boat parameters such as their size and speed. The categories are detailed in the Table 4 and are - small and fast ship; large and "slow" ship; large and fast ships - where we consider the pleasure craft as small but fast, cargo and tanker as large but slow and finally the passenger ship as fast and large.

Table 4: Boat categories an macrocategories from EMODnet, associated to their average speed and sizes

Categories	Macrocategories	Speed (in knots)	Size (in m)
small and fast	pleasure craft	> 20	< 30
large and "slow"	cargo, tanker, tug and towing	<=20	>30
large and fast	passenger	> 20	> 30

3.4.2 *Terrestrial variables*

In order to analyse the vegetation role on the bird preferences in Canada, the Vegetation Zones of Canada [125] was downloaded. This dataset presents the different types of vegetation for the whole Canada with a precision of approximately 1:5 m to 1:10 m as showed in Figure 13. In this study, we analysed data from stations within distinct vegetations: Temperate, Boreal, and Arctic. The Temperate zone includes the Acadian Temperate Forest, Eastern Temperate Deciduous Forest, and Eastern Temperate Mixed Forest. The Boreal zone comprises the Eastern Boreal Forest and Northern Boreal Woodland, while the Arctic zone encompasses the Low Arctic Shrub Tundra, Mid-Arctic Dwarf Shrub Tundra, and Subarctic Woodland-Tundra. Recording sites sampled diverse biotopes, including marshes, tundra, forest and peatlands/bogs.



source : https://open.canada.ca/data/en/dataset/22b0166b-9db3-46b7-9baf-6584a3acc7b1
https://www.naturalearthdata.com/

Figure 13: Vegetation Zones of Canada in 2020 from [125] : This map highlights three different regions: the Temperature region in the south, the Boreal region in the centre of the country, and the Arctic region in the north of Québec.

Also, the Atmosphere datastore from Copernicus was used to download variables data such as daily temperature, wind (u - Eastward - and v - Northward - components) at 10 metres and the total precipitation. The temperature data were extracted from the EAC4 (ECMWF Atmospheric Composition Reanalysis 4) model, which provide 25 pressure level and a resolution of 0.75 x 0.75 degree every 3 hours while the wind and precipitation were extracted from the CAMS global atmospheric composition forecasts, which offer a precision of 0.4 x 0.4 degree.

Finally, the pvlib package [126] was used to obtain information regarding solar activity. Using this package allows access to solar parameters provided by multiple models, or data from satellites and ground stations. The data were downloaded every five minutes. The different phases were considered to be daylight when the sun's elevation was above 0°, civil twilight when the elevation was below 0° and above -6°, nautical twilight when the elevation was below -6° and above -12°, nautical twilight when the elevation was below -12° and above -18°, and night when the elevation was below -18°.

4

METHODS

4.1 Training and optimising a YOLOv5 model 38
4.1.1 Workflow 38
4.1.2 Annotation 40
4.1.3 Training 47
4.1.4 Active learning 48
4.2 BirdNET analysis 49
4.3 Transformer model 49
4.4 Maximising the scores by adjusting the detection threshold 50
4.4.1 Bird model 50
4.4.2 Humpback whale model 51
4.5 Post-processing the detections 51
4.5.1 Filtering and call density estimation 51
4.5.2 Humpback whale phrases reconstruction 52
4.6 Species Distribution Modelling (SDM) 52
4.6.1 Presence-only model 53
4.6.2 Presence-absence model 56
4.7 Cumulative Utilisation Impact (CUI) 59
4.8 Acoustic indices 60
4.9 Estimation of the Repertoire Sharing (RS) value for the Humpback whale 60
4.10 Statistical analysis 62

Key points

- The humpback whale vocal repertoire, comprising **23 distinct units with 2,957 annotations**, and the **27 bird species dataset with 29,795 annotations**, were meticulously annotated by hand using the Raven annotation tool;
- The **YOLOv5 architecture** was employed to facilitate the detection of species or units;
- The best model was used to predict the entire dataset, and the call density was estimated based on the number of detections per hour of recordings.

4.1 TRAINING AND OPTIMISING A YOLOV5 MODEL

Studying a species sound production at the level of the repertoire requires either the bibliography to determine the different types that compose the vocal repertoire, or to annotate different signal and use automatic processes in order to split them into different groups, as in [127, 128]. In this thesis, we first perform manual annotations and then use the literature to fit the different types to the existing literature.

4.1.1 *Workflow*

This thesis set out to develop a complete workflow for detecting species in acoustic data. In order to achieve this objective, a series of scripts were developed. The primary function of these scripts was to process the annotation. The secondary function of the scripts was to train an artificial neural network model. The third function of the scripts was to perform active learning based on the previously trained models. The workflow that as been developed is compatible with the Raven signal annotation tools [129] and the LabelMe image annotation tools. As presented in Figure 14, the use of Raven facilitates the annotation of the signal whilst enabling synchronous listening. Nonetheless, whether employing Raven or LabelMe, both systems provide annotations linked to a signal. These annotations are then addressed in the 'get_train_annot.py' file, as presented in the Figure 15 (green part). The function of this script is to extract the annotations, convert them into the YOLO format and subsequently divide them into a training set, a testing set and a validation set. In addition, it calculates the spectrograms and creates annotations files (txt files containing the label and the box coordinates).

The result of the script is a command that instructs the user to train the model with the train.py script from Yolov5, and a list of weights to add in the hyperparamters for each class in recommendation.

Following the validation of the model, the precision, recall, mAP@50 (i.e. mAP with an IoU of 50%), mAP@50-95 metrics, precision recall curve and F1 score as a function of the confidence curve for each class were obtained. The use of the model for the detection of new signals is then possible. For this, we adapted the original Yolov5 model in order to consider acoustics signal, processed with a short time Fourier transform (STFT) so that it is loaded as a spectrogram and then an image. Other scripts were also written in order to collect detections and re-adapt to the appropriate formats, as well as creating Raven annotation file to verify and correct it into the software (Figure 15 orange part).

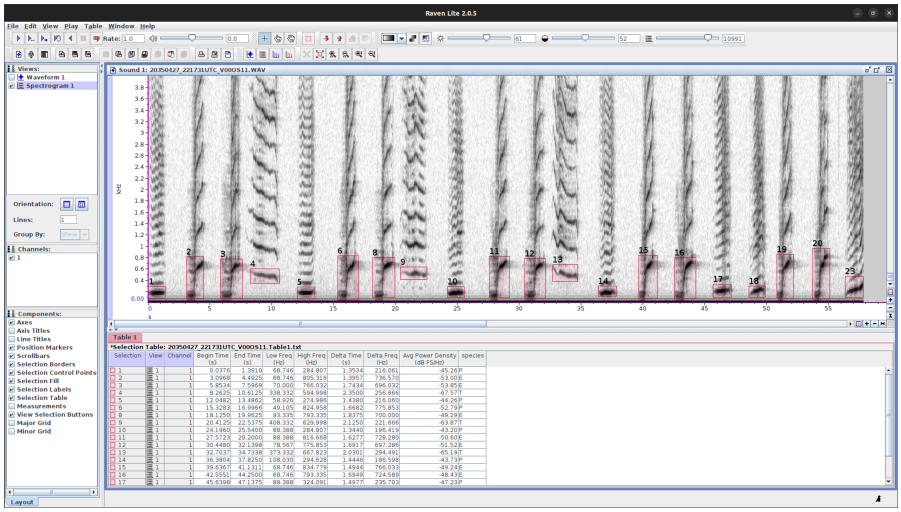


Figure 14: Example of a Raven annotation file with bounding box in red and relative information in the bottom table.

Contributions

A full workflow was made available in order to transpose Raven annotations into a format suited to train a YOLO model. This open source methods has already been used in multiple study, for detecting orca, fin whale, or dolphin vocalisations [130, 131].

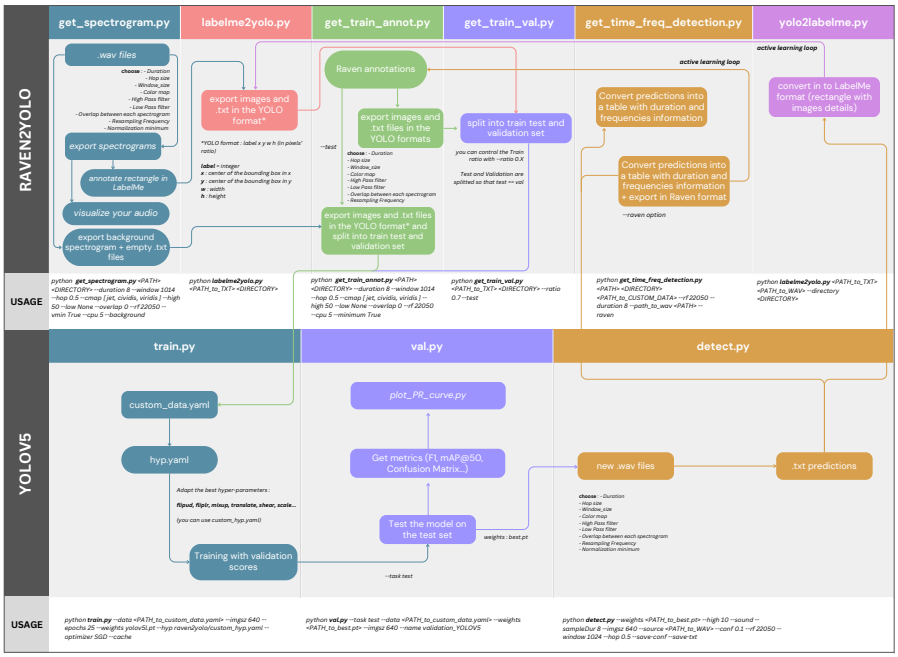


Figure 15: Workflow of the RAVEN2YOLO method

4.1.2 *Annotation*

4.1.2.1 *Humpback whale vocal repertoire*

To gather an initial set of ground truths to train an automatic units detector, we manually annotated a sample of 110 1-minute long recordings from 7 different stations (Figure 41). Specifically, 56 files were selected from 3 stations in Guadeloupe on different dates (from February 2021 to April 2022), 38 from Bermuda, 8 from Anguilla 5 from Saint-Barthélemy and 1 each from Sint Eustatius, Martinique Prêcheur and Saint-Martin, ensuring a large spatio-temporal coverage to reduce the probability of missing parts of the repertoire.

An important variability was observed in the annotated files, whether regarding the number of singing individuals, or their distance to the recorder. Each noticeable units was marked in time-frequency using the Raven software [129], resulting in a database of 2,957 calls amongst 23 units. The annotated units are made available in a public repository : here). We used published repertoires from different regions for class differentiation, such as the 3 main unit categories (low-frequency, mid-frequency and high-frequency) [132–134]. Additionally, around 1,500 8-seconds excerpts were added, comprising background noise and other signals that could cause false detection (*e.g.* human voices, boat sounds, bird songs, and other noises). Then, spectrograms were extracted from audio files at 8-second intervals, with a sampling rate of 13,000 Hz, applying a high-pass Butterworth filter (order 2 with a cut-off frequency of 40 Hz), and applying a short-term Fourier transform with a window of 1024 samples (0.078 s) and 50% overlap (0.039 s). The end of each files (which are exactly 58 seconds) were padded with noise from recordings without the presence of humpback whales to yield 8 contiguous 8-seconds chunks. The YOLO model necessitates square images; consequently, padding is added to the spectrogram when it is rectangular. However, if the spectrogram is excessively long and the image size is not optimised, the precision will be reduced because the resolution of the entire spectrogram will be low. The duration of the spectrograms was then determined by taking into consideration the approximate duration of units, which is approximately two seconds. In addition, the silence that occurs between one and two seconds was factored into this calculation, with the aim of ensuring that at least three units were included in each spectrogram.

The reported vocal repertoire for the North Atlantic humpback whale population during the breeding season is described in Table 5, with detailed characteristics such as duration, fundamental frequency characteristics, along with their associated name in the bibliography and each unit is represented in spectrograms in Figure 16. A letter was used to represent each individual unit, with an apostrophe being

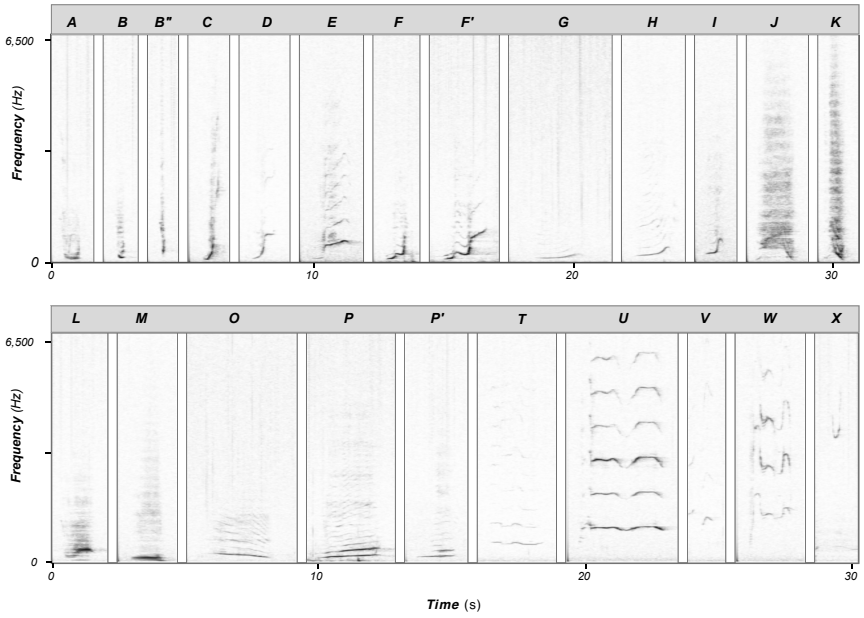


Figure 16: Spectrogram for each unit of the North Atlantic humpback whale's vocal repertoire on breeding grounds : The global spectrogram was generated using a Short-Term Fourier Transform (STFT), signals resampled at 13 kHz, 2048-point Hanning window and 1400-point overlap

placed after the letter when the type was found to be similar to the first unit associated with the letter, albeit shorter or longer.

Contributions

The vocal repertoire of the North Atlantic population during their breeding grounds has been the subject of only a very limited amount of documentation. This work has, however, contributed to **characterising and describing the repertoire of 2021**.

One of the primary outcomes of this work is the report of a vocal repertoire for the North Atlantic humpback whale population during the breeding season. By manually annotating sampled recordings, a total of 23 different units were identified, which are associated to humpback whale units described in previous studies. The spectrograms of each of these units are shown in Figure 16, with detailed characteristics reported in Table 5 such as duration, fundamental frequency characteristics, along with their associated name in the bibliography.

Organised into three main categories — low-frequency sounds, mid-frequency sounds and high-frequency sounds— [132, 134] the units in the repertoire have centre fundamental frequencies ranging from 90 Hz to 4,105 Hz, and their durations vary from 0.20 to 2.07 seconds.

Low-frequency units are characterised by an average frequency usually below 250 Hz [132, 134]. They typically last more than one second, and have a relatively low frequency modulation. For instance, one of the longest units in this repertoire, "oo" (unit P), has an average duration of 1.39 seconds (std: 0.42).

The mid-frequency category includes units with a low frequency modulation and an average frequency between 250 Hz and 600 Hz [132, 134]. To more precisely organise this repertoire, this category was then split into two sub-categories -pulsed and ascending sounds- [135, 136] and complex sounds [135]. Pulsed and ascending sound (B", C, D, E, F, F′ and G) are either very brief in duration, around one second, and have significant fluctuation between the initial and final frequency. The unit C is a prime example of this sub-category (Figure 16). Some of these units have a plateau, either in the middle of the unit (F, F′) or at the end (D, E). The complex sounds sub-category encompasses all continuous sounds that are usually longer than one second and contain complex frequency and/or amplitude modulation patterns.

The high-frequency category consists of units with an average frequency above 600 Hz [132, 134]. These units can be very short, such as the "repeated cries" (unit V : 0.37 s on average, std: 0.13), or as long as the longest unit in this repertoire, "long cries" (unit U : 2.07 s on average, std: 0.82). These high-frequency units are highly variable in form and frequency, which required their division into six classes. For example, units W and X are high-frequency, with centre frequencies above 2 kHz. The observed variations in the measurements, *i.e.* the high standard deviation values, can indeed be attributed to the scarcity of these units in the annotations.

As shown in Figure 17, applying a Uniform Manifold Approximation and Projection (UMAP) [139] technique to the minimum and maximum frequency and duration of each annotation and colouring by category (low, mid or high frequency) makes the separation of the categories visible in the representation. This finding confirms the accuracy of the annotations at this level.

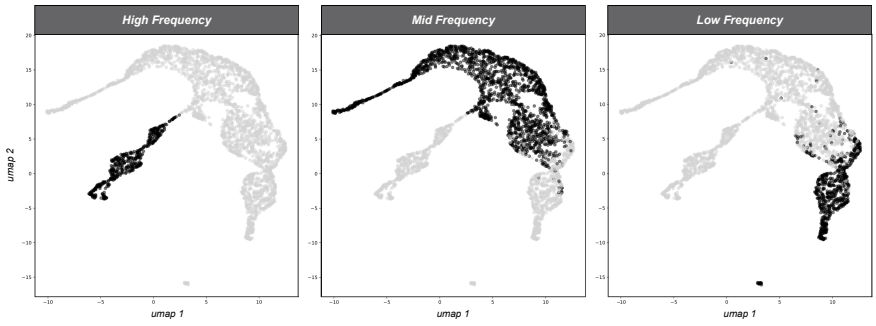


Figure 17: Representation of the humpback whale vocal repertoire categories using 2 dimension UMAP

Table 5: Mean lower, higher and centre frequency and duration of annotation in bold and their std : These characteristics were extracted from the Raven Annotation Tool. The centre frequency is calculated by taking the middle point between higher frequency and lower frequency. We reported previous studies that used the unit names with symbols (* for [134] in Caribbean Sea, ° for [136] in Northeastern Newfoundland, † for [133] in East Australia, ‡ for [137] in Hawaii Mexico, § for [135] in Southeast Alaska and □ for [138] in Norway).

Category	Unit	Name	duration (s)	Low Freq (Hz)	High Freq (Hz)	Center Freq. (Hz)
Low Freq.	A	snore *	**0.59** ± 0.14	**73** ± 36	**256** ± 109	163
	B	snore *	**0.21** ± 0.06	**93** ± 29	**263** ± 48	179
	L	snore *, scream †	**0.87** ± 0.23	**53** ± 57	**186** ± 156	119
	M	growl °§	**0.95** ± 0.24	**41** ± 17	**140** ± 35	90
	P	oo *	**1.39** ± 0.42	**98** ± 47	**285** ± 110	192
	P′	oo *	**0.98** ± 0.19	**104** ± 52	**236** ± 64	168
Mid Freq.	B"	snore *	**0.20** ± 0.04	**274** ± 64	**500** ± 87	390
pulsed and ascending	C	droplet ° □, bark †	**0.59** ± 0.21	**66** ± 36	**1,1120** ± 462	597
	D	droplet °, ouip □, bark †	**0.73** ± 0.25	**90** ± 63	**935** ± 142	531
	E	ascending shriek † fluct_3 □	**0.94** ± 0.37	**156** ± 138	**793** ± 83	499
	F	trumpet †	**0.56** ± 0.14	**97** ± 59	**986** ± 167	548
	F′	trumpet †	**1.04** ± 0.19	**186** ± 58	**823** ± 175	483
	G	snore *	**0.91** ± 0.30	**167** ± 40	**493** ± 86	333
Mid Freq.	H	reverse wo ‡	**1.38** ± 0.23	**174** ± 52	**496** ± 76	330
complex	I	wo *	**0.64** ± 0.13	**191** ± 33	**632** ± 94	417
	J	yelps †	**1.07** ± 0.37	**73** ± 49	**618** ± 168	358
	K	short yelps †, swop □	**0.68** ± 0.15	**76** ± 32	**722** ± 1289	399
	O	"descending" snore *	**0.96** ± 0.33	**188** ± 40	**444** ± 74	323
	T	waver *	**1.73** ± 0.50	**428** ± 44	**618** ± 72	527
High Freq.	U	long cries *	**2.07** ± 0.82	**814** ± 74	**1,022** ± 110	924
	V	"repeated" cries *	**0.37** ± 0.13	**1,090** ± 275	**1,556** ± 308	1,319
	W	cries ‡	**1.04** ± 0.37	**1,247** ± 361	**3,894** ± 915	2,598
	X	high cries	**0.64** ± 0.26	**3,128** ± 534	**5,827** ± 638	4,105

When looking at similar units, for example T and U or C and D on Figure 19, we observed that it can be sometimes difficult to differentiate both unit with just these three parameters. While U and T

are two distinct cluster, some units of the type D and C are mixing together. Indeed, it is imperative to acknowledge that a multitude of parameters, in addition to duration and the range of minimum and maximum frequencies, must be considered when identifying an unit. For instance, the number of inflection points is also an important feature in this type of analysis. However, to take the latter into consideration in automatic processes, contour analysis would be necessary, but it is difficult to process when there are overlapping signal, as is the case in these data. However, we also performed a Random Forest analysis on the annotations for background validation and obtained a score of 75% (see Figure 18 for the confusion between unit types), with the same observations as for the UMAP, such as the absence of important information, such as contour information.

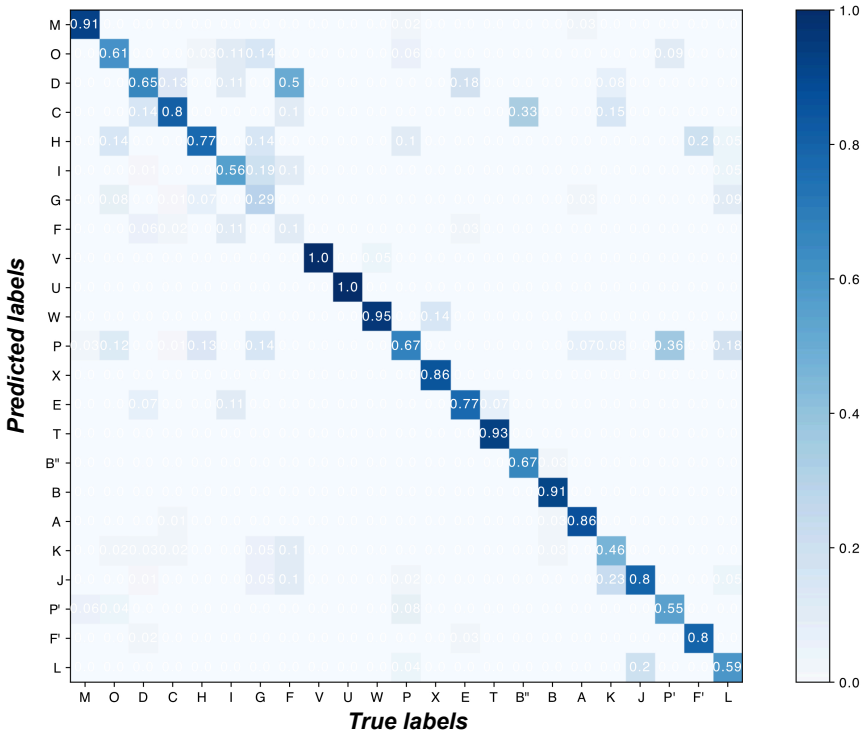


Figure 18: Random Forest confusion matrix over the 23 units of the humpback whale vocal repertoire. : The y-axis corresponds to the model's predictions, while the x-axis corresponds to the annotations.

To assess the quality of the annotated signals, the Signal-to-Noise Ratio (SNR) was computed. First, signal power was computed as the mean of squared waveform values after a 40 Hz high-pass filter within the annotated segments. Then, the mean noise power was extracted by performing the same calculations on noise segments between annotations. The SNR is then formulated as SNR $= 10 *$ $\log_{10}$(mean signal power/mean noise power). Annotated units had a

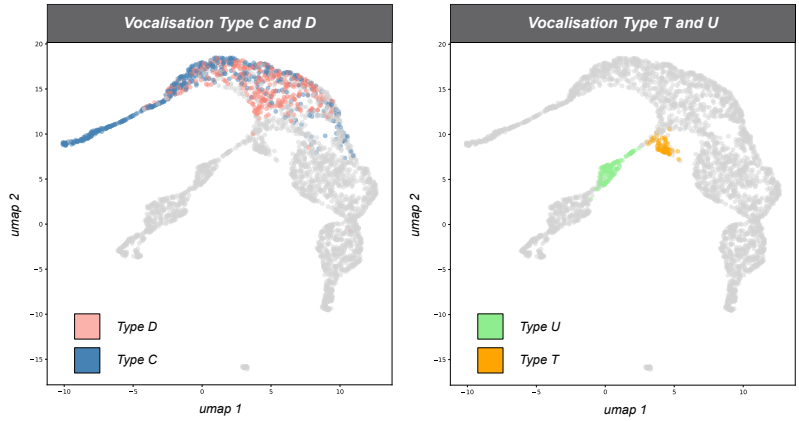


Figure 19: Representation of the humpback whale's vocal repertoire using two-dimensional UMAP : Units C and D are represented on the left, while T and U are on the right.

mean SNR of 9.9 ± 8.6 dB, including 16 files with average SNR under 2 dB and 44 files over 10 dB.

4.1.2.2 *Bird species catalogue*

With the aim of detecting the presence of several species in highly heterogeneous environments, this study focuses exclusively on the detection of bird songs from 27 different species presented in Table 6.

These species were chosen for their acoustic diversity and relative ease of recognition in audio recordings. Figure 20 shows the spectral representation of the sounds of the 27 species used for identification purposes. Annotations were performed on 34 files (approximately 22.5 hour of recording) from 22 different recording stations between May and June of 2021, 3 different habitat types (forests, bog and marshes), and at different times of the day (from 3:00 to 23:00) to obtain multiple levels of bird activity and choruses. A total of 29,795 annotations were made using the Raven annotation tool [129] and are available here. Particular attention was paid to annotating all song patterns for each of the selected species. Indeed, even in the case of strong overlap among several vocalisations, or low Signal to Noise Ratio (SNR), it is important that all vocalisations from the listed species are annotated, as the model will consider non-annotated songs as background noise. Unselected species were not annotated. As a result, they can be considered as noise for the model.

Then, to prepare the data for the model, audio were split into 15-second chunks with a sampling rate of 22,050 Hz, a window size of 1024 samples (0.046 s) and an overlap of 50% (0.023 s). Annotations that were located between two chunk of 15-seconds were kept only if they retain at least 20% of the signal. If the annotation is split into two parts, one of which is less than 20%, the smaller part is removed from the annotation set and thus from the training.

Table 6: Bird Species used in the model with their four-letters codes

Code	Scientific Name
alfl	Alder Flycatcher (*Empidonax alnorum*)
amre	American Redstart (*Setophaga ruticilla*)
blpw	Blackpoll Warbler (*Setophaga striata*)
btbw	Black-throated Blue Warbler (*Setophaga caerulescens*)
btnw	Black-throated Green Warbler (*Setophaga virens*)
coye	Common Yellowthroat (*Geothlypis trichas*)
gcki	Golden-crowned Kinglet (*Regulus satrapa*)
heth	Hermit Thrush (*Catharus guttatus*)
lisp	Lincoln's Sparrow (*Melospiza lincolnii*)
nawa	Nashville Warbler (*Oreothlypis ruficapilla*)
nopa	Northern Parula (*Setophaga americana*)
oven	Ovenbird (*Seiurus aurocapilla*)
rcki	Ruby-crowned Kinglet (*Regulus calendula*)
revi	Red-eyed Vireo (*Vireo olivaceus*)
rwbl	Red-winged Blackbird (*Agelaius phoeniceus*)
savs	Savannah Sparrow (*Passerculus sandwichensis*)
scta	Scarlet Tanager (*Piranga olivacea*)
sosp	Song Sparrow (*Melospiza melodia*)
swsp	Swamp Sparrow (*Melospiza georgiana*)
swth	Swainson's Thrush (*Catharus ustulatus*)
tewa	Tennessee Warbler (*Leiothlypis peregrina*)
veer	Veery (*Catharus fuscescens*)
wcsp	White-crowned Sparrow (*Zonotrichia leucophrys*)
wiwr	Winter Wren (*Troglodytes hiemalis*)
wtsp	White-throated Sparrow (*Zonotrichia albicollis*)
ybfl	Yellow-bellied Flycatcher (*Empidonax flaviventris*)
yrwa	Yellow-rumped Warbler (*Setophaga coronata*)

4.1.2.3 *External validation dataset*

To evaluate the bird model, we predicted species on 884 new 15-second recordings from the Biodiversity Monitoring Network of Québec. These recordings (available on this public repository) were annotated by experts according to the species identified in the recordings with

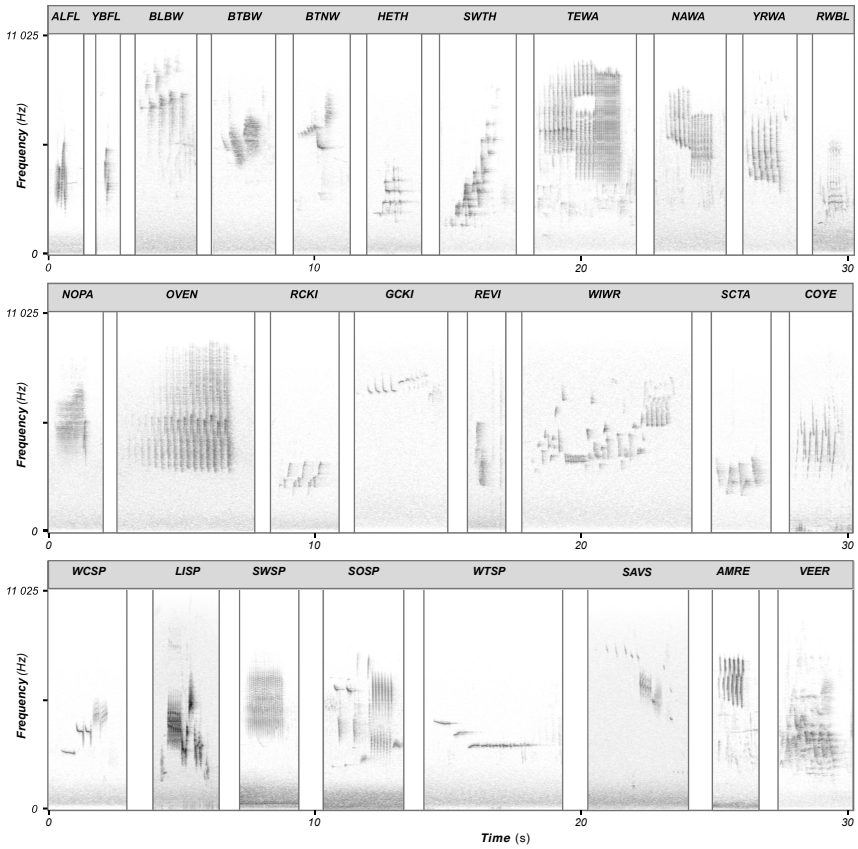


Figure 20: 27 bird species repertoire : All spectrograms were generated using a Short-Term Fourier Transform (STFT) (signals sampled at 22,050 Hz, 300 Hz High Pass filter, 9000 Hz Low Pass filter, 2048-point Hanning window and 90% overlap)

start and stop annotations (3,405 annotations). The files were recorded in 94 different sites, in different ecosystems and at different hours from 2016 to 2020. In addition, the annotator classifies the recording into 3 classes - good, medium and bad - according to the level of chorus in the recording (Figure 21), which will be used as low, mid, high in this work, with "high" for files with a high level of chorus. The distribution of chorus levels in this dataset was 348 low chorus, 277 mid chorus and 259 high chorus. The most annotated species in these recording was the White-throated Sparrow, *wtsp* (*Zonotrichia albicollis*) (476 annotations) and the species with the lowest number of annotation was the Yellow-bellied Flycatcher, *ybfl* (*Empidonax flaviventris*) (12 annotations) revealing an unbalanced dataset.

4.1.3 *Training*

The annotations that were produced, were then randomly split into three sets — training, validation and test — with a ratio of around 70:15:15. Validation data allowed us to track model performance after

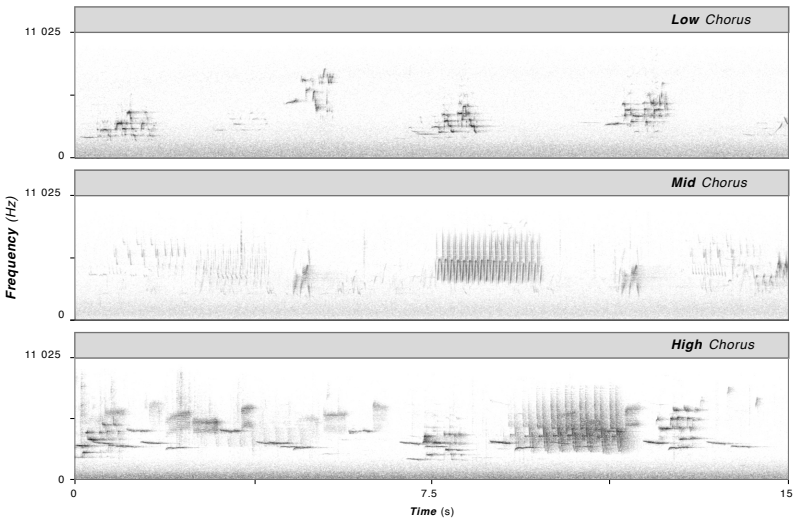


Figure 21: Representation of the different levels of Chorus : Top panel represents a low chorus, without overlap, the middle panel shows a mid chorus, with little overlap while the bottom panel represents a high chorus with much overlap.

each epoch, while the test set served as a benchmark post-training. The performances that outcome from the different sets, allowed us to choose the best settings amongst optimisers (SGD versus Adam), image size (640x480 versus 224x144 pixels), and data augmentations (mix-up, copy-paste), and other hyper-parameters. Some parameters from YOLOv5 were not modified for the different models. These include the learning rate, which was set as recommended depending on the optimiser (SGD=1E-2 and Adam=1E-3), and the OneCycle learning rate, which has a final learning rate of 0.1. Models were initialised with weights pre-trained on the COCO image dataset [140], and trained on NVIDIA A40 GPU. During and after training, performances were evaluated based on various metrics including precision, recall, area under the precision/recall curve (mean average precision at 50% and between 50% and 95% of intersection over union), and various loss metrics to optimise bounding box placement and predictions. The primary metric used for evaluation was mAP@50, as it combines multiple metrics and is less strict than mAP@50-95, which requires very precise boxes. However, for certain comparison, F-score were also important to consider.

4.1.4 *Active learning*

To obtain a better model with greater generalisation over new signals, it is important to add new training samples. However, as previously mentioned, manual annotation is time-consuming. Therefore, a method combining automatic detection and manual verification can be used. This method, called active learning, requires original annota-

tions and an already-trained model to predict over new signals. With the collected ground truth annotations, YOLOv5 models were trained to automatically detect humpback whale unit types for one and bird vocalisations for the other.

With the best performing models, we created new spectrograms from new audio files that are in the database, with the same parameters and predict using the models. YOLO predictions were converted into the appropriate format in order to import them in Raven. This enabled to verify them, and perform corrections if necessary (discarding a false detection, readjusting bounding boxes...). The new annotations that was manually verified were then used and another split was done to keep the ratios that was initially set. This step of active learning can be done multiple times in order to improve the learning of the model by correcting its previous errors and also adding variations in the class which will help the model to generalise. [1]

4.2 BIRDNET ANALYSIS

We evaluated our model based on the reference model BirdNET. We uploaded the V2.4 BirdNET Analyser [141] and used this model to predict species on each files of the validation set and the soundscape evaluation set. It is important to note that the model was used as proposed, meaning that no fine-tuning was done. Also, the geographical threshold was not applied to the detection, enabling the model to reduce the number of potential species in the prediction based on geographical information. This decision was made because this threshold is based on what is already known about the species' habits, and is therefore not applicable to all species. After retrieving all the predictions made every 3 seconds (with a confidence threshold set to 0), we removed the predictions from other species that are not in our 27 species list. After that, we kept the predictions made over the 15-second audio by grouping the five 3-second chunks. It resulted in a BirdNET prediction of the species present in each 15-second files for both datasets.

4.3 TRANSFORMER MODEL

In order to facilitate a comparison of the detection scores from YOLO, a transformer architecture, originally designed for click detection, was utilised. As illustrated in Figure 22, the model under consideration features an Encoder-Only architecture with 8 heads and 8 blocks, and takes a Short-Term Fourier Transform (STFT) as input. The model's optimiser is an AdamW, its loss is a binary cross-entropy (BCE) loss, and it contains 2.2 million parameters. The model was

1 The necessary code for adapting Raven annotations to the YOLOv5 format and training the model is documented and available at: raven2yolo.

trained on the same training set and evaluated on the same recordings as YOLO [**Ferre_etal_2026**].

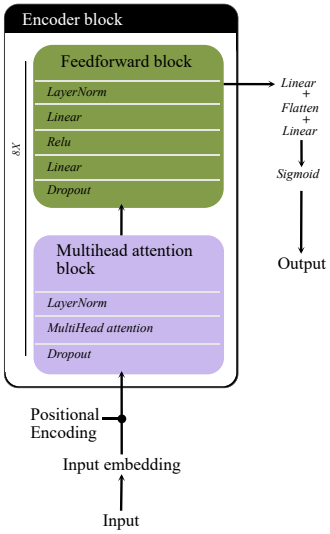


Figure 22: Transformer Encoder-Only Architecture

4.4 MAXIMISING THE SCORES BY ADJUSTING THE DETECTION THRESHOLD

4.4.1 *Bird model*

From our bird model, we obtained boxes around the detections with a confidence threshold and an associated class. From BirdNET, we obtained predictions associated with a confidence threshold, but for 3-second chunks. In order to compare the two models, we verified the presence of the species annotated by the expert, in the models' predictions. The average precision scores, micro, macro and weighted were computed using the scikit-learn average_precision_score function [142] on the 884 files soundscape dataset. In order to improve both results, we computed the Receiver Operating Characteristic (ROC) curve and associated Area Under Curve (AUC) for each species, both our model and BirdNET to find the optimum threshold to fix, on the validation set. This threshold will be used to determine whether a detection is considered positive (if above) or negative (if below). From this, we created 3 different scenarios based on the True Positive Rate (TPR) : 0.1; 0.5; 0.9; which resulted on a threshold value per class as presented in Table 14. In order to provide greater clarity regarding these scenarios, given the heterogeneity of the study's objective, it is necessary to determine whether the selection of a model is to be made on the basis of its high precision, which would result in a species never being confused, but at the cost of reduced recall, or a model that occasionally confuses but consistently detects signals,

which would result in lower precision but higher recall. In the first scenario, TPR 0.1, the model misses ten times more signals than it correctly predicts, resulting in low recall. In the second scenario, TPR 0.5, the model misses the same number of signals as it correctly detects, aiming to combine high recall and high precision. In the final scenario, TPR 0.9, the model almost misses all vocalisations, resulting in high recall. With these adapted threshold, we then measured the precision, recall, F1-score and the F05-score (which gives more weights on precision than recall compared to F1-score) for each model in different chorus level and for each scenario on the 884 files evaluation dataset.

4.4.2 *Humpback whale model*

For the Humpback whale model, we also adapted the threshold for each unit type based on the F1 score curve. Through the observation of precision and recall as a function of confidence, we noticed that the edges between 0 and 0.1 and between 0.8 and 1 had significant variability, with high recall but very low precision or conversely. We therefore constrained optimal confidence thresholds between 0.1 and 0.8 to ensure more reliable detection for each class. By cutting at the maximum F1 between these two part, we then found the optimal threshold for each type, that will be applied after the detection, as a filter of false positives.

4.5 POST-PROCESSING THE DETECTIONS

4.5.1 *Filtering and call density estimation*

The first part of the analysis after obtaining the YOLO predictions over new files consists in measuring the number of units detected in the recording, and make these results comparable between different stations. As some of the detections are false alarm, the choice has been done to remove all detections that are under the fixed threshold estimated with the methodology explained before. Then, for humpback whale only, to avoid counting false or sporadic detections, we discard files with less than 3 detections (a song typically contains an unit at least every 6 seconds, making about 10 detections per file). With regard to avian species, all detections were retained, as the purpose of this protocol is to detect birds during their migratory patterns. Even sporadic detections are of significance. Then, to account for recording effort variation across stations, we normalised the detection count by the number of recorded hour, and report this normalised detection rate per week. For the analysis of humpback whale presence, we considered weeks with a detection rate lower than 7 (*i.e.* comprising less

than 196 units in total), to be weeks with no humpback whale presence, so they were removed for future analysis.

4.5.2 *Humpback whale phrases reconstruction*

In order to analyse the repetition of each unit and, more particularly, to reconstruct the phrases, a filter is applied at the level of the recording. Initially, in order to filter recordings with multiple singers, all files containing at least two units with less than 0.5 seconds of silence are removed. The process is designed to eliminate files that have been identified as having overlapping detections. Consequently, it ensures that only files that have been accurately identified as clean are retained. Secondly, all units are aligned into the recording, and a symbol is added between each units depending on the time between both – one symbol for at least one second, two symbols for at least two seconds, and three symbols for at least three seconds – which results in a list of units for the entire duration of the recording file. In order to facilitate the visualisation of the different phrases, the recordings are then arranged in accordance with the date of recording. The initial 60 recordings are then presented in a colour-coded manner, with each unit type represented by a specific colour and letter. As a visual representation is provided, a statistical measure is also obtained by means of a method of enumeration, whereby the frequency of occurrence of each phrase is determined. In order to accomplish this, we used phrases of varying sizes, ranging from 5 to 12 entries, with the acknowledgement that silence constitutes a component of the analysis. These phrases are designated as 'kernels' within the context of this process. The kernel then convolves over the list of units (with a step of 1) to ascertain the frequency with which each pattern occurs. Following the convolution process, a comparison is made between all the different patterns. These are then ranked according to their frequency, with the result that the most frequently used patterns are identified.

4.6 SPECIES DISTRIBUTION MODELLING (SDM)

Modelling the habitat or distribution of a species requires a lot of parameters and can be difficult for scarce species. Species distribution modelling (SDM) is a tool that can be used to understand the parameters preferred by a species. SDM can then be used to analyse how a species' distribution will change in response to changes in these parameters. The models under consideration can be divided into two main groups: the presence-only models, which require observations to operate; and the presence-absence models, which necessitates observations and absence of a species in a specific location

to align with the model. The presence-only MaxEnt model and the presence-absence model GAM were used in this thesis.

4.6.1 *Presence-only model*

MaxEnt is a software [143] that relies on maximum entropy and machine learning techniques. The MaxENT process is based on the presence of the target species and the environmental parameters of a defined area. It is from these two components that the algorithm randomly selects 10,000 background points (pseudo absence) in order to capture the full environment parameter distribution. The model is then trained with the aim of finding the most spread-out distribution, or closest to uniform, throughout the study region while meeting the constraint of matching the real observations given to the model. The evaluation of the models is made using the area under the curve (AUC) on the receiver operating characteristic (ROC) curve, similar to the method employed for machine learning. Indeed, the objective is to measure the sensitivity (1 - omission rate) as a function of the fraction of the total study area predicted to be present (1 - specificity). The omission rate is measured using different thresholds, with the prediction of the map and the area that will be over or under that threshold.

In order to predict the habitat suitability of the sperm whale, we used our visual observations and different environmental variables as described in Table 7. As the model requires a specific region with standardised data, environmental data was sampled for all the subregions of the Mediterranean Sea and Black Sea Figure 10 characterised by a rectangle extending from longitude 0.04° to 30.3° and latitude between 41.71°N and 47.3°N. As the model requires different environmental parameters, multiple layers were prepared for this area, and the data was oversampled to correspond to 0.083 x 0.083 deg using QGIS tools.

The primary objective of the L181 mission was to identify sperm whales. Thus, our observations were biased towards the area, as we were in an area where their presence had been definitively confirmed, rather than following a specific transect [146]. To this end, we have developed a bias layer for the MaxENT models. In order to accomplish this objective, a compilation of all GPS positions obtained from different missions was undertaken, subsequently leading to the generation of a density raster encompassing a spatial extent of 0.083 x 0.083 degrees. The squares that were not sampled have been assigned a value of 0.002, while the squares that were sampled have been normalised to a maximum value of 1 as recommanded from previous study [147]. The bias layer was subsequently incorporated into each MaxENT model.

Table 7: Environmental variables and their interest for the model of the sperm whale in the Mediterranean : The sources of the parameters corresponds to : A : GEBCO [120]; B : Geomorphology of the oceans [122]; C : Global Ocean Physics Analysis and Forecast model [123], cmems_mod_glo_phy_anfc; D : Global Ocean Biogeochemistry Analysis and Forecast model [123] cmems_mod_glo_bgc-bio_anfc.

Group	Environmental variable	Original resolution in degree	Final resolution in degree	Source	Justification from [144, 145]
Static parameters	Depth (m)	0.004	0.083	A	Sperm whale feed on squids and fish that live in the deep water
	Roughness	0.004	0.083	A	High roughness indicates a large escarpment and greater prey richness
	Slope (°)	0.004	0.083	A	Associated with currents, high slope induce prey aggregation or enhanced primary production
	Distance to canyons	0.0083	0.083	B	Canyons are suitable for deep diver as it contains all the favourable parameter
Dynamic parameters	Sea surface temperature (SST) (°C)	0.083	0.083	C	Reveal front locations, potentially associated with prey aggregations
	Temperature at 600m (°C)	0.083	0.083	C	-
	Temperature gradient (°C)	0.083	0.083	C	-
	Salinity	0.083	0.083	C	-
	Mixed Layer depth (m)	0.083	0.083	C	Proxy of prey availability
	SSH (m)	0.083	0.083	C	High SSH is associated with high mesoscale activity and enhanced prey aggregation or primary production
	Net Primary Production	0.25	0.083	D	Proxy of prey availability
	Surface O_2 concentration	0.25	0.083	D	-
	O_2 concentration at 600m	0.25	0.083	D	-
	Surface current	0.083	0.083	C	Strong currents induce the mixing of waters and aggregation of prey

The variable environmental parameters, including sea surface temperature (SST), salinity, surface current intensity, sea surface height (SSH), mixed layer and dissolved oxygen, were compiled and averaged from the record between 2022 and 2025, encompassing the period from May to October, to align with the data observation period. The data regarding dissolved oxygen and temperature were divided into two segments: the first corresponding to the surface, and the second corresponding to a depth of 600 metres.

The execution of a MaxENT model can be undertaken in two distinct ways: the first option involves the operation of the model with all parameters, whereas the second option entails the optimisation of the model through the selection of the most effective parameters. In the ensuing experiment, both methods were implemented: firstly, all fixed parameters were used, and subsequently, a second model was executed with all parameters (fixed and dynamic). In a second experiment, in order to ascertain the most significant variables for predicting sperm whale habitat suitability using MaxEnt, two different methods were used. The initial approach involves the use of our observation dataset, with 75% of the observations allocated for training and the remaining 25% designated for testing the model's predictions. With this final metric, it is feasible to introduce numerous variables individually and to try the AUC optimisation that ensues from the training and testing processes. The second method involves the use of 100% of the observations, followed by the employment of the OBIS dataset as a test. In both experiments, the initial step was to compute a MaxENT model with only the fixed variable. The resultant data from both models provides insight into the contribution of each fixed parameter over the OBIS dataset or our observations. Subsequently, the same model is run with a dynamic parameter, with every possible combination being attempted. The result of this can indicate which parameter adds information and contributes to a better prediction. If the parameter is found to increase the AUC by 0.1%, it is retained for the subsequent stage of the process; otherwise, it is excluded. The same method is repeated by adding another dynamic parameter, until the model showed no further improvement in terms of the area under the curve in the test set.

It should be noted that a single detail is distinguishable from the comparison derived from the OBIS dataset. This distinction arises from the fact that, in the context of the OBIS dataset, the K-fold method was employed as a test, whereby the training dataset is divided into K segments, with each segment being replicated ten times. This approach is undertaken to prevent the occurrence of training bias or dependence on the dataset. Thanks to the use of a variety of models, a range of maps is obtained in addition to AUC performance values, facilitating their comparisons.

4.6.2 *Presence-absence model*

Generalised Additive Model (GAM) is another method for modelling complex phenomena resulting from various parameters, including modelling species absences and presence in SDM contexts. It is a regression-based techniques but with a non-linear representation. It relies on the use of splines, which correspond to multiple functions that are adjusting on each parameter. The sum of many splines forms a GAM that can then be applied to new data and presented in Figure 23. The resulting Akaike's Information Criterion (AIC) value corresponds to the likelihood of the model to fit to the data. However, it should be noted that this is only applicable in instances where the data are comparable and only the model parameters are subject to modification. The R2 value is also an indicator of the model's fit over the data. Furthermore, the GAM models produces results with effective degrees of freedom (EDoF) for each parameter. This provides information regarding the importance of each parameter, as well as indicating its statistical significance.

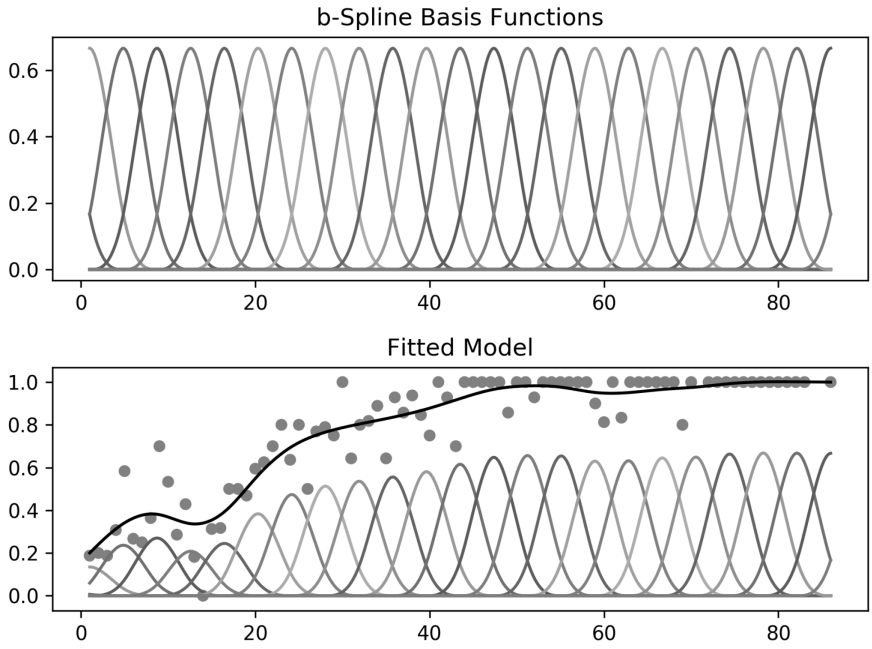


Figure 23: Representation of the splines that make up the Generalised Additive Model (GAM) (top), and the fitted model representation (bottom) : The figure is extracted from pyGAM [148].

In this thesis, we used Generalised Additive Models (GAMs) from the pygam package in Python [148], to model the presence of humpback whales and avian species in Québec. Given that the model under consideration is of a presence-absence type, the standardised data presented above were used for the purpose of performing the model. For birds and humpback whales, the GAM model was made using

the detection per hour of recording average per weeks, along with the corresponding environment variable mean for that specific week. For whales, it is established that Bermuda does not serve as a breeding ground; rather, it functions as a seasonal stopover site. Consequently, Bermuda was excluded from the data observations. The environmental parameters that were retained for the humpback whale in the model comprised surface salinity, sea surface temperature, mixed layer depth and chlorophyll-a concentration as presented in Table 8. The methodology employed for the avian study involved the use of total precipitation, temperature, and the two components of wind to ascertain wind intensity (Table 9. Furthermore, the photo period and the altitude of each station were considered.

Table 8: Environmental variables and their interest for humpback whale : The sources of the parameters corresponds to : A : GEBCO [120]; C : Global Ocean Physics Analysis and Forecast model [123], cmems_mod_glo_phy_anfc; D : Global Ocean Biogeochemistry Analysis and Forecast model [123] cmems_mod_glo_bgc-bio_anfc.

Group	Environmental variable	Original resolution in degree	Final resolution in degree	Source	Justification
Static parameters	Distance to 5,000 meters depth (m)	0.004	0.083	A	Deep water could be used by male for sound propagation [149]
	Distance to shore	0.004	0.083	A	Closer to shore can offer more stability in the environment and protection for mother and calves
Dynamic parameters	Sea surface temperature (SST) (°C)	0.083	0.083	C	Humpback whale have already shown negative relationship to sea surface temperature
	Salinity	0.083	0.083	C	Reveal slight variations in marine parameters
	Mixed Layer depth (m)	0.083	0.083	C	Can play a role in sound propagation
	Chlorophyll-a	0.25	0.083	D	Proxy of prey availability

With regards to humpback whales, the propagation of sound from the source to a considerable distance is well documented. In addition, the positioning of the stations is known with a high degree of certainty, but the position of the singer is not. This presents a challenge to analyse the effect of fixed parameters. Hence, the decision was taken to remove any fixed parameter, such as depth or roughness when creating a GAM model for whale. To execute a GAM model, it is first possible to compute the model using only a parameter as splines, given that the data are not linear, in order to ascertain the appropriate distribution between linear, binomial, Poisson and gamma distributions. In the Caribbean context, the humpback whale model was constructed using four parameters based on a linear regression distribution. The number of iterations was fixed at 500. The model

was developed by adding each parameter in turn, as illustrated below:

$$GAM = LinearGAM(s(0) + s(1) + s(2) + s(3)).fit(X, y) \quad (9)$$

with s(0) defined as temperature, s(1) salinity, s(2) for chlorophyll-a concentration, and s(3) for the mixed layer depth while y is the detections associated to each X line.

Following the evaluation of the humpback whale model, it was used for the purpose of predicting new data. In order to accomplish this objective, the daily values of the parameters were used over an area extending from 1.5° S to 51.75° N and from 48.25° W to 87° W.

A similar process was conducted for birds as we obtain the weekly mean call rate for each weeks, years and at different latitudes (from 45 to 62°N). Then, associated with these detections, we used the mean temperature over that same latitude as well as the total precipitation, and the wind speed as presented in Table 9. Using the same linear regression distribution, we computed the models and used the results to adapt and add or remove parameters. Finally, the same process was performed for each species of the survey in order to analyse specific preferences.

Table 9: Environmental variables and their interest for birds : The sources of the parameters corresponds to : A : GEBCO [120]; E : Natural Resources Canada [125] ; F : ECMWF Atmospheric Composition Reanalysis 4 [150] ; G : pvlib-python [126]

Group	Environmental variable	Original resolution in degree	Final resolution in degree	Source	Justification
Static parameters	Altitude	0.004	0.083	A	Impact the vegetation distribution
	Latitude	0.004	0.083		Higher latitudes are indicative of extended migratory patterns and more inhospitable environmental conditions
	Habitat composition	0.004	0.083	E	Certain species may demonstrate a marked preference for a particular type of forest or general habitat type
Dynamic parameters	Temperature (°C)	0.083	0.083	F	Reveal the seasonal changes
	Wind intensity (m/s)	0.083	0.083	F	Can affect migration
	Total precipitation (cm)	0.083	0.083	F	May have a masking effect on communication
	Elevation of the Sun	0.25	0.083	G	Linked to photo period, which is key to migration

4.7 CUMULATIVE UTILISATION IMPACT (CUI)

In order to evaluate the impact of boat traffic on sperm whales, the different categories of boat were presented above, based on the AIS data collected. Following [151], a log transform was applied on the normalised values of the densities (between 0 and 1). Following the oversampling of the map to the same grid size as the model, the level of risk for each category was estimated based on the table proposed by Maxwell et al. [151]. The passenger categories, which include ferries, are defined as large boats with a high level of speed and the capacity to adjust their trajectory to a medium extent. The risk associated with this phenomenon was assessed to be of moderate severity, with a rating of 12 out of 20 presented in Table 10.

Table 10: Boat categories and their associated impact values on the sperm whale population, along with the final CUI impact.

Categories	Frequency /4	Direct /Indirect impact /3	Resistance (Likelihood of mortality) /3	Recovery time of individual (years) /4	Reproductive Impacts /3	Population Effects /3	Total /20
small and fast	3	3	1	1	1	1	**10**
large and "slow"	2	3	2	1	3	1	**12**
large and fast	2	3	2	1	3	1	**12**

The presence of these vessels is notable, though not to the same extent as the estimated frequency of pleasure craft. For all three categories, the level of impact was estimated to be 3 out of 3, as it is a direct impact on the animal and can lead to mortality. Nevertheless, as previously stated, certain vessels possess the capacity to modify their trajectory to a greater extent, thereby yielding disparate outcomes with regard to their reproductive impact. For instance, the value of smaller vessels such as pleasure craft is assigned a value of 1 out of 3. This is due to the fact that they have the capacity to impact certain aspects, such as disturbance. However, they are less likely to result in fatalities, in contrast to larger vessels. A comprehensive evaluation of all pertinent factors reveals that the pleasure craft possess a value of impact that has been designated as 10 out of 20. In contrast, the cargo and other merchandise transporters, which are of a larger nature but characterised by reduced velocity, have been assigned a value of 12.

Using Eq.10 facilitates the identification of the potential area where the risk is elevated, contingent on the categorisation of the vessels, but also in a general sense. In this study, the cumulative utilisation impact value for each pixel is calculated, thus delineating the "danger" area where there is a higher probability of a collision between a ship and a sperm whale.

$$CUI = \sum_{i=1}^{n} \sum_{j=1}^{m} D_i * S_j * u_{ij} \tag{10}$$

where D_i is the normalised between 0 and 1 log-transformed value of intensity of an anthropogenic impact for a pixel i, S_j is the probability distribution of species j from MaxENT model for that same pixel and u_i, j is the weight from the impact i to the species j as presented in [151] and similar to [152]. In the present study, the impact corresponded to the intensity of boat traffic from each categories, which were then normalised collectively.

4.8 ACOUSTIC INDICES

Where the primary objective of a study does not involve the collection of information on the species recorded, acoustic indices can be used to obtain a proxy for avian diversity or to estimate the impact of anthropogenic activities. To do so, the module sound from maad was used and the ACI, NDSI, H, ADI, and BI indices were computed. These measures were made on full audio and full frequency band, except for the AEI and ADI which were computed over the 0 to 20 kHz frequency band.

Acoustic indices can also be the number of Region of Interest (nROI) present in a signal [29]. We then compute the nROI, which is also used as a proxy of the bird species richness [153] in a recording. To do so, we used the scikit-maad package over all the evaluation soundscape dataset. The validity of this dataset is ensured by the fact that it was annotated by experts and not used for training purposes. This guarantees a correct comparison. The maximum dB value was set to 96 (which is the default value) and we then summed the number of ROI for each files. To compare the result of nROI with the true number of species into the recording, *i.e.* the species richness, we used the annotations from specialists and count the total of different species identified (part of the 27 species dataset and other species that has been identified).

4.9 ESTIMATION OF THE REPERTOIRE SHARING (RS) VALUE FOR THE HUMPBACK WHALE

As the purpose was to analyse the evolution of the vocal repertoire throughout the breeding season, we tried to estimate the resemblance

between two repertoires. Grouping detections by recording weeks and stations allowed us to generate call type distributions and characterise vocal repertoire usage at a given place and time. Across weeks and stations, vocal repertoire usage can then be compared using the Jaccard index, also known as the Repertoire Sharing (RS) [154]. This measure is formulated by Eq.11, where A and B are unit type distributions each at specific times / places, $|A \cap B|$ represents the number of shared vocal units between A and B, and $|A \cup B|$ represents the total number of vocal units in both.

$$RS(A, B) = \frac{|A \cap B|}{|A \cup B|}. \tag{11}$$

Such index allows us to estimate the similarity between songs produced at different times / places (the higher the index, the higher the similarity). We use this as a proxy to unveil time / places with more or less song variation. Firstly, in order to study how song evolves over time we compute the average weekly RS value (calculated by measuring the RS per recording day) of every active station pair. This yields a distribution of RS values per week, a high distribution indicating similar repertoire usage across the Caribbean region, and hence a low level of local song variations during that week.

However, preliminary analyses showed that the RS is affected by the recording effort and the number of active stations. To compensate for this, for each day, we sample 3 stations and 92 units (4 times the size of the vocal repertoire) which were picked equitably between each station. We then compute RS values between each station pairs, and repeat this process a 100 times to yield standardised trends of cross-station similarity (the curve was not correlated with recording effort, Pearson r = -0.37, p-value >0.5). We applied this procedure to the days between 9 February and 5 May 2021, smoothing the resulting curve with a rolling 7-day average. The slope between each day then allows us to test whether there are particular phases of innovation during the breeding season. As the most frequently detected unit, unit D, was measured in almost all weeks at all stations over the course of the year, it was removed from that particular analysis. The reason for this is that it accounts for 50% of the detections and thereby impacts the random sampling and RS evaluation, damping its evolution over time.

In a secondary analysis, to get a sense of how song innovation might be distributed through space, the RS between consecutive weeks of each station was computed (week n and week n+1 pairs, yielding a distribution of RS values per station). Here, a high distribution of RS values indicates a low amount of variations in that station (repertoire usage was similar between each consecutive week).

4.10 STATISTICAL ANALYSIS

A range of methodologies were employed in order to verify the significance of the results obtained in this study. Firstly, in order to verify significant results, the Pearson test was performed using the SciPy package [155]. With regard to the nROI analysis, the use of Spearman from the same package was implemented. In addition, in order to ascertain whether the presence of recording stations had a significant impact on RS for humpback whale analysis across consecutive weeks, the Kruskal-Wallis H test was used from R Studio [156].

Subsequently, as the RS across space seemed to be impacted by weeks, we attempted to describe its evolution with temporal models. In order to verify the hypothesis concerning the two modes, we first performed a piecewise linear regression of RS values, with one part from early February to late April, and another from mid-April to mid-May. The R^2 and p-value of each curve were measured using the Pearson method, available in the SciPy package [155]. Furthermore, local slopes were computed, and slope distribution of the two parts were compared using the Mann-Whitney U test. As the RS curve contains an almost complete absence of data between weeks 12 and 14, the initial statistical analysis was conducted using two sets : slopes between weeks 6 and 12, and the slopes between weeks 14 and 17. The same test was performed to compare slopes from week 6 to 14 with those from week 14 to 17. The Cohen's d was estimated by dividing the difference of the mean of each slope distribution by the standard deviation of the data.

5

DETECTION AND CLASSIFICATION

5.1 A YOLOv5 model on 23 different units for Humpback whale . . . 64
5.1.1 Generalisation of the model . . . 67
5.1.2 Comparison to another architecture . . . 68
5.2 A YOLOv5 model on 27 bird species . . . 71
5.2.1 Bird model evaluation . . . 71
5.2.2 Comparision to BirdNET . . . 75
5.3 Comparing the box detection to nROI index for bird species richness estimation . . . 78
5.4 Discussion . . . 80
5.4.1 Humpback whale model scores . . . 80
5.4.2 Birds model scores and comparison with BirdNET 81
5.4.3 Importance of the confidence threshold adjustment . . . 82
5.4.4 Improvement in detection in high chorus level . 83
5.4.5 Box detection for analysis . . . 84
5.4.6 Difficulties and bias . . . 85

The objective of this chapter is firstly to report on the metrics obtained by the two models, humpback whale and birds. Secondly, it is to compare the results with existing state-of-the-art in order to evaluate the model and ascertain the extent to which this thesis contributes to the development of neural network use in bioacoustics. The two models we developed for species detection were made using the YOLOv5 architecture. This model predict bounding boxes based on the training data, such as presented in Figure 24 for bird vocalisations. With these predictions and the confidence threshold that is assigned to a box, we were able to compute metrics and then compare to the literature.

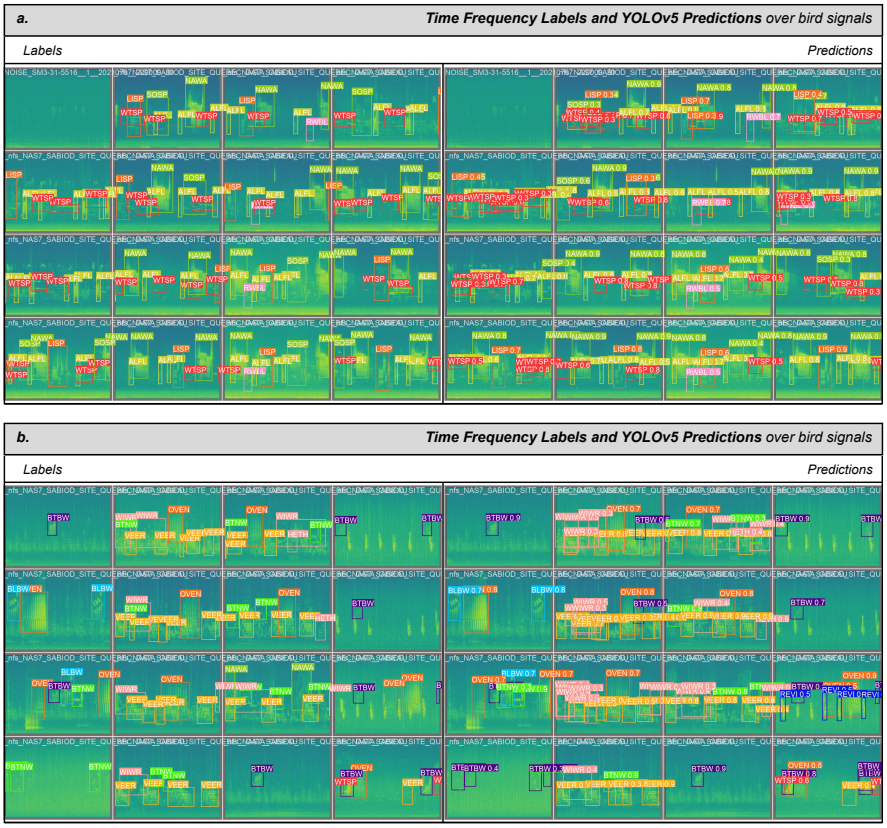


Figure 24: Example of the labels given to our model and the resulting predictions with their associated confidence score on bird chorus.

5.1 A YOLOV5 MODEL ON 23 DIFFERENT UNITS FOR HUMPBACK WHALE

Key points

- **The optimal YOLOv5 model for humpback whale** was determined to be the 'large' model architecture, SGD optimiser, image size of 640, batch size of 64 and personalised weights per class, achieving a **mAP@50 of 74%**;
- The model's predictions indicate a degree of confusion between similar and under-represented units, yet a **relatively low level of confusion between units** on a global scale;
- The model demonstrated the capacity to predict humpback whale vocalisations from various years, locations and populations. However, there was a notable level of low confidence and high confusion in unit allocation;
- A comparison of the model with a transformer architecture revealed superior performance for the former, with an **F1 score of 72.9%** compared to the latter's 66.0%.

The YOLO model trained to detect specific vocalisation units in spectrograms achieved a mean Average Precision (mAP) at 50% of Intersection over Union (IoU), denoted as mAP@50, of 74% on the test set as presented in the Table 11. This score is for the best performing hyper-parameters, which were to use the 'large' model architecture, the Stochastic Gradient Descent (SGD) optimiser, an image size of 640x480 pixels, batches of 64 samples, and a higher weight in the loss function for classes that are less represented in the dataset set.

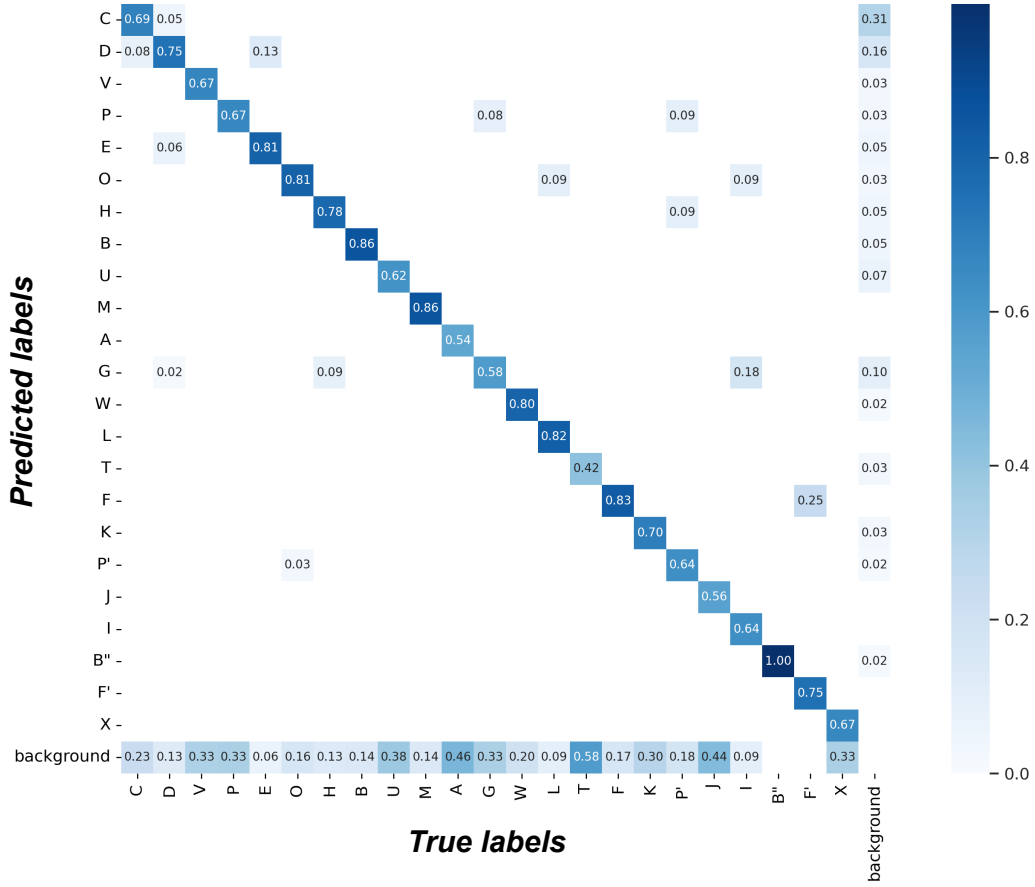


Figure 25: Confusion matrix of YOLO model over humpback whale units : y-axis represent the Predictions of the model while the x-axis represent the ground truth. The value at the intersection of the two represents the rate of correct classification or confusion if not in the diagonal line. The "background" line in terms of predictions corresponds to the false negative (FN), while for the true axis it corresponds to the false positive (FP).

Our model was also employed to compute the attention map using a method known as GradCAM [157]. As illustrated in Figure 26, the analysis of attention maps derived from various layers of the model (layers 0, 1 and -1) reveals a sequential pattern of activity. Initially, on the first layer of the model, which corresponds to the very first convolutional layer at the beginning of the network's backbone, the focus begins to shift towards units (layer 0), while noise is retained.

Subsequently, on the second layer (layer 1), which corresponds to a layer of convolution for feature extraction, the majority of the noise is removed (see Figure 26.b). In the final layer (layer -1), which corresponds to the detection head responsible for predicting confidence and bounding boxes, a substantial region is identified where information is extracted to predict the label. The results presented herein illustrate the model's focal point in predicting the label and the bounding boxes.

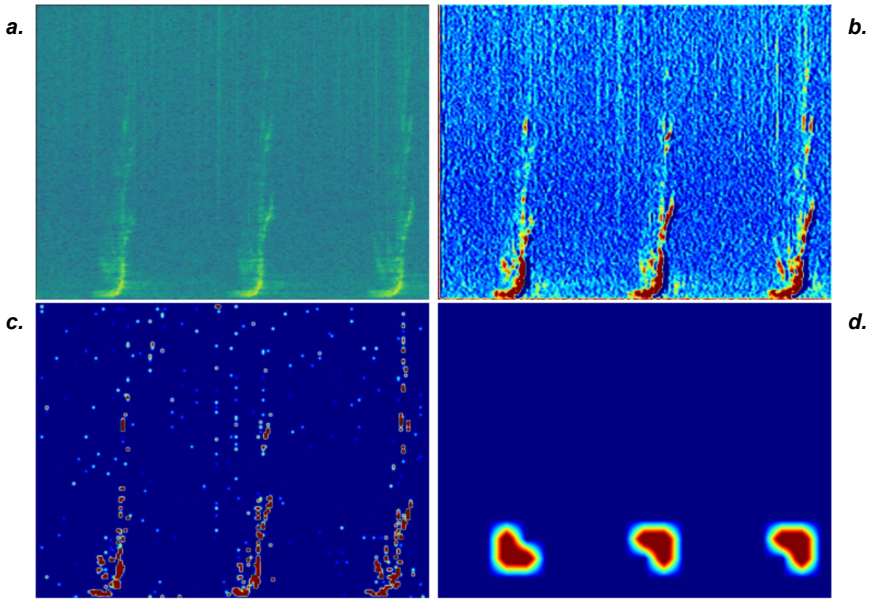


Figure 26: Original spectrogram (a) with the attention map extracted from the model, at the layer 0 (b), layer 1 (c) and -1 (d)

A notable aspect of this analysis is the model's avoidance of focusing on noise, which could have served as a warning sign regarding the potential for over-fitting. When looking at a noise file as presented in Figure 27, we can see that the resulting layer does not focuses on anything. Indeed, some datasets allow models to learn around the annotation when the data and splits are not well distributed, due to the presence of bias in the data and the fact that some information is helpful in predicting outcomes outside the informative part.

As presented in the confusion matrix Figure 25, apart from the confusion between certain low-represented units (*e.g.* F and F′ or G and I see Table 11), most of the predictions are good for the test set. To go into a bit more detail about the confusions, the F and F′ units, for example, are very similar in terms of sound and modulation (see Figure 16), and both are low-represented in the dataset, same for the G and I. These two parameters can strongly influence the measurements. These classification errors highlight the difficulties in accurately separating these units. Additionally, as illustrated by the confusion ma-

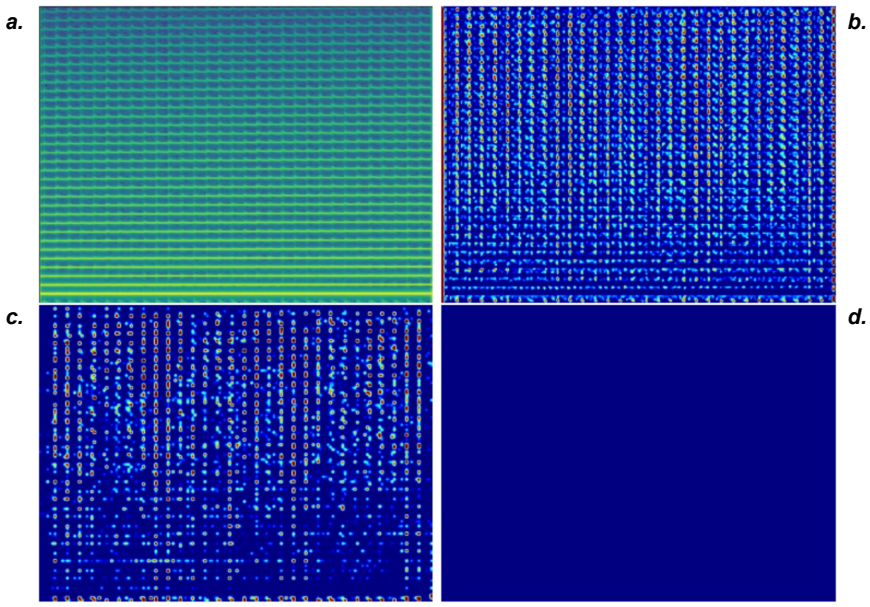


Figure 27: Original spectrogram of noise (a) with the attention map extracted from the model, at the layer 0 (b), layer 1 (c) and -1 (d)

trix, the model failed to accurately identify a significant proportion of the annotations, consequently leading to mispredictions in the background. This finding indicates that the training may require further low-SNR annotation and additional overlapping vocalisations.

To further confirm the performance of the model on a real-world scenario, the recall was estimated on a random sample of 11 files *a posteriori* (by comparing predictions with exhaustive manual annotations). The post-hoc recall reached 84% on vocalisations at least 5 dB over the noise, and 59% when counting the vocalisations of low energy as presented in Figure 28. However, in low SNR files, the maximum missed detection reaches 25, while 6 of the 11 files have less than 10 missed detections. Consequently, the model was deemed sufficiently efficient for the tasks of vocalisation detection and unit assignment. Parallel to this post-hoc recall analysis, in order to measure post-hoc precision, we computed the number of detections on dates known for not having any humpback whale in the Caribbean. After filtering out files with fewer than three detections and analysing the remaining detections in areas without whales, the model's false detection rate did not exceed 0.4 per hour.

5.1.1 *Generalisation of the model*

In order to verify the generalisation of the model, which mean trying to see if it still works in different sea conditions or different locations in the world, we tried to predict the vocalisation from recordings far

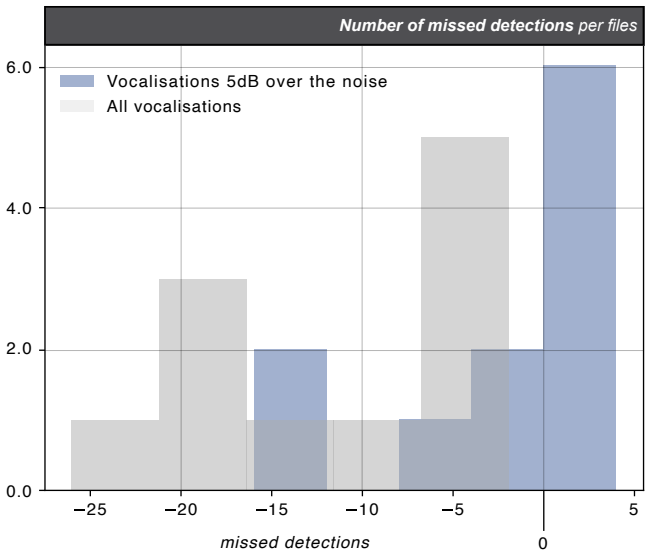


Figure 28: Post hoc analysis of the missed detection per file over 11 files : The y-axis corresponds to the number of files for which x units were missed, while the x-axis is the number of units missed.

from the Caribbean, in Norway and Moorea in French Polynesia, and also with files from different years as the vocal repertoire is modified during the years. Our results show that the model is still able to predict vocalisations as presented in Figure 29. However, as it is visible on these predictions, the confidence of the model is low.

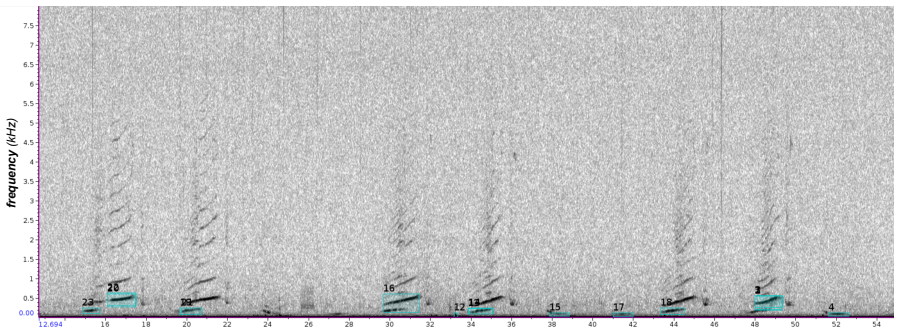


Figure 29: Detection of our YOLO model for humpback whale units over a Antigua recordings in 2025.

5.1.2 *Comparison to another architecture*

In order to compare the proposed model with an other architecture, a transformer architecture was utilised. The methodology employed in training the model, the dimensions of the image, and the classification were all consistent. Following the detection, the maximum confidence score for each species is filtered at an interval of 8 seconds. As YOLO

Table 11: Units number of annotation, split train, validation and test with associated Precision, Recall map@50 scores on the test set for YOLOv5 : mAP@50 scores under 0.5 are presented in bold.

Unit	N	Train	Val	Test	Precision	Recall	mAP@50
all	3111	2119	481	511	0.836	0.702	0.739
C	513	361	90	77	0.721	0.662	0.706
D	359	260	51	63	0.736	0.754	0.750
V	253	170	49	43	0.921	0.651	0.692
P	227	169	45	30	0.850	0.567	0.652
E	183	127	33	31	0.877	0.839	0.851
B	129	88	30	14	1.000	0.821	0.858
H	131	95	22	23	0.961	0.870	0.868
U	116	87	20	21	0.656	0.546	0.585
A	101	75	16	13	0.848	0.538	0.530
M	113	75	24	21	0.982	0.857	0.858
W	80	57	14	15	0.883	0.667	0.761
G	93	73	15	12	0.399	0.583	**0.481**
O	163	123	21	31	0.858	0.777	0.835
T	65	48	11	12	0.675	0.333	**0.379**
F	61	44	8	12	0.912	0.865	0.909
K	57	39	10	10	0.764	0.650	0.700
L	75	57	12	11	0.946	0.818	0.821
J	49	36	10	9	1.000	0.607	0.667
P′	56	42	9	11	0.656	0.545	0.577
B"	33	22	7	4	0.758	1.000	0.995
X	24	19	3	3	0.907	0.667	0.698
F′	27	17	6	4	1.000	0.889	0.995
I	49	35	5	11	0.914	0.636	0.823

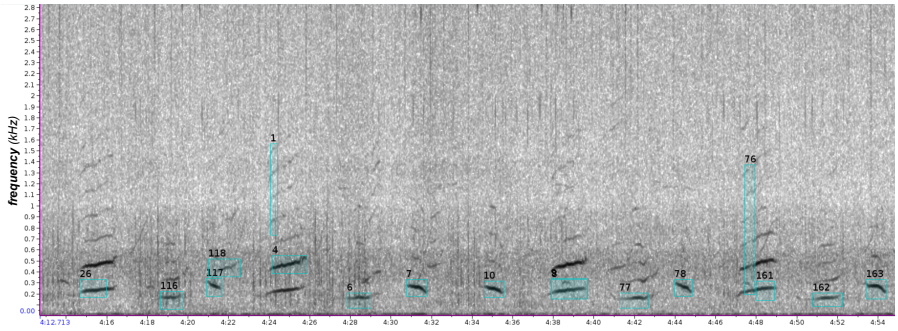


Figure 30: Detection of our YOLO model for humpback whale units over a Moorea recordings in 2025.

provides bounding boxes, but not a single score per species, reducing these boxes into only one confidence per class enable the comparison to a transformer for the test dataset.

As presented in Table 12 and Figure 31, our model performed better in term of precision, recall and F1 score. In fact, the YOLO model demonstrated a higher performance with an F1 score of 72.9%, surpassing the transformer by 15% for this particular task. By comparing each class and measuring the gain or loss between the two models,

Table 12: Metrics comparison between YOLO and a simple transformer

metrics	YOLOv5	Transformer
F1 score	**0.729**	0.570
Precision	**0.952**	0.687
Recall	**0.637**	0.570

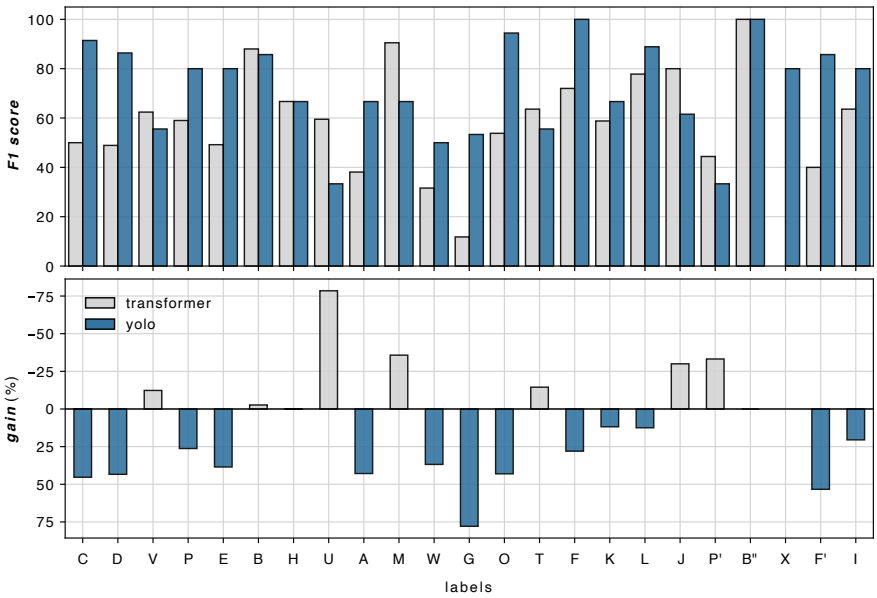


Figure 31: F1 score for the YOLO model compared to the transformer : The top part shows the F1 score for each model per unit type, while the bottom part shows the gain and loss using YOLO or the transformer.

we can see that our YOLO model perform better for 13 of the 23 classes. However, the transformer increases the F1 score for 7 of the 23 classes. For example, using YOLO, the type U has a F1 score bellow 40%, while it reaches around 60% with the transformer 31.

Contributions

The proposed model demonstrates **high scores in the analysis of the humpback whale recording**, with even high generalisation to recognise the species. The observed confusion between certain units **necessitates the development of more extensive annotations and a greater variety of units**, particularly for units that are currently under-represented.

5.2 A YOLOV5 MODEL ON 27 BIRD SPECIES

Key points

- For **the 27 bird species**, the efficacy of the models is optimised when using the YOLOv5 'large' architectures, the Adam optimiser, images of a size of 640, batches of 32, and special weights for each species. The optimal model attained a **mAP@50 of 82.0%**.
- There are **minimal confusion across the various species**. However, the presence of **certain species is predicted in the background**;
- In comparison to the BirdNET Analyser, our model achieves a micro mAP of 69.1% in a soundscape test with mixed chorus, while the BirdNET model achieves 55.3%. With regard to the weighted cmAP metric, our model attained 70.6%, in comparison to BirdNET's 61.5%.
- It was demonstrated that the **implementation of a species-specific threshold** adjustment in the detection process can result in an **enhancement of the results**.
- The use of box detection has been demonstrated to facilitate the incorporation of supplementary information regarding detections, whilst demonstrating efficacy in the prediction of species richness (Spearman 61.8% *p-value* <0.001).

5.2.1 *Bird model evaluation*

The highest achieved mAP@50 score during training and evaluation on the validation set was 84.6% for the bird best model (Table 13). On the test set, the corresponding mAP@50 score reached was 82.0% (Precision = 79.0%; Recall = 79.9%) (5th line of Table 13). These scores were obtained with the large pre-trained weights, Adam optimiser, an image size of 640, batch size of 32 as well as the addition of special weights for under-represented classes. We note that with the 'small' architecture, with the SGD optimiser and batch size of 16 and the same weight than for our best model (4th line of Table 13), a test mAP@50 of 81.3% is reached while training in less than 20 minutes and requiring 5 times less GPU memory and reduce the inference time from 4.9 ms to 1.7 ms. Also, the same parameters without the personalised weights per class reach a test mAP@50 of 81.5%. Our results then showed that it is recommended to process an image with

a minimal size of 640 pixels, because the reduction to 224 pixels drops the score by around 6%, which is considerable.

After performing the K-fold cross-validation with the best performing model, metrics were mAP@50 81.8% ± 0.011, precision 80.9% ± 0.007 and recall 77.8% ± 0.011 which is consistent with the metrics we obtained previously and therefore validates the fact that reported scores are not specific to the test set used previously. As shown in the confusion matrix Figure 32, the model seems to miss some of the annotations by classifying them in the background, especially the White-throated sparrow *wtsp* with 23% ± 3% of the test annotations. Except the confusion between the Song sparrow *sosp* and the Lincoln's sparrow *lisp* (13% ± 9%) confusion between classes is low and remains below 6% with the highest confusion between *nawa* and *yrwa* (5%), *amre* and *yrwa* (5%). For the species classification scores, the species with the best scores is Northern Parula, *nopa* (*Setophaga americana*) (mAP@50 = 93.1% ± 0.3%) while the Winter Wren, *wiwr* (*Troglodytes hiemalis*) is the worst predicted one (mAP@50 = 42.1% ± 7.6%) (Table 14).

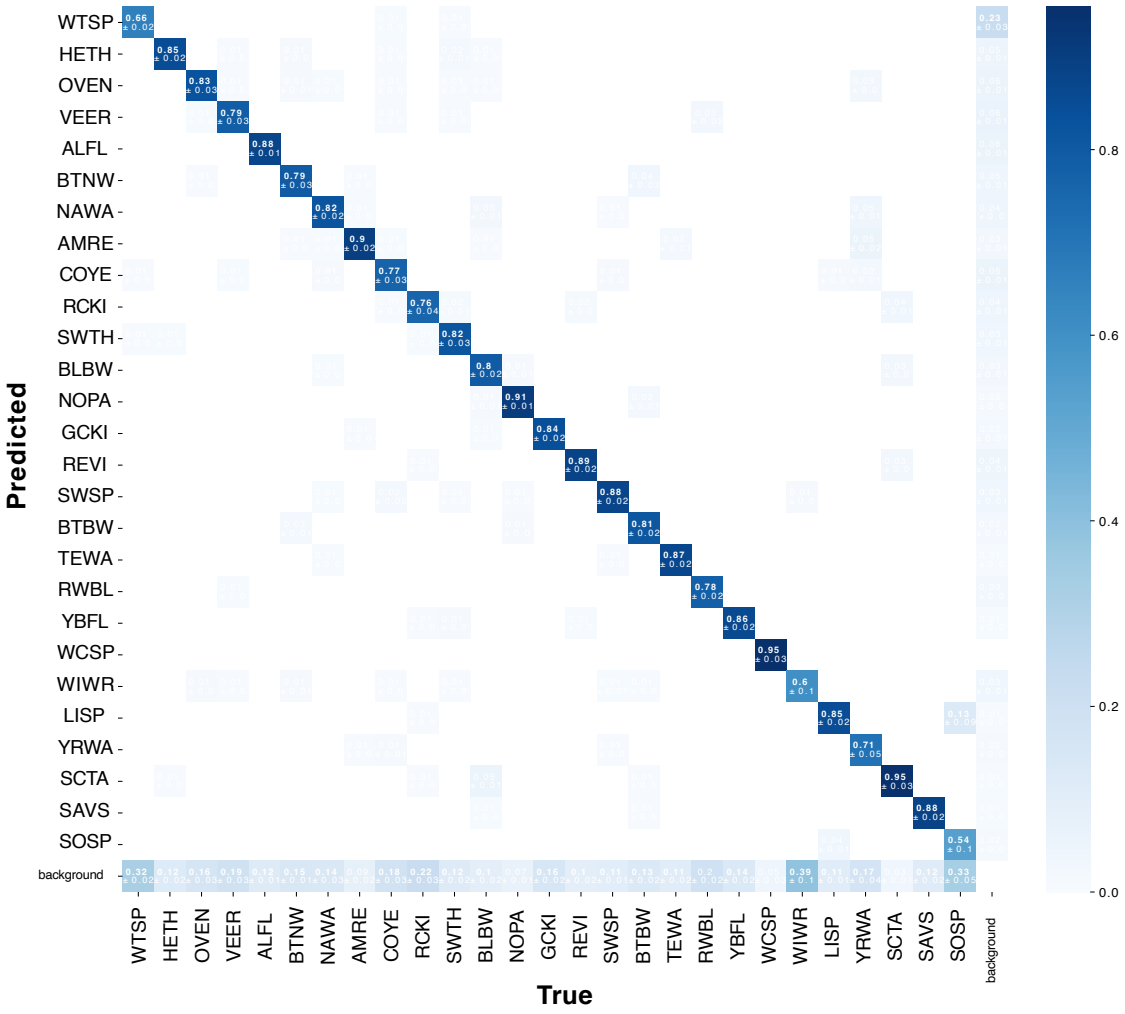


Figure 32: Confusion matrix on the test set of the annotations from the Québec, Canada database, with a total of 27 species : The standard deviation is measured with the Kfold cross validation with k = 10. The X-axis corresponds to the annotations, while the Y-axis shows the model's predictions. Diagonals indicate good predictions, while background predictions correspond to missed annotations.

Table 13: Model performance with different parameters for 30 epochs on the annotations from the Québec, Canada database : The columns imgsz correspond to the 'image size' in pixels while pw is used for 'classes weight' as we modified the weight of each classes during the training. Trainings were performed on a NVIDIA A40 GPU.

Size	duration (min)	GPU (Go)	optimiser	imgsz (pixels)	batch	pw	Train Precision	Train Recall	Train mAP@50	Train mAP@50-95	Test Precision	Test Recall	Test mAP@50	Test mAP@50-95	inference (ms)
L	23	11.9	SGD	640	32	Y	0.798	0.827	0.842	0.482	0.772	0.820	0.813	0.455	5.2
L	30	6.33	SGD	640	16	Y	0.782	0.843	0.843	0.483	0.775	0.822	0.814	0.458	7.7
S	12	4.82	SGD	640	32	Y	0.777	0.812	0.83	0.470	0.749	0.833	0.802	0.446	2.4
S	18	2.48	SGD	640	16	Y	0.789	0.825	0.845	0.477	0.774	0.816	0.813	0.45	1.7
L	**21**	**11.9**	**Adam**	**640**	**32**	**Y**	**0.798**	**0.82**	**0.846**	**0.476**	**0.79**	**0.799**	**0.820**	**0.452**	**4.9**
L	28	6.51	Adam	640	16	Y	0.795	0.802	0.841	0.479	0.785	0.785	0.815	0.453	5.0
L	14	2.07	SGD	224	32	Y	0.742	0.831	0.799	0.449	0.715	0.805	0.760	0.419	1.7
L	23	1.57	SGD	224	16	Y	0.744	0.833	0.795	0.448	0.719	0.793	0.759	0.421	1.5
L	20	11.9	SGD	640	32	N	0.764	0.838	0.806	0.456	0.700	0.796	0.725	0.409	30.4
L	27	6.33	SGD	640	16	N	0.791	0.838	0.841	0.477	0.787	0.819	0.819	0.451	6.5
S	11	4.82	SGD	640	32	N	0.794	0.833	0.846	0.477	0.785	0.813	0.815	0.451	2.4
S	17	2.48	SGD	640	16	N	0.774	0.813	0.812	0.462	0.775	0.824	0.815	0.453	1.7
L	23	11.9	Adam	640	32	N	0.800	0.839	0.849	0.485	0.773	0.827	0.818	0.46	5.3
L	31	6.83	Adam	640	16	N	0.774	0.830	0.831	0.476	0.765	0.824	0.812	0.454	6.0
L	15	2.07	SGD	224	32	N	0.753	0.850	0.808	0.454	0.718	0.815	0.763	0.415	3.4
L	26	1.57	SGD	224	16	N	0.770	0.834	0.810	0.456	0.726	0.827	0.773	0.424	2.0
S	11	0.719	SGD	224	32	Y	0.728	0.801	0.776	0.419	0.691	0.785	0.740	0.392	0.6
S	20	0.457	SGD	224	16	Y	0.726	0.794	0.784	0.417	0.712	0.779	0.748	0.391	0.7

5.2.2 *Comparision to BirdNET*

5.2.2.1 *ROC AUC and threshold estimation*

In order to improve the results and get an optimum threshold associated with each species, we examined the ROC curve for each species on the validation set Figure 33 and calculated the Area Under Curve as presented in Table 14. We compared different true positive (TPR) scenarios — TPR 0.1, TPR 0.5 and TPR 0.9 — to find the best parameter and therefore the best model. The results obtained for the non-finetuned BirdNET are lower than YOLO for most of the species, except *sosp*, *savs* and *rwbl* where we observe a very low confidence threshold (maximum between 0.6 and 0.15) for each scenario. We observed a large distribution with BirdNET's confidence threshold, which ranges from 0.015 to 0.905 for a TPR of 0.1 depending on the species, whereas it ranges from 0.425 to 0.89 for YOLO in the same scenario. This suggest a better learning of certain classes compared to others in the case of BirdNET. This finding highlights the importance of adapting thresholds by class for more optimised results. We also calculated the False Positive Rate (FPR) for each scenario, which gives with a TPR of 0.1 a FPR < 1e-3 for YOLO and 0.007 ± 0.031 for BirdNET. With a TPR of 0.5, the FPR is 0.001 ± 0.001 (YOLO) and 0.037 ± 0.087 (BirdNET). Finally, with a TPR of 0.9 the FPR is 0.012 ± 0.011 for YOLO and 0.163 ± 0.125 for BirdNET. As we can see, the higher the TPR, the higher the FPR, but this increase is much more pronounced with BirdNET than with our YOLO model. Achieving the right balance between a low FPR and a high TPR is key to creating an effective model with strong scores. In this experiment, our model seems to perform better with the 27 trained species.

After retrieving the predictions of our model and BirdNET on the 884 annotated files dataset, we were able to measure different metrics as presented in Table 15.

The class mean Average Precision (cmAP) scores weighted with the number of annotations in the dataset in all chorus levels (*low, mid and high*) is 70.6% with our model while it is 61.5% with BirdNET. In high chorus files, the cmAP weighted is 73.0% for YOLO and 63.6% with BirdNET. In general, these results show that our model performs well at all levels of chorus, and even better than BirdNET, which allows us to consider our model effective for the task we intend to perform. A closer examination of the metrics Figure 34 shows that, as the TPR increases, precision scores decrease (Figure 34 a.), while recall scores increase (Figure 34 b.) for BirdNET and our model, which is induced by the reduction of the thresholds (Table 14). The lower the threshold, the more detections will be retained and therefore the higher the recall will be. However, among these detections there will be errors that will reduce accuracy. The mean F1-score (Figure 34 d.) are better for our model than BirdNET with a mean F1-score of 65.6%, 62.5%

Table 14: Area Under the ROC Curve of each species for our model and BirdNET with the different TPR scenarios associated with the positive threshold to set for the detections on the soundscape dataset from Québec, Canada database : The corresponding scientific names are provided in Table 6

	AUC ROC		BirdNET Thresholds			YOLO Thresholds		
Species	BirdNET	YOLO	TPR 0.1	TPR 0.5	TPR 0.9	TPR 0.1	TPR 0.5	TPR 0.9
wtsp	0.974	**0.988**	0.105	0.04	0.0	0.82	0.7	0.435
yrwa	0.946	**0.988**	0.145	0.03	0.0	0.685	0.685	0.225
nawa	0.923	**0.995**	0.56	0.13	0.015	0.635	0.635	0.42
sosp	**0.999**	0.993	0.015	0.0	0.0	0.505	0.14	0.015
lisp	0.96	**0.996**	0.225	0.225	0.015	0.665	0.665	0.115
gcki	0.936	**0.996**	0.17	0.0	0.0	0.775	0.775	0.5
coye	0.981	**0.992**	0.055	0.015	0.0	0.645	0.645	0.37
ybfl	0.952	**0.998**	0.1	0.1	0.015	0.43	0.43	0.065
alfl	0.988	**0.996**	0.76	0.635	0.045	0.63	0.63	0.205
wiwr	0.942	**0.992**	0.275	0.025	0.0	0.52	0.455	0.255
nopa	0.959	**0.99**	0.175	0.09	0.0	0.785	0.785	0.045
rcki	0.972	**0.987**	0.07	0.015	0.0	0.81	0.725	0.3
revi	0.971	**0.994**	0.495	0.05	0.0	0.625	0.625	0.52
amre	0.825	**0.993**	0.08	0.015	0.0	0.715	0.715	0.38
heth	0.948	**0.994**	0.84	0.13	0.0	0.78	0.78	0.57
wcsp	0.987	**0.997**	0.1	0.1	0.0	0.425	0.425	0.425
btbw	0.931	**0.998**	0.485	0.22	0.04	0.89	0.8	0.61
btnw	0.873	**0.996**	0.905	0.19	0.0	0.835	0.835	0.565
tewa	0.948	**0.999**	0.28	0.115	0.0	0.425	0.425	0.425
blbw	0.644	**0.995**	0.03	0.0	0.0	0.695	0.695	0.09
swth	0.954	**0.997**	0.38	0.09	0.0	0.755	0.755	0.48
scta	0.951	**1.0**	0.355	0.13	0.02	0.81	0.81	0.665
savs	**0.991**	0.99	0.06	0.0	0.0	0.81	0.615	0.19
rwbl	**0.996**	0.991	0.04	0.0	0.0	0.655	0.655	0.44
veer	0.906	**0.98**	0.83	0.075	0.0	0.755	0.645	0.2
swsp	0.952	**0.996**	0.325	0.105	0.0	0.835	0.47	0.28
oven	0.953	**0.988**	0.655	0.08	0.0	0.8	0.69	0.36

Table 15: Average Precision score for both models : Mixed chorus corresponds to all different chorus level mixed together.

	mAP (micro)		cmAP weighted		cmAP macro	
Chorus Level	YOLO	BirdNET	YOLO	BirdNET	YOLO	BirdNET
mixed	**0.691**	0.553	**0.706**	0.615	**0.600**	0.553
low	**0.662**	0.551	**0.693**	0.614	**0.610**	0.598
mid	**0.700**	0.558	**0.720**	0.623	**0.598**	0.573
high	**0.711**	0.558	**0.730**	0.636	**0.629**	0.538

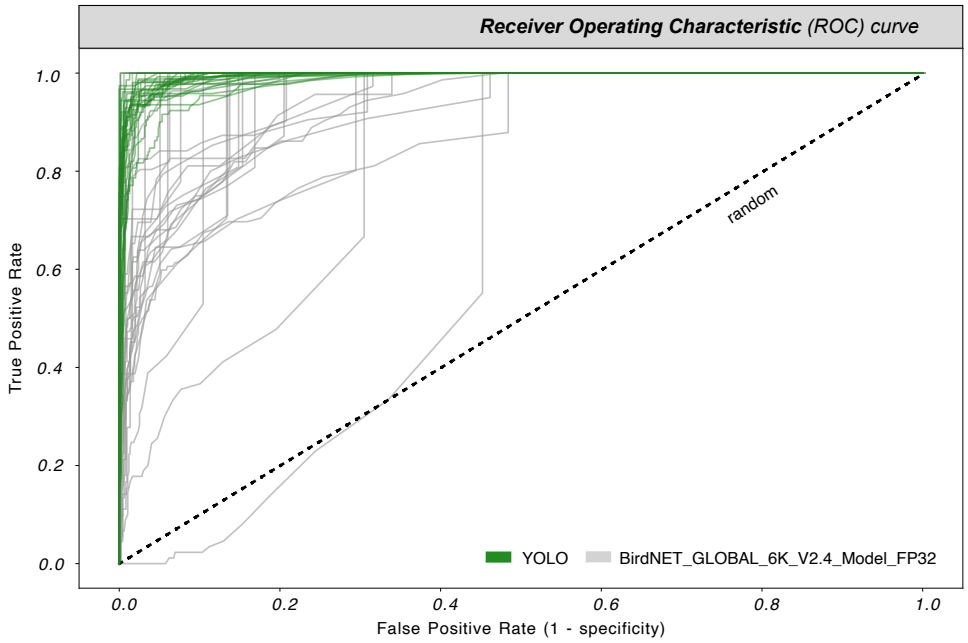


Figure 33: Receiver Operating Characteristic (ROC) curve of the 27 species for our model compared to BirdNET on the soundscape dataset from Québec, Canada database : The random classification is placed in dotted line.

and 56.7% at TPR 0.9, 0.5 and 0.1 respectively, while for BirdNET the F1-score is 23.7%, 57.1% and 56.3% for TPR 0.9, 0.5 and 0.1. However, as we focused on being more precise in the prediction rather than having a good recall, we investigated the F0.5-score (Figure 34 c.) and concluded that the best scenario is TPR 0.5 for YOLO, with a mean F0.5-score of 66.4%, respectively 65.7%, 67.4% and 66.2% for *low, mid, high* chorus level. For BirdNET, the best scenario is rather TPR 0.1 with a mean F0.5-score of 67%, respectively 72.8%, 64.1% and 64.2% for *low, mid, high* chorus level. The F0.5-score weighted by the class weights verified that hypothesis.

5.2.2.2 *Species classification*

As presented on Figure 35, when taking the best scenario for each model, *i.e.* TPR 0.5 for YOLO and 0.1 for BirdNET, the species F0.5-score is highly variable between species. We observed that YOLO misses more species than BirdNET, disregarding the chorus level. However, these species are not the most represented in the 884 files, as classes *scta* and *ybfl* with 17 and 12 annotations respectively, nevertheless *amre* was more frequent (75 annotations). We observed that the *amre* threshold is 0.715 in scenario 0.5 of YOLO, and is exactly the same for scenario 0.1, while most *amre* detections were made around 0.2, which shows a possible non-representativeness of the validation set that calculates the threshold. It would therefore be appropriate to

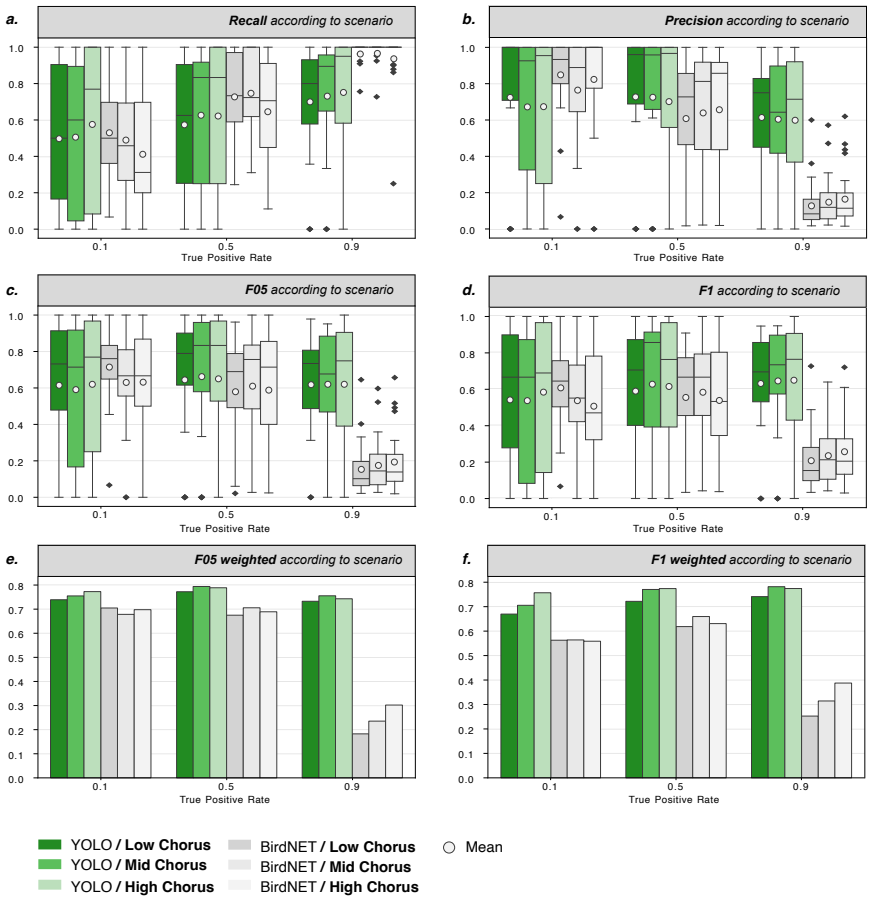


Figure 34: Evaluation of our model and BirdNET over the three different scenarios on the soundscape final validation dataset : The average for each metric is represented by a dot.

reduce the threshold of the species that are missed in the detections. For the mid chorus level, we observe that BirdNET missed *btnw* and *blbw* and for the high chorus level it missed the *gcki* and *blbw*. In general, YOLO is as good as BirdNET with even better results for highly represented species such as *wtsp*, *coye*, *oven* and *heth*, respectively 476, 338, 281 and 217 occurrences to detect.

Contributions

The model we developed here using box detection seems to be better adapted to high chorus recordings than BirdNET.

5.3 COMPARING THE BOX DETECTION TO NROI INDEX FOR BIRD SPECIES RICHNESS ESTIMATION

As the nROI index measures the number of regions of interest in a recording — potentially the number of vocalisations — and is correlated to species richness, we decided to compare our boxes, which

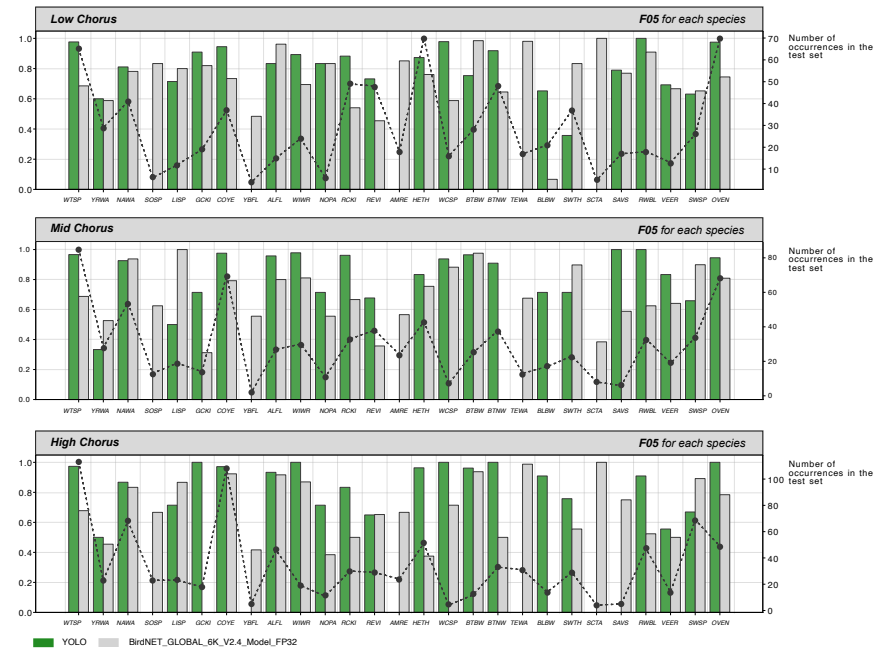


Figure 35: F0.5-score for BirdNET at a true positive rate scenario of 0.1 and our model at a true positive rate scenario of 0.5 for the 27 species on the soundscape dataset from Québec, Canada database : The dotted line represent the number of each species to detect in each chorus level.

are similar to the nROI, to see if we obtained the same results. After computing the nROI index for each files of the evaluation dataset, we measured a spearman ρ of 0.179 *p-value* < 0.001 between the number of ROI in the signal and the species richness of the same file, which imply a low correlation as presented in Figure 36.

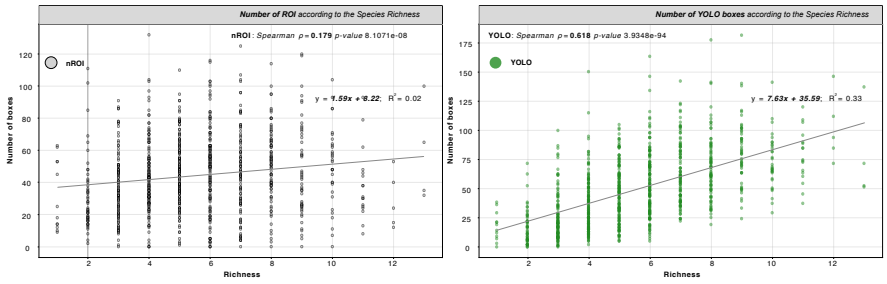


Figure 36: Number of detected boxes with the nROI index compared to the number of boxes from YOLO on the soundscape dataset from Québec, Canada database : The species richness take all the species in the recording, not only the one that compose the dataset.

The maximum species in a 15 seconds file is 13 and the number of boxes from the nROI range between 0 and 132. With our method, we obtained a spearman ρ of 0.618 *p-value* < 0.001 which resulted

in a higher correlation. For our model, the number of boxes varies between 2 and 182, and we observed that when there are more than 6 species in a file, the number of boxes with YOLO is always greater than 20, while with the nROI method there are files without ROI. This may be due to incorrect settings for the nROI method, particularly in the case of files with low SNR. In a recordings which contains birds songs, YOLO seems to be better to predict more region of interest, or box, rather than the nROI index. As we previously observed that our model performs better with high chorus files, this finding confirms its efficacy in detecting and differentiate signals in mixed soundscapes with high choruses.

5.4 DISCUSSION

5.4.1 *Humpback whale model scores*

The results presented previously for humpback whale show promising precision with a satisfactory recall. However, it is important to note that certain units do not exceed a mAP of 50%, and in some cases, there is also low recall, as evidenced by unit T, which exhibits a recall of 33% and a precision of 67.5%. In addition, the type G demonstrates a low level of precision (39.9%) and a recall that approaches 50%. In order to provide a more detailed account of the results obtained, it is necessary to discuss the confusion matrix. This analysis reveals that unit T is not confused with another unit, indicating that the model is missing a significant number of units when making predictions in the background. One potential explanation for these overlooked detections is that the T unit may be less discernible in the spectrogram when the signal-to-noise ratio (SNR) is low. Alternatively, the training set may comprise a limited variety of this unit, while the test and validation sets contain more complex examples, which could lead to a higher degree of difficulty in identifying the T unit. In the case of unit G, it is evident that 58% of the annotations are accurately predicted, while the remaining 18% are erroneously categorised as unit I. This misclassification is also evident in the Random Forest analysis (see Figure 18), where unit G is classified as G, I or H, which are visually similar units. However, the random forest analysis reveals a confusion between units F and D, which is not observed in our model. Indeed, certain vocalisation-related parameters, such as duration, frequency and features, exhibit variation in the number of inflexion points, thereby resulting in divergent shapes. This feature is not present in the random forest, which explains why our YOLO model performs better on this task. Nonetheless, the residual uncertainty can be attributed to annotation inaccuracies or, alternatively, a lack of variability in the annotations from the training set, which can result in erroneous predictions. A comparison of the results obtained

with YOLO and another architecture (transformer) revealed that the former yielded superior outcomes. However, the transformer architecture comprises a total of 2 million parameters, whereas YOLO encompasses 53 million parameters. Furthermore, it was observed that the transformer model appears to be more effective in the case of longer and more stationary signals, as evidenced by the units "U" and "M". This observation can be explained by the nature of the transformer, which is designed to detect dependencies on the temporal axis, as opposed to the YOLO model, which extracts features such as contours on the spectrograms. This enables the YOLO model to perform better with highly variable units, such as units "C", "D" or "F'". However, a potential approach to enhance transformer scores would be to extend the duration of the input, either to 15 seconds or to the entire duration of the recording file. By incorporating this additional data, the model would be able to identify the recurrent pattern of song more accurately, thereby enhancing the overall performance metrics.

5.4.2 *Birds model scores and comparison with BirdNET*

The objective was to develop a methodology that would facilitate the identification of diverse taxa through the recognition of species-specific vocalisations, even in circumstances where signals from multiple species overlap. We showed that using box-annotated vocalisations on a local database improves the species detection scores compared to the reference BirdNET model. In addition, we have shown that the YOLO model, based on object detection on images, was effective in detecting acoustic signals despite the chorus. The good efficiency of YOLO for vocalisation was previously shown in multiple studies [63, 130, 131, 158–161]. However, even though the results are correct, with a mean F05-score of 66.4% on the 27 species and 78.5% when measuring weighted F05-score for all chorus level, some species remained undetected. Compared to the literature models, such as BirdNET, that reached F05-score of 67.0% and a weighted F05-score of 68.9%, we similarly missed vocalisation, revealing the complexity of species detection in some recordings. The hypotheses explaining these missed detections could be related to not accounting for all the different types of songs for each species, particularly those with several variations (*e.g. rcki* [162] song's is composed of 3 units A, B and C but not necessarily produced mathematically). Moreover, our dataset is not representative of local populations and therefore does not take into account the non-linearity in birdsong [163]. Indeed, songs can vary regionally or seasonally [164, 165] which makes model generalisation challenging. Nevertheless, we consider that both models are effectively detecting the presence of species as long as the recording duration is greater than 15 seconds. Seeing several chunks of the same

recording, would increases the probability of detecting a vocalisation. Post-processing allow to filter out low-confidence detections.

The results obtained here for BirdNET are similar to those previously reported in the literature [141]. Using BirdNET to asses european birds, a study attained a F1-score ranging from 40% to 52% [166], while other obtained an average precision ranging from 72 to 85% and recall rate ranging from 33 to 84% [167]. The similarity between our BirdNET results and those from other studies validate our comparison. It support the efficiency of our model for the desire task and appears even better than BirdNET, perhaps due to the small number of classes (27 compared to the + 6,000 for BirdNET).

Nevertheless, it is important to note that even with good precision and recall, these two methods remain less accurate than manual analysis and should therefore be used to simplify and/or speed up the analysis of a file or large database. The use of automatic detection methods must be adapted to the objectives of each project. In addition, we have seen that the model we presented can be effective with 5 times lighter weights and way faster in inference. To reduce the impact of training or forward on a large database, lighter models are recommended, even if they are sometimes less accurate, in order to reduce inference time, computing power and therefore processing costs. In this work, we tried to improve the metrics by training with one of the latest version of the YOLO model, *i.e.* YOLOv12, which led to very similar results during training, except that it rather focus on high annotated species, but using twice as many GPUs memory and taking about three times longer to train (over 1 hour for 25 epochs on a NVIDIA A40) compared to our best YOLOv5 (around 20 minutes).

5.4.3 *Importance of the confidence threshold adjustment*

In order to improve model predictions, we decided to set a threshold value for each species. This method has been use for birds and for the humpback whale. By using different values of True Positive Rate (TPR) over the Receiver Operating Characteristic (ROC) curve, we found the optimal point to get an average TPR and avoiding too much false detection (*i.e.* a low False Positive Rate, FPR). A similar process was carried out on the F1 curve while working on the humpback whale, which then helped to filter the detections. However, it is sometimes impossible to find the dataset allowing these threshold. There is for example a limit relative to the possible differences with the validation set, on which the ROC curve is computed, and the final test set. This can lead to an over estimation of the threshold which resulted on missed detections after detections processing. To improve results accuracy, for bird detector, we should have reduced the threshold of some classes (*amre*, *ybfl* and *tewa*) to 0.2. We observed that the confidence scores of YOLO are higher than BirdNET that seems to be

usually low, even in previous study [168]. Moreover, the distribution of the BirdNET thresholds was not distributed equally, with high confidence (0.905) for some classes and very low for others (0.015) in the best scenario (*i.e.* TPR 0.1). These observations were not applicable to our model, except in the case of the higher TPR scenario (*i.e.* TPR 0.9), where the threshold ranged between 0.015 and 0.665. However, for both model, the lowest threshold is associated to *sosp*, for which BirdNET is better than our model due to a too high confusion with *lisp*. The threshold value to set will then depend directly on the training phase and the dataset on which it is measured. Indeed, a dataset based on recordings with a single species and a low chorus level will likely result in over estimated thresholds. If thresholds cannot be set by class, its likely to reduce the quality of the results compared to what we achieved.

5.4.4 *Improvement in detection in high chorus level*

Whether it is for bird choruses or humpback whale singing together, the models presented above reached good results with overlapping vocalisation in term of detection. In fact, for the bird model, one of the key results of this work is that we did not observe significant variation in scores depending on the level of the chorus. Even if the BirdNET model was a little lower that ours, this result suggests that BirdNET can also accurately detect birdsong, even in files with a high level of chorus, as long as the thresholds are set correctly. Nevertheless, our YOLO model improves the results in high chorus files, and even more than in low chorus file. As the training set is composed of various files but many overlapping annotations, it is possible that YOLO model works better in high rather than low chorus.

To determine what might influence YOLO's predictions compared to BirdNET, we analysed missed detections and false predictions. We also performed this on humpback whale and reached a similar conclusion. We found out that our model was more confused in files with a low signal-to-noise ratio than BirdNET. Low SNR files increase the confusion, particularly between similar vocalisations. For example, for birds, the *heth* and *swth* are very similar. The model then is likely to predict both species on the same vocalisation and the filtering will then be done by taking the highest confidence and also the confidence that is above the species threshold. Once again, this result shows the importance of using class-specific thresholds. We also observed that some false predictions were not linked to confusion between the species or unit, but with other bird species. For example, by using our model of humpback whale on recording from different populations, it appears to predict vocalisations, but the confidence were low and the type unit was not correct. For bird, we saw for example that species such as White-throated Sparrow (*Zonotrichia albicollis*)

and Black-capped Chickadee (*Poecile atricapillus*), as presented in Figure 37, appear to be confused also. To avoid these previous points, we suggest to perform active learning loops with low SNR files and other species in background, and therefore improve the results in these scenarios. However, it is worth pointing out that the model confuses classes but does not miss vocalisations, which will simplify active learning because our model already recognises the structure of vocalisations and is able to detect them. As presented in an example 37, BirdNET missed 4 species in one recording, but found 2 of these later in the recording. One hypothesis for these missed detections is the possibility that they occurred between two 3-second windows, which may have rendered them more difficult to detect. However, setting an overlap for the analysis could avoid this [166, 169]. As it is set to 0 by default, this observation confirms that it is better to run on longer files to verify the presence of a species in a recording.

5.4.5 *Box detection for analysis*

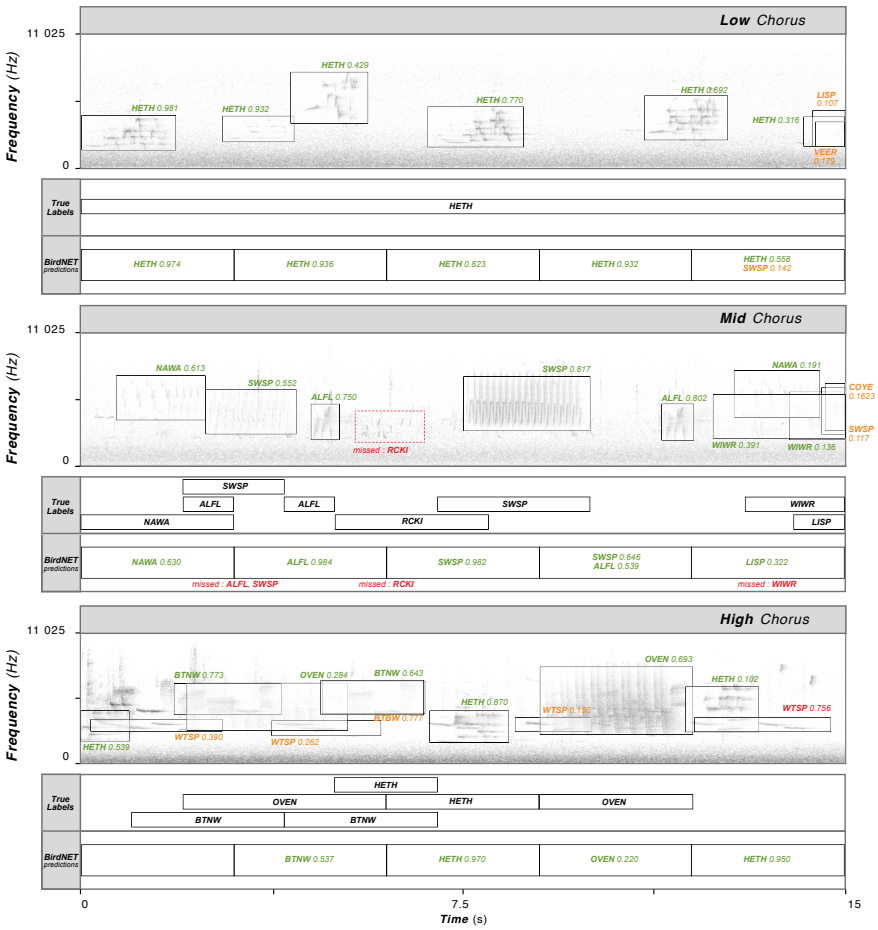


Figure 37: Example of the time annotations, the BirdNET predictions and our model boxes over three examples of the chorus levels.

One of the advantageous features of our models is that, compared to predictions with confidence scores based on seconds of signal, we obtain a box around the vocalisation with an associated confidence score. This box is useful in multiple ways: first, it verifies the prediction observed in the spectrograms; second, it detects overlapping vocalisation and finally, it prevents confusion between classes as we can verify the overlap in time and frequency between the prediction and the annotation. Moreover, box detection can improve the estimation of populations abundance, which until now, was done by measuring the call rate, *i.e.* the proportion of total audio windows containing a target vocalisation [170]. Box can allow to analyses the shift in frequency that can occur, for example, in response to anthropophony [171]. Also, as species share the same environment, box can be used to characterised soundscape ecology, by knowing which part of the frequency each species is using [172]. Finally, our results demonstrated that the number of YOLO boxes can allow to analyse the species richness in a recording, similarly to the nROI index [153]. Indeed, we measured a strong correlation in our evaluation files between the number of boxes and species richness. It suggests that our model has learned to recognise the bird songs that compose an audio signal, being able to box them by assigning a label with confidence. While the species composition of a sample is not the main focus of the study, the number of YOLO boxes can be used as an indicator of species richness.

5.4.6 *Difficulties and bias*

In this work, we first characterise the vocal repertoire of humpback whales in the Caribbean Sea during the 2021 breeding season. When run manually, categorisation processes may be susceptible to subjective biases, especially given that units can exhibit gradual variations [134]. Hence, to validate the reliability of the present repertoire, we confirm that units have a low level of overlap in spectro-temporal features (based on visualising a 2D projection and a random forest classifier's performance). Furthermore, the size of the repertoire found is comparable to that found in other studies [132, 133]. Since units vary depending on populations and breeding seasons, the construction of the present repertoire was not based on that of previous studies. However, several units were found to be similar to those in other studies [132, 133, 135, 136] (Table 5). In particular, some of them are part of the repertoire of non-song calls and song calls from Alaska [135], Australia [133] or the North Atlantic population during the feeding period [136, 138]. It has been observed that some units of the repertoire are different but are named the same in the literature. For example, units A, B, B", L and O are all referred to as "snore" [134]. Nevertheless, upon meticulous examination of these units, as substantiated by the random forest analysis, it was ascertained that they exhibited

divergent spectro-temporal features. This finding justifies their categorisation as distinct unit types in the analysis. We thus characterise a total of 23 units, organised into three categories (Low, Mid and High Frequency).

In the present repertoire, thirteen of the twenty-three units are classified as mid-frequency units. These are organised as either ascending or complex sounds, accounting for 1,792 of the 3,111 annotations in the set. In comparison, we found only four high-frequency units, accounting for 473 annotations in total. Therefore, high-frequency calls may be challenging to detect due to their under-representation in the neural network model's training set. Although song structures are highly stereotyped [19], the non-song calls within these songs can vary greatly [135] which may present a generalisation challenge for the model.

Despite the fact that some non-song calls also appear in songs —hence their presence across all sessions— they are sometimes altered and become less recognisable. Additionally, propagation effects that can distort their appearance on spectrograms can complicate the classification task. With a small dataset (2,957 annotations for 23 classes), there might be a lack in vocalisation diversity. This may be an explanation for class confusion and also low detection number for some classes.

If the aim is to develop a general model which will be able to work in every breeding ground, it is therefore crucial to create a training dataset to avoid biases in subsequent analyses. Furthermore, as the classification of certain units can be based on the presence of harmonics [135], it is important to define, for future studies, whether these harmonics should be included in the annotation boxes. We observed that including harmonics is essential for low-frequency vocalisations, such as units L and M, since their fundamental is less visible than their harmonics.

6

RELATIONS BETWEEN DETECTION AND FIXED ENVIRONMENT

6.1 Coastal parameters for the humpback whale 88
6.2 Habitat composition for birds in Québec 92
6.3 Importance of bathymetric characteristics for the sperm whale in the Mediterranean 95
6.4 Discussion 100
6.4.1 Habitat preferences 100
6.4.2 Detecting only songs can reduce the predicted densities 104
6.4.3 Sperm whale sampling bias 105

The purpose of this chapter is to analyse only fixed parameters. These parameters will be considered as potential predictors, as they are believed to be relevant to the species objectives in the area. The term 'fixed environment' may be defined as the environment component that will not be modified during a period of one year or over the surveyed period. In this context, the parameters of the underwater environment are considered to be constant. These include latitude, depth, slope, rugosity, and parameters such as canyons. On land, fixed parameters may include altitude, latitude, and the composition of the environment, such as the type of land or vegetation.

Key points

Using model detections and visual observations, we performed a statistical analysis of the potential habitat suitability of different species.

- We propose a **map of suitability for humpback whales and sperm whales**, and **suggest preferences for bird species** related to the fixed parameters;
- The analysed parameters explain much of the presence; however, **they lack information on the timing of migration**. Furthermore, they make positive predictions in regions where no observations were made, which is probably characterised by the absence of dynamic parameters in the models.

6.1 COASTAL PARAMETERS FOR THE HUMPBACK WHALE

The study of the results obtained from the detection of humpback whales provides valuable insights into their presence in proximity to specific islands. However, as the position of the singer are not precisely known with our bioacoustics protocol, it is difficult to know in which distance the singer is. In order to analyse the impact of fixed parameter on their presence, we therefore consider the island as the fixed parameter, which all have their own characteristics such as the size of the continental shelf. The YOLOv5 models presented above was used to detect vocalisation units on a dataset spanning nearly 10,000 hours of recordings collected from December 2020 to August 2022, covering regions from Bermuda to Aruba. Initially, 2,072,851 vocalisations were detected across 278,237 files out of nearly 600,000 in the database. After applying the filtering criteria detailed in the methods section, only 659,222 detections remained between the 1st and 24th weeks of 2021 and 2022 (they are made available in a public repository). Notably, the most frequently detected vocalisation was unit D, totalling 359,266 detections, while the least detected units were W (172 detections), X (102 detections) and B" (20 detections). Seven units were detected over 10,000 times (D, E, C, O, T, P, V), while others ranged from 305 to 9,464 detections.

Among the 175 weeks recorded across stations, between the first and 24th weeks of 2021 and 2022, only 109 weeks exceeded the threshold to be considered as positive (averaging 7 detections per hour), 92 in 2021 and 17 in 2022. These weeks were recorded in Bermuda, Anguilla, Saint-Martin, Sint Eustatius, Saint-Barthélemy, Guadeloupe, and Martinique. No positive weeks were found in Bahamas, Jamaica, Bonaire, or Aruba. The week with the highest average detection rate occurred in Guadeloupe Anse Bertrand in mid February 2021, with a mean of 1,180 detections per recorded hour. Guadeloupe Saint-François, Anguilla, Saint-Barthélemy and Saint-Martin also exhibited notable detection rates around 600 detections per hour (Figure 38).

During the breeding season, the time with the highest detection rate varied by island. It occurred in February and March for some (Bermuda, Anguilla, Sint Eustatius, Guadeloupe Anse Bertrand and Guadeloupe Deshaies), and in March and April for others (Saint-Martin, Saint-Barthélemy, Guadeloupe Saint-François, Martinique).

Overall, detection rates increased in late February and declined between May and June. No detection was recorded in the first week of 2021, but humpback whale songs began in Saint-Barthélemy in the second week. In 2022, singing also started in the second week of the year in Saint-Martin, but unfortunately the limited amount of data available prevents a comparison. While no detection occurred in the Bahamas during 2021, recordings from the first week of February 2022 confirmed humpback whale songs in the night between the 2nd

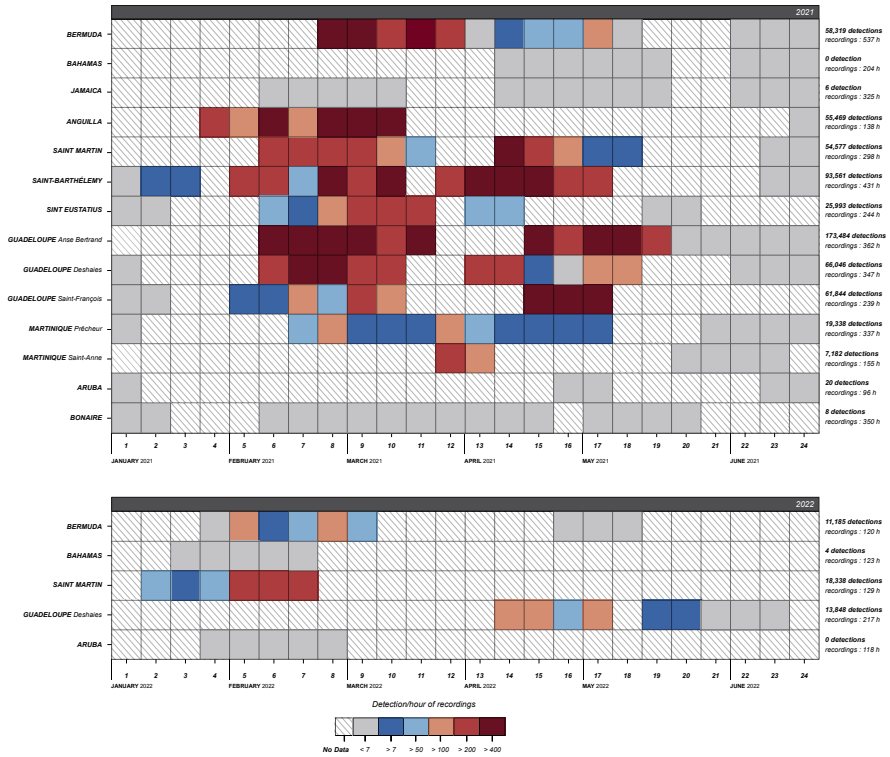


Figure 38: Weekly mean detection per recording hour during the breeding season and over the 14 considered stations : 2021 is represented at the top while 2022 at the bottom. Over the thousands of hours of recordings from the first 6 months, a total of 659,222 detections were kept. A threshold was set to 7 detections per hour of recording to define a week as positive or not. Given that one week represents approximately 27 hours of recording, this represents at least 190 detections, or several dozen minute-long files containing at least 3 detections. The maximum average detection rate is 1,180 per recorded hour.

and the 3rd of February, but the number of detections did not exceed the set threshold. No other positive recording was found in Bahamas, suggesting it is a transitory migration passage.

It has been observed that the depth in this region can be particularly steep, a phenomenon that is particularly pronounced in areas adjacent to the Atlantic Ocean. In this study, the relationship between the distance to the 200 m depth and the total detection over the recording time was investigated. The results showed that 10 out of the 13 stations were within 5 km from the 200 m depth, and only 7 were under 30 km from the 2000 m depth. However, no correlation was observed between the distance to these depths and the total detection over the recording time. For instance, Guadeloupe Anse Bertrand has the highest detection rate, with 173,454 detections over 362 hours of recording. This corresponds to 479 detections per hour. It is located at a depth of 200 m and 2000 m, respectively, only 3.5 km and 11 km away from the

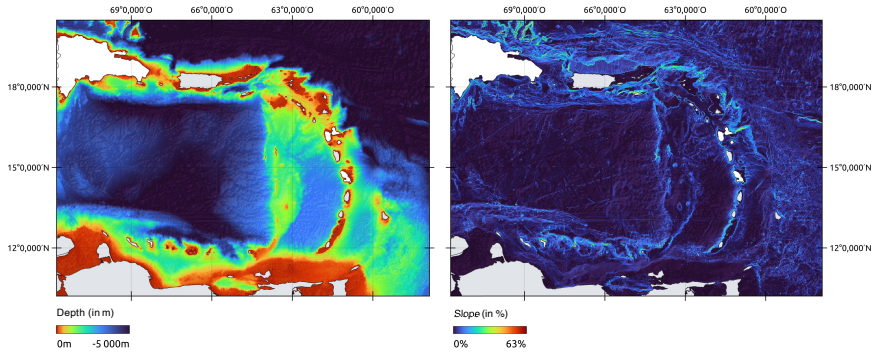


Figure 39: Bathymetric and slope map of the Caribbean region : The informations were extracted from the GEBCO 2023 dataset.

200 m and 2,000 m depths, respectively. Meanwhile, Anguilla, which has the second highest detection rate (401 detections per hour), is located at a depth of 200 m and 2,000 m, respectively, 32 km and 32 km away from the 200 m and 2,000 m depths, respectively. Nevertheless, an examination of the distance to the 5000 m reveals a robust negative correlation with a coefficient of -0.77 (*p-value* <0.005). The figure is less than 0.005. Indeed, six of the stations exhibiting the lowest detection rates are situated at a depth greater than 100 km, while the three stations with the highest detection rates, namely Guadeloupe Anse Bertrand, Anguilla and Guadeloupe Saint-François, are located at a depth below 60 km.

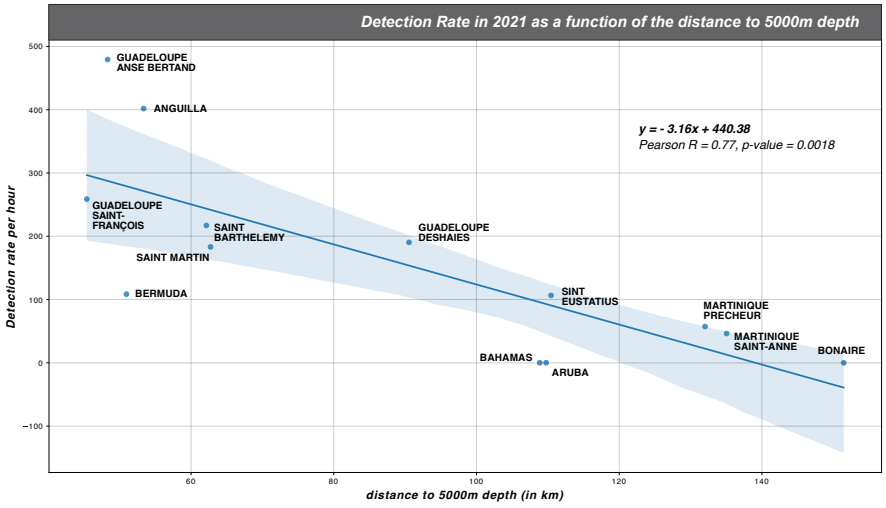


Figure 40: Detection Rate of humpback whale unit in 2021 as a function of the distance to 5,000 m depth.

In the absence of a demonstrable correlation between distance from the shore and detection rate, with the majority of recordings situated less than 1 km from the shore, it can be concluded that the pivotal parameter is the distance to a significant slope in proximity to the shore.

Using the aforementioned two parameters, the potential breeding areas in which the humpback whale may be located have been delineated and are presented in Figure 41

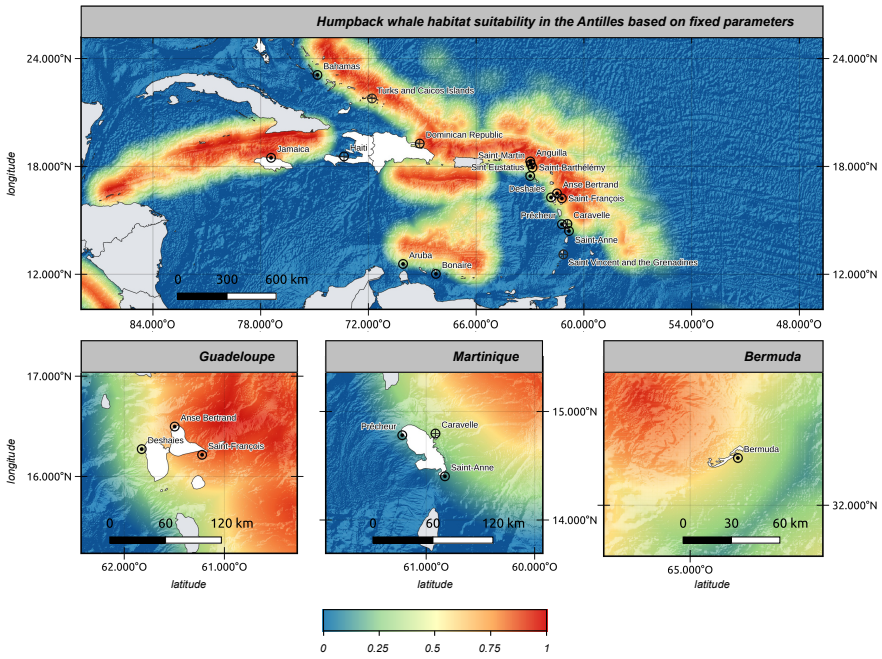


Figure 41: Predicted habitat suitability using the combination of the distance to the 5000 meter depth and the distance to the shore.

The distribution of the species is indicated on the map, which shows its presence throughout the Bahamas, along the Dominican Republic and in proximity to Jamaica, as well as along the Caribbean until Martinique. In the Caribbean Sea, the potential breeding areas are less pronounced, with evidence of presence in Aruba and Bonaire, as well as south of Puerto Rico.

Contributions

- The total number of units collected between 2021 and 2022 in the various regions was **659,222**;
- The maximum detection rate per hour of recording was measured in Guadeloupe Anse Bertrand, with a rate of **over 1,000 detections per hour**;
- A **strong negative correlation** was measured between the **detection rate per hour and the distance of a station to a depth of 5,000 m**;
- A map of the potential breeding area was proposed based on the observations.

6.2 HABITAT COMPOSITION FOR BIRDS IN QUÉBEC

Following the execution of the model over the data of the PAM in Québec, and the subsequent filtration of results based on each species' threshold, a total of 22,641,658 detections were obtained, distributed across 125,240 files from 254 station. In addition to the 3,853 hours of recordings conducted in 2020 (Figure 42), a total of 504,218 detections were made, amounting to approximately 4.5 million in 2021, 2022 and 2023 (25,487, 29,027 and 35,808 hours of recordings, respectively) and ultimately reaching 8.16 million in 2024 (53,893 hours of recordings). The present study revealed that all species were detected at least once. The most frequently detected species was the White-throated sparrow (*wtsp*), with 3,382,170 detections (15%), while the least frequently detected species was the Scarlet tanager (*scta*), with only 410 detections.

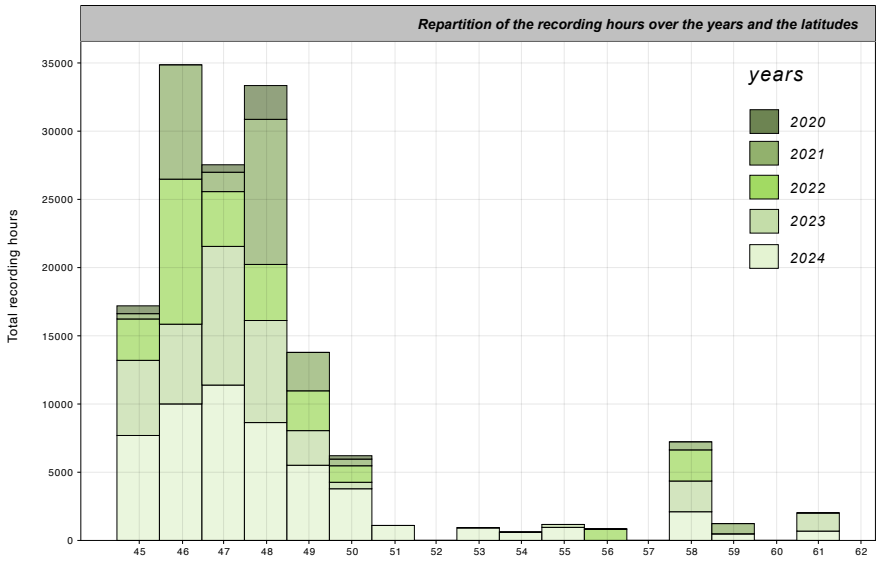


Figure 42: Distribution of the total recording time in hours for each year, depending on the latitude of the station

In order to analyse the avian species present and their relationship to the fixed parameters, the following factors must be taken into consideration: the presence or absence of the birds at different latitudes at the stations, the altitude at which the birds are found, and the different habitats in which the birds are present. As illustrated in Figure 43, the regression analysis of the data from 2020 to 2024 reveals a negative correlation between the detection rate and latitude. This indicates that as the latitude increases, the detection rate decreases. Subsequently, a high correlation was measured, yielding a highly significant Pearson R value of 90% ($p\text{-value}<0.001$). From Figure 44, which illustrates the density of detections per hour across the various stations, it is evident that there is a notable increase in avian activity between the 18th and 28th weeks of all years. Furthermore, this

activity coincides with the migration path from southern latitudes to Québec.

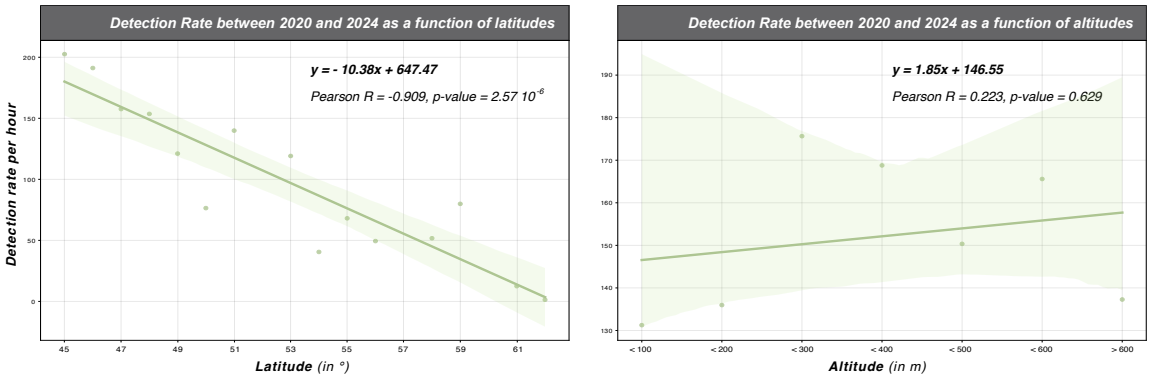


Figure 43: Linear regression between the detection rate and the latitudes (a.) and altitudes (b.).

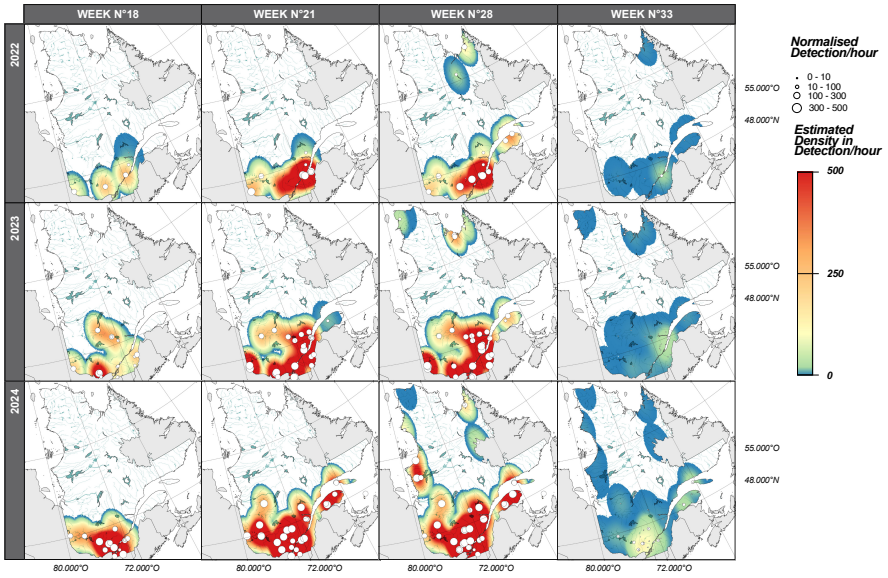


Figure 44: Evolution of detection density per hour of recording across Québec between weeks 18 and 33 of 2022, 2023 and 2024.

However, an analysis of the detection rate per hour of recordings in relation to the altitude of the stations reveals no discernible correlation. As the preceding results analysis have been conducted on a global average, accounting for all species simultaneously, it is acknowledged that species habits may vary between species. For instance, some species are more likely to be present at high latitudes, while others remain at lower latitudes. A species-specific analysis was conducted on the ovenbird, a species that was detected 1,009,992 times between 2020 and 2024. The analysis revealed a preference for forested habitats located between 45 and 48° of latitude (Figure 45). However, observations of the detection rate in relation to altitude

within this geographical area have not yielded results that can inform hypotheses regarding altitude preferences, such as Ovenbird (*oven*) who was detected at every altitude.

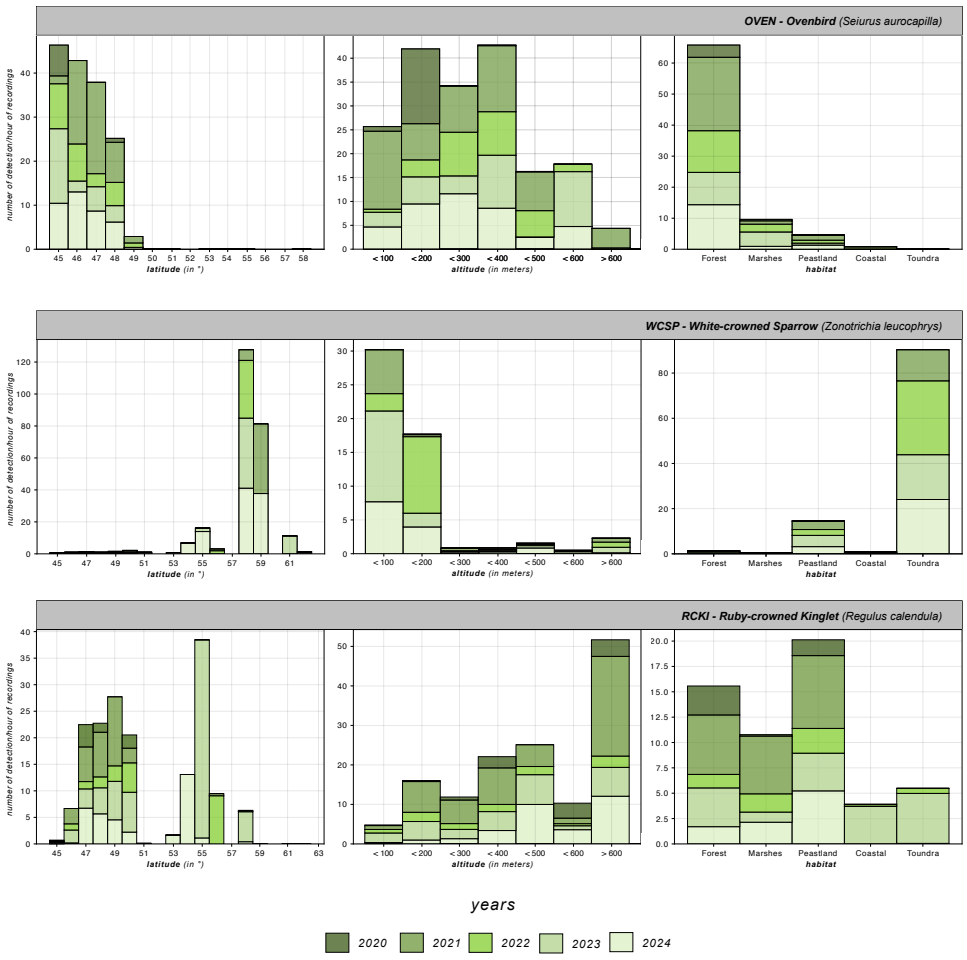


Figure 45: Preferences for latitude, altitude and habitat of the three sample species (OVEN, WCSP and RCKI) between 2020 and 2024.

In contrast, the white-crowned sparrow (*wcsp*), which was detected 387,398 times, exhibits a marked preference for peatlands and tundra. Furthermore, the majority of detections were made between 55 and 61° latitude, with a maximum at 58°. With regard to altitude, almost no detections were made at altitudes above 200 metres. A comparison of the years under consideration reveals that the detection rate is higher at latitude 59° during 2020, while it is at 58° during 2022 and 2023.

Finally, the Ruby-crowned kinglet (*rcki*) species, detected 523,158 times over the course of this recording period, does not exhibit specific preferences over the years. Despite the apparent affinity for higher latitudes, the species was observed in a wide range of habitats, span-

ning from 46° to 55° latitude, thus demonstrating a substantial ecological breadth.

Contributions

- A total of **22 million bird detections from 27 species** were collected;
- An analysis of the calling rate for each species, depending on latitude, altitude and habitat, revealed that each species exhibited different preferences.;
- A **strong negative correlation** was measured between the **call rate and the latitude**, as all species do not migrate to the Arctic region.

6.3 IMPORTANCE OF BATHYMETRIC CHARACTERISTICS FOR THE SPERM WHALE IN THE MEDITERRANEAN

An analysis of the distribution of observations across various geographical areas reveals that the majority of observations are made within a 10-kilometre radius of a canyon (Figure 46). A more precise analysis of the data revealed that 85 of the 232 observations were conducted within 1.5 km of a canyon (i.e. inside or less than 1.5 km away). In terms of canyon size, 39 were found in a canyon smaller than 250 km², 36 in a canyon between 250 and 500 km², and 10 in a canyon larger than 500 km².

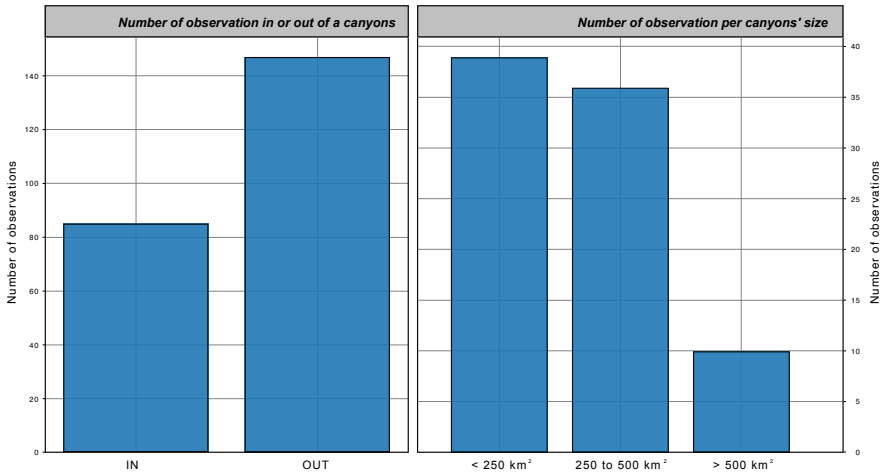


Figure 46: Number of sperm whale observations inside a canyon (with a 1.5km range around) compared outside (left) and the details of the canyon' surfaces (right)

Figure 47 illustrates the fixed parameters derived from the GEBCO. The rugosity and slope exhibit a high degree of similarity in terms of representation on the map. The bathymetry, on the other hand, delin-

eates the continental shelf in red and the deep sea in blue. The emplacement of the high slope and rugosity corresponds to the decrease in depth. Furthermore, the distance to canyon map demonstrates the proximity between the coast and canyons, as these geological structures are predominantly formed by erosion.

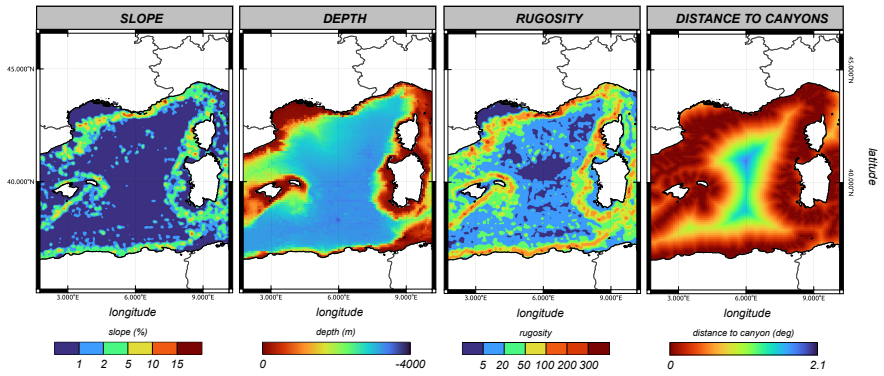


Figure 47: Fixed parameter maps with slope (a) depth (b) rugosity (c) and distance to canyons (d) in the western basin of the Mediterranean

When computing a MaxENT model using only one fixed parameter, it is possible to identify the major contributor. As presented in Figure 48, the AUC for the OBIS dataset attained 87.3% using depth only, with the optimal depth value recorded as 540 m and the optimal range between 200 and 2500 m.

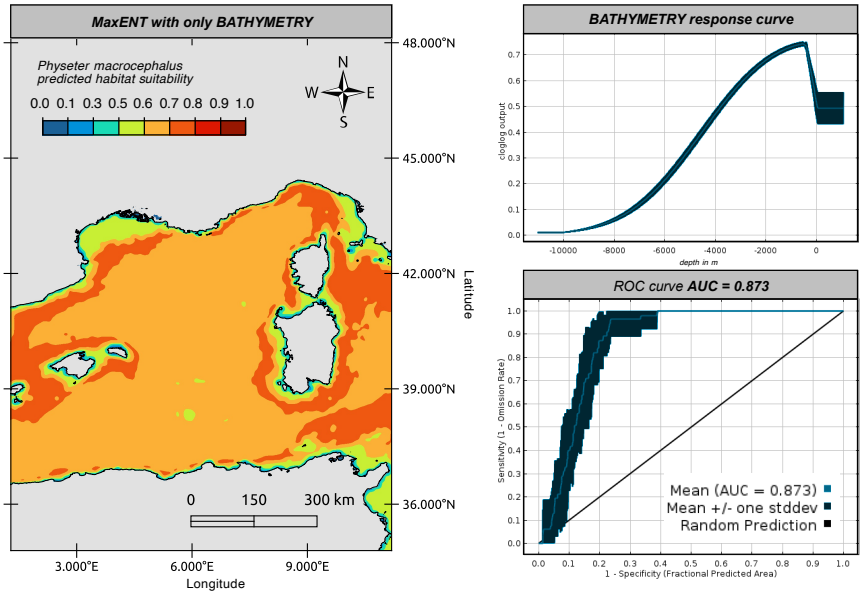


Figure 48: MaxENT model projection using the bathymetry, with the response curve and its ROC AUC over the test set OBIS.

As shown in Figure 51, the implementation of a slope-based model resulted in an AUC of 81.5% over the OBIS dataset, substantiates the hypothesis that the probability increases under the condition that the slope is not equal to zero. The resultant figure is analogous to that of the rugosity-only model, as illustrated in Figure 49, exhibiting an Area Under the Curve (AUC) of 84.9%.

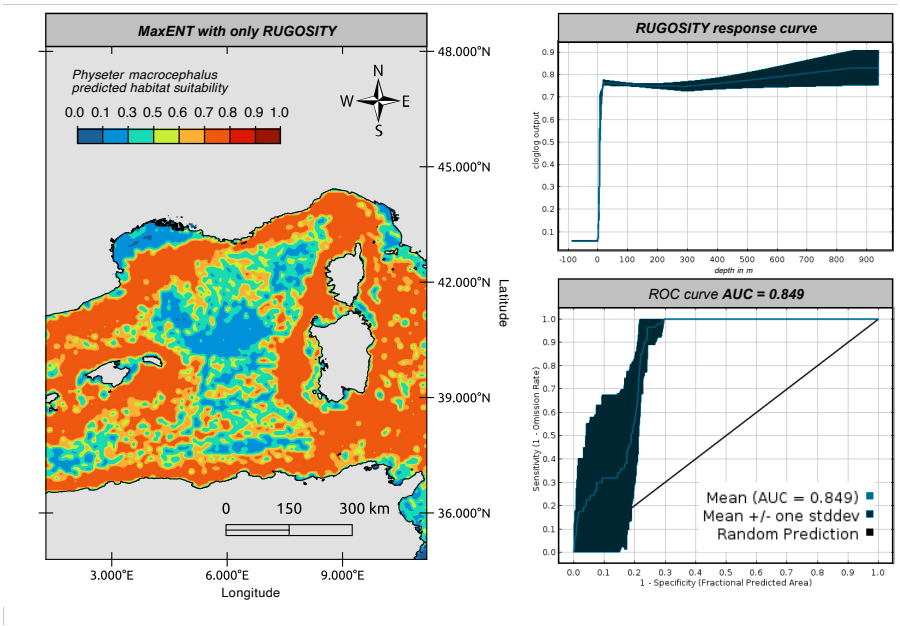


Figure 49: MaxENT model projection using the rugosity, with the response curve and its ROC AUC over the test set OBIS.

Nevertheless, in comparison with all models comprising a single variable, the one that yields promising results is the one in which the distance to the canyon is the sole variable presented in Figure 50. The area under the curve (AUC) of the probability of sperm whale presence, as determined by the OBIS dataset, was found to be 94.1%. This suggests a relationship between the probability of sperm whale presence and distance to a canyon. A decrease in probability was observed as the distance to a canyon increased, with a 1-degree (110 km) margin being reached at which the probability was almost zero. The maximum probability of occurrence is observed when the distance to a canyon is approximately 0.07 degrees (approximately 7 km).

The combination of all the parameters and the execution of the same model resulted in the attainment of a mean AUC of 91.6% over the OBIS dataset. The map resulting from the implementation of the aforementioned model is presented in Figure 52 . The contributions of each parameter in combination are presented in the following jackknife figure. As demonstrated in the preceding analysis, the distance to the canyon is a significant contributing factor, accounting for 24% of the total variance. However, it is estimated that the major parameter is the slope, with 58.4% of the contribution. It is imperative that

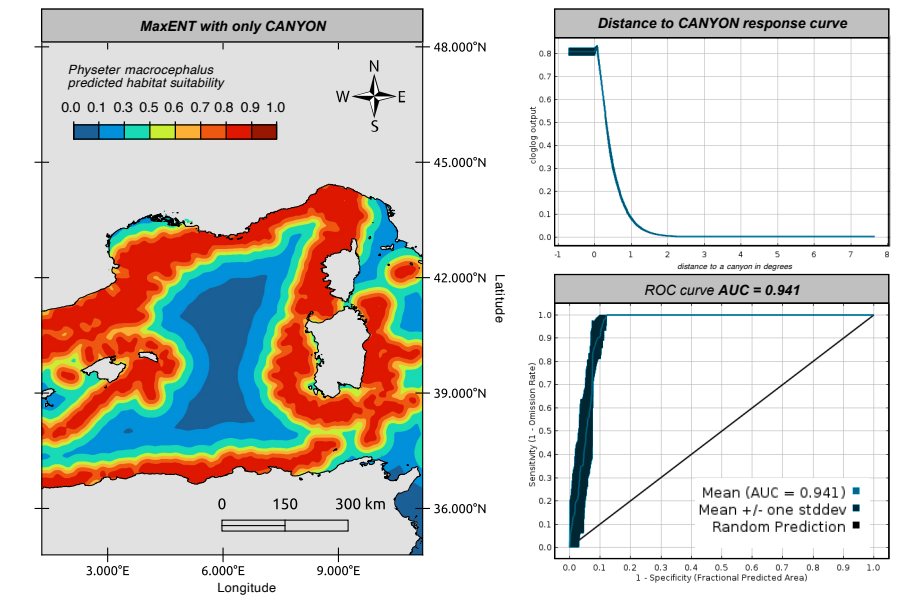


Figure 50: MaxENT model projection using only the distance to canyons, with the response curve and its ROC AUC over the test set OBIS.

the results of this study are interpreted with caution, given the correlation between the slope and the canyons. However, both roughness and bathymetry contributed to a maximum of 12.8% and 4.8%, respectively, which were the least significant contributors.

The use of observational data to predict the habitat suitability of sperm whales in the Mediterranean has revealed that a significant proportion of the observations were conducted in the proximity of canyons. Subsequent analysis, employing a MaxENT model with all fixed parameters, has substantiated this observation and has further demonstrated that the probability increases within the initial 10 km radius of a canyon before decreasing. It appears that canyons, characterised by high slopes and significant roughness, offer a comprehensive explanation for a substantial proportion of the observed phenomena in the Mediterranean region. Consequently, our research will concentrate on canyons as a primary subject to facilitate a more profound comprehension of these observations. As the observations were conducted in the vicinity of the Stoechades Canyon, this particular location will serve as the focal point for the ensuing analysis of dynamic variables.

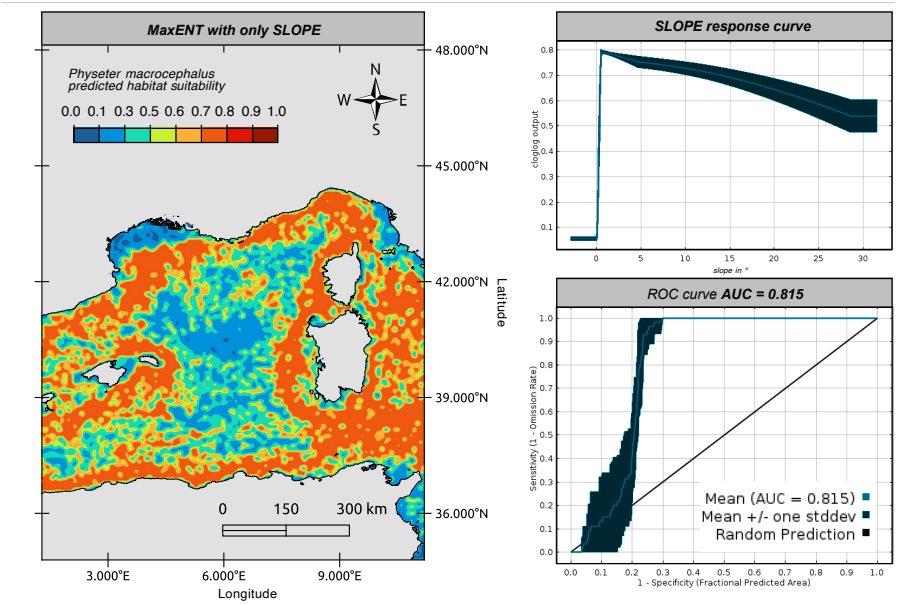


Figure 51: MaxENT model projection using the slope, with the response curve and its ROC AUC over the test set OBIS.

Contributions

- Over the 232 diving observations, **85 were done inside or at least 1.5km away from a canyon**;
- With four fixed parameters, we obtain an **AUC of 91.6% over the OBIS dataset** with as a major contributor the **slope** (54%) and the **distance to a canyon**(24%).

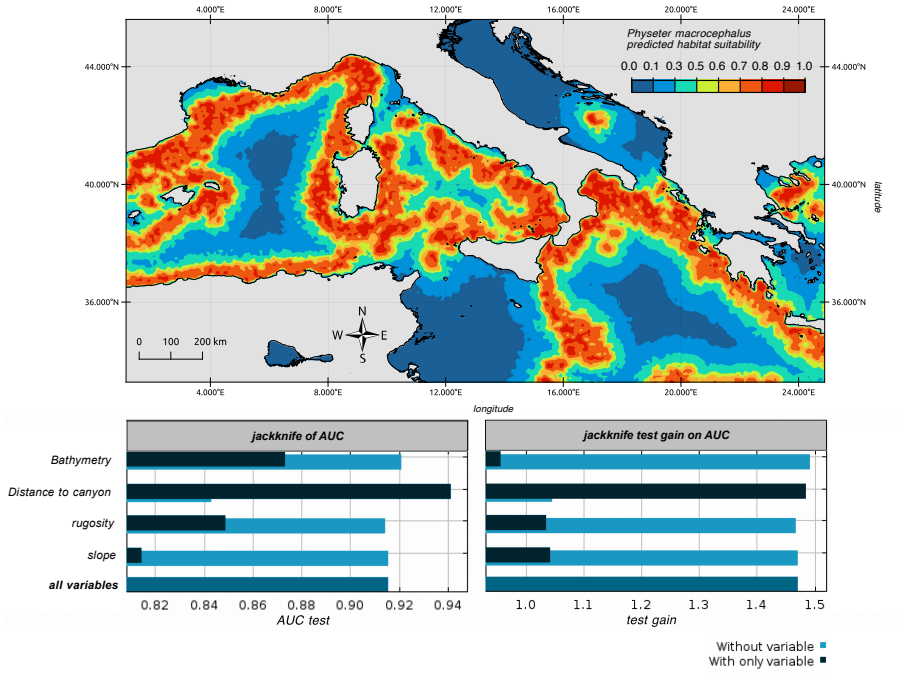


Figure 52: MaxENT model projection using all four fixed parameters, with the jackknife representation of the AUC and gain of each parameters.

6.4 DISCUSSION

6.4.1 *Habitat preferences*

6.4.1.1 *Humpback Whale*

The results of the present study indicate a clear preference among humpback whales for islands situated in close proximity to deep waters. Studies conducted on the feeding grounds have also observed a correlation between the presence of the species and bathymetric features, particularly the slope and the distance to the 100-m isobath [173]. This finding, when considered in conjunction with the observed parameters, yields a map that exhibits a high degree of consistency with the observed data. Indeed, it is evident that the Caribbean region, which is situated adjacent to the Atlantic Ocean, constitutes a suitable habitat for humpback whales. Furthermore, the Dominican Republic and Jamaica have been identified as regions within the Caribbean where the presence of humpback whales has been documented [97]. Nonetheless, analysis of this parameter revealed that the habitat is conducive to cetacean habitation in Aruba and Bonaire, despite the rarity of observations in these locations [174]. These results suggest that further parameters should be considered when assessing habitat preferences.

Our detection results showed that peak detection in Bermuda occurs between late February and mid-March, with almost no detection in May. This is consistent with the previous description in this area [175] *i.e.*, a maximum detection rates in late February or the beginning of March. A more recent study analysed a decade of humpback whale sighting in Bermuda, from 2010 to 2020, and found that the maximum sighting generally occurs in March [176]. It is also said that Bermuda is a stopover zone during migration [175, 176] which means that humpback whales, coming from Iceland, Norway or Northern Canada, stop here for a reason as yet little understood, before going down to the Caribbean. Our study observations show that humpback whales are present in the Caribbean Sea as early as mid-January on specific islands. Furthermore, in early February 2022, a 6-hour passage of humpback whales was recorded in the Bahamas. This shows that there are several migration routes, with passage zones, stopovers zones, and destinations, as mentioned in previous studies [177]. The literature also corroborates that maximum period of presence in the Caribbean is observed in late March to early April, with a decline in May [98], which is consistent with our measurements. In previous studies, it has been shown that peak detection occurs in mid to late February in Anguilla meanwhile it is in April that the peak occurs in Guadeloupe [97]. This difference in dates can be explained by two phenomena, firstly the North Atlantic population migrates from the north to the south [178] creating an arrival delay between the islands located at the highest latitudes and those further south, and secondly the two segments of the North Atlantic population are estimated to migrate within 6 weeks of each other [179] and seem to have their own preferred breeding grounds with for the North West segment tending to frequent the high latitudes of the Caribbean (Anguilla in particular) and the North East segment tending to visit the low latitudes of the Caribbean (below Antigua *i.e.* 17°N). The consistency between our passive acoustic approach and previous knowledge of migratory routes confirms the efficiency of this technique to monitor soniferous animals.

6.4.1.2 *Birds of Québec*

When analysing the avian species' preferences, a strong negative correlation was observed between their singing activity and latitude. Indeed, the singing activity has been demonstrated to be closely related to their densities [180]. In consideration of the aforementioned results, it can be assumed that avian densities are diminished in Arctic regions. Nevertheless, it is important to note that this result should be regarded as a generalisation rather than a specific observation. The data revealed a tendency for certain species to be found at higher latitudes, while others were observed only in lower latitudes, and some were present in all latitudes. The tendency of a species to demon-

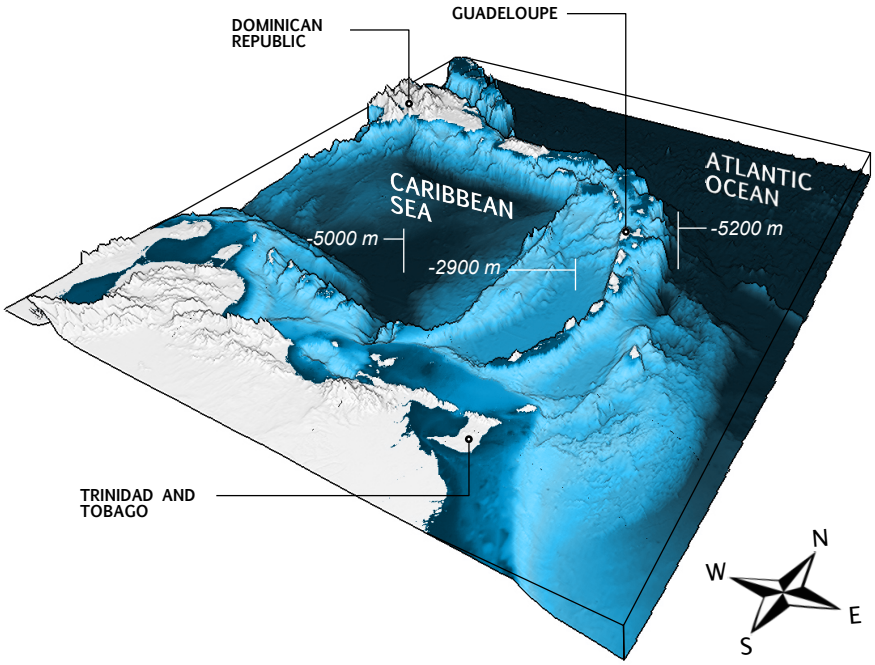


Figure 53: Three-dimensional representation of the Caribbean region incorporating bathymetric information.

strate a preference for a specific region or location can be directly associated with the availability of food resources in that area. It is an established fact that certain species of bird, for example woodpeckers, have developed feeding strategies that exploit specific prey types that inhabit only older trees [181]. In addition, some waterbirds will prefer aquatic invertebrates that are more prevalent in aquatic biomes. As previously outlined, the White Crowned Sparrow (*wcsp*) was presented, and the results obtained demonstrated a clear preference for high latitude and tundra habitat, thus indicating a preference for Arctic habitats. This finding is consistent with the conclusions drawn in the preceding literature [182]. This species is distributed extensively throughout the United States throughout the year. However, it undergoes migration from the southern reaches of Québec to the higher latitudes, including the Arctic regions (see [182]).

The second example, the Ruby-crowned Kinglet (*rcki*), exhibited no discernible preference for specific habitats or latitudes. Its presence was documented in a variety of habitats, with the exception of Arctic regions. Nevertheless, an examination of the extant literature reveals that the study of this species remains challenging due to its nesting habits [183]. Observations of the species in question have revealed a preference for nesting in high and old coniferous forests, a characteristic that is particularly pronounced in the boreal region [184]. As

demonstrated by the high detection rate obtained at 55° latitude and the high detection rate in the forest habitat, the collected data has been confirmed. In addition, the aforementioned paper analysed the different habitats of *rcki* and concluded that the species is more generalist [183, 184]. This finding is in accordance with the results observed in the present study. It is evident from the results that there is a general tendency for the species to be found at higher latitudes. As the species has a marked preference for coniferous trees, and given that the cover of these trees is decreasing in the Boreal region as altitude is reduced [185], the search for these forests has led to higher altitudes, as was observed in the results.

In the final example, the Ovenbird (*oven*) exhibited a marked preference for forests in the low-latitude regions of Québec, situated between 45 and 48°N. This observation indicates the presence of a geographical area characterised by restricted access, situated within the lowest regions of Québec. The area in question is typified by the presence of temperate mixed forests and deciduous woodlands. As with the preceding species, we encountered literature investigating their habits, with the present paper proposing *oven* as "a common member of the deciduous forest breeding bird community in North America" [186, 187]. Moreover, the avian species under consideration is demonstrated to possess a breeding ground that extends from the central regions of the United States of America to the lower latitudes of Québec [186]. The congruence between the earlier documented observations and the results of our study indicates that the model we developed attains a satisfactory degree of accuracy in the study of avian species in diverse habitats during the breeding period. Nonetheless, the use of geographical parameters such as latitude, altitude, and vegetation zones alone is inadequate for predicting migratory patterns. The prediction of such phenomena is further complicated by the influence of other variables, including temperature and photoperiod, which have been shown to impact migratory behaviour [55].

It has been observed that each species exhibits a distinct preference for a particular habitat. This observation highlights the importance of conserving natural habitat diversity to ensure the biodiversity of avian species is maintained [188]. Indeed, the study also revealed the potential effects of habitat fragmentation, which constitutes a component of human impact on the environment. It is evident that certain forest types have been subject to modification due to agricultural practices or forestry activities [185, 189]. This has resulted in variations in species composition or abundance. It has been demonstrated that certain species are capable of adapting to a variety of habitats, as evidenced by the behaviour of generalist species. However, in response to alterations in the environment resulting from human modification, some species may be compelled to modify their breeding ground in order to avoid areas of altered habitat. This has been previously ob-

served in the context of a comparison between the response of natural fire and that of logging [189]. These phenomena are of particular importance in Canada, and also in Québec. The findings of this study indicate that the abundance and diversity of bird populations are influenced by the duration of logging rotations. Furthermore, it has been demonstrated that areas of forest that have been subjected to fire provide a habitat for certain species that have the habit of nesting in burned logs. Consequently, it can be hypothesised that the logging of these trees may result in the displacement of these species. On a global scale, the process of logging is carried out at a time scale that may be both shorter and more recurrent than fire. It is important to note that this activity has the potential to induce variation in species composition in certain areas.

6.4.1.3 *Sperm whale*

The analysis of diving observations of sperm whales in a limited area, encompassing the region between Marseille and Nice, facilitates the generation of a map illustrating the potential habitat suitability of the entire Mediterranean Sea. Nevertheless, as previously stated, these parameters continue to account for a significant proportion of the observations, albeit with reduced precision. This finding indicates the necessity for more refined parameters. Indeed, with an AUC of approximately 91% of the OBIS dataset, the areas predicted as potentially interesting are all located along the coast. This is in contrast to the predictions that have been previously published in the literature [145]. Moreover, the model demonstrated that the optimal depth was identified as approximately 500 metres, a finding that aligns with the results of prior studies [146]. However, given that depth has been proven to be a reliable predictor of results, as evidenced by previous research [85], which is based on the foraging behaviour of the sperm whale, the observed depth was comparatively low in relation to the contributions of the canyons and slope. This significant contribution has already been expressed in the state of the art in studies carried out around the globe [88, 89].

6.4.2 *Detecting only songs can reduce the predicted densities*

As the implications of the parameters in the elaboration of potential habitat preference maps are discussed, it is important to consider the potential bias of the measurements taken. It is evident that the training set for the birds and humpback whales comprised exclusively of songs. As demonstrated in the preceding analysis of humpback whale data, the model demonstrates proficiency in generalising across a diverse array of recordings from disparate regions. However, the exclusive detection of this particular aspect of communication may result in the exclusion of a substantial proportion of the total sounds pro-

duced. In the context of humpback whales, the deployment of detection call units separate from song units would facilitate the identification of habitat preferences for singing males and females with calves. In the context of ornithology, the capacity to detect specific calls, such as those associated with avian migration, has garnered significant interest. This includes the use of auditory stimuli, such as the so-called "flying call" [50, 190], to delineate the migratory pathways of birds.

6.4.3 *Sperm whale sampling bias*

The research protocol that was implemented with the objective of studying sperm whales involved the use of acoustics to locate and monitor their dives, and even follow individual specimens to study their behaviours. Whilst the majority of studies that seek to estimate the habits of species tend to do transects [145], this was not the case in the present study. However, the results obtained were consistent with the existing literature, as it was found that canyons and slopes are significant parameters for the presence of sperm whales. In order to circumvent the possibility of bias arising from the protocol, a bias layer is employed. The presence of the bias layer had a marginal impact on the outcomes. The absence of the layer, as illustrated in Figure 54, appears to exhibit over-fitting to the data from our observation. This phenomenon results in a minimal potential area and elevated confidence levels exclusively in the regions where the input data is available.

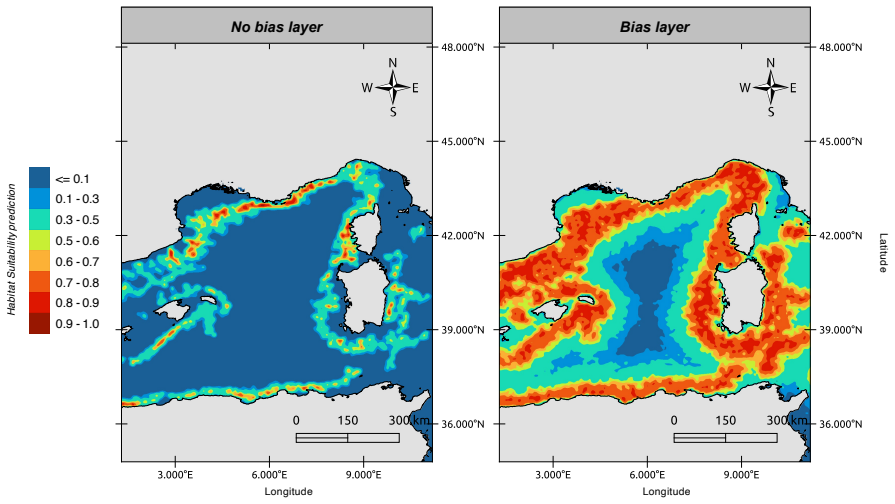


Figure 54: Comparison between a MaxENT model without bias layer (left) and with (right) using only fixed parameters.

This observation lends further support to the notion that the bias layer plays a significant role in this particular type of analysis when MaxENT is employed in the context of biased sampling effort. Furthermore, as illustrated in the prediction map, the confidence in the

proximity of the slope of the Golf of Lion is high, while observations in the OBIS dataset are limited. It is possible to provide a justification for these results within the context of two hypotheses. Firstly, it is observed that the fixed parameters employed in this study are insufficient for the purpose of predicting habitat suitability. Secondly, the area is deemed suitable, yet the number of scientific missions capable of conducting surveys in this region is limited. This may be due to the meteorological conditions, which are often more challenging due to stronger winds and waves than those experienced along the coast between Marseille and Nice, or the Balearic Islands.

7

RELATIONS BETWEEN DETECTION AND LONG TERMS DYNAMIC PARAMETERS

7.1 Humpback whale presence 108
7.2 Seasonal variation of humpback whale vocal repertoire 114
7.3 Sperm whale suitable habitat 117
7.3.1 Importance of surface and deep parameters . . 117
7.3.2 Increasing human pressure 121
7.4 Seasonal changes for birds migration in Québec 123

As demonstrated in the preceding chapter, the prediction of a species' potential habitat is feasible with a limited number of fixed parameters. However, it should be noted that the resulting maps merely indicate the location, rather than providing insights into the temporal aspect, particularly in the context of species that undergo migration. As has been previously outlined, a multitude of variables have the capacity to exert influence over the phenomenon of migration. Moreover, the objective of the aforementioned migration is also a contributing factor. It is important to note that for sperm whales, food resources represent the most significant parameter [85]. The analysis has facilitated the prediction of potential fixed parameters that contribute to their presence. Nevertheless, the resulting map does not provide clear evidence regarding the extent to which the Mediterranean Sea is favourable, or whether this is the case for a specific region only. However, in the case of humpback whales, a greater reliance is observed on areas that are both safe and calm. In this chapter, the impact of dynamic parameters will be examined through a two-pronged approach. Firstly, parameters that are anticipated to undergo long-term evolution, typical of seasonal fluctuations, will be delineated. Secondly, parameters that are expected to exhibit variation across the entire duration of the survey, but not necessarily over the course of a single day, will be identified.

Key points

In this chapter, we used GAMs with dynamic parameters for birds and humpback whale and the main results are :

- The **optimal temperature** for the breeding ground of humpback whales is approximately **26°C**, while temperatures above 27°C have been shown to result in the absence of whales;
- The produced model was used to predict migration, with a good accuracy;
- The **activity of birds singing is highly dependent on the photoperiod and the temperature** of the breeding
- A Generalised Additive Model (GAM) was used to predict the abundance of birds during the breeding season in Québec, with latitude, temperature and week of the year (linked to the photoperiod) being the independent;
- **Sperm whales have been observed to be present near canyons** that are also close to the major current of the area;
- The Sea Surface Height (SSH) map between May and October is close to the predicted habitat suitability of sperm whales.

7.1 HUMPBACK WHALE PRESENCE

The construction of a GAM was achieved by using a range of environmental parameters, including temperature, salinity, and chlorophyll concentration. As outlined in the methodology, the mean detection per island was calculated on a weekly basis, with the mean of the variable parameter for the same week used as a reference. The response curve of each parameter resulting from the model is presented in Figure 55.

The model's Akaike's Information Criterion, denoted AIC, reached 2406, with a R2 of 0.53. The temperature is found to have the greatest contribution, with an effective degrees of freedom (EDoF) of 11.2 and a significant p-value. The salinity variable is found to have an EDoF of 10.1 ($p\text{-}value > 0.1$), while chlorophyll-a has an EDoF of 7.1 ($p\text{-}value > 0.1$). Mixed layer depth is found to have an EDoF of 6.9 ($p\text{-}value > 0.1$). A more detailed analysis of the temperature data reveals a clear distinction between two distinct temperature ranges: 25.5°C and 28.5°C. The model predicts that the likelihood of recording a humpback whale is minimal in an area where the temperatures is above

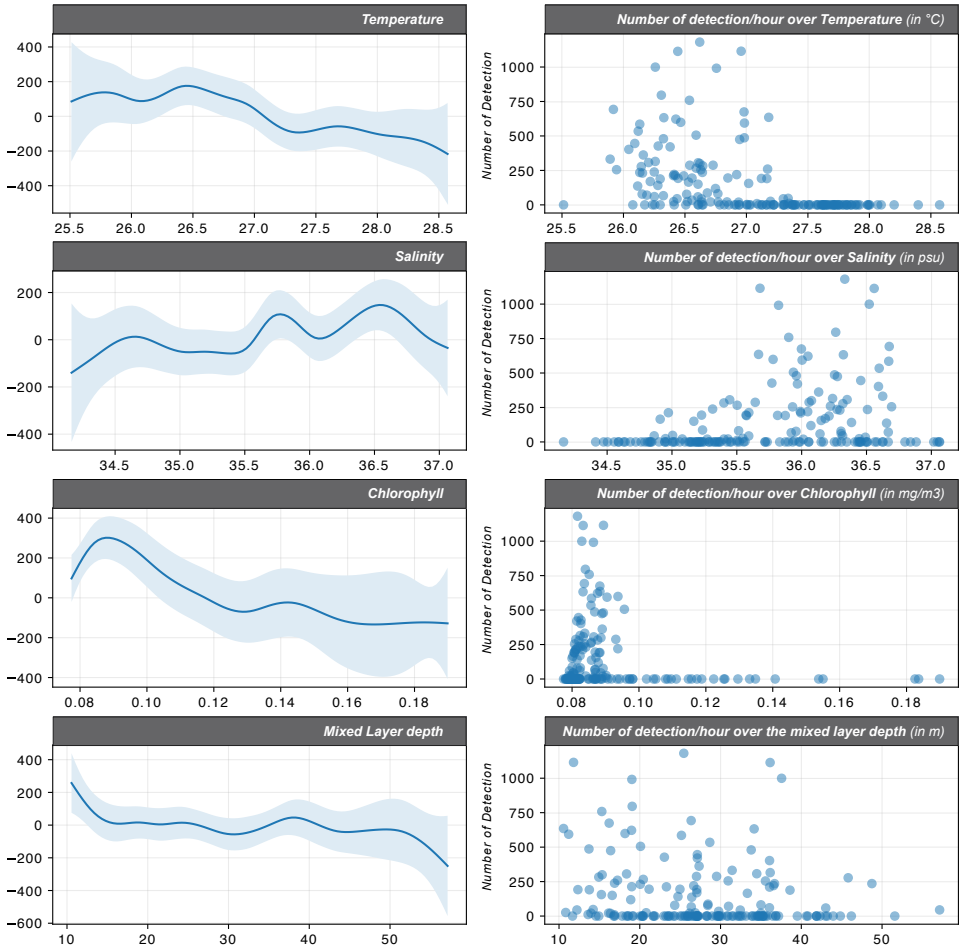


Figure 55: Results of the humpback whale GAM with the response curves of its components. : The y-axis of the graph represents the impact of the corresponding parameter on the number of detections. In the instance of a positive response, the number of detections is increased, whereas in the negative instance, it is decreased.

27.1°C, while the probability increases significantly around 26.4°C. With regard to the salinity, the impact on the humpback whale is negligible at low levels. However, chlorophyll-a concentration above 0.12 mg/m^3 has been shown to have a negative effect. It is also notable that the mixed layer depth does not appear to have a significant impact, as evidenced by the low EDoF and the subsequent curve.

The Figure 56 presents the variation of the chlorophyll-a concentration between January and June. The results indicate that the concentration across the Caribbean is minimal, with the exception of the waters originating from the Amazon River, which exhibit a high degree of concentration and extend as far as Grenada Island in the southern Caribbean. Should the chlorophyll-a concentration prove deleterious

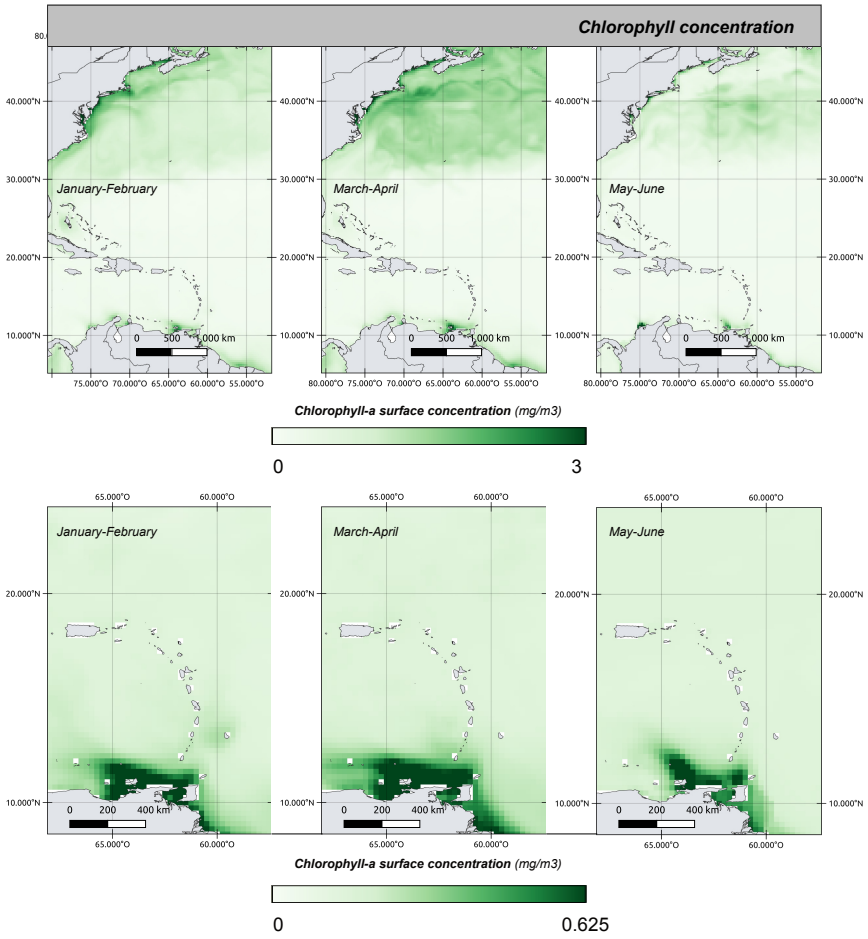


Figure 56: Chlorophyll-a concentration over 3 periods of time in the Northern Atlantic (top) and the Caribbean (bottom).

to the humpback whale, it should result in their absence in proximity to such patches.

With regard to the salinity levels, it is observed that these levels tend to impact the presence of the species in areas of low salinity. A seasonal variation across the Caribbean is evident, with a decrease in salinity between March and May, which is particularly pronounced in June, as illustrated in Figure 57.

Upon analysis of the mixed layer depth, it was observed that this parameter did not appear to have any impact on the humpback whale, as evidenced by the GAM. The depth of the mixed layer was found to be more pronounced in the months of March to April, and conversely, it was observed to be less deeper in the water columns during the months of January to February and May to June.

Finally, the most effective parameter is observed to demonstrate strong seasonality, with elevated temperatures recorded after the month of April. Globally, temperatures are lower in March and April than in other months, with most stations recording temperatures below

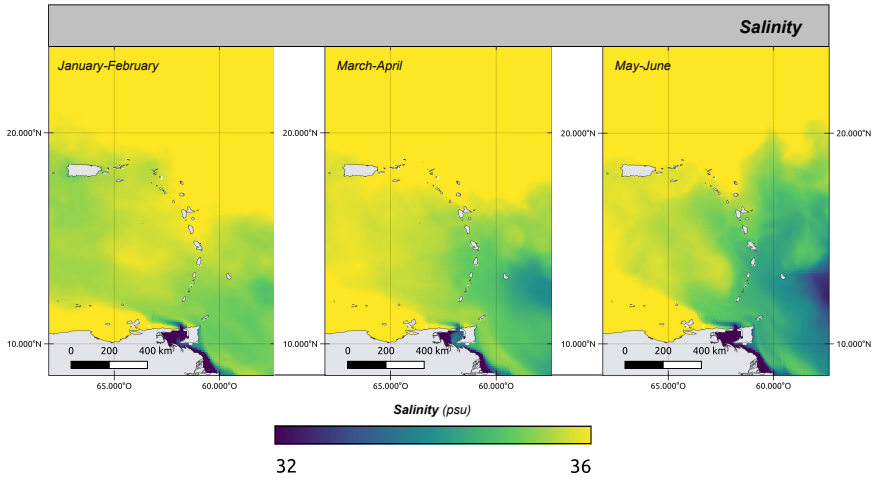


Figure 57: Surface salinity evolution over 3 periods of time in the Caribbean.

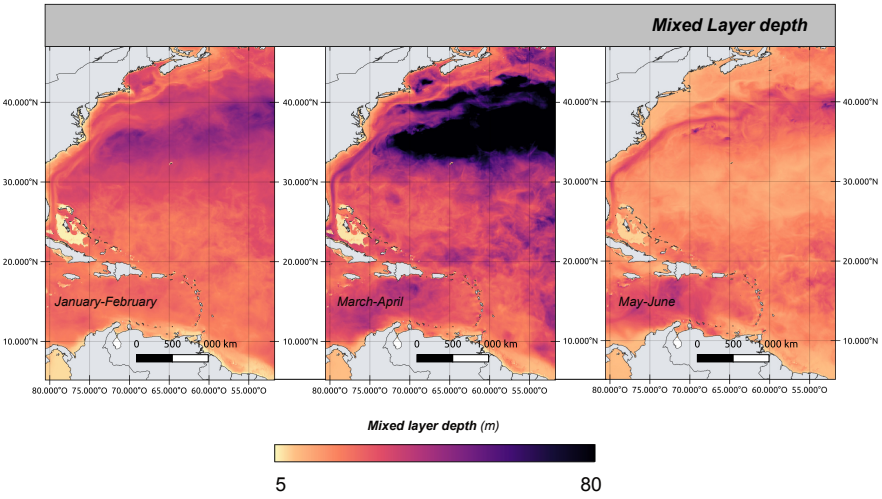


Figure 58: Mixed layer depth over 3 periods of time in the Caribbean.

27°C. However, the islands situated to the south of the Caribbean archipelago exhibit higher temperatures. It is notable that the maximum temperature recorded for a breeding ground is 28°C, and 27.1°C was the result obtained in this study. This indicates that the temperature in May and June is excessively high for most islands in the Caribbean, potentially influencing the migration patterns of the species.

The use of the aforementioned model for the duration of a breeding season enabled the prediction of maximum detection over the course of a year, with the daily oceanic conditions being entered into the model. As illustrated in Figure 60, there is a notable decrease in the number of possible humpback whales in the area during mid-December, followed by a significant increase in the number observed

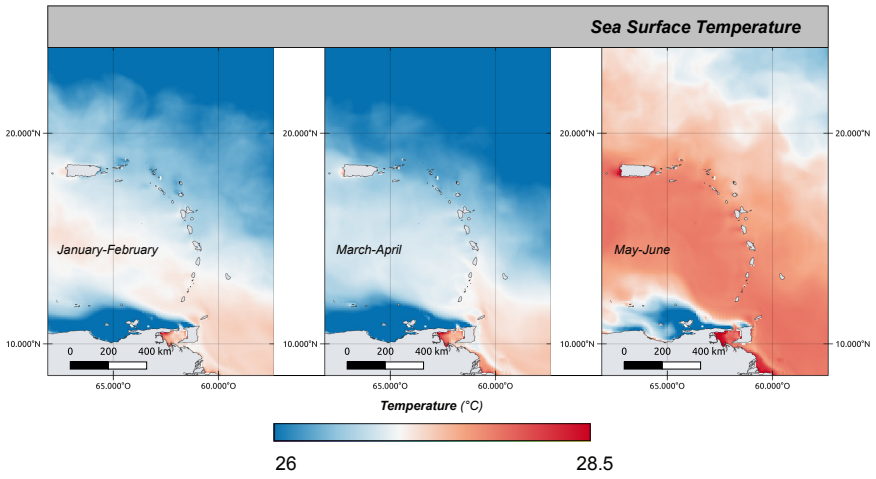


Figure 59: Temperatures over 3 periods of time in the Caribbean.

in early April. By the end of June, the predicted detection rate per hour is minimal in the Caribbean, but high in higher latitudes, above Bermuda, which corresponds to the route between the breeding and feeding areas.

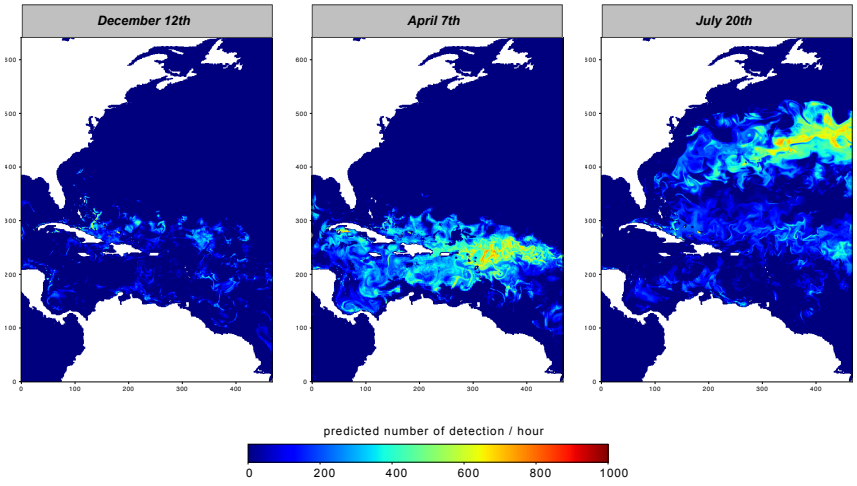


Figure 60: Results of the prediction of humpback whale distribution on December 12th 2021 (a), April 7th (b) and June 20th (c), using the Generalised Additive Model (GAM)

Moreover, as is evidenced by the present study, the season for each location can be predicted on a daily basis. Consequently, Figure 60 presents the potential detection rate for the 2021 breeding season, calculated by averaging the mean of all days for each week. As illustrated in Figure 61, the calendar exhibits a high degree of similarity to the one observed in the real data Figure 38. The maximum detection of the phenomenon occurs around Guadeloupe, while it is low in the lowest latitudes, such as Martinique. The onset of the season

is anticipated to occur in the Bahamas, with a subsequent development in Saint Martin. It is observed that there is a delay between the northern and southern stations in terms of the first positive week and maximum. As the maximum is recorded at the beginning of March for high latitudes (above 17°), it occurs in mid-April for the lowest in Guadeloupe and even in Martinique. For all stations, the termination of the season is predicted to occur in mid-May. Nevertheless, a discrepancy was observed between the original results and the predicted outcomes for Bermuda. Indeed, the results demonstrate a high prevalence of detection throughout the entire breeding season. This is attributable to the fact that the location functions predominantly as a migratory stopover point as opposed to a breeding area. In this particular instance, the prediction indicates that the conditions will be favourable after June, at a time when conditions in the Caribbean are not conducive to this activity. The present study establishes a correlation between the resultant data and the map presented previously (Figure 55). The analysis revealed that the optimal conditions are shifting from the Caribbean to higher latitudes as the season comes to a close.

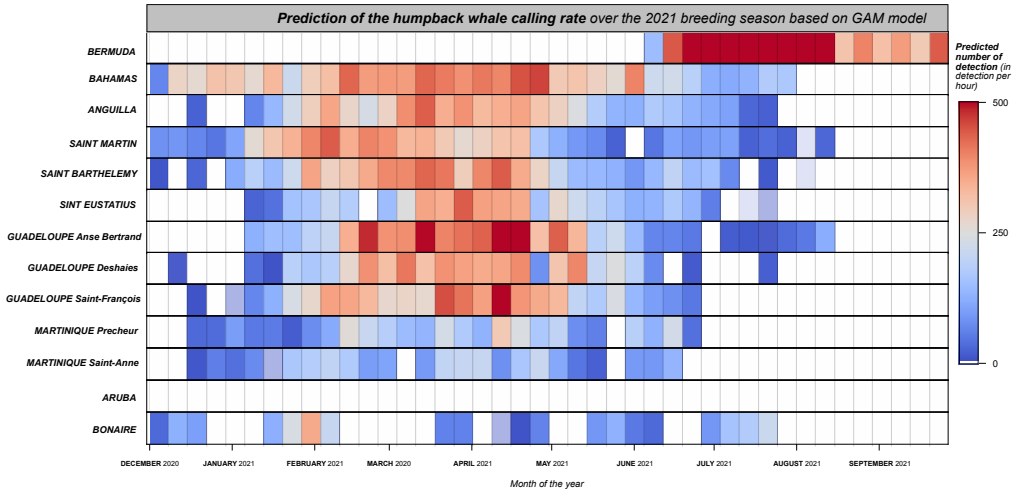


Figure 61: GAM estimated call rates of humpback whales throughout the entire breeding ground during the 2021 breeding season and until the end of September.

The findings of this study indicate that a substantial number of effective parameters have been identified for predicting the presence of humpback whales. However, there remains a component that has not been incorporated into the prediction model to detect the end of the season. Nonetheless, by using the GAM approach, we were able to successfully predict areas where humpback whales were not detected or where detections were sparse. For instance, in Martinique, favourable conditions prevail over a shorter period, from February to the beginning of May, exhibiting high variability during the month,

with detection rates ranging from 0 to 400 per hour. This is analogous to the observations documented in the data. Conversely, in Aruba, no humpback whales were detected, and the model did not detect any either, as the conditions were not conducive to detection. The optimal temperature range for this species is reported to be between 25 and 27°C (obtained in this study and in the literature [96]), with salinity levels ranging from 35.5 to 37 and chlorophyll-a concentrations above 0.08 and 0.12 mg/m3. However, during this season, the temperature in this area is approximately 27°C, which is considered too warm, and the chlorophyll-a concentration can reach levels of 0.2 to 1 mg/m3.

Contributions

- A GAM obtained **53%** of R2 with 4 variable parameters : **Temperature, salinity, mixed layer depth and chlorophyll-a concentration**;
- The model confirm the **maximum temperature of 27.1°C** over which no whale were detected;
- While no detection were made in Aruba and Bonaire, the GAM predicted some potential whale in Bonaire but not in Aruba due to too high temperatures.

7.2 SEASONAL VARIATION OF HUMPBACK WHALE VOCAL REPERTOIRE

Analysis of the presence of humpback whales in a specific area has also been shown to facilitate the study of their vocal repertoire over time. In order to analyse the evolution of vocal repertoire usage across time and space, RS values were computed using pairs of positive recording weeks (with a mean detection rate higher than 7 per hour). In this study, a RS value of 1 indicates identical repertoires, and a value of 0 indicates repertoires without any unit in common.

The results of this analysis, presented in Figure 62, highlight the weeks with more or less song variations (suggested by a low similarity of repertoire usage across stations), each day, 92 units were sampled from 3 randomly selected actives stations, in order to compute the RS between each station pair. This recording effort standardisation prevented the RS to be influenced by it (the rolling average curve was not dependant to the recording effort, Pearson r = -0.37 p-value >0.05). By computing the slope between days of the average curve (Figure 62), we demonstrate that the RS variation between the beginning of February and the beginning of April 2021 are significantly different to the one between the beginning of April and the first week of May (MannWhitney U p-value <0.05, Cohen's effect size d = 1.59). If we compare the slopes between the beginning of Febru-

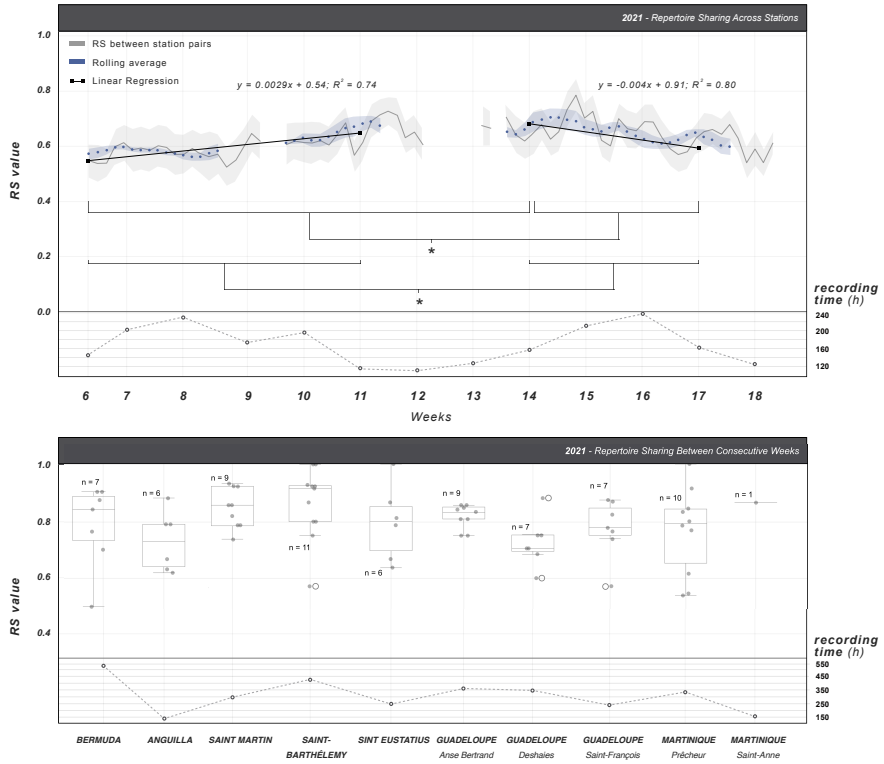


Figure 62: Spatial repertoire sharing as a function of time (top), and temporal repertoire sharing for each station (bottom) : The top panel shows, per recording day, the RS between station pairs (with a standardised sampling effort). Temporal slopes of the spatial RS curve (in blue) are significantly different between the start and the end of the season. The bottom panel shows, per station, RS distributions for consecutive recording weeks, with boxes denoting Q1, Q2 and Q3 quartiles. * : p-value <0.05

ary and the middle of March with the slopes between the beginning of April and the first week of May, they also appear to differ significantly (MannWhitney U p-value <0.05, Cohen's effect size d = 1.47). Indeed, the RS increases at the beginning of the season and tends to decrease from the middle of April to the end of May (Figure 62). This phenomenon is further supported by the measurement of the linear regression curves, with a positive slope at the initial stage and a negative one after the 14^{th} week. The positive part of these linear regression has a slope of +.0029 of RS per day, which has a R^2 of 0.74 (p-value <0.01). The shorter decreasing part has a slope of -.004 of RS per day, with a R^2 of 0.80 (p-value <0.05) as shown in Figure 62. To further assess the reliability of this finding, a randomisation test shuffling the weeks order showed no significant slope differences between the start and the end of the breeding season (MannWhitney U p-value >0.05).

As a parallel investigation to unveil potential areas of higher or lower song variation, we computed the RS between consecutive weeks

of each station (bottom panel of Figure 62). The Kruskal-Wallis H-test did not demonstrate any significant effect of stations over the RS of consecutive weeks (p-value >0.05). However, the fact that RS values ranged from 50% to 100% indicates that, at a given location, songs can vary greatly from one week to the next. Nonetheless, it seems unlikely that biased sampling of specific units would be responsible for the observed trends of increase and decrease in repertoire sharing, and hence this does not hinder the main finding of this study. Saint-Barthélemy was found to have the highest median RS (91.6%), while Guadeloupe Deshaies had the lowest (70.5%). Only two weeks had enough detections to be counted positive in Martinique Saint-Anne, giving one RS value of 86.6%. Martinique Prêcheur displayed variable RS values between weeks, with a maximum of 100% and a minimum of 53.8%.

Due to the irregular nature of the recording schedule, and the 1-minute on/5-minute off duty cycle, it is not feasible to describe the sequences that constitute the songs in full. Given that the objective of CARI'MAM is to study all cetaceans, including odontocetes, a long recording period with shorter recording intervals was selected. Nevertheless, through a more meticulous examination of repeated unit sequences, it was possible to reconstruct some of the recorded phrases. The implementation of an automated filtration process enables the elimination of recordings exhibiting overlapping or excessively proximate units (with a temporal separation of less than 1 second). This facilitates the consolidation of units into a cohesive sequence for the purpose of analysing repetitive patterns.

This highlighted that certain phrases at two different locations were exactly the same in terms of composition as presented in Figure 63. For instance, the phrase 'PEET', originally denoted 'QEET' before changes in the nomenclature of our repertoire, was recorded in Bermuda on 24th February 2021, as well as the day after, at a distance of 1,800 km away, in Anse Bertrand, Guadeloupe. However, an analysis of the silence between the phrase from Bermuda and Guadeloupe reveals a discrepancy in the duration of the silence, as it is 'P..E.E..T' (with '.' being a one-second pause) in Guadeloupe and 'P...E..E...T' in Bermuda. A second example is provided by Bermuda, where the 15th and 5th of April 2021. The phrase 'KCMMJ' was present in February 2022. These findings highlight the potential efficacy of the proposed model not only in the detection of units but also in the automatic reconstruction of phrases and, conceivably, entire songs. This finding provides further support for the hypothesis that phrases can exhibit similarity among individuals within the same population or across different males sharing a common breeding area [191, 192]. Furthermore, it demonstrates that these phrases can maintain stability from the conclusion of one season to the subsequent one [193].

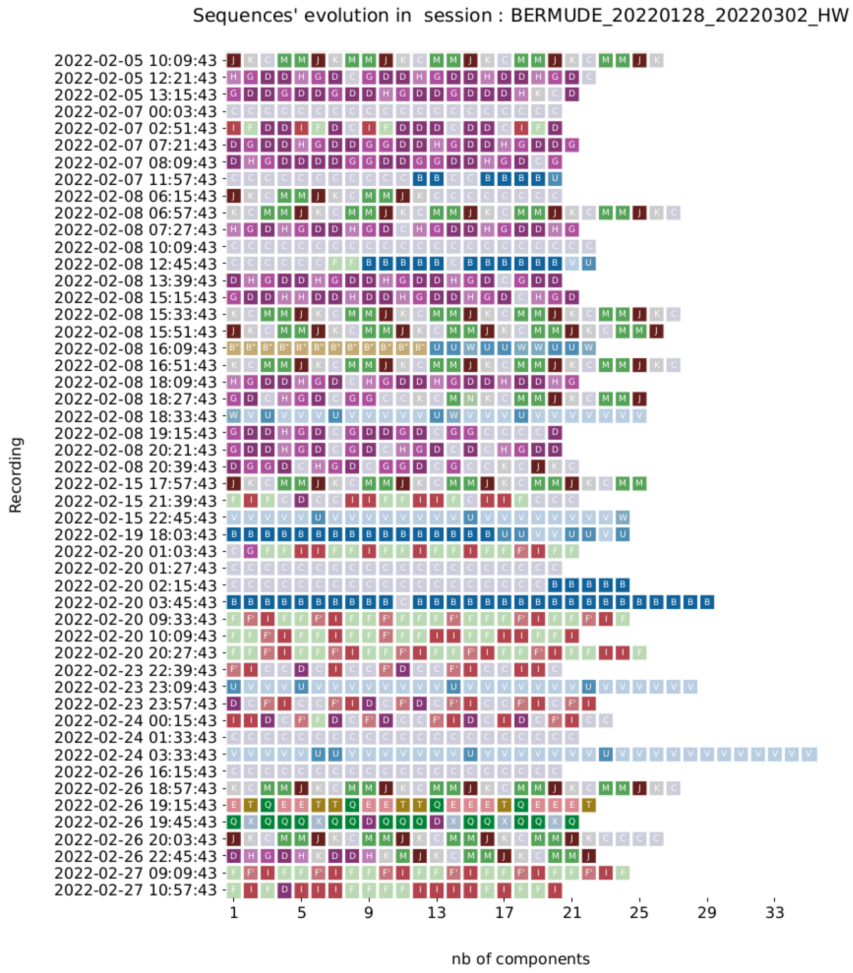


Figure 63: Example of the succession of different units and clear phrases from a humpback whale's song, as recorded in the Caribbean : The y-axis represents multiple files with the dates, while the x-axis represents the number of units inside each file.

7.3 SPERM WHALE SUITABLE HABITAT

7.3.1 *Importance of surface and deep parameters*

As illustrated in Figure 64, the mean values of the selected parameters for the period under consideration are presented for the Western basin of the Mediterranean. These parameters have been selected to predict the habitat suitability of the sperm whale are presented. The surface current and the temperature gradient have been shown to be significant factors in the identification of water fronts. The dissolved oxygen levels (at the surface and at 600 m depths) have been found to be more closely linked to the productivity of plankton, which is a fundamental component of the ecosystem. It is noteworthy that plankton productivity is recognised as one of the lowest levels in the food chain. The analysis of mixed layer depth, SSH, surface temperature,

and 600 m depth temperature, in conjunction with surface salinity, has been shown to reveal areas of strong evaporation or the presence of warmer waters. The data have been collated over the period May to October, and while they do not reveal any specific areas of interest, they do provide a comprehensive overview of the seasonal patterns observed in the sperm whale population during this time.

Initially, an attempt was made to ascertain the feasibility of optimising the MaxENT models based on the AUC score. In order to accomplish this objective, the model incorporating solely fixed parameters was used. The introduction of dynamic parameters was then pursued, with experimentation conducted until a configuration comprising five parameters was attained. A comparison of the AUC was conducted between the OBIS dataset and a segment of the author's own dataset. It was observed that the incorporation of additional parameters resulted in an enhancement of the AUC across both datasets until a maximum of four parameters was reached. At this point, the AUC began to stabilise or decline. The increase varied from 94.4% without dynamic parameter on our dataset and 96.3% over OBIS, to 98.8% over OBIS with four parameters (surface current intensity, temperature at 600 m, as well as the concentration of O2 at 600 m and the temperature surface gradient). The findings of the present study reveal that scores increased to 98.2% over the dataset, with only three dynamic parameters. These are the summer mixed layer, the concentration of oxygen at 600 m, and the sea surface height. However, it was observed that the maximisation of the AUC using the most adapted parameter could lead to over-fitting of the model, resulting in a prediction map that is only where the observations are. In the subsequent analysis, it is proposed that all the parameters will be used within the same model.

As was previously carried out using only the fixed environment parameters, the MaxENT model was computed using all dynamic and fixed parameters. Subsequently, all the variable parameters presented in Figure 64 were added. While an AUC of 91.6% is achieved when using solely fixed parameters, when employing all variables, it increases the AUC to 96.5% over the OBIS dataset. The five principal contributors, which are pivotal in achieving optimal results, are as follows: surface current intensity (44.7%), distance to a canyon (12.3%), oxygen concentration at 600 m depth (10.2%), slope (9.2%), and temperature gradient (7.9%). The use of these results serves to substantiate the significance of canyons within the habitat of the sperm whale. However, it is also elucidated that there exists a multitude of variable parameters that have the capacity to exert an influence upon the prevailing conditions.

An analysis of the response curves of the model Figure 66, with particular attention to the top five contributors, reveals that the current does not demonstrate a clear preference. However, in terms of dis-

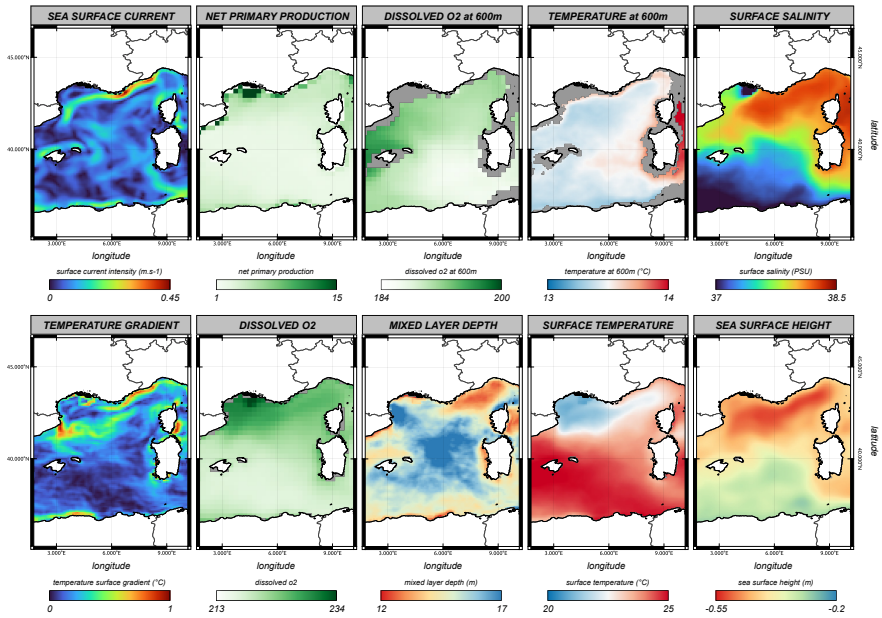


Figure 64: Mediterranean dynamic parameters averaged between May and October.

tance to the canyon, proximity is associated with a higher response. With regard to the dissolved O_2 concentration at a depth of 600 metres, it is preferable for the level to be as high as possible. As the depth increases, the predictions decrease concomitantly. With regard to the temperature gradient, an optimal value of approximately 0.5°C is identified. However, it is observed that predictions are higher with elevated delta temperatures, suggested by the surface temperature gradient response. It is evident from the jackknife analysis of Figure 65 that when the number of parameters is reduced to a single one, *i.e.* the SSH, the AUC for the global model is increased. However, if the SSH is removed from the model, the AUC for the OBIS dataset is increased, albeit to a lower extent. The contribution of SSH to the model is estimated to be the sixth most significant, accounting for 6.5% of the total. With regard to the slope, the maximum prediction is only at an angle of 1°, although it remains high for all values of slope.

In order to analyse the quality of our results, we also conducted a measure of the proportion of OBIS dataset observations over the resulting value of confidence of the model.

As illustrated in Figure 67, the proportion of detections that are well predicted is presented as a function of MaxENT thresholds. The results obtained show that approximately 70% of the OBIS observations are located within the area where the MaxENT model predicts a value of 0.5 for habitat suitability. However, it should be noted that only 20% of the OBIS dataset falls within the area with a value of 0.8, which is more restricted. The outcomes of this study may indicate a

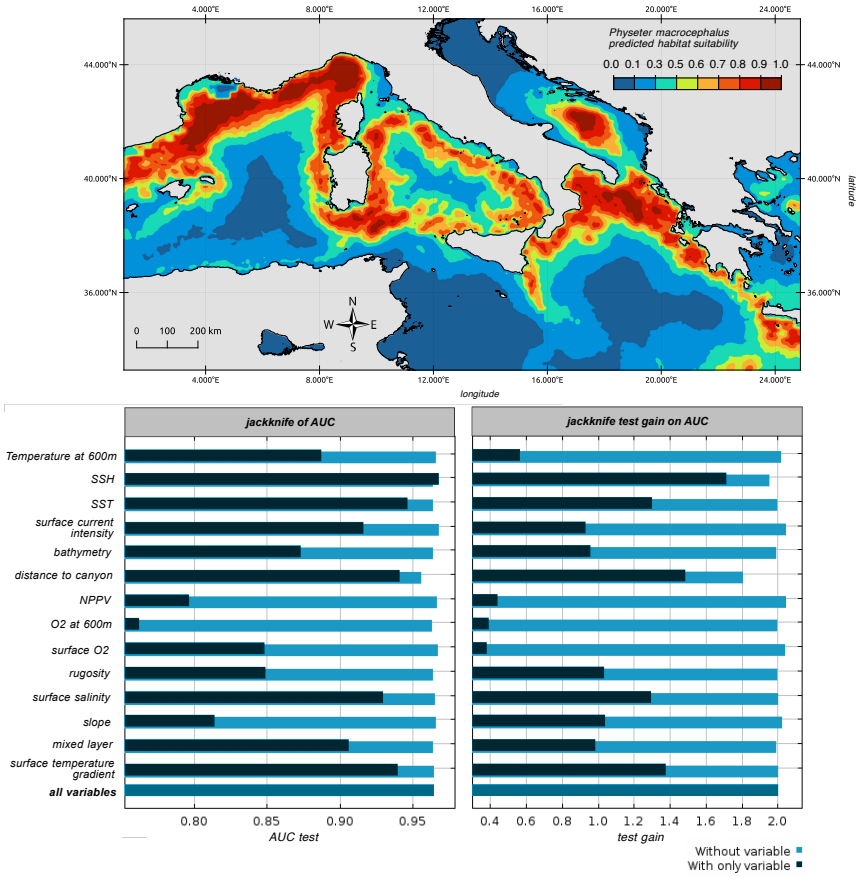


Figure 65: Result of the MaxENT model using all fixed and variable parameters averaged between May and October.

range of behavioural habits, given that our dataset is derived from foraging individuals, whereas OBIS is based on a comprehensive array of observational data. It has been demonstrated that certain areas where sperm whales have been observed do not function as foraging areas, but rather serve as routes for transit or socialisation.

Contributions

- The MaxENT model reached an **AUC over the OBIS dataset of 96.5%**;
- The most important parameters are the **surface current intensity**, the **distance to a canyon**, the **concentration of O2 at 600 m** depth, the **slope** and the **temperature gradient**;
- The northern part of the Western basin, as well as Mallorca is predicted to be suitable to sperm whale.

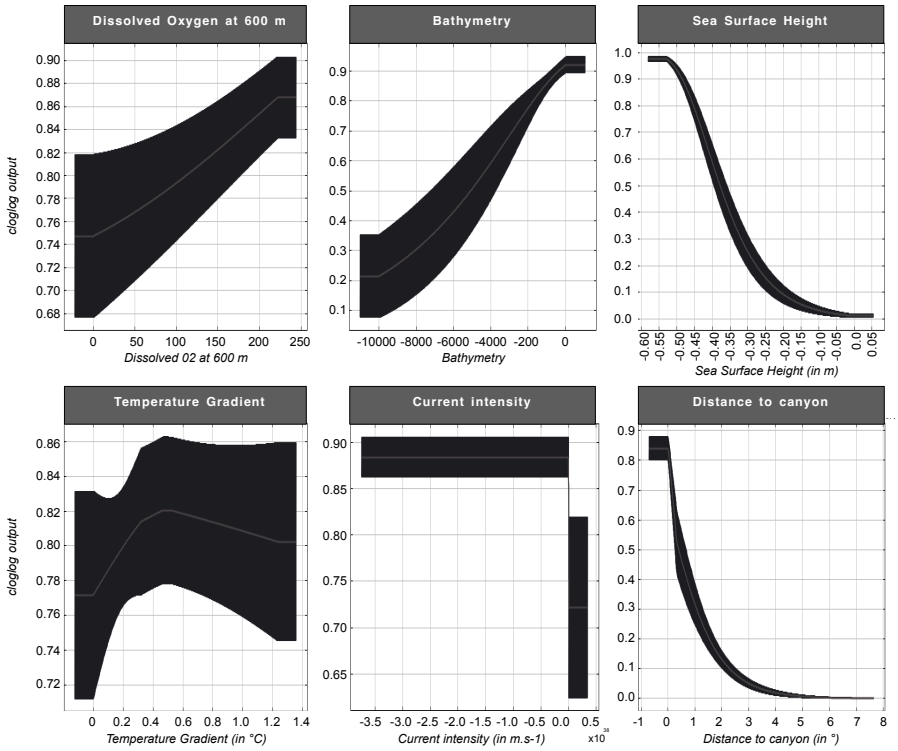


Figure 66: Response curve of some of the parameters that composes the MaxENT model.

7.3.2 *Increasing human pressure*

Throughout this study, the term 'dynamic parameters' is employed to denote the environmental factors that are subject to variation over the course of a season. As only natural parameters were presented, the human pressure was also studied. The use of AIS data from vessels facilitated the analysis of the density of each vessel category presented in Table 4. Indeed, using the preceding map of the sperm whale's presence in the Mediterranean, and acknowledging that collisions with vessels represent a significant concern for the viability of the sperm whale population, the global and category-specific areas of potential risk have been calculated.

As illustrated in Figure 68, large and fast boats (ferries) typically follow direct routes across multiple destinations (Toulon, Ajaccio, Majorca, Genoa, etc.), while smaller, faster vessels are more prevalent along the coast, extending their coverage to the entire Pelagos Sanctuary. Finally, the final category, which can be defined as large and slow, includes tanker boats and other large vessels. These vessels tend to follow some routes (wider ones), but are also present in a variety of locations. Combining the map of sperm whale habitat suitability with the boat density map shows that the area at risk of collision with 'small and fast' boat, is smaller than the area at risk of colli-

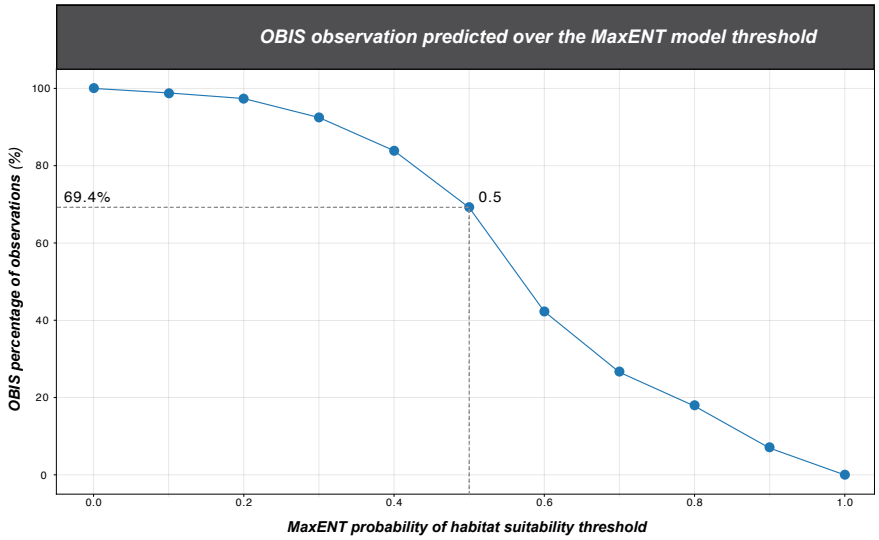


Figure 67: Proportion of OBIS observations that fall within the areas predicted by our model, at different confidence levels.

sion with 'large and fast' boats. These collisions may occur over three main routes: Genoa to Corsica, Toulon to Corsica, and Toulon to Nice. However, 'large and slow' boats represent a danger to sperm whales in a wider area, such as the Gulf of Lion.

Upon examination of the resultant data from the three distinct categories that have been determined to be within the global danger area for sperm whales, it is evident that there are three primary areas: As illustrated in Figure 69, the following locations have been identified as main areas of potential concern for sperm whale traffic: the city of Genoa, where traffic density is high; the coast between the canyons near Toulon to Nice, where habitat is predicted to be favourable; and finally, the waters around the Costa Brava, where boats transit from Barcelona to Marseille for example.

A more detailed analysis, as illustrated in Figure 70, reveals that the Pelagos Sanctuary is particularly prone to collisions between whales and boats, irrespective of their categorisation. Furthermore, while the CUI value is an average of 5.18 ± 3.96, which is relatively low, it is approximately 9.18 ± 4.04 in the Pelagos Sanctuary which is significantly higher (t-test $p\text{-}value < 0.001$). This suggests that the probability of a collision between a boat and a sperm whale in this area is almost double that of other parts of the Mediterranean Sea. Nevertheless, it is important to acknowledge the potential for variation in the regulation of AIS usage between countries in the Mediterranean region. Furthermore, there is a general underestimation of maritime traffic that is a consequence of AIS data.

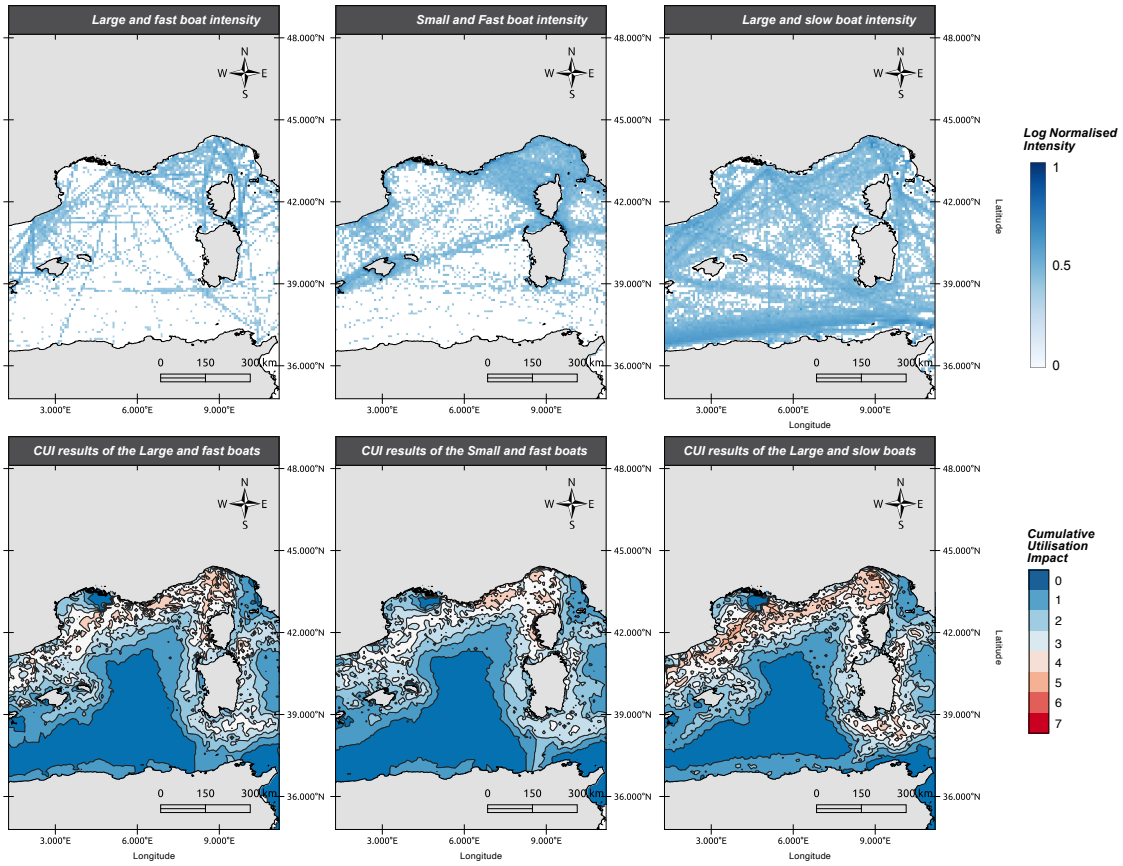


Figure 68: Result of the Cumulative Utilisation Impact (CUI) for each boat categories.

Contributions

- Cumulative utilisation impact measurement revealed that **the collision risk is more extended for the cargo, tanker and in general large and slow boats**;
- Ferries routes are areas where the CUI is high;
- The collision **CUI** measure reveal that it is almost **two times higher in the Pelagos sanctuary rather than in the whole Mediterranean**.

7.4 SEASONAL CHANGES FOR BIRDS MIGRATION IN QUÉBEC

As previously stated, there are notable preferences for the bird's habitat during the breeding season. Nevertheless, the provision of precise dates of arrival remains unfeasible based on fixed parameters.

However, the results from the detection process have provided preliminary insights into the seasonal variations. As presented in Figure 71, the maximum detection in the southern regions, designated as

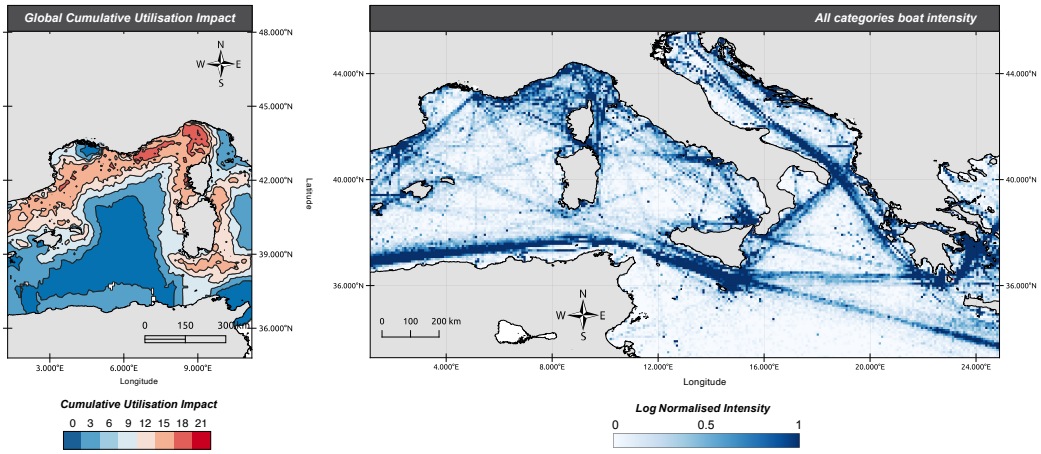


Figure 69: Result of the Cumulative Utilisation Impact of all boat categories summed together.

temperate, exhibits a broader temporal distribution than the boreal regions and the Arctic region. This finding indicates that the onset of favourable conditions in the northern regions is expected to occur at an earlier time. It is evident from the figure that the species most frequently detected in the Arctic region is the White-crowned sparrow (*wcsp*). This is due to the fact that, as previously demonstrated, it exhibits a preference for higher latitudes and tundra, which are characteristics of this particular region of Québec.

In order to achieve superior outcomes, a GAM analogous to that employed for humpback whales has been used. The development of that GAM was achieved by incorporating the temperature, total precipitation and wind data to create a comprehensive model, as illustrated in Figure 72. In the present model, which displays a R2 of 18.3% and an AIC of 10,358, it was determined that precipitation (with an EDoF of 11.5) exhibited no correlation with a *p-value* above 0.05. Conversely, temperature (with an EDoF of 27) was found to be correlated with a *p-value* of 0.016. Finally, wind (with an EDoF of 11.1) exhibited a strong correlation with a *p-value* below 0.001. The models indicate that the presence of wind is detrimental to the efficacy of the system, with the impact of wind being less significant than that of temperature. It has been observed that in conditions of temperature below 2.5°C, the system is rendered incapable of detecting birds. The findings of the study indicate that precipitation exerts a negligible influence on the detection process. However, when the precipitation level exceeds 0.008 m, a decline in detections is observed. This low impact can result in rain events lasting for a shorter duration than previously observed. Specifically, precipitation may be limited to several hours, with avian activity continuing uninterrupted before and after the rain. However, observations on this model indicate that higher temperatures are associated with improved performance. As previ-

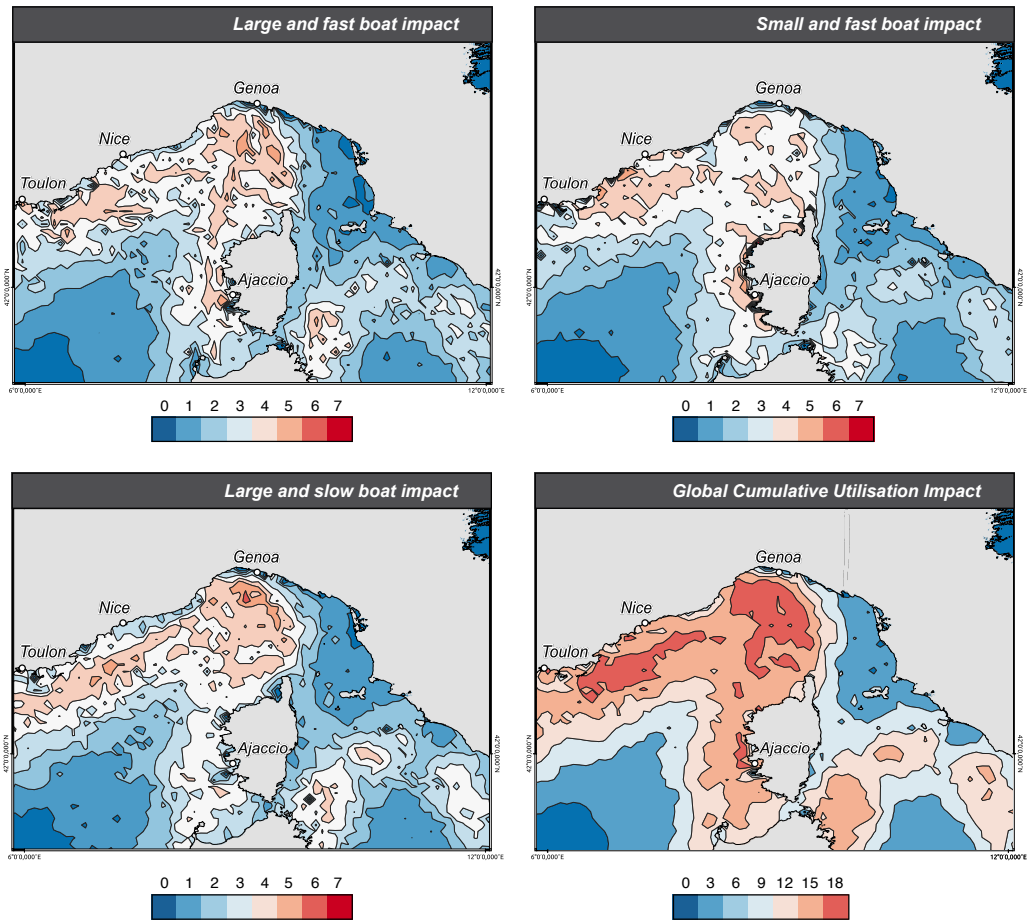


Figure 70: Zoom on the Pelagos Sanctuary for the different boat categories Cumulative Utilisation Impact.

ously stated, the impact of temperature on migration appears to have been overlooked. It is imperative to consider the impact of elevated temperatures on detections, particularly in the context of warmer stations.

Given that the former model demonstrates a high level of importance attributed to temperature, a decision was taken to formulate an alternative model using the fixed parameter of latitude, in addition to incorporating the week number, as illustrated in Figure 73]. The model obtained an AIC of 9,330, which is lower than the previous model. However, it presented a R2 value of 74%, with a contribution from the temperature, an EDoF of 27.6, months with an EDoF of 10.2, and finally, latitude with an EDoF of 1. All parameters were significant, with *p-values* lower than 0.001. As demonstrated in this section, the latitude parameter has been shown to result in a decrease in detection when the latitude is decreasing, as was previously observed. In addition, an increase in detection has been observed with temperature, which is consistent with the findings of the previous model. However, the significance of temperature in this instance is greater

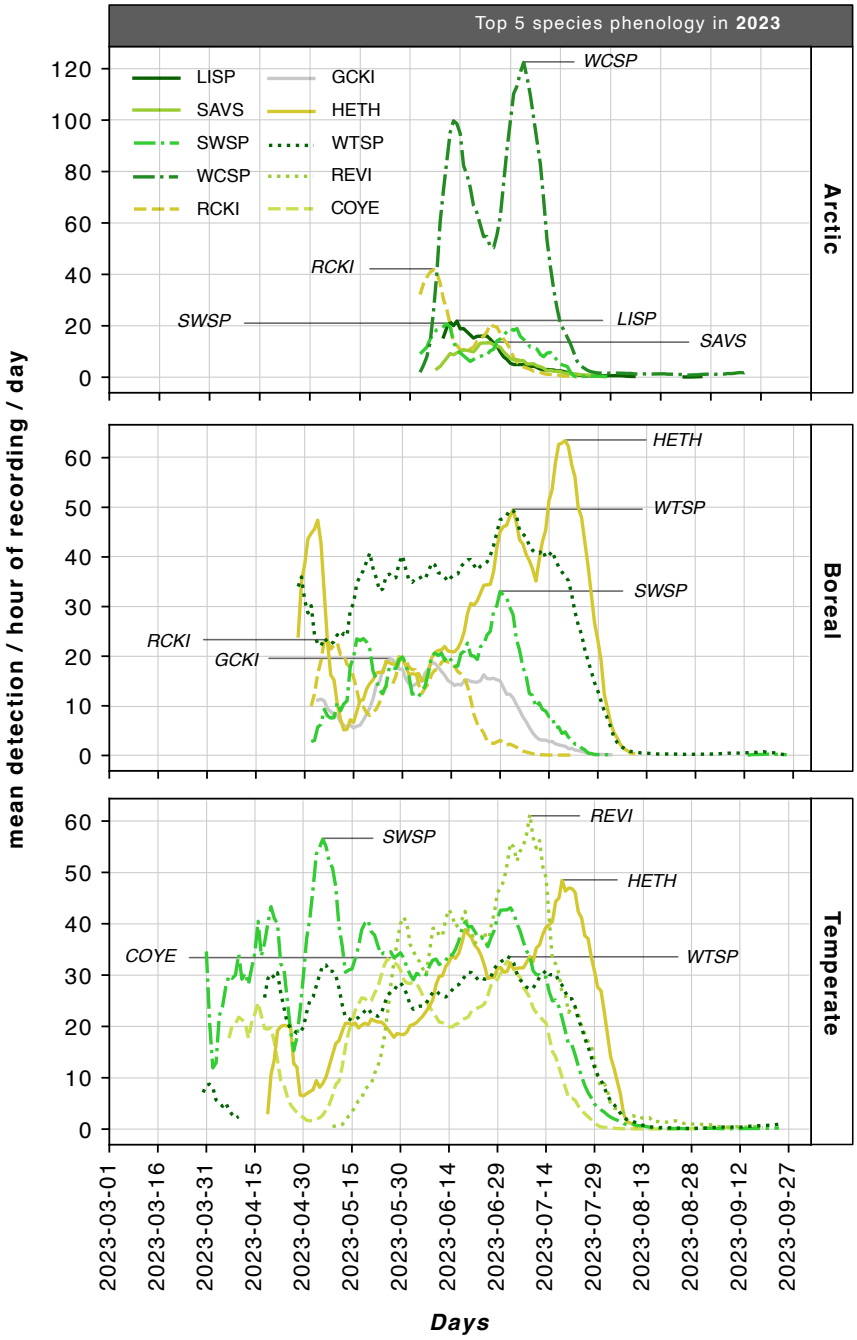


Figure 71: Mean detection per hour of recording for the 3 different areas for the top 5 detected species in 2023 : The Arctic area, which is the one more at north have *swsp*, *wcsp*, *lisp*, *rcki* and *savs* as top 5 species while Boreal area has *heth*, *rcki*, *gcki*, *swsp* and *wtsp*. Finally, Temperate region, which is the more at south, has *revi*, *swsp*, *coye*, *heth* and *wtsp* as top 5 species.

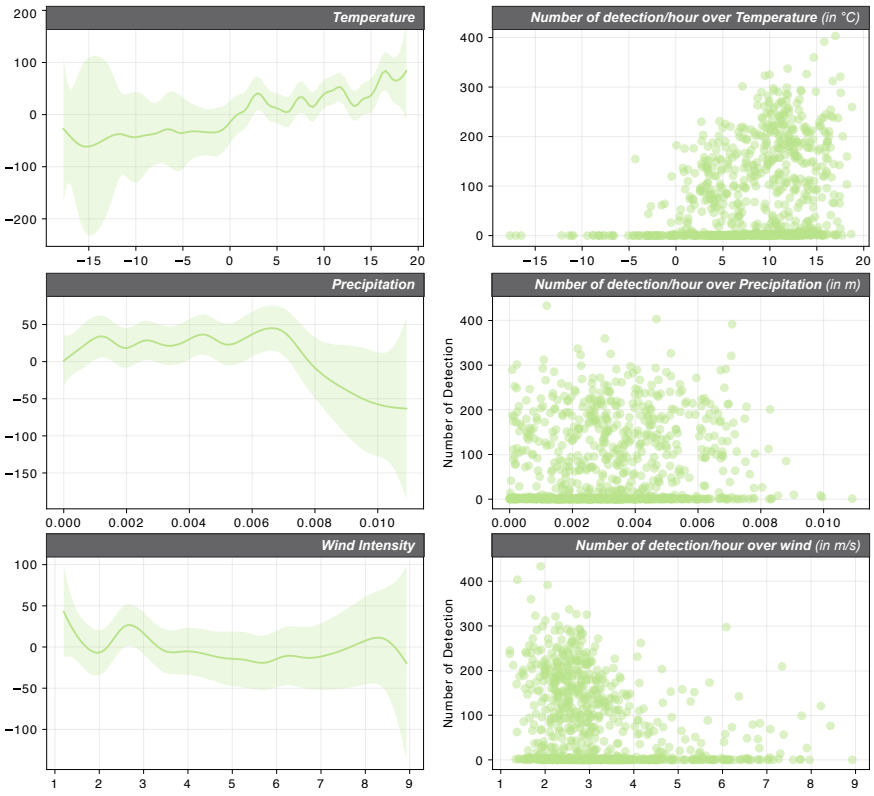


Figure 72: Results of the bird GAM with the response curves of temperature, total precipitation and wind intensity. : The y-axis of the graph represents the impact of the corresponding parameter on the number of detections. In the instance of a positive response, the number of detections is increased, whereas in the negative instance, it is decreased.

than in the previous model. The week number is a salient parameter in the model, as evidenced by the observed increase in value since the thirteenth week of the year, which corresponds to the end of March and beginning of April. A slight decrease is noted until the thirtieth week of the year, which is the end of July. It is also noteworthy that the value is significantly negative after the favourable weeks, indicating that even if the parameter were favourable, it would result in a reduction of the model's prediction, as evidenced by the week 35 example.

A GAM was implemented for each species individually, and the resulting responses and p-values are reported in Table 16. Evidence suggests a clear relation between the week number and the activity of various bird species, indicating a seasonal variation in the number of detections. The temperature, moreover, has been demonstrated to be significantly linked with the following species *wtsp*, *oven*, *yrwa*, *wiwr*, *blbw*, *swsp*, *revi* and *alfl*. For these species, it appears that an increase in temperature is associated with an increase in the number of detection. With regard to the relationship between latitude and species, it was

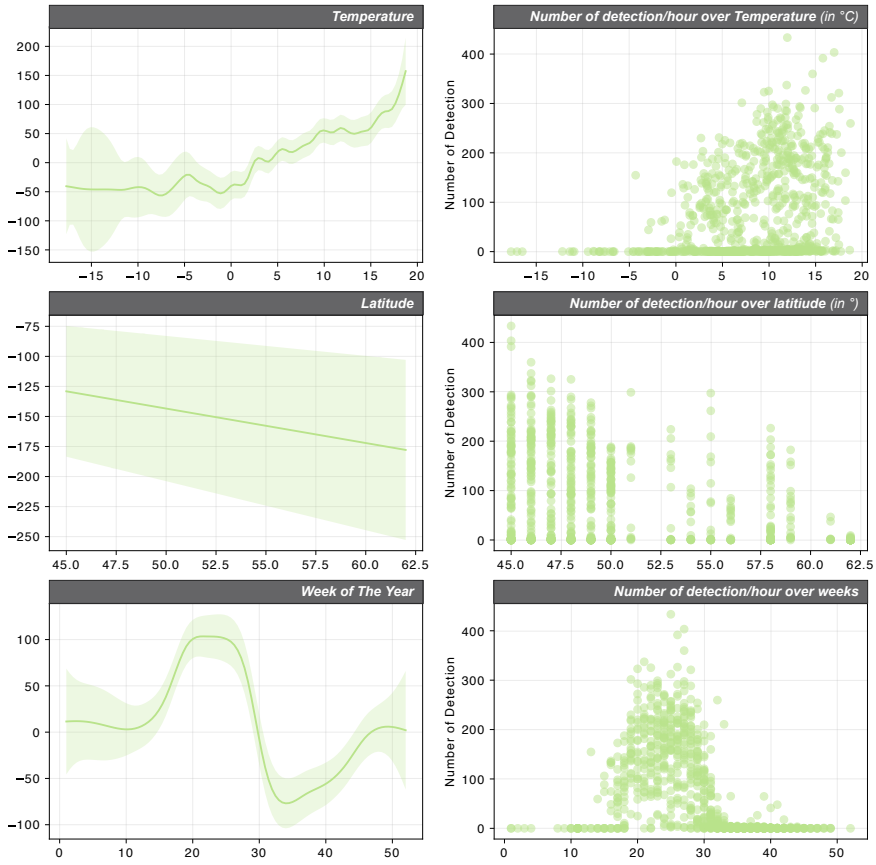


Figure 73: Results of the bird GAM with the response curves of temperature, latitude and week number : The y-axis of the graph represents the impact of the corresponding parameter on the number of detections. In the instance of a positive response, the number of detections is increased, whereas in the negative instance, it is decreased.

observed that certain species exhibited a significant correlation, such as *oven*. This is consistent with the earlier findings that the species' abundance typically decreases with increasing latitude. However, evidence suggests a strong correlation for *wcsp*, which is also consistent with the previous results which indicate higher detection rates at greater latitudes. On a global scale, GAM has been demonstrated to offer an effective explanation of the response to the parameters. Nevertheless, for certain species for which very few detections were made, such as scta, the efficacy of the GAM is diminished.

The same process as for the humpback whale was used to predict daily detection per hour, with the time taken being 9 in the morning. The results indicate that the southern region is more advantageous than the northern region, and furthermore, it is more extensive in length. This observation was also measured on real detection, as presented above.

Table 16: Bird Species GAM model and response to each parameters : The *p-value* significance is referred as : * < 0.05; ** < 0.01 and *** < 0.001.

species	**temperature** *p-val*	**latitude** *p-val*	**week** *p-val*	R^2	AIC	*p-value*
GCKI	3.10e-01	5.46e-02	**1.11e-16** ***	34.59	4583	1.67e-02 **
WTSP	**9.91e-07** ***	3.39e-01	**1.11e-16** ***	46.06	7117	1.04e-01
RCKI	9.24e-01	3.52e-01	**1.11e-16** ***	28.49	6005	5.72e-01
OVEN	**1.29e-03** **	**1.93e-02** *	**1.11e-16** ***	39.09	5360	**6.67e-03** ***
WCSP	9.68e-01	**2.91e-08** ***	**7.42e-13** ***	23.48	7213	**1.14e-07** ***
SOSP	1.48e-01	**4.24e-02** *	**1.11e-16** ***	19.33	3565	1.27e-01
NAWA	2.98e-01	**4.35e-04** ***	**1.11e-16** ***	34.6	6211	**1.35e-04** ***
TEWA	8.99e-01	2.64e-01	**1.10e-03** **	9.3	4593	2.24e-01
HETH	9.19e-02	**2.15e-03** **	**1.11e-16** ***	43.21	7400	**2.90e-04** ***
YRWA	**4.72e-12** ***	7.73e-01	**1.11e-16** ***	21.39	3244	5.15e-01
WIWR	**1.05e-02** *	7.90e-01	**1.11e-16** ***	29.68	4452	7.98e-01
BTBW	4.63e-01	**3.57e-02** *	**1.11e-16** ***	19.17	3958	**1.48e-02** *
VEER	1.65e-01	**5.73e-04** ***	**1.11e-16** ***	24.17	5426	**1.68e-04** ***
COYE	9.62e-02	**6.01e-04** ***	**1.11e-16** ***	34.84	6300	**1.32e-04** ***
BLBW	**7.41e-03** **	5.54e-01	**1.11e-16** ***	17.22	3944	7.41e-01
SWSP	**9.28e-05** ***	**8.84e-04** ***	**1.11e-16** ***	42.2	7035	**9.91e-05** ***
YBFL	8.12e-01	6.98e-01	**6.53e-09** ***	12.47	3090	8.20e-01
BTNW	6.20e-01	6.61e-02	**1.11e-16** ***	24.98	4618	**3.64e-02** *
SWTH	4.82e-01	1.43e-01	**1.11e-16** ***	20.53	5069	9.60e-02
REVI	**1.11e-16** ***	**4.23e-06** ***	**1.20e-09** ***	30.48	7637	**8.17e-08** ***
SAVS	4.48e-01	2.52e-01	**1.00e-12** ***	15.09	5708	3.27e-01
NOPA	9.94e-01	5.10e-02	**2.97e-12** ***	15.63	2701	**2.97e-02** *
AMRE	8.35e-01	7.52e-01	**1.11e-16** ***	18.67	2098	5.93e-01
ALFL	**1.59e-03** **	2.09e-01	**2.33e-15** ***	20.2	6371	1.14e-01
LISP	9.48e-01	**3.32e-05** ***	**2.72e-11** ***	16.02	4660	**1.15e-04** ***
RWBL	8.62e-01	**2.86e-03** **	**6.28e-14** ***	18.33	5791	**1.53e-03** **
SCTA	9.63e-01	4.96e-01	4.39e-01	0.391	-4863	5.56e-01

Further results pertaining to this particular aspect were obtained; however, the temperature was not included as a parameter. It was observed that another factor was not part of the equation, yet it demonstrated a high degree of correlation with the number of weeks. Indeed,

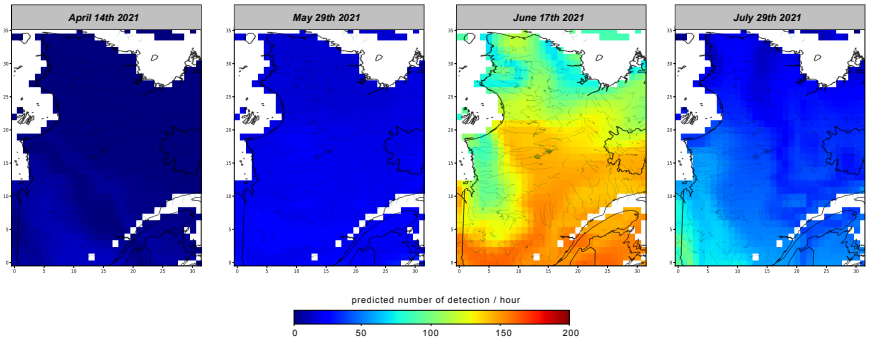


Figure 74: Prediction of the potential birds distribution across Québec at different times of 2021 based on the GAM.

an analysis of the total duration of days between weeks, analogous to the photographic period, reveals that the duration of daylight is different at stations at 46° latitude, which is south of Québec, and at 58° latitude, which is high north (Figure 75). The longest day of the year is June 21st, which corresponds to week 25. As has been observed, the number of detections over time and across different periods of the day appear to demonstrate a certain pattern in relation to avian activity. Indeed, the majority of birds initiate their vocalisations at sunrise, persisting until 8-9am, after which there is a decline in song activity, followed by a resumption of singing after sunset. Furthermore, it has been observed that the onset of sunrise, particularly during the weeks of June, is directly correlated with the start of avian activity. It is evident from the data presented that the period of heightened bird activity in higher latitudes occurs during the third to fourth weeks of the study period. This corresponds to the late 12th week of June to the 30th week of July in the temperate region. The onset of bird activity in higher latitudes is observed to occur in the 12th week, while the culmination of activity is recorded in the 30th week. These results demonstrate a high degree of similarity with the detections that were collected from the various stations.

Contributions

- The best **GAM reached a R2 of 74%** with the following predictors : **temperature**, **latitude** and **week of the year**;
- **Favourable period** is estimated to be from the **beginning of April, to the end of July**;
- The daily peak in detection rates is **highly variable** and follow the **photoperiod**, whether on lower and higher latitudes.

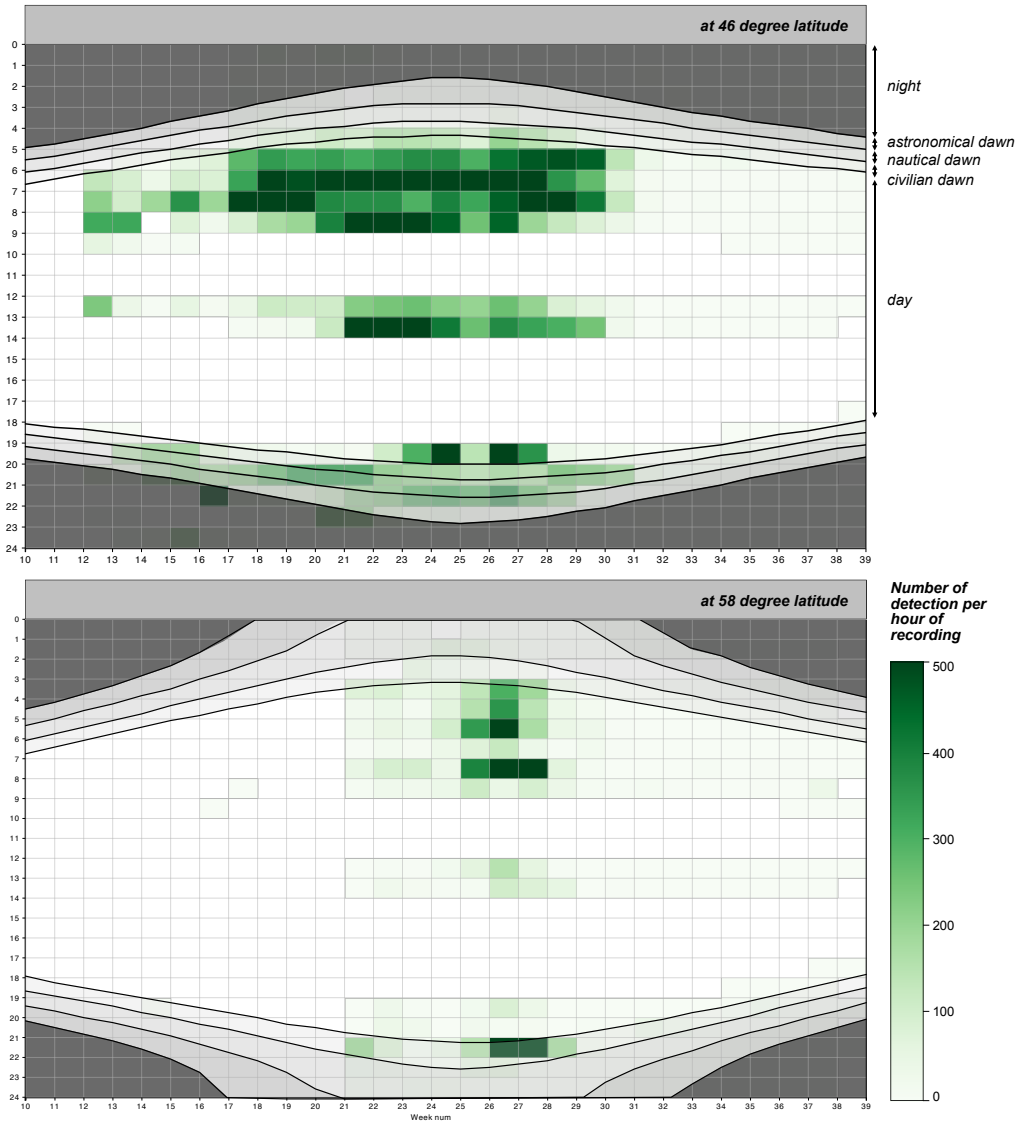


Figure 75: The evolution of sunset and sunrise times for a station located at 46° (a) and a station located at 58° (b), in relation to the call rate of birds in the same station.

8

RELATIONS BETWEEN DETECTION AND SHORT TERMS DYNAMIC PARAMETERS

8.1 Brief evolution of the oceanic conditions in the Stoechades canyon . . . 134
8.2 Response to higher temperatures for the bird detection rates . . . 141
8.3 Discussion on dynamic parameters . . . 143
8.3.1 Sperm whale preferences on habitat and dynamic parameters . . . 143
8.3.2 Habitat suitability is not abundance or density estimation . . . 144
8.3.3 Bird preferences and habitat . . . 145
8.3.4 GAM and MaxENT model bias . . . 146
8.3.5 Human pressure . . . 148

In the present study, a range of models were employed to predict the habitat suitability of various species. These included an absence-presence Generalised Additive Model (GAM) and a presence-only MaxENT model. The results obtained from this study indicated that humpback whales are sensitive to high temperatures, while sperm whales tend to prefer areas with strong currents in proximity to canyons. Furthermore, a correlation between bird detection and temperature was identified, with higher temperatures resulting in increased detection. However, it should be noted that these results were obtained at the seasonal level, a methodological approach that has been shown to minimise the impact of rare and extreme events [194]. The purpose of this chapter is to concentrate on rare but significant events. To this end, the focus will be on the Stoechades canyon regarding the sperm whale as it is notable that canyons are among the most effective predictors for them. In addition, an investigation will be conducted on the temperatures at various stations and the daily detection of birds in the province of Québec. The objective is to identify any potential events and to observe the subsequent impact on avifauna.

Key points

The analysis of special events yielded the following results:

- The **Stoechades canyons experienced downwelling** (descent of chlorophyll-a in depth) a month prior to the observations;
- **Peak temperature** in Québec was followed by a **decrease in bird singing activity**.

8.1 BRIEF EVOLUTION OF THE OCEANIC CONDITIONS IN THE STOECHADES CANYON

Over the 232 observations that were made during all the missions 74 were done around the same canyon which is called Stoechades.

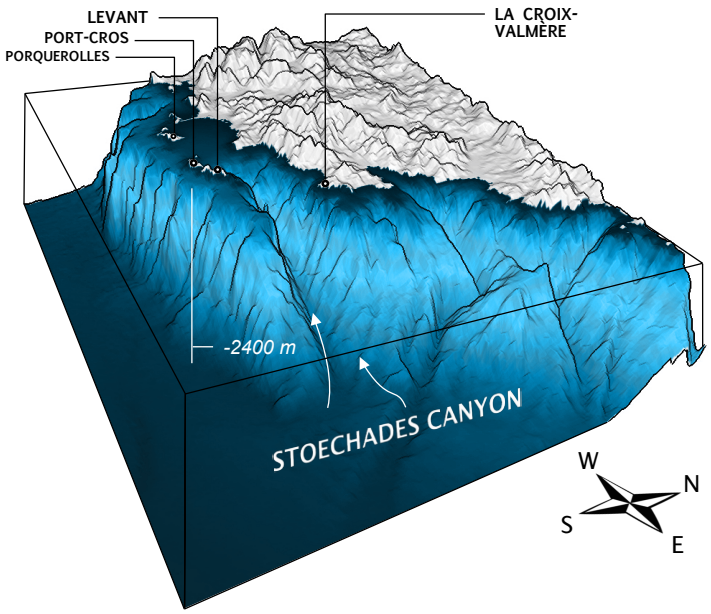


Figure 76: Stoechades canyon 3D representation

As demonstrated in Figure 76, the Stoechades canyon is situated in proximity to La Croix Valmère and the islands of Hyères. The canyon measures approximately 40 kilometres in length and is up to 2,200 metres deep. It has previously been demonstrated that canyons are a highly effective predictor of the habitat suitability of sperm whales, given that they encompass a variety of factors that influence their prey. These include elevated levels of roughness and slopes that interact with the currents. However, the orientation of Stoechades to the Northern Current (NC) distinguishes it from other canyons. Indeed,

the NC characteristically enters the canyon, which can result in the ascent of nutrients from the bottom. As illustrated in Figure 77, the NC is located in close proximity to the coastline in this region. Upon examination of the figure, it is evident that the Stoechades canyon is situated within the range of 43.09° and 43.13° latitude. This indicates that, in regions where current intensity is high, the canyon may potentially be entered by the current. At shallower depths, and even at considerable depths, as evidenced by the 300 metre depth measurement, the structure may be susceptible to being positioned against the slope.

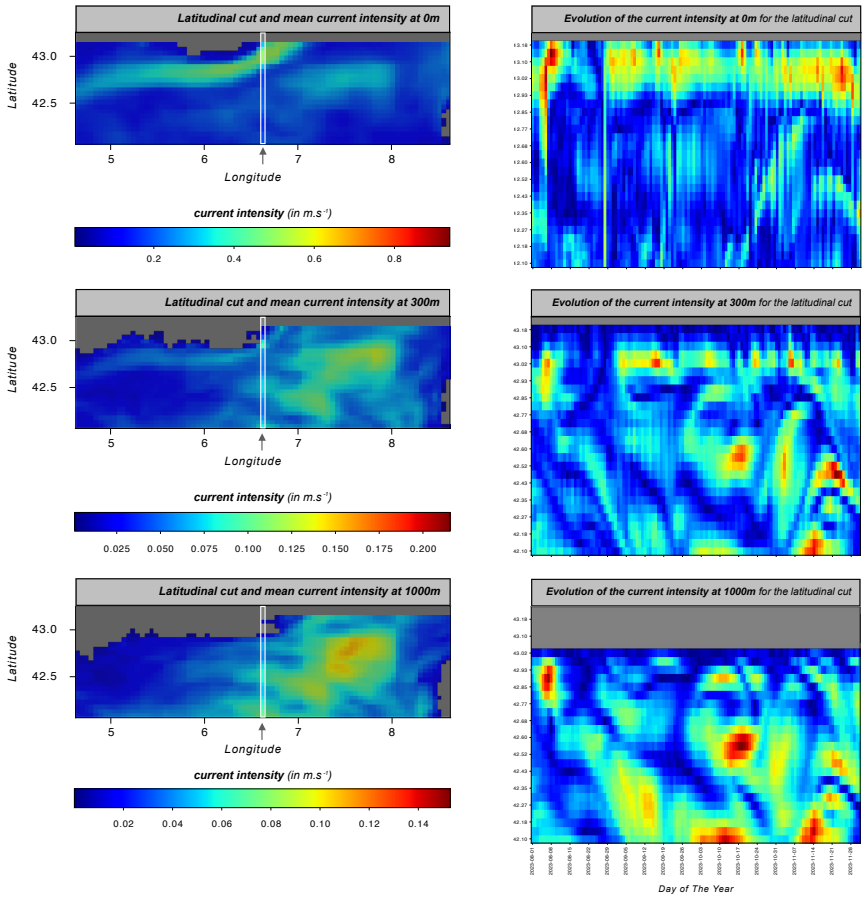


Figure 77: Current intensity following a latitudinal cut above the Stoechades canyon between August and December 2023

The analysis of various events within this canyon facilitated the monitoring of rare occurrences that have the potential to enhance primary production, thereby resulting in an increase in the presence of sperm whales. The following investigation was conducted to observe the variations in the NC over a latitudinal cut from the coast (43.2°) to the deep sea (42.1°) between the beginning of August and the end of November 2023. The results of this investigation can be observed in Figure 77. The initial segment of the figure, which denotes the surface current, reveals a pronounced current during the first days of August.

The presence of a strong current has been observed at depths of up to 300 metres and 1,000 metres. However, following this occurrence, the NC is observed to be almost non-existent for a period of one to two weeks. Subsequent to this, the current starts again at the beginning of September with notable intensity at a depth of 300 metres. An examination of the orientation of the current during the specified period reveals that the presence of the current was observed on August 7th, as illustrated in Figure 78. However, subsequent analysis indicates that the current undergoes modification until August 26th, resulting in a southward current that does not extend to the canyon. However, on August 28th, the surface current is observed to be particularly strong, exhibiting a north-to-south orientation, a phenomenon attributed to a significant wind event. Also, on October 8th, the Figure 78 shows a contact between two currents, the Northern Current (NC) and a secondary current, which originates from the circulation loop of return initiated by the Balearic current that we will call the Balearic Return Current (BRC).

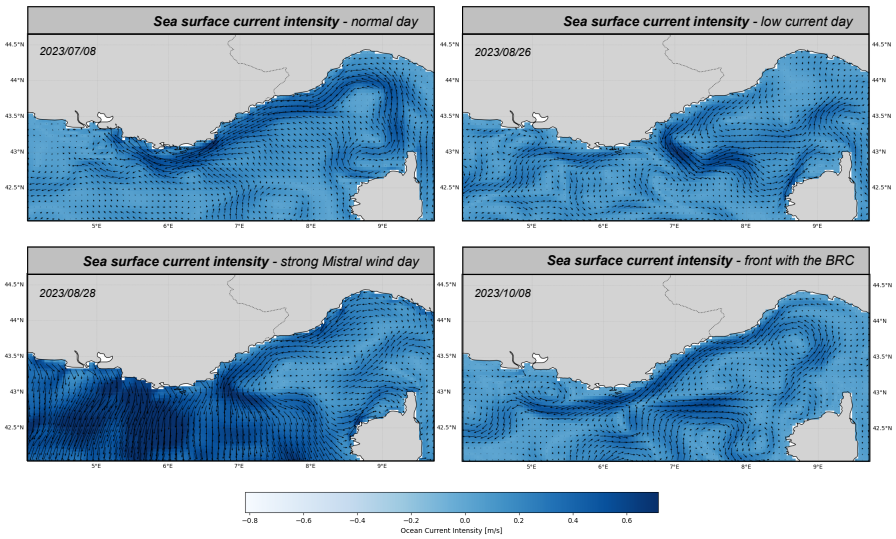


Figure 78: Different sea surface current conditions with different event types : a 'normal' sea surface current (a); a modified current to the south (b); a strong wind event (c); and a front between the northern and the Balearic Return Current (BRC) (d).

In order to comprehend the potential consequences of the cessation and subsequent resumption of the NC at a higher intensity, the chlorophyll-a concentration was observed using a depth cut over the same latitudinal line.

As illustrated in Figure 79, the initial observation reveals that the deep chlorophyll maximum (DCM) is situated between 60 and 80 metres in this region. On the first day of August, observations were made of a small patch of concentration at a certain depth over the canyon. Then, it is apparent that the patch is more visible on August

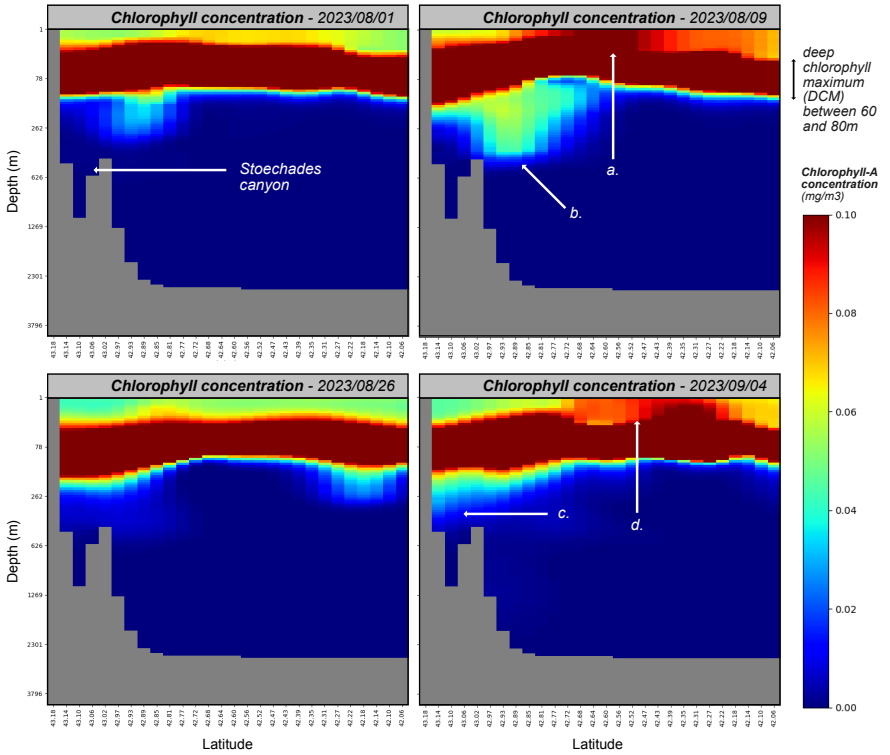


Figure 79: Chlorophyll-a concentration during different days for a depth latitudinal cut : a. the surface chlorophyll-a concentration is high; b. there is a big increase of the concentration of chlorophyll-a in the deep (up to 600 m); c the deep chlorophyll-a concentration is high into the canyon; d : the surface chlorophyll-a concentration increase again at the surface.

9th, eight days hence. It is also visible from the data that an increase in chlorophyll-a concentration in the deep layer (b) is concomitant with an increase in the surface layer (a). On August 26th, the DCM is observed at a shallower depth within the canyon, measuring below 100 metres. Following the occurrence of the strong wind event on September 4th, as illustrated in Figure 78, an increase in the chlorophyll-a concentration was observed within the canyon at a depth of c and at the surface in the offshore region.

It is hypothesised that the occurrence of a high-intensity wind event may have precipitated a descent of the surface chlorophyll-a in the deep layers. However, when that event stopped, an increase in surface chlorophyll-a concentration was observed. The current component, both northward and eastward, is analysed in Figure 80. The eastward component (denoted uo) is represented in this figure, with variation across the specified dates. As presented in Figure 80, the NC (blue) exhibits a weak and offshore trajectory, while the BRC (a) displays an offshore orientation. However, on August 9th, the NC is attached to the shore, stronger and also deeper (b). As previously observed, the interruption of the current was noted at the end of Au-

gust. Figure 80 shows that on August 26th, no current is visible for that component. However, on September 4th, the NC once again surpasses the canyon, with the BRC (c) demonstrating a closer proximity. This observation is further corroborated by the finding of an increase in the current at depths exceeding 1200 metres.

That strong wind event may have produced current variation that induce the descent of surface chlorophyll-a in the deep, while its reduction in intensity increase the surface concentration. Analysing the current component - Northward and Eastward - we represent on Figure 80 the Eastward component (denoted uo) variation across these dates. On the first day of August, the NC (in blue) is weak and over the canyon, while the BRC is off-shore (a). However, on August 9th, the NC is attached to the shore, stronger and also deeper (b). As mentioned before, there was an interruption of the current at the end of August, and on August 26th, no current is visible for that component in the figure. However, on September 4th, the NC will once again be above the canyon, with the BRC closer to it (c). We also noticed that the current at depth was stronger than 1,200 m.

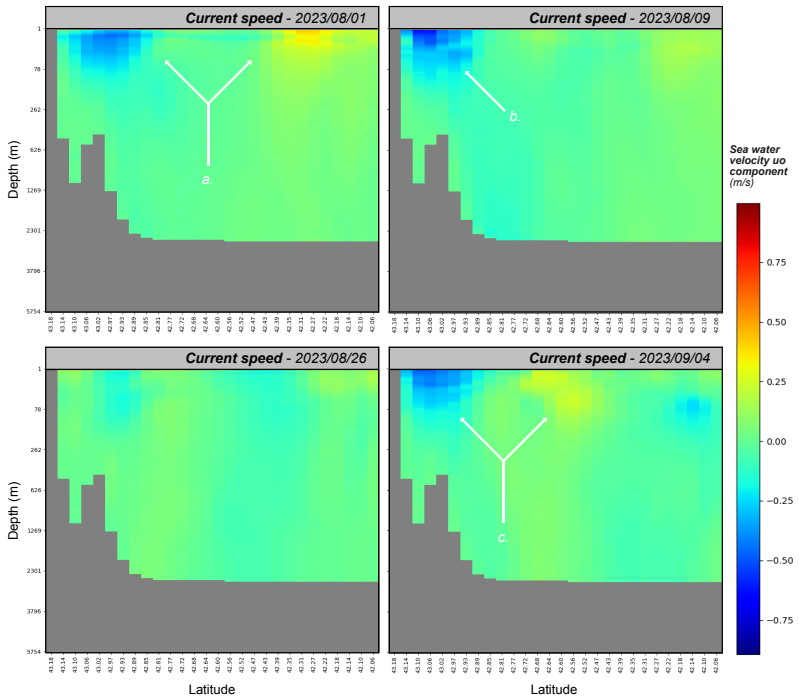


Figure 80: Current eastward component evolution during different days for a depth latitudinal cut : a. there is the Northern current and the Balearic Return Current (BRC); b. the Northern current is closer to the shore, and stronger, it can create downwelling; c. the Northern current and the BRC front is again and closer, with the increase of current in the deep

Finally, the vertical component (Northward, denoted vo) is represented on Figure 81. On the first day of August, the current is ob-

served to be within normal parameters. However, on August 9th, a marked increase in surface current strength is recorded, likely attributable to the presence of a strong wind at the surface. On August 26th, in the absence of current activity along the coastline, a substantial volume of water (b) is observed to traverse the area from a southern to a northern direction. It is hypothesised that the observed phenomenon may be attributable to the departure of water at a certain depth, as evidenced on August 9th. It is observed that on September 4th, the NC once again demonstrates a marked strength and depth, with an orientation that is oriented in a southward direction. As previously asserted, the occurrence of a substantial wind event serves to reinforce the capacity of these phenomena to influence surface currents and, moreover, to contribute to variations in deep water.

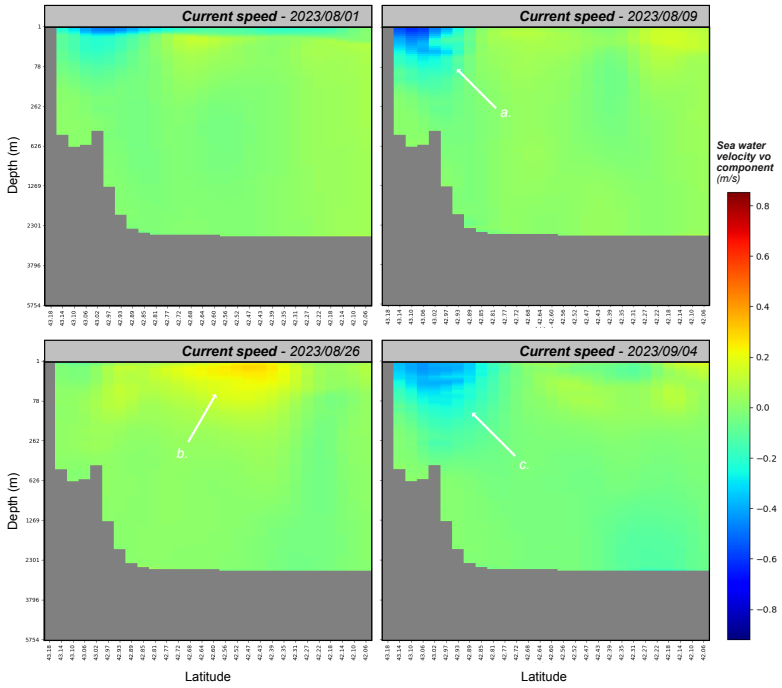


Figure 81: Current northward component evolution during different days for a depth latitudinal cut : a. the current is from the coast to the sea, which can create downwelling in the area; there is a strong current from the sea to the coast; c : once again a strong current from the coast to the sea, even in deep water of the canyon.

Overall, it was observed that multiple wind events resulted in strong movement of the Northern Current (NC) and high variation of the chlorophyll-a concentration. It is observed here a potential downwelling, which corresponds to the descent of water from the surface to the deep. This increase in chlorophyll-a within the deep ecosystem has the potential to result in an increase of biomass. In the course of the Longitude 181 mission, the observations from the mission WW4 were conducted in this area on September 25th and at the start of Oc-

tober of the same year as the oceanic event described above. Throughout the observation period, multiple specimens were recorded in the area, from the beginning to the end of the mission, with 93 positive points in 14 days. This is the highest number of points from all L181 missions, as the mean number of points per day is 3.56, whereas this mission achieved 6.64.

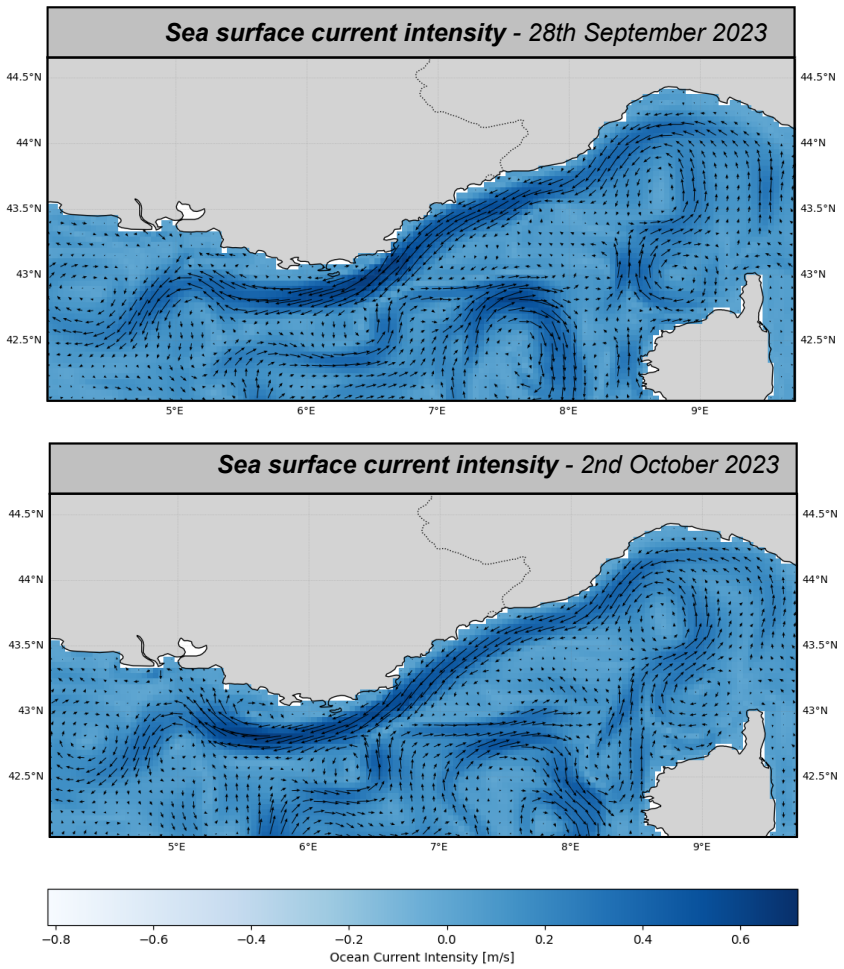


Figure 82: Sea surface current orientation on September 28th and October 2nd with a front off-shore the islands of Hyères.

An additional oceanographic occurrence was also documented during the period in which the observations were conducted, in the same area. As illustrated in Figure 82, the NC is in fact confronted by an opposing current. On September 28th and subsequently in October, a front was measured offshore from the islands of Hyères. The term 'front' is used to denote the boundaries between two or more water masses. In this particular instance, the measurement is taken of the velocity; however, it is possible for the phenomenon to occur in relation to the temperature. It is plausible that the front measured here can be linked to potential vortexes. In circumstances where two currents

of opposing direction are in proximity, the ascent of organic matter from the depths may be a contributing factor. This phenomenon can be of significance for sperm whales, as it results in the availability of their preferred prey. These observations are consistent with the regular observations of sperm whales in this area, as recorded by the missions.

Contributions

- Analysing the Northern Current (NC) before observations of sperm whale allow to detect a potential downwelling in the Stoechades canyon 1 month prior the observations;
- A **potential front** was also observed **between the Northern Current (NC) and the Balearic Return Current (BRC)**.

8.2 RESPONSE TO HIGHER TEMPERATURES FOR THE BIRD DETECTION RATES

As demonstrated in the preceding chapter, there was a direct relationship between temperature and song activity. As illustrated in Figures 84 and 83, there is a clear association between rising temperatures and an increase in detections in both Abitibi and Côte-Nord. However, given that the mean temperature in Côte-Nord is between 10 and 17.5°C (Figure 83), it is notable that in Abitibi, situated further south, temperatures can reach up to 21°C (Figure 84). Furthermore, in 2022, a peak detection was observed in the first weeks of July in Côte-Nord, while in Abitibi in 2023 it occurred in the last week of June. In order to facilitate a comparison between the two stations, an analysis of the detection rate reveals that it has remained above 250 since mid-May in Abitibi, persisting until mid-July, a period of two months. Conversely, in Côte-Nord, the detection rate has remained between the last week of June and late July, constituting a duration slightly in excess of one month. As previously stated, the favourable period was quicker for northern regions, which is also observed here.

As shown in Figure 84, the response to high temperatures can be observed. Indeed, an increase in temperature at the end of May has also been demonstrated to result in a decrease in detection. In instances where the temperature exceeds 20°C on two consecutive days, a decline in detection is observed in the subsequent days, irrespective of the recording time. In the region of Côte-Nord, the maximum temperature is recorded at the onset of August, coinciding with the period of minimal detection. During the period in which peak detection for birds in that region was being conducted, the temperature was recorded as being below 15°C. From the data, a potential relationship

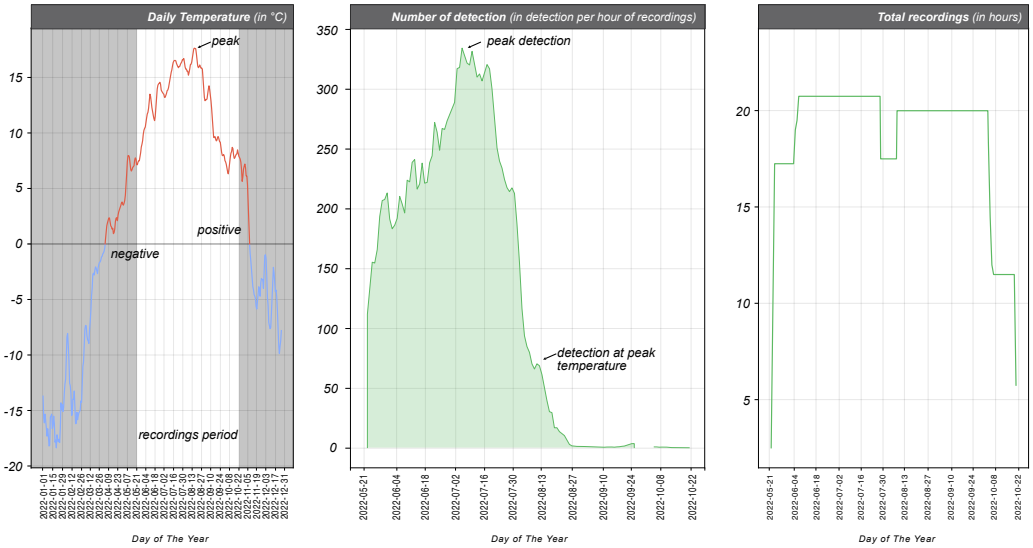


Figure 83: Daily temperature and detection rate with total recording time for 2022 season in the Côte-Nord regions.

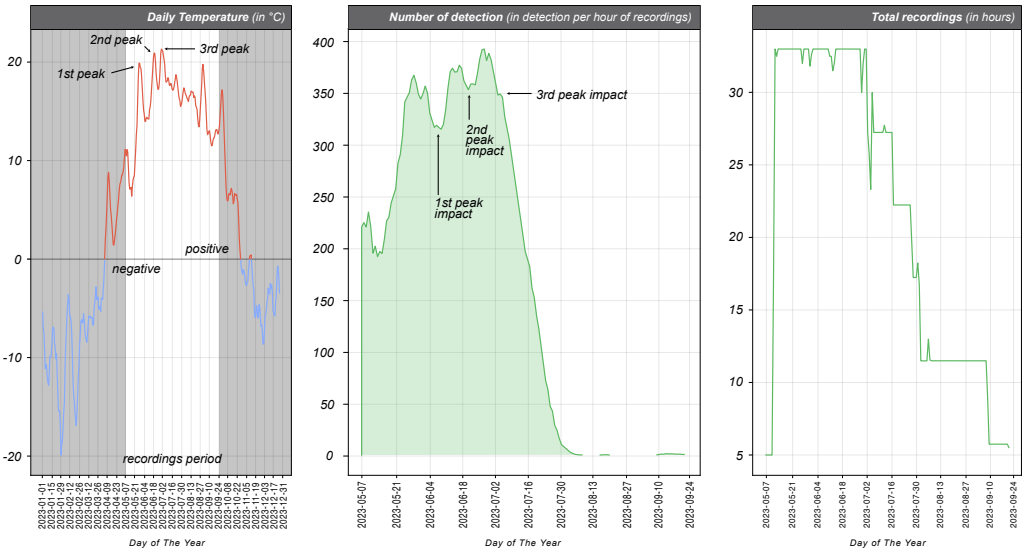


Figure 84: Daily temperature and detection rate with total recording time for 2023 season in the Abitibi Témiscamingue region.

between rising temperatures and a decline in bird song activity can be observed. This observation suggests the presence of a critical temperature threshold, beyond which avian song behaviour is reduced. This hypothesis, however, requires further investigation in order to ascertain the precise temperature parameters that trigger this response in birds.

Contributions

- The bird detection rate is observed to **decrease** when the temperature reaches a particular value, which is **above 15°C in the northern stations and 20°C for the on more south**;
- Following 3 peaks of temperature (reaching an average of 20°C to 21.3°C) results in 3 detection rate decreases in Abitibi area.

8.3 DISCUSSION ON DYNAMIC PARAMETERS

8.3.1 *Sperm whale preferences on habitat and dynamic parameters*

As outlined in the preceding chapters, the influence of dynamic parameters on the temporal and spatial distribution of particular species has been a subject of discussion. These analyses are dependent on statistical models, using observations as valid points where the species is found to be present. By handling a range of fixed parameters, it was determined that sperm whales exhibit a preference for areas characterised by canyons. However, employing dynamic parameters revealed that the current also plays a significant role. The integration of these findings with those related to canyons and the current suggests that the impact of the current on canyons, as evidenced by the results, may provide substantial food sources for the prey of sperm whales, thereby contributing to their observed presence. As canyons are already known to be of importance to deep divers [195], their influences on currents were also studied in response to the presence of sperm whales [196]. The conclusions of the aforementioned paper determined that canyon influence on prey availability is achieved through the modification of the current, thereby resulting in the creation of upwelling or downwelling [196]. The findings of the Mexican sperm whale population study also indicate that sperm whales were encountered in areas exhibiting a sea surface height lower than average, a characteristic feature of cyclonic regions [197]. The results obtained from the study indicated that the SSH (Sea Surface Height) exhibited a capacity to predict the majority of the OBIS observations. It was observed that the predictive capability of the SSH was found to be enhanced in scenarios where the SSH values were found to be lower. This observation is in alignment with the findings reported in the extant literature on the subject. The results of the study indicated that the dissolved oxygen concentration was among the top five contributing factors to sperm whale populations in the Mediterranean Sea.

It has been previously established that the depth of the maximum oxygen concentration in deep-foraging mammals may be indicative of the vertical exchange of water masses, thus serving as an indicator of potential downwelling [198]. From our study we observed a relationship between the depth-related concentration of oxygen and the resulting prediction. It was observed that an increase in oxygen concentration at a given depth results in a corresponding increase in the prediction. The dissolved oxygen concentration we used was for an average for the entire period under investigation. This observation may suggests the potential area where downwelling is expected. Furthermore, a potential downwelling event was observed a month prior to the sighting of the sperm whale, which could be consistent. Indeed, in canyons, downwelling has been shown to enhance primary production, thereby contributing to the augmentation of the food chain process and thus attracting sperm whales. However, the interval between the occurrence of the event and the presence of the sperm whale has been documented to be approximately four weeks [100]. Additionally, the presence of sperm whales in proximity to the temperature front, particularly the North Balearic Front, which is offshore, has been documented [199]. The results obtained in this study demonstrate that the Northern Current is subject to fluctuations, and that it generates a front with the BRC when the latter approaches the coast. Indeed, the interaction of these two distinct bodies of water can give rise to the formation of a vortex, which, in turn, can serve as a potential habitat for sperm whales. The hypothesis is that these areas are conducive to the development of trophic webs offshore, where fixed parameters are inapplicable [199].

8.3.2 *Habitat suitability is not abundance or density estimation*

The predictions derived from the model that was proposed have been shown to demonstrate strong statistical performance, with a high degree of accuracy in the majority of observations from the OBIS dataset. OBIS is the result of many years of observations, with some of this research undertaken using transects. The map that was constructed from the results of our study displays notable similarities to the findings of preceding studies [145, 200, 201]. These earlier studies indicated higher densities in the Western basin and particularly elevated levels in the Liguro-Provençal basin. However, the predictions of previously published models indicate the presence of sperm whales in Algerian waters, where the model predictions for our study are below 0.5. The geographical areas in question are the Ligurian-Provençal basin, the region encompassing Costa Brava, the western portion of Corsica and Sardinia, and the southernmost region of Italy. Following the analysis of the model's results, an area within the Adriatic Sea has been identified with a high degree of confidence. A survey

of the extant literature reveals a certain lack of consensus amongst researchers regarding the abundance of sperm whales. While some models make no prediction [145], others predict low densities (estimated at 0.07 individuals per 1,000 km^2) [200], and still others predict high densities [201]. Nevertheless, an analysis of the OBIS dataset revealed the presence of some sperm whales in that particular region, thereby substantiating the hypothesis that the area is indeed suitable. Additionally, the model indicated a higher abundance of sperm whales in the northern Balearic Islands, while the southern region continued to demonstrate a significant level of uncertainty in the data. This outcome is analogous to that reported [201], yet it appears to diverge from the findings of the aforementioned publication on this specific region, which suggests a higher probability of occurrence in the southern part of the Balearic Islands [146]. The results presented herein demonstrate the potential for comparison with existing literature, as they predict the degree of suitability of a habitat for sperm whales, as opposed to other species. It is therefore not possible to estimate sperm whale abundance or density. However, it is possible to determine the locations where these cetaceans can be found. Nevertheless, this less precise approach may assist in the prediction of movement from one habitat to another, as it is possible to estimate the locations where the sperm whale will not be present.

8.3.3 *Bird preferences and habitat*

The use of GAMs in this study incorporated presence-absence data, which, in this particular instance, equated to a specific number of detections per hour of recording, in contrast to zero detections for absence. This approach facilitated the analysis of various parameters that were found to be effective in predicting the preferred breeding areas of avian species. It was determined that temperature is a significant parameter, and it is considered to be one of the most effective. The findings indicate a direct correlation between temperature and detection rate, with higher temperatures resulting in increased detection probability. Nevertheless, it should be noted that the aforementioned result does not take into account species preference. The findings, with the exception of those derived from the models, indicate that elevated temperatures result in a decline in the detection rate. This suggests the presence of an optimal temperature at which avian activity ceases, but at higher temperatures, this activity resumes. However, it is important to note that temperature has already been shown to be responsible for the reduction of singing behaviour rather than defence [116]. As demonstrated in preceding studies, the probability of avian population decline from one geographical location to another is hypothesised to be predominantly influenced by the environmental conditions available for their breed-

ing. Indeed, there is a heightened risk for avian species breeding in boreal forests, as climate change is predicted to engender increased drought and heat, which can result in elevated wildfire frequency and subsequent impact on bird communities [202].

The employment of an automatic detection model over a substantial database in Québec facilitated the identification of analogous avian community preferences and the corroboration of a latitudinal gradient, characterised by enhanced detection in temperate regions relative to the Arctic. It has been demonstrated that species can be classified as either generalists or specialists, with the latter exhibiting a preference for a specific habitat. Furthermore, it has been established that the period during which species are present is shorter in the Arctic than in temperate regions. This observation, made with regard to *Orthoptera*, may also be applied to predators (birds). It is evident that avian species exhibit a south-to-north migratory pattern. Consequently, a temporal discrepancy is observed between the earliest and latest migratory groups. A study of the delays in question was undertaken, drawing upon diverse population data. The findings indicated that the geographical location of breeding had a significant impact on the migratory schedules of the population under study. This impact was characterised by a delay in the arrival date, a delay in the first egg in the nest, and a subsequent delay in departure [203]. The findings of this study appear to provide a rationale for the observed variation in the temperate region detection rate. Specifically, the rate exhibited a peak between March and July, while for stations located further north, it remained relatively consistent from the end of May to the end of June. Indeed, as the initial egg is formed at a subsequent point in time at higher latitudes [203], the first hatching occurs at a later stage, consequently extending the return date. Furthermore, research has indicated that ambient temperature exerts an influence on the duration of the incubation, with a shorter period being observed in warmer regions [204]. Subsequently, during the return migration of avian species from the northern regions, these birds make intermittent stops within the study area. The PAM system continues to record these individual birds, thereby contributing to an augmentation in the detection rate over the specified period.

8.3.4 *GAM and MaxENT model bias*

It is acknowledged that the selection of parameters is a potential source of bias in both the GAM and MaxENT models, given their use of environmental data for analysis. It is important to note that, with the exception of fixed parameters, which are measured from satellite and precise sonar, dynamic parameters are not as precise as those extracted from real data and simulation models. Nevertheless, these models are accurate and have previously demonstrated good re-

liability, as evidenced by prior studies [205]. Furthermore, the study observed that positive data is of significant importance in terms of position. In the MaxENT model, for instance, the use of solely positive data from the mission observation yielded a map of a highly specific nature, predicting the presence of sperm whales exclusively in areas where observations were made. This phenomenon can be attributed to the overfitting of the model, whereby specific parameters were incorporated within a highly constrained domain, resulting in predictions being made exclusively within the observed parameters. In order to avoid the potential for such bias, we elected to follow the advice of previous studies [147] and apply a bias layer. The incorporation of a bias layer within the model has been demonstrated to mitigate the issue of overfitting when the area under study is limited. The use of this bias layer was also motivated by the protocol for data collection, which diverged from the transect approach employed in multiple studies [145, 201]. In the context of modelling sperm whale habitat suitability, the efficacy of the opportunistic observation protocol can be attributed to the incorporation of a bias layer, which was facilitated by the GPS data acquired from the vessel. Indeed, using solely observational data would have led to predictions being made exclusively in regions where observation density was higher. However, by using the model, we predicted that the habitat was suitable for sperm whales after the continental shelf of the Gulf of Lion. This finding differed from the predictions made by the literature model. However, sperm whales have been recorded in this area of the Mediterranean during the winter months, and it is hypothesised that they may use different foraging strategies in this season [206]. It can be hypothesised that the presence of more challenging oceanic conditions, which preclude observation from boats, may account for the paucity of observations in this area.

In the MaxENT model, an error was observed in the computation of NaN values. The current intensity was consequently set to a very low value. Nevertheless, it is observed that the current is the most significant contributor to the model, yet its response curve does not demonstrate a tendency for a preferred level of current, given the very low value of the layer that was added. Given that all the observations from our dataset were made within or in close proximity to the Northern Current, it is possible that a bias may have been introduced, resulting in the identification of the most effective predictors. However, should this parameter contribute to over 40% of the prediction, the resulting map is also impacted by the other parameter, given that our prediction map is not equivalent to the sea surface current intensity map.

8.3.5 *Human pressure*

In the preceding chapter, an analysis was conducted of the potential area in which sperm whales were susceptible to fatal collisions with boats. The findings presented herein were derived from the application of a habitat suitability model in combination with Automated Identification System (AIS) data collected during the month of August 2022. It is important to note that the density of boats can be underestimated. As has been demonstrated in various studies, few boats emit AIS, with sometimes less than 50% of boats in a study conducted on the Scottish coast doing so [207]. The findings of the study demonstrated that the collision risk is twice as high in the Pelagos Sanctuary than in the entire Mediterranean Sea. The evidence presented indicates that vessels of a larger size are associated with an elevated risk of danger. Indeed, a categorisation was established for the purpose of distinguishing between "large and slow" boats and those ferries that exceed a speed of 20 knots. Nevertheless, at a velocity of 20 knots, the likelihood of a fatal collision is nearly 100% [208]. This indicates that the probability is consistent for both "slow" and "fast" in this particular context. It has been asserted that these large boats, which are characterised as "slow" in this context, are not in fact slow. Rather, they are already fast, a factor which can account for their elevated level of danger. As previously stated, a reduction in speed has the potential to mitigate the consequences of a collision. For instance, a decrease to 10 knots has been shown to reduce the fatality rate of such events by up to 45%. The observed result is indicative of a relationship with the dense marine traffic that characterises this area, which is comprised of multiple significant harbours, including those of Marseille, Toulon and Genoa. In general, the regions that were identified as having elevated levels of risk correspond to those previously delineated in the Pelagos Sanctuary study [209]. Furthermore, in the event that the vessel does not collide with a sperm whale and subsequently impact the population, the noise produced by the boat constitutes a significant factor in the disturbance of the animal. Furthermore, the sonar and propeller of the vessel can be a source of disturbance for the species, given its reliance on sound for foraging purposes. Observations of humpback whales reveal that certain stations exhibit noise profiles corresponding to boat traffic, while others display nocturnal activity of the reef, as illustrated in Figure 85. Indeed, Guadeloupe Deshaies exhibits higher decibel levels during the night-time hours, with a distinctive 'U' shape to the daily mean dB curve. In contrast, the daily dB activity in Guadeloupe Anse Bertrand exhibits an "M" shape, characterised by peaks in the morning and evening. Such a profile may be indicative of an area with significant boat traffic, particularly ferry services. It is probable that the presence of humpback whales in the area of Guadeloupe Anse Bertrand is not

influenced by boat traffic, as this location has been identified as one of the stations with the highest detection of these cetaceans.

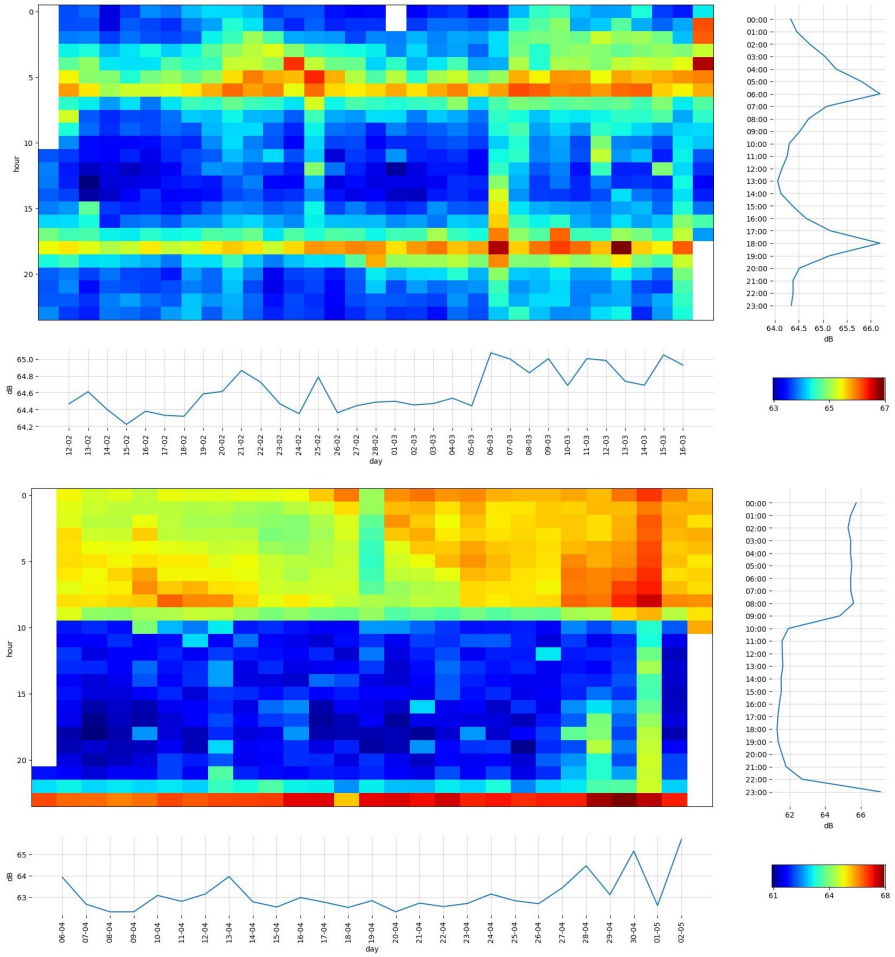


Figure 85: Daily and hourly evolution of the decibel levels for (a.) Guadeloupe Anse Bertrand and (b.) Guadeloupe Deshaies between 6500 and 12,500 Hz : The power spectral density (PSD) was computed for the 6,500–12,500 Hz frequency band in 10-second segments.

It can be posited that the ferry or large boat traffic is the cause of the noise, which is only present for two or three hours a day. This is less than the area that is most frequently used by pleasure craft and exhibits an inverted "U" shape. This suggests that the only favourable time, with less anthropogenic noise, is during the night. As previously demonstrated in preceding studies, significant behavioural alterations in humpback whales have been observed in the presence of boats [210, 211]. These alterations include an increase in speed, a decrease in dive duration, and a reduction in overall resting time. These changes have a direct impact on the whales' energy consumption. In addition, it was observed that the presence of noise from boats

altered the singing activity, which consequently affected individual mating success [212].

The impact of human noise pollution on avian species has been a subject of investigation in the extant literature. As demonstrated in the relevant literature, avian species exhibit an increase in minimum song frequencies in response to human noise [213]. This adjustment is accompanied by a maintenance of key acoustic parameters, including amplitude, maximum frequency, peak frequency, duration, and rate of calling, thereby ensuring the preservation of vocal characteristics despite environmental influences. In the present study, no analysis was conducted on the impact in question. However, the measurement of the Normalised Difference Soundscape Index (NDSI) could have been a mean to perform the analysis. As previously stated, the NDSI quantifies the ratio between biophony and anthrophony. Figure 86 illustrates the mean NDSI value per hour and per day for the Onatchiway station, which is situated at 49° latitude in Québec.

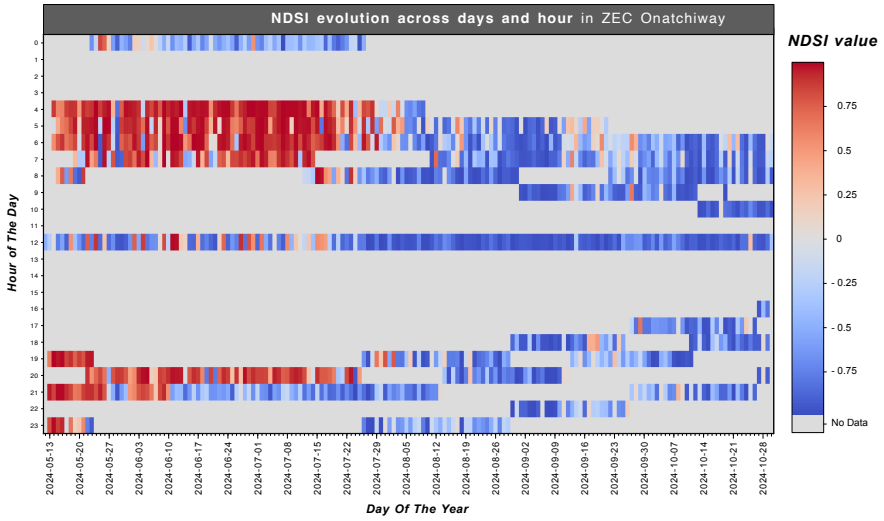


Figure 86: Evolution of the NSDI value across days and hours in the ZEC Onatchiway station

In the instance of a positive NDSI value (red), this indicates that biophony has surpassed anthropophony. Conversely, a negative NDSI value (blue) signifies the reverse. It is observable that the breeding season is characterised by a large red patch from March to the end of July, while the subsequent period is marked by a blue patch. Furthermore, an increase in the NDSI is observable during the morning and night-time periods, whilst a variability is observed during daylight hours. This figure is intended to illustrate the various aspects that were presented in the results. The breeding season, as well as the daily bird activity, which occurs primarily after sunset and sunrise, are represented. However, it is interesting to note that the level of activity is limited during the midday period. This could be due to

either low levels of song activity in the birds or high levels of human activity.

9

GENERAL DISCUSSION

The final sections of this thesis will address the broader implications of the findings and will also be accompanied by a critical evaluation and recommendations for future research direction. Indeed, the integration of automatic detection with artificial neural networks and species distribution modelling has the potential to provide good results however it can introduce considerable complications. In our attempts to predict how a species would respond to different parameters, whether fixed or dynamic, we did not used verified observations to run the GAM models. In contrast, the MaxENT model for sperm whale was developed on the basis of observation, incorporating data derived from diving animals. It is evident that, in order to ensure an optimal fit of the model, the GAM models require both positive and negative values that are of a high quality. Consequently, the implementation of automatic detection in this particular context has the potential to introduce bias to the measure. Following the verification of the observation of certain species, which was found to be consistent with existing literature, the potential for erroneous detection in the data must be considered. As was discussed in the preceding chapters, sound does not propagate in a similar manner when the parameters are altered. This can result in variation in the signal's shape, which consequently presents a more challenging task for the model to detect on the spectrogram. This observation gives rise to an interesting question, which will be discussed here. Are ANN always applicable in research? Before attempting to respond to the aforementioned question, it is first necessary to consider the results and their implications.

9.0.1 *The growing impact of human activity on natural habitats*

As was stated in the thesis and as is already acknowledged in the literature, changes occurring in the environment impact the various populations that inhabit it. It was demonstrated, for instance, that the optimal temperature for the humpback whale breeding ground is below 27.1°C. The aforementioned data, which has previously been documented in other breeding grounds, indicates a probable shift in the breeding grounds or an adaptation in the humpback whale population, as the global ocean temperature continues to rise. The investigation of their potential breeding ground remodelling is imperative to be investigated. Furthermore, it has been observed that marine traffic of all types is occurring in proximity to the habitat of

the sperm whale. This has the potential to result in noise disturbance and, in the most severe cases, fatal collisions. It was also highlighted that the risk of collision is almost double in the marine mammal sanctuary due to its significant location in the Mediterranean Sea. A study has revealed that, for speeds ranging from 10 to 14 knots, there is a probability of between 45% and 75% of a collision resulting in serious injury or death. This risk increases to above 90% when the vessel's speed exceeds 17 knots [208]. As collisions with ships represent a significant cause of mortality among marine mammals, particularly in the Mediterranean Sea, where there is dense marine traffic, the 2019 ACCOMBAMS Resolution 7.12 and 2022 Resolution 8.18 underscore the necessity of establishing conservation plans to reduce these ship strikes. Such plans must be implemented using adapted protocols and solutions. In the province of Québec, it has been observed that certain avian species exhibit a preference for specific forest types. Nevertheless, the ongoing shifts in climate and increasing forestry activities are modifying the distribution of these forests, compelling birds to seek alternative nesting areas. It is notable that there has been an increase in both wildfires and the fragmentation of bird habitats, in addition to rising temperatures at lower and higher latitudes. This suggests that the breeding grounds of birds in the Boreal Forest of Québec may be subject to significant changes in the far to near future. It is evident that further studies are required to analyse the precise bird responses to climatic conditions and their impact on migration, as well as the humpback whale population worldwide. Furthermore, it is imperative to acknowledge the regulatory framework governing marine traffic in areas where marine mammals are known to feed or socialise.

9.0.2 *Defining the objective of the research*

It is conceivable that a multitude of environmental studies can be conducted. It is widely acknowledged that there is a considerable biodiversity loss occurring on a global scale; as a result, there is an imperative to collect data on biodiversity. Nonetheless, the process of data collection is accompanied by inherent costs, including both temporal and financial investments. Additionally, less evident but no less substantial are the carbon footprints associated with research activities. The selection of a clearly defined objective is of fundamental importance prior to this. As previously outlined, the environment is a complex system that demands a sophisticated understanding of numerous specialist subjects. The study of a single species, as evidenced by the research conducted on the sperm whale, has revealed a significant ecological relationship with its prey, specifically squid. It can thus be deduced that the link is of greater importance, given that squids are linked to lower resources in the food chain, which rely on

nutrients. In this study, we observed that the environmental mapping of the sperm whale was achieved through the analysis of the evolution of chlorophyll-a in the ecosystem and the impact of canyons on this process. The prediction of these oceanographic conditions for upwelling or downwelling is contingent upon the use of specific models developed by oceanographers and physicians. The analysis of sperm whale habitat suitability necessitates a substantial degree of knowledge from a variety of scientific disciplines.

Furthermore, it has been shown that a substantial volume of application can be accomplished with a single dataset. As described in the aforementioned work, the CARI'MAM dataset was initially collected with the purpose of documenting the seasonal movements of dolphins and humpback whales across the islands during the winter months. The dataset was used in this study to investigate the habitat preferences of humpback whales. Additionally, it was employed to examine the evolution of their vocal repertoire over time. This dataset offers a valuable opportunity to explore the cultural processes that occur in the animal kingdom. However, as discussed in this paper, since we were able to obtain interesting results on how the vocal repertoire evolves over the entire breeding season, the choice of a duty cycle of 1 minute ON/5 minute OFF does not allow the analysis of the entire song of the humpback whale, which is what is most commonly used in the literature for studying song evolution. It is therefore essential that choices on methods are adapted to the objective of the research that will be done after.

9.0.3 *Choosing the best methods*

As bioacoustics emerges as a significant monitoring tool for biodiversity, it has been the focus of extensive research, resulting in the establishment of voluminous databases. Large-scale monitoring systems, such as those implemented in Québec, necessitate the allocation of substantial storage capacity, typically in the order of multiple terabytes. This requirement is associated with financial implications. However, the same dataset has been employed for birds, as seen in this work, but also for insects [113]. It can be hypothesised that a large-scale monitoring study of this nature, incorporating approximately 10 years of data, could yield significant insights into the future of various taxa, including amphibians and mammals. Furthermore, it has the capacity to unveil alterations over time in the context of climate change and the augmentation of anthropogenic noise within natural habitats. However, it is important to note that the aforementioned quantity of recorders is not feasible for all researchers, nor is it required. As discussed in this study, only 27 species of birds have been the subject of research, while hundreds of others have not been analysed. In the context of research that aims to map the movement

patterns of species between different environments, large-scale monitoring studies can offer significant insights. However, when investigating the arrival and subsequent departure of species at a particular location, the use of limited recorders and visual observations is often sufficient.

This prompts the question of whether automatic detection and artificial neural networks (ANNs) can be successfully applied in the domain of bioacoustics. The advent of these technologies in research has enabled the analysis of a greater quantity of data. This thesis demonstrates that both the humpback whale and bird models are capable of analysing a considerable volume of recordings, with the capacity to predict the species present within a time frame that is unattainable for human analysts (less than 10 milliseconds for 15 seconds of signal). Nevertheless, it should be noted that this level of speed is accompanied by a certain degree of bias, which manifests in the form of a compromise between high recall, but lower precision, and high precision, but lower recall. The choices that are made have a significant impact on the results, whether the abundance (when low recall) or the diversity (with low precision). Indeed, a model that confuses two species in a recording will tend to predict both species, resulting in subsequent analysis that is biased. In the aforementioned thesis, the use of the object detection model YOLOv5 was proposed, which employs boxed annotation in time and frequency. In addition, a methodology was proposed for identifying the optimal model parameter, with a threshold value designated for each species. It has been demonstrated that models are more prone to confusion at higher levels of chorus, as evidenced in this study. To address this issue, we propose a methodology to mitigate errors in soundscape recordings. Nevertheless, the model that was presented is complex, requires a significant amount of annotation, and necessitates GPU capacity in order to be operational. Despite the presence of annotation (approximately 30,000 for birds and 3,000 for humpback whales), the performance metrics may still fall beneath the required standards for certain research applications, which demand highly precise and error-free data. Annotations represent a significant subject in the context of ANNs, given their capacity to exert a substantial influence on the outcomes of these models in their entirety. The optimal solution is the selection of manual annotations, accompanied by expert verifications. However, as the large models that are now in use require an increasing number of annotations, the task is no longer feasible for experts alone. Indeed, the employment of a combination of automatic and manual annotations has become a prevalent methodology, as it facilitates the augmentation of the quantity of annotations while maintaining a satisfactory level of accuracy.

Consequently, the present thesis observes that the use of the NDSI index in a single station unveils a pattern that is consistent with the

findings of the detection, which pertains to daily activity in relation to photoperiod, in addition to arrival and departure date. The use of the aforementioned index, which quantifies the ratio between biophony and anthropophony, has the potential to yield outcomes that are analogous to those obtained through automatic detection. These outcomes may exhibit comparable response curves to those observed in the GAM models. Nevertheless, NDSI does not facilitate the determination of species, as previously outlined in this research. Similarly, the nROI which was studied also does not contribute to this process.

In conclusion, the selection of methodology is contingent upon the objectives of the study in question. Indeed, the requirement for automatic detection using an ANN varies significantly between studies. Consequently, the presence or absence of a particular species within the recordings necessitates a different methodology. The employment of ANNs has the capacity to yield a more substantial amount of information, albeit with the possibility of false detections. However, it can be used on a global scale, thereby reducing errors. Manual detection has been demonstrated to yield precise information, thus facilitating the study of specific traits of the studied species. Then, acoustic indices have the capacity to be used across a variety of protocols, thereby facilitating the acquisition of insight and the facilitation of comparison between disparate regions, provided that the recording protocol is analogous. In conclusion, the selection of methods is contingent on the objectives of the study. ANNs should not be regarded as the sole means of obtaining results for biodiversity monitoring. In scenarios where the quantity of files is substantial, which would be laborious for a human to manage, ANN can be employed, taking into account their inherent biases and error rates.

10 CONCLUSION

In conclusion, bioacoustics has been demonstrated to be an effective tool with which to monitor the presence of various species. In combination with automated analysis, there is considerable potential for the acquisition of valuable results, which may assist in the analysis of species behaviour. In addition, alongside the utilisation of species distribution modelling (SDM), the automatic detection and environmental features can be employed to analyse species preferences with greater precision. In this study, the YOLO architecture was employed to detect and classify 23 humpback whale units and 27 different birds species. The models obtained mAP scores above 70%, and the utilisation of these models on extensive databases facilitates the determination of seasonal fluctuations. Furthermore, bioacoustic monitoring was utilised to confirm the presence of sperm whales in the Mediterranean region. The analysis of the obtained results, in relation to environmental features, enabled the prediction of the potential sperm whale habitat and the identification of areas where there is a high probability of boat collisions. The present study highlights the multifaceted relationship between bioacoustic, automatic detection with deep learning and species distribution modelling employing diverse methodologies.

11

CONTRIBUTIONS

Here are the main contributions of this thesis :

- The present thesis sets out a workflow with all the necessary scripts and open-source materials, with the aim of assisting bioacousticians in the use of time-frequency models for detection tasks in acoustic recordings.

- Furthermore, the present thesis encompasses the publication of two datasets in the European database Zenodo, which are open source. Firstly, the detection of humpback whales (*Megaptera novaeangliae*) was published, with a total of 600,000 detections documented. In addition, all the verified annotations for 23 distinct classes were made available here. Secondly, the dataset containing annotations of 27 species of bird in Quebec has also been published on Zenodo here.

- A bird detector was released in GitHub as well as a humpback whale detector with all the scripts to run it again on new datasets here.

- Finally, the research reports were published online and at different events where the public could come and talk about the results, discuss them and even help to share them (ORCID) .

- Final contribution is a repository with multiple script to perform sound analysis, such as acoustic indices, spectral density power or Time Delay of Arrival for click analysis or to download and analyse the data from Copernicus Ocean dataset, with map visualisation or Hovmöller representation (git_tools).

—

"The mountains [and oceans] are calling and I must go."
John Muir

—

BIBLIOGRAPHY

[1] Vir Singh. *Textbook of environment and ecology*. Springer, 2024.

[2] Nathan L Stephenson. "Estimated ages of some large giant sequoias: General Sherman keeps getting younger". In: *Madroño* (2000), pp. 61–67. URL: https://sierranaturenotes.yosemite.ca.us/SequoiaAges.htm.

[3] David C Coleman, DA Crossley, and Paul F Hendrix. *Fundamentals of soil ecology*. Academic press, 2004. DOI: https://doi.org/10.1016/B978-0-12-179726-3.X5000-X.

[4] Jinfei Zhang, Ying Liu, Shunan Zhang, Houqing Zeng, Wona Ding, Dajian Zhang, and Guohua Xu. "Plant nitrogen nutrition: enhancing plant resilience to abiotic stresses". In: *Journal of Genetics and Genomics* (2026). ISSN: 1673-8527. DOI: https://doi.org/10.1016/j.jgg.2026.03.004.

[5] Zachary Sylvain and Diana Wall. "Linking soil biodiversity and vegetation: Implications for a changing planet". In: *American journal of botany* 98 (Mar. 2011), pp. 517–27. DOI: 10.3732/ajb.1000305.

[6] David Moore, Gemma Cranston, Anders Reed, and Alessandro Galli. "Projecting future human demand on the Earth's regenerative capacity". In: *Ecological Indicators* 16 (2012), pp. 3–10. DOI: 10.1016/j.ecolind.2011.01.008.

[7] Nafiu Ahmed, Taherul Islam Khan, and Aboh Augustine. "Climate change and environmental degradation: a serious threat to global security". In: *European Journal of Social Sciences Studies* (2018). DOI: 10.5281/zenodo.1307227.

[8] Bradley J Cardinale, J Emmett Duffy, Andrew Gonzalez, David U Hooper, Charles Perrings, Patrick Venail, Anita Narwani, Georgina M Mace, David Tilman, David A Wardle, et al. "Biodiversity loss and its impact on humanity". In: *Nature* 486.7401 (2012), pp. 59–67. DOI: https://doi.org/10.1038/nature11148.

[9] David U Hooper, E Carol Adair, Bradley J Cardinale, Jarrett EK Byrnes, Bruce A Hungate, Kristin L Matulich, Andrew Gonzalez, J Emmett Duffy, Lars Gamfeldt, and Mary I O'Connor. "A global synthesis reveals biodiversity loss as a major driver of ecosystem change". In: *Nature* 486.7401 (2012), pp. 105–108. DOI: 10.1038/nature11118.

[10] Muzafar Shah Habibullah, Badariah Haji Din, Siow-Hooi Tan, and Hasan Zahid. "Impact of climate change on biodiversity loss: global evidence". In: *Environmental Science and Pollution Research* 29.1 (2022), pp. 1073–1086. DOI: 10.1007/s11356-021-15702-8.

[11] Intergovernmental Panel On Climate Change. "Climate change 2007: Impacts, adaptation and vulnerability". In: *Genebra, Suíça* (2001).

[12] Erik Meijaard, Muiz Wafiy, Safwanah Ni'Mattulah, Rona Dennis, Panut Hadisiswoyo, Douglas Sheil, Adrià Descals, David L.A. Gaveau, Nabillah Unus, Hjalmar Kühl, Friederike E.L. Otto, Jatna Supriatna, Edvin Aldrian, David Petley, and Serge Wich. "Extreme rainfall further endangers the world's rarest great ape". In: *Current Biology* 36.12 (2026), 3176–3183.e2. ISSN: 0960-9822. DOI: https://doi.org/10.1016/j.cub.2026.05.029. URL: https://www.sciencedirect.com/science/article/pii/S0960982226006342.

[13] Yi Zhou and Baojing Gu. "The impacts of human activities on Earth Critical Zone". In: *Earth Critical Zone* 1.1 (2024), p. 100004. ISSN: 2950-4767. DOI: https://doi.org/10.1016/j.ecz.2024.100004.

[14] Florian Borgwardt, Leonie Robinson, Daniel Trauner, Heliana Teixeira, Antonio J.A. Nogueira, Ana I. Lillebø, Gerjan Piet, Mathias Kuemmerlen, Tim O'Higgins, Hugh McDonald, Juan Arevalo-Torres, Ana Luisa Barbosa, Alejandro Iglesias-Campos, Thomas Hein, and Fiona Culhane. "Exploring variability in environmental impact risk from human activities across aquatic ecosystems". In: *Science of The Total Environment* 652 (2019), pp. 1396–1408. ISSN: 0048-9697. DOI: https://doi.org/10.1016/j.scitotenv.2018.10.339.

[15] Benjamin Halpern, Kimberly Selkoe, Fiorenza Micheli, and Carrie Kappel. "Evaluating and Ranking the Vulnerability of Global Marine Ecosystems to Anthropogenic Threats". In: *Conservation biology : the journal of the Society for Conservation Biology* 21 (Nov. 2007), pp. 1301–15. DOI: 10.1111/j.1523-1739.2007.00752.x.

[16] Rachel Carson. "Silent spring. 1962". In: *New York* (2009).

[17] Gary M Fellers. "Aggression, territoriality, and mating behaviour in North American treefrogs". In: *Animal Behaviour* 27 (1979), pp. 107–119. DOI: https://doi.org/10.1016/0003-3472(79)90131-3.

[18] Danielle M. Cholewiak, Salvatore Cerchio, Jeff K. Jacobsen, Jorge Urbán-R., and Christopher W. Clark. "Songbird dynamics under the sea: acoustic interactions between humpback

whales suggest song mediates male interactions". In: *Royal Society Open Science* 5.2 (Feb. 2018), p. 171298. ISSN: 2054-5703. DOI: 10.1098/rsos.171298.

[19] Roger Payne and Scott McVay. "Songs of Humpback Whales". In: *Science (New York, N.Y.)* 173 (Sept. 1971), pp. 585–97. DOI: 10.1126/science.173.3997.585.

[20] Marcos Maldonado-Coelho, Sidnei S. dos Santos, Morton L. Isler, Maria Svensson-Coelho, Manuelita Sotelo-Muñoz, Cristina Y. Miyaki, Robert E. Ricklefs, and John G. Blake. "Evolutionary and Ecological Processes Underlying Geographic Variation in Innate Bird Songs". In: *The American Naturalist* 202.2 (2023). PMID: 37531273, E31–E52. DOI: 10.1086/725016.

[21] Chiara De Gregorio, Filippo Carugati, Vittoria Estienne, Daria Valente, Teresa Raimondi, Valeria Torti, Longondraza Miaretsoa, Jonah Ratsimbazafy, Marco Gamba, and Cristina Giacoma. "Born to sing! Song development in a singing primate". In: *Current Zoology* 67.6 (Dec. 2021), pp. 597–608. ISSN: 2396-9814. DOI: 10.1093/cz/zoab018.

[22] Katie Kowarski, Salvatore Cerchio, Hal Whitehead, and Hilary Moors-Murphy. "Where, when, and why do western North Atlantic humpback whales begin to sing ?" In: *Bioacoustics* 31.4 (2022), pp. 450–469. DOI: 10.1080/09524622.2021.1972838.

[23] Paul Best, Lise Habib-Dasetto, Jules Cauzinille, Ricard Marxer, Fabienne Delfour, Thierry Legout, and Marie Montant. *Underwater behaviour of Globicephala melas*. IBAC 2025. Poster. Sept. 2025. URL: https://hal.science/hal-05497429.

[24] Lara Berkenbaum, François Sarano, Toinon Flecher, Walter M.X. Zimmer, Olivier Adam, René Heuzey, Axel Preud'Homme, and Hervé Glotin. *Analysis of sperm whale (Physeter macrocephalus) dialogues, click by click: an ethoacoustic approach*. One Ocean Science Congress. Poster. June 2025. URL: https://univ-tln.hal.science/hal-05281331.

[25] C Abrahams. "Bioacoustics as a research tool for avian ecology and conservation". PhD thesis. Nottingham Trent University, 2022. URL: https://irep.ntu.ac.uk/id/eprint/47203/.

[26] V. Kandia and Y. Stylianou. "Detection of sperm whale clicks based on the Teager–Kaiser energy operator". In: *Applied Acoustics* 67.11 (2006). Detection and localization of marine mamals using passive acoustics, pp. 1144–1163. ISSN: 0003-682X. DOI: https://doi.org/10.1016/j.apacoust.2006.05.007.

[27] Maxence Ferrari. "Study of a biosonar based on the modeling of a complete chain of emission-propagation-reception with validation on sperm whales. General Mathematics [math. GM].

Université de Picardie Jules Verne". In: *English. NNT: 2020AMIE0006 tel-03626254* (2020). DOI: 10.70675/bc53afd3z7e48z418czac64ze2d3ce020ada.

[28] Jérôme Sueur, Almo Farina, Amandine Gasc, Nadia Pieretti, and Sandrine Pavoine. "Acoustic Indices for Biodiversity Assessment and Landscape Investigation". In: *Acta Acustica united with Acustica* 100 (Aug. 2014). DOI: 10.3813/AAA.918757.

[29] Sylvain Haupert, Manon Ducrettet, Frédéric Sèbe, and Jérôme Sueur. "Is monitoring biodiversity with acoustic indices a cul-de-sac?" In: (Apr. 2025). DOI: 10.21203/rs.3.rs-6481480/v1.

[30] Frederic B. Fitch. "Warren S. McCulloch and Walter Pitts. A logical calculus of the ideas immanent in nervous activity. Bulletin of mathematical biophysics, vol. 5 (1943), pp. 115–133." In: *Journal of Symbolic Logic* 9.2 (1944), 49–50. DOI: 10.2307/2268029.

[31] Hervé Goëau, Pierre Bonnet, and Alexis Joly. "AI-based Identification of Plant Photographs from Herbarium Specimens". In: *Biodiversity Information Science and Standards* 5 (Aug. 2021). TDWG 2021, virtual Conference, pp. 1–4. DOI: 10.3897/biss.5.73751.

[32] Stefan Kahl, Connor M. Wood, Maximilian Eibl, and Holger Klinck. "BirdNET: A deep learning solution for avian diversity monitoring". In: *Ecological Informatics* 61 (2021), p. 101236. ISSN: 1574-9541. DOI: https://doi.org/10.1016/j.ecoinf.2021.101236.

[33] Long Cao, Ken Caldeira, and Atul K. Jain. "Effects of carbon dioxide and climate change on ocean acidification and carbonate mineral saturation". In: *Geophysical Research Letters* 34.5 (2007). DOI: https://doi.org/10.1029/2006GL028605.

[34] Tatiana Ilyina, Richard Zeebe, and Peter Brewer. "Future ocean increasingly transparent to low-frequency sound owing to carbon dioxide emissions". In: *Nature Geoscience* 3 (Dec. 2009), pp. 18–22. DOI: 10.1038/ngeo719.

[35] Jérôme Defrance, Philippe Jean, and Nicolas Barrière. "Les arbres et les forêts peuvent-ils contribuer à l'amélioration de l'environnement sonore ?" In: (), pp. 187–195. DOI: 10.3917/spub.190.0187.

[36] Martin Obrist, Gianni Pavan, Jérôme Sueur, Klaus Riede, Diego Llusia, and Rafael Márquez. "Chapter 5. Bioacoustics approaches in biodiversity inventories". In: vol. 8. Jan. 2010, pp. 68–99. ISBN: 1784-1291. URL: https://api.semanticscholar.org/CorpusID:209423763.

[37] Salvatore Cerchio and Marilyn Dahlheim. "Variation in feeding vocalizations of humpback whale *Megaptera novaeangliae* from Southeast Alaska". In: *J. Bioacoustics* 11 (2001), pp. 277–295. DOI: 10.1080/09524622.2001.9753468.

[38] Rebecca Dunlop, Douglas Cato, and Michael Noad. "Non-song acoustic communication in migrating humpback whales (*Megaptera novaeangliae*)". In: *Marine Mammal Science* 24 (2008), pp. 613–29. DOI: 10.1111/j.1748-7692.2008.00208.x.

[39] Louis M Herman, Adam A Pack, Scott S Spitz, Elia YK Herman, Kathryn Rose, Siri Hakala, and Mark H Deakos. "Humpback whale song: who sings?" In: *Behavioral Ecology and Sociobiology* 67.10 (2013), pp. 1653–1663. DOI: 10.1007/s00265-013-1576-8.

[40] Howard Elliott Winn and Lois King Winn. "The song of the humpback whale *Megaptera novaeangliae* in the West Indies". In: *Marine Biology* 47 (1978), pp. 97–114. DOI: https://doi.org/10.1007/BF00395631.

[41] Whitlow Au, Adam Pack, Marc Lammers, Louis Herman, Mark Deakos, and Kimberly Andrews. "Acoustic properties of humpback whale song". In: *J. Acoustical Soc. of America* 120 (2006), pp. 1103–10. DOI: 10.1121/1.2211547.

[42] Stephen Handel, Sean K Todd, and Ann M Zoidis. "Rhythmic structure in humpback whale (Megaptera novaeangliae) songs: Preliminary implications for song production and perception". In: *The Journal of the Acoustical Society of America* 125.6 (2009), EL225–EL230. DOI: https://doi.org/10.1121/1.3124712.

[43] Danielle Cholewiak, Renata Sousa-Lima, and Salvatore Cerchio. "Humpback whale song hierarchical structure: Historical context and discussion of current classification issues". In: *Marine Mammal Science* 29 (2013), pp. 312–32. DOI: 10.1111/mms.12005.

[44] Véronique Sarano, François Sarano, Justine Girardet, Axel Preud'homme, Hugues Vitry, René Heuzey, Marion Sarano, Fabienne Delfour, Hervé Glotin, Olivier Adam, Bénédicte Madon, and Jean-Luc Jung. "Underwater photo-identification of sperm whales (Physeter macrocephalus) off Mauritius". In: *Marine Biology Research* 18.1-2 (2022). Ed. by Informa UK Limited, pp. 131–146. DOI: 10.1080/17451000.2022.2040737.

[45] Christian Lydersen, Marie-Anne Blanchet, Kit M Kovacs, Tiu Similä, Carla Freitas, Zoë Morange, Ove M Pedersen, Emma F Vogel, Marten Bril, Guttorm Christensen, et al. "Migration to breeding areas by male sperm whales Physeter macrocephalus from the Northeast Atlantic Arctic". In: *Scientific Reports* 15.1

(2025), p. 7861. DOI: https://doi.org/10.1038/s41598-025-91266-8.

[46] Sally A Mizroch and Dale W Rice. "Ocean nomads: Distribution and movements of sperm whales in the North Pacific shown by whaling data and Discovery marks". In: *Marine Mammal Science* 29.2 (2013), E136–E165. DOI: 10.1111/j.1748-7692.2012.00601.x.

[47] Stéphanie L. Watwood, Patrick J. O. Miller, Mark Johnson, Peter T. Madsen, and Peter L. Tyack. "Deep-diving foraging behaviour of sperm whales (Physeter macrocephalus)". In: *Journal of Animal Ecology* 75.3 (2006), pp. 814–825. DOI: https://doi.org/10.1111/j.1365-2656.2006.01101.x.

[48] H. Whitehead, J. Barlow, S.M. Dawson, A. Eguiguren, B. Miller, and F. Shabangu. "Physeter macrocephalus. The IUCN Red List of Threatened Species 2025: e.T41755A50382216". In: (2025). DOI: https://dx.doi.org/10.2305/IUCN.UK.2025-2.RLTS.T41755A50382216.en.

[49] Heather Williams. "Birdsong and Singing Behavior". In: *Annals of the New York Academy of Sciences* 1016.1 (2004), pp. 1–30. DOI: https://doi.org/10.1196/annals.1298.029.

[50] Justin Salamon, Juan Pablo Bello, Andrew Farnsworth, Matt Robbins, Sara Keen, Holger Klinck, and Steve Kelling. "Towards the automatic classification of avian flight calls for bioacoustic monitoring". In: *PloS one* 11.11 (2016), e0166866. DOI: https://doi.org/10.1371/journal.pone.0166866.

[51] F Lincoln. "The migratory flyways of North America". In: *US Department of Agriculture. Circular* 342 (1935), p. 12.

[52] John M Hagan, Trevor L Lloyd-Evans, and Jonathan L Atwood. "The relationship between latitude and the timing of spring migration of North American landbirds". In: *Ornis Scandinavica* (1991), pp. 129–136. DOI: 10.2307/3676543.

[53] Jay Zaifman, Daoyang Shan, Ahmet Ay, and Ana Gabriela Jimenez. "Shifts in bird migration timing in north American long-distance and short-distance migrants are associated with climate change". In: *International Journal of Zoology* 2017.1 (2017), p. 6025646. DOI: https://doi.org/10.1155/2017/6025646.

[54] Eberhard Gwinner. "Circannual rhythms in bird migration". In: *Annual Review of Ecology and Systematics* (1977), pp. 381–405. DOI: 10.1146/annurev.es.08.110177.002121.

[55] Vinod Kumar, John C Wingfield, Alistair Dawson, Marilyn Ramenofsky, Sangeeta Rani, and Paul Bartell. "Biological clocks and regulation of seasonal reproduction and migration in birds". In: *Physiological and Biochemical Zoology* 83.5 (2010), pp. 827–835. DOI: 10.1086/652243.

[56] Frank Chapman Bellrose. "Waterfowl migration corridors east of the Rocky Mountains in the United States". In: *Biological notes; no. 061* (1968). DOI: 10.5962/bhl.title.15160.

[57] Michael G. Buhnerkempe, Colleen T. Webb, Andrew A. Merton, John E. Buhnerkempe, Geof H. Givens, Ryan S. Miller, and Jennifer A. Hoeting. "Identification of migratory bird flyways in North America using community detection on biological networks". In: *Ecological Applications* 26.3 (2016), pp. 740–751. DOI: https://doi.org/10.1890/15-0934.

[58] Herbert Robbins and Sutton Monro. "A stochastic approximation method". In: *The annals of mathematical statistics* (1951), pp. 400–407. DOI: 10.1214/aoms/1177729586.

[59] Diederik P Kingma and Jimmy Ba. "Adam: A method for stochastic optimization". In: *arXiv preprint arXiv:1412.6980* (2014). DOI: https://doi.org/10.48550/arXiv.1412.6980.

[60] Cailey I Kerley, Leon Y Cai, Yucheng Tang, Lori L Beason-Held, Susan M Resnick, Laurie E Cutting, and Bennett A Landman. "Batch size go big or go home: counterintuitive improvement in medical autoencoders with smaller batch size". In: *Medical Imaging 2023: Image Processing*. Vol. 12464. SPIE. 2023, pp. 106–115. DOI: 10.1117/12.2653643.

[61] Kim Bjerge, Jamie Alison, Mads Dyrmann, Carsten Eie Frigaard, Hjalte MR Mann, and Toke Thomas Høye. "Accurate detection and identification of insects from camera trap images with deep learning". In: *PLOS Sustainability and Transformation* 2.3 (2023), e0000051. DOI: https://doi.org/10.1371/journal.pstr.0000051.

[62] Margarita Mulero-Pázmány, Sandro Hurtado, Cristóbal Barba-González, María Luisa Antequera-Gómez, Francisco Díaz-Ruiz, Raimundo Real, Ismael Navas-Delgado, and José F Aldana-Montes. "Addressing significant challenges for animal detection in camera trap images: a novel deep learning-based approach". In: *Scientific Reports* 15.1 (2025), p. 16191. DOI: https://doi.org/10.1038/s41598-025-90249-z.

[63] Stéphane Chavin, Jérôme Couvat, Paul Best, Laurent Bouveret, Julien Chalifour, Tacumba Duncan, Sébastien Gréaux, Cathy Lacourbas, Sarah Manuel, Benjamin de Montgolfier, Marit Pistor, and Hervé Glotin. *Time-Frequency Exploration of the Repertoire and Evolution of Humpback Whale Songs in the Caribbean Sea*. DCLDE. Poster. June 2024. URL: https://hal.science/hal-04917511.

[64] Bart van Merriënboer, Vincent Dumoulin, Jenny Hamer, Lauren Harrell, Andrea Burns, and Tom Denton. *Perch 2.0: The Bittern Lesson for Bioacoustics*. 2025. arXiv: 2508.04665 [cs.LG]. URL: https://arxiv.org/abs/2508.04665.

[65] Connor M Wood, Felix Günther, Angela Rex, Daniel F Hofstadter, Hendrik Reers, Stefan Kahl, M Zachariah Peery, and Holger Klinck. "Real-time acoustic monitoring facilitates the proactive management of biological invasions". In: *Biological Invasions* 26.12 (2024), pp. 3989–3996. DOI: https://doi.org/10.1007/s10530-024-03426-y.

[66] Douglas Gillespie, DK Mellinger, JONATHAN Gordon, David Mclaren, PAUL Redmond, Ronald McHugh, PW Trinder, XY Deng, and A Thode. "PAMGUARD: Semiautomated, open source software for real-time acoustic detection and localisation of cetaceans". In: *Journal of the Acoustical Society of America* 30.5 (2008), pp. 54–62. DOI: ttps://doi.org/10.1121/1.4808713.

[67] Joanna Sarnocinska, Jakob Tougaard, Mark Johnson, Peter T Madsen, and Magnus Wahlberg. "Comparing the performance of C-PODs and SoundTrap/PAMGUARD in detecting the acoustic activity of harbor porpoises (Phocoena phocoena)". In: *Proceedings of meetings on acoustics*. Vol. 27. 1. Acoustical Society of America. 2016, p. 070013. DOI: https://doi.org/10.1121/2.0000288.

[68] AM von Benda-Beckmann, C Binder, H Johnson, J MacDonnell, J Theriault, A Vanderlaan, and D Thomson. "Northern right whale sonobuoy localisation dataset for the DCDLE workshop". In: *Technical Report Final report* (2022). URL: https://dclde2024.com/site/assets/files/1034/dclde2024_dataset_v5_0-1.pdf.

[69] KJ Palmer, Emma Cummings, Michael G Dowd, Kait Frasier, Fabio Frazao, Alex Harris, April Houweling, Jasper Kanes, Oliver S Kirsebom, Holger Klinck, et al. "A public dataset of annotated orcinus orca acoustic signals for detection and ecotype classification". In: *Scientific data* 12.1 (2025), p. 1137. DOI: 10.1038/s41597-025-05281-5.

[70] Maxence Ferrari, Hervé Glotin, Ricard Marxer, and Mark Asch. "DOCC10: Open access dataset of marine mammal transient studies and end-to-end CNN classification". In: *2020 International Joint Conference on Neural Networks (IJCNN)*. IEEE. 2020, pp. 1–8. DOI: 10.1109/IJCNN48605.2020.9207085.

[71] Miles Parsons, Audrey Looby, Kranthikumar Chanda, Lucia Di Iorio, Christine Erbe, Fabio Frazao, Michelle-Nicole Havlik, Francis Juanes, Marc Lammers, Songhai Li, Matthias Liffers, Tzu-Hao Lin, Simon Linke, Aran Mooney, Craig Radford,

Aaron Rice, Rodney Rountree, Laela Sayigh, Renata Sousa-Lima, and Sophie Nedelec. "A Global Library of Underwater Biological Sounds (GLUBS): An Online Platform with Multiple Passive Acoustic Monitoring Applications". In: Oct. 2024, pp. 2149–2173. ISBN: 978-3-031-50255-2. DOI: 10.1007/978-3-031-50256-9_123.

[72] Arik Kershenbaum et al. "Automatic detection for bioacoustic research: a practical guide from and for biologists and computer scientists". In: *Biological Reviews* 100.2 (2025), pp. 620–646. DOI: https://doi.org/10.1111/brv.13155.

[73] Dena Jane Clink and Johny Tasirin. "The potential for passive acoustic monitoring and automated detection to improve conservation efforts of tarsiers in Sulawesi, Indonesia". In: (2026). DOI: https://doi.org/10.32942/x2dt0m.

[74] Daniel Romero-Mujalli, Tjard Bergmann, Axel Zimmermann, and Marina Scheumann. "Utilizing DeepSqueak for automatic detection and classification of mammalian vocalizations: a case study on primate vocalizations". In: *Scientific reports* 11.1 (2021), p. 24463. DOI: https://doi.org/10.1038/s41598-021-03941-1.

[75] Ella Browning, Rory Gibb, Paul Glover-Kapfer, and Kate Jones. "Passive acoustic monitoring in ecology and conservation". In: (Oct. 2017). DOI: 10.13140/RG.2.2.18158.46409.

[76] Tristan Carsault, Mohamed Alila, Madiop Lo, Achraf Drira, and Alessio Maglio. "North Atlantic Right Whale upcall detection in passive acoustic monitoring: reproducible benchmark scoring and evaluation-protocol effects". In: *Available at SSRN 6956543* (). DOI: http://dx.doi.org/10.2139/ssrn.6956543.

[77] Masato Hagiwara, Benjamin Hoffman, Jen-Yu Liu, Maddie Cusimano, Felix Effenberger, and Katie Zacarian. *BEANS: The Benchmark of Animal Sounds*. 2022. arXiv: 2210.12300 [cs.SD]. URL: https://arxiv.org/abs/2210.12300.

[78] Khanh Truong, Jo Eidsvik, Robin Andre Rørstadbotnen, Jan Petter Morten, Laurine Andres, and Anthony Sladen. "Automated detection of fin whales with distributed acoustic sensing in the Arctic and Mediterranean". In: *The Journal of the Acoustical Society of America* 158.6 (Dec. 2025), pp. 5057–5074. ISSN: 0001-4966. DOI: 10.1121/10.0041855.

[79] Vicent Avaria-Avaria, Dídac Diego-Tortosa, Carles Gallardo, Sergio Morell-Monzó, and Carlos Alberto Quiroz-Rangel. "Exploring You Only Look Once v8 for automatic detection of dolphin whistles in spectrograms". In: *Bioacoustics* (2026), pp. 1–27. DOI: 10.1080/09524622.2025.2612276.

[80] Rahima Khanam and Muhammad Hussain. *What is YOLOv5: A deep look into the internal features of the popular object detector*. 2024. arXiv: 2407.20892 [cs.CV]. URL: https://arxiv.org/abs/2407.20892.

[81] Adam A Pack, Louis M Herman, Alison S Craig, Scott S Spitz, James O Waterman, Elia YK Herman, Mark H Deakos, Siri Hakala, and Carley Lowe. "Habitat preferences by individual humpback whale mothers in the Hawaiian breeding grounds vary with the age and size of their calves". In: *Animal Behaviour* 133 (2017), pp. 131–144. DOI: https://doi.org/10.1016/j.anbehav.2017.09.012.

[82] Astrid Frisch-Jordán, Nicola Ransome, Oscar Aranda-Mena, and Fernando Romo-Sirvent. "Intensive feeding of humpback whales (Megaptera novaeangliae) in the breeding ground of Banderas Bay, Mexico". In: *Latin American Journal of Aquatic Mammals* 14.1 (2019), pp. 27–33. DOI: 10.5597/lajam00244.

[83] Jay Zaifman, Daoyang Shan, Ahmet Ay, and Ana Gabriela Jimenez. "Shifts in Bird Migration Timing in North American Long-Distance and Short-Distance Migrants Are Associated with Climate Change". In: *International Journal of Zoology* 2017.1 (2017), p. 6025646. DOI: https://doi.org/10.1155/2017/6025646.

[84] Violaine Dulau, Alexandre Gannier, and John Goold. "Diving and Feeding Behaviour of Sperm Whales (Physeter macrocephalus) in the Northwestern Mediterranean Sea". In: *Aquatic Mammals* 30 (Dec. 2004), pp. 419–426. DOI: 10.1578/AM.30.3.2004.419.

[85] Hal Whitehead and Megan Shin. "Current global population size, post-whaling trend and historical trajectory of sperm whales". In: *Scientific reports* 12.1 (2022), p. 19468. DOI: 10.3354/meps242295.

[86] David Grémillet, Sue Lewis, Laurent Drapeau, Carl D van Der Lingen, Jenny A Huggett, Janet C Coetzee, Hans M Verheye, Francis Daunt, Sarah Wanless, and Peter G Ryan. "Spatial match–mismatch in the Benguela upwelling zone: should we expect chlorophyll and sea-surface temperature to predict marine predator distributions?" In: *Journal of Applied Ecology* 45.2 (2008), pp. 610–621. DOI: https://doi.org/10.1111/j.1365-2664.2007.01447.x.

[87] E. Papale et al. "Seasonal habitat suitability and distribution patterns of Mediterranean fin whales". In: *Ecological Informatics* 90 (2025), p. 103362. ISSN: 1574-9541. DOI: https://doi.org/10.1016/j.ecoinf.2025.103362.

[88] Hilary B Moors-Murphy. "Submarine canyons as important habitat for cetaceans, with special reference to the Gully: a review". In: *Deep Sea Research Part II: Topical Studies in Oceanography* 104 (2014), pp. 6–19. DOI: 10.1016/j.dsr2.2013.12.016.

[89] Daniela Silvia Pace, Antonella Arcangeli, Barbara Mussi, Carlotta Vivaldi, Cristina Ledon, Serena Lagorio, Giancarlo Giacomini, Gianni Pavan, and Giandomenico Ardizzone. "Habitat suitability modeling in different sperm whale social groups". In: *The Journal of Wildlife Management* 82.5 (2018), pp. 1062–1073. DOI: https://doi.org/10.1002/jwmg.21453.

[90] Robert L Pitman, John A Totterdell, Holly Fearnbach, Lisa T Ballance, John W Durban, and Hans Kemps. "Whale killers: prevalence and ecological implications of killer whale predation on humpback whale calves off Western Australia". In: *Marine Mammal Science* 31.2 (2015), pp. 629–657. DOI: https://doi.org/10.1111/mms.12182.

[91] Laurène Trudelle, Salvatore Cerchio, Alexandre Zerbini, Ygor Geyer, François-Xavier Mayer, Jean-Luc Jung, Maxime Hervé, Stephane Pous, Jean-Baptiste Sallée, Howard Rosenbaum, Olivier Adam, and Jean-Benoit Charrassin. "Influence of environmental parameters on movements and habitat utilization of humpback whales (*Megaptera novaeangliae*) in the Madagascar breeding ground". In: *Royal Society Open Science* 3.12 (2016), p. 160616. DOI: 10.1098/rsos.160616.

[92] Alexandre N Zerbini, Artur Andriolo, Mads Peter Heide-Jørgensen, José Luis Pizzorno, Ygor G Maia, Glenn R VanBlaricom, Douglas P DeMaster, Paulo César Simões-Lopes, Sérgio Moreira, and Cláudia Bethlem. "Satellite-monitored movements of humpback whales Megaptera novaeangliae in the Southwest Atlantic Ocean". In: *Marine Ecology Progress Series* 313 (2006), pp. 295–304. DOI: https://doi.org/10.3354/meps313295.

[93] Sophie Bestley, Virginia Andrews-Goff, Esmee van Wijk, Stephen R Rintoul, Michael C Double, and Jason How. "New insights into prime Southern Ocean forage grounds for thriving Western Australian humpback whales". In: *Scientific Reports* 9.1 (2019), p. 13988. DOI: https://doi.org/10.1038/s41598-019-50497-2.

[94] Eduardo Mercado and Neil Frazer. "Environmental constraints on sound transmission by humpback whales". In: *J. Acoustical Soc. of America* 106.5 (Nov. 1999), pp. 3004–3016. ISSN: 0001-4966. DOI: 10.1121/1.428120.

[95] Qiongyu Huang, Brooke L. Bateman, Nicole L. Michel, Anna M. Pidgeon, Volker C. Radeloff, Patricia Heglund, Andrew J. Allstadt, A. Justin Nowakowski, Jesse Wong, and John R. Sauer. "Modeled distribution shifts of North American birds

over four decades based on suitable climate alone do not predict observed shifts". In: *Science of The Total Environment* 857 (2023), p. 159603. ISSN: 0048-9697. DOI: https://doi.org/10.1016/j.scitotenv.2022.159603.

[96] Solène Derville, Leigh G. Torres, Renee Albertson, Olive Andrews, C. Scott Baker, Pamela Carzon, Rochelle Constantine, Michael Donoghue, Cyril Dutheil, Alexandre Gannier, Marc Oremus, Michael M. Poole, Jooke Robbins, and Claire Garrigue. "Whales in warming water: Assessing breeding habitat diversity and adaptability in Oceania's changing climate". In: *Global Change Biology* 25.4 (2019), pp. 1466–1481. DOI: https://doi.org/10.1111/gcb.14563.

[97] Amy Kennedy and Phillip Clapham. "From Whaling to Tagging: The Evolution of North Atlantic Humpback Whale Research in the West Indies". In: *Marine Fisheries Review* 79 (Feb. 2018), pp. 23–37. DOI: 10.7755/MFR.79.2.2.

[98] Peter Strevick, Laurent Bouveret, Nadege Gandilhon, Caroline Rinaldi, Renato Rinaldi, Fredrik Broms, Carole Carlson, Amy Kennedy, Natalie Ward, Frederick Wenzel, et al. "Migratory destinations and timing of humpback whales in the Southeastern Caribbean differ from those off the Dominican Republic". In: *J. Cetacean Res. Manage.* 18 (2018), pp. 127–133. DOI: https://doi.org/10.47536/jcrm.v18i1.442.

[99] Cynthia Barile, Simon Berrow, Jonathan Gordon, Rossa Meade, Morgane Pommier, and Joanne O'Brien. "Sperm whale hotspots off western Ireland and the importance of dynamic variables as shown by a multiscale Bayesian additive regression trees workflow". In: *Frontiers in Marine Science* Volume 13 - 2026 (2026). ISSN: 2296-7745. DOI: 10.3389/fmars.2026.1767540. URL: https://www.frontiersin.org/journals/marine-science/articles/10.3389/fmars.2026.1767540.

[100] Sarah NP Wong and Hal Whitehead. "Seasonal occurrence of sperm whales (Physeter macrocephalus) around Kelvin Seamount in the Sargasso Sea in relation to oceanographic processes". In: *Deep Sea Research Part I: Oceanographic Research Papers* 91 (2014), pp. 10–16. DOI: 10.1016/j.dsr.2014.05.001.

[101] Ilias Foskolos, Niki Koutouzi, Lysimachos Polychronidis, Paraskevi Alexiadou, and Alexandros Frantzis. "A taste for squid: the diet of sperm whales stranded in Greece, Eastern Mediterranean". In: *Deep Sea Research Part I: Oceanographic Research Papers* 155 (2020), p. 103164. ISSN: 0967-0637. DOI: https://doi.org/10.1016/j.dsr.2019.103164.

[102] M Merino and MA Monreal-Gómez. *Ocean currents and their impact on marine life*. Vol. 1. In: Encyclopedia of life support systems (EOLSS), developed under the auspices of the UNESCO, 2009, pp. 47–52.

[103] Graeme C Hays. "Ocean currents and marine life". In: *Current Biology* 27.11 (2017), R470–R473. DOI: 10.1016/j.cub.2017.01.044.

[104] Shoshiro Minobe, Akira Kuwano-Yoshida, Nobumasa Komori, Shang-Ping Xie, and Richard Justin Small. "Influence of the Gulf Stream on the troposphere". In: *Nature* 452.7184 (2008), pp. 206–209. DOI: 10.1038/nature06690.

[105] Jaime B Palter. "The role of the Gulf Stream in European climate". In: *Annual review of marine science* 7.1 (2015), pp. 113–137. DOI: https://doi.org/10.1146/annurev-marine-010814-015656.

[106] Marta Pascual, Borja Rives, Celia Schunter, and Enrique Macpherson. "Impact of life history traits on gene flow: A multispecies systematic review across oceanographic barriers in the Mediterranean Sea". In: *PLOS ONE* 12 (May 2017), e0176419. DOI: 10.1371/journal.pone.0176419.

[107] Claude Millot and Isabelle Taupier-Letage. "Circulation in the Mediterranean sea". In: *The Mediterranean Sea*. Springer, 2005, pp. 29–66. DOI: https://doi.org/10.1007/b107143.

[108] M-A Ahumada-Sempoal, María del Mar Flexas, Raffaele Bernardello, Nixon Bahamon, and Antonio Cruzado. "Northern Current variability and its impact on the Blanes Canyon circulation: A numerical study". In: *Progress in Oceanography* 118 (2013), pp. 61–70. DOI: 10.1016/j.pocean.2013.07.030.

[109] Anne A Petrenko. "Variability of circulation features in the Gulf of Lion NW Mediterranean Sea. Importance of inertial currents". In: *Oceanologica acta* 26.4 (2003), pp. 323–338. DOI: 10.1016/S0399-1784(03)00038-0.

[110] Susana García-Monteiro, JA Sobrino, Y Julien, Guillem Sòria, and Drazen Skokovic. "Surface Temperature trends in the Mediterranean Sea from MODIS data during years 2003–2019". In: *Regional Studies in Marine Science* 49 (2022), p. 102086. DOI: https://doi.org/10.1016/j.rsma.2021.102086.

[111] Fatima Ezzahra Ait Ballagh, Christophe Rabouille, Françoise Andrieux-Loyer, Karline Soetaert, Bruno Lansard, Bruno Bombled, Gael Monvoisin, Khalid Elkalay, and Karima Khalil. "Spatial variability of organic matter and phosphorus cycling in rhône river prodelta sediments (NW mediterranean sea, france): A model-data approach". In: *Estuaries and Coasts* 44.7 (2021), pp. 1765–1789. DOI: 10.1007/s12237-020-00889-9.

[112] Catherine Périé and Sylvie de Blois. "Dominant forest tree species are potentially vulnerable to climate change over large portions of their range even at high latitudes". In: *PeerJ* 4 (2016), e2218. DOI: 10.7717/peerj.2218.

[113] Joëlle Spooner. "Distribution et phénologie d'insectes et d'insectivores le long d'un gradient de température induit par la latitude". In: (2024). URL: https://hdl.handle.net/20.500.11794/152123.

[114] John R. Moran, Janice M. Straley, Jacek M. Maselko, Lauren A. Wild, and Robert M. Suryan. "The Decline of Humpback Whales in Prince William Sound, Alaska, Following the 2014–2016 Northeast Pacific Marine Heatwave". In: *Marine Mammal Science* 42.3 (2026). e70195 5542213, e70195. DOI: https://doi.org/10.1111/mms.70195.

[115] CM Coomes and EP Derryberry. "High temperatures reduce song production and alter signal salience in songbirds". In: *Animal Behaviour* 180 (2021), pp. 13–22. DOI: 10.1016/j.anbehav.2021.07.012.

[116] Marion Cordonnier, Amanda R Ridley, Thierry Lengagne, and Mylène Dutour. "The impact of high temperatures on bird responses to alarm calls". In: *Behavioral Ecology and Sociobiology* 77.7 (2023), p. 82. DOI: https://doi.org/10.1007/s00265-023-03354-2.

[117] Valentin Barchasz, Valentin Gies, Sebastian Marzetti, and Hervé Glotin. "A novel low-power high speed accurate and precise DAQ with embedded artificial intelligence for long term biodiversity survey". In: *e-Forum Acusticum 2020*. 2020, pp. 3217–3224. URL: https://hal.science/hal-03230835v1.

[118] Hervé Glotin, Maxence Ferrari, Paul Best, Marion Poupard, Nicolas Thellier, Audrey Monsimer, and Pascale Giraudet. *CARIMAM REPORT BIOACOUSTIC DATA PROCESSING*. Research Report. DYNI LIS, Oct. 2021. URL: https://hal.science/hal-03629286.

[119] Laura González García, Marc Fernández, and José MN Azevedo. "MONICET: The Azores whale watching contribution to cetacean monitoring". In: *Biodiversity Data Journal* 11 (2023), e106991. DOI: https://doi.org/10.3897/BDJ.11.e106991.

[120] Compilation Group GEBCO. In: (2023). DOI: doi:10.5285/f98b053b-0cbc-6c23-e053-6c86abc0af7b.

[121] Nyall Dawson et al. *qgis/QGIS: 3.22.5*. Version final-3_22_5. Mar. 2022. DOI: 10.5281/zenodo.6367783.

[122] P.T. Harris, M. Macmillan-Lawler, J. Rupp, and E.K. Baker. "Geomorphology of the oceans". In: *Marine Geology* 352 (2014). 50th Anniversary Special Issue, pp. 4–24. ISSN: 0025-3227. DOI: https://doi.org/10.1016/j.margeo.2014.01.011.

[123] Copernicus Marine Service. *GLobal Ocean Physics Analysis and Forecast*. 2023. DOI: https://doi.org/10.48670/moi-00016.

[124] *Emodnet-humanactivities.eu EU Vessel Density Map. Detailed Method*. 2019. URL: https://www.emodnet-humanactivities.eu/documents/Vessel%20density%20maps_method_v1.5.pdf.

[125] Kenneth A Baldwin. *Vegetation zones of Canada: A biogeoclimatic perspective*. Natural Resources Canada= Ressources naturelles Canada, 2020. URL: publications.gc.ca/pub?id=9.885047&sl=0.

[126] William F. Holmgren, Clifford W. Hansen, and Mark A. Mikofski. "pvlib python: a python package for modeling solar energy systems". In: *Journal of Open Source Software* 3.29 (2018), p. 884. DOI: 10.21105/joss.00884.

[127] Paul Best, Sébastien Paris, Hervé Glotin, and Ricard Marxer. "Deep audio embeddings for vocalisation clustering". In: *PLOS ONE* 18.7 (July 2023), pp. 1–18. DOI: 10.1371/journal.pone.0283396.

[128] Marion Poupard, Paul Best, Jay Morgan, Gianni Pavan, and Hervé Glotin. "A first vocal repertoire characterization of long-finned pilot whales (Globicephala melas) in the Mediterranean Sea: a machine learning approach". In: *Royal Society Open Science* 11 (Nov. 2024). DOI: 10.1098/rsos.231973.

[129] K. Lisa Yang Center for Conservation Bioacoustics at the Cornell Lab of Ornithology. *Raven Light: Interactive Sound Analysis Software*. Version 2.0.5. 2023. URL: https://www.ravensoundsoftware.com/.

[130] Loïc Lehnhoff, Hervé Glotin, Yves Le Gall, Eric Menut, Hélène Peltier, Alain Pochat, Krystel Pochat, Olivier Van Canneyt, and Bastien Mérigot. "Whistles characterisation using artificial intelligence reveals responses of short-beaked common dolphins to a bio-inspired acoustic mitigation device for fishing nets". In: *Scientific Reports* 15.1 (2025), p. 40618. DOI: https://doi.org/10.1038/s41598-025-24256-5.

[131] Justine Girardet, Hervé Glotin, Stéphane Chavin, Marion Poupard, Julie Guiderdoni, and Véronique Sarano. "Arctic diel and circadian acoustic pattern of Orcas, Fin, and Humpback whales revealed by deep learning from two months of continuous recordings". In: *Ecological Informatics* 93 (2026), p. 103564. ISSN: 1574-9541. DOI: https://doi.org/10.1016/j.ecoinf.2025.103564.

[132] LK Winn and HE Winn. *Wings in the Sea: The humpback whale*. Hanover and London: University of Rhode Island, 1985. DOI: doi:10.1017/S0030605300026508.

[133] Rebecca Dunlop, Michael Noad, Douglas Cato, and Dale Stokes. "The social vocalization repertoire of East australian migrating humpback whales (*Megaptera novaeangliae*)". In: *J. Acoustical Soc. of America* 122 (Dec. 2007), pp. 2893–905. DOI: 10.1121/1.2783115.

[134] Eduardo Mercado and Christina E. Perazio. "All units are equal in humpback whale songs, but some are more equal than others". In: *Animal Cognition* 25.1 (2022), pp. 149–77. DOI: 10.1007/s10071-021-01539-8.

[135] Michelle Fournet, Andy Szabo, and David Mellinger. "Repertoire and classification of non-song calls in Southeast alaskan humpback whales (*Megaptera novaeangliae*)". In: *J. Acoustical Soc. of America* 137 (Jan. 2015). DOI: 10.1121/1.4904504.

[136] Mikala V. Epp, Michelle E. H. Fournet, and Gail K. Davoren. "Humpback whale call repertoire on a Northeastern Newfoundland foraging ground". In: *Marine Mammal Science* 38.1 (2022), pp. 256–273. DOI: https://doi.org/10.1111/mms.12859.

[137] H. E. Winn, T. J. Thompson, W. C. Cummings, J. Hain, J. Hudnall, H. Hays, and W. W. Steiner. "Song of the Humpback Whale: Population Comparisons". In: *Behavioral Ecology and Sociobiology* 8.1 (1981), pp. 41–46. ISSN: 03405443, 14320762. DOI: https://doi.org/10.1007/BF00302842. (Visited on 07/15/2024).

[138] Hervé Glotin, Jean-Louis Etienne, Stéphane Jespers, Justine Girardet, Pascale Giraudet, Valentin Gies, Véronique Sarano, François Sarano, Jean-Marc-Prevot, Nathalie d'Alvise ans Sébastian Marzetti, Valentin Barchasz, Marion Poupard, Maxence Ferrari, Lionel Camus, Pierre Priou, Malik Chami, Julie Guiderdoni, and Sébastien Paris. *Orca, Humpback, Fin and Sperm whales all together into an anthropized Arctic Fjord: the 2021 to 2024 CIAN Expeditions*. Tech. rep. University of Toulon, CIAN ; Laboratoire d'informatique et des Systèmes - LIS (UMR 7020), 2025. URL: https://univ-tln.hal.science/mnhn-04785408.

[139] Leland McInnes, John Healy, Nathaniel Saul, and Lukas Grossberger. "UMAP: Uniform Manifold Approximation and Projection". In: *J. of Open Source Software* 3.29 (2018). DOI: 10.21105/joss.00861.

[140] Tsung-Yi Lin, Michael Maire, Serge J. Belongie, Lubomir D. Bourdev, Ross B. Girshick, James Hays, Pietro Perona, Deva Ramanan, Piotr Doll'a r, and C. Lawrence Zitnick. "Microsoft COCO: Common Objects in Context". In: *CoRR* abs/1405.0312

(2014). arXiv: 1405.0312. URL: http://arxiv.org/abs/1405.0312.

[141] Stefan Kahl, Connor M Wood, Maximilian Eibl, and Holger Klinck. "BirdNET: A deep learning solution for avian diversity monitoring". In: *Ecological Informatics* 61 (2021), p. 101236. DOI: https://doi.org/10.1016/j.ecoinf.2021.101236.

[142] F. Pedregosa, G. Varoquaux, A. Gramfort, V. Michel, B. Thirion, O. Grisel, M. Blondel, P. Prettenhofer, R. Weiss, V. Dubourg, J. Vanderplas, A. Passos, D. Cournapeau, M. Brucher, M. Perrot, and E. Duchesnay. "Scikit-learn: Machine Learning in Python". In: *Journal of Machine Learning Research* 12 (2011), pp. 2825–2830. URL: http://jmlr.org/papers/v12/pedregosa11a.html.

[143] Steven J Phillips and Miroslav Dudík. "Modeling of species distributions with Maxent: new extensions and a comprehensive evaluation". In: *Ecography* 31.2 (2008), pp. 161–175. DOI: https://doi.org/10.1111/j.0906-7590.2008.5203.x.

[144] Auriane Virgili et al. "Combining multiple visual surveys to model the habitat of deep-diving cetaceans at the basin scale". In: *Global Ecology and Biogeography* 28.3 (2019), pp. 300–314. DOI: https://doi.org/10.1111/geb.12850.

[145] Clara Lerebourg, Oliver Boisseau, Vincent Ridoux, and Auriane Virgili. "Summer distribution of the Mediterranean sperm whale: insights from the acoustic Accobams survey initiative". In: *Frontiers in Marine Science* Volume 10 - 2023 (2023). ISSN: 2296-7745. DOI: 10.3389/fmars.2023.1229682.

[146] Enrico Pirotta, Jason Matthiopoulos, Monique MacKenzie, Lindesay Scott-Hayward, and Luke Rendell. "Modelling sperm whale habitat preference: a novel approach combining transect and follow data". In: *Marine Ecology Progress Series* 436 (2011), pp. 257–272. DOI: https://doi.org/10.3354/meps09236.

[147] Stephanie Kramer-Schadt et al. "The importance of correcting for sampling bias in MaxEnt species distribution models". In: *Diversity and Distributions* 19.11 (2013), pp. 1366–1379. DOI: https://doi.org/10.1111/ddi.12096.

[148] Daniel Servén and Charlie Brummitt. *pyGAM: Generalized Additive Models in Python*. Mar. 2018. DOI: 10.5281/zenodo.1208723.

[149] Anke Kügler, Marc O Lammers, Adam A Pack, Ludovic Tenorio-Hallé, and Aaron M Thode. "Diel spatio-temporal patterns of humpback whale singing on a high-density breeding ground". In: *Royal Society Open Science* 11.1 (2024), p. 230279. DOI: 10.6084/m9.figshare.c.7018211.

[150] Antje Inness, Melanie Ades, Jérôme Agustí-Panareda, Jérôme Barré, Anna Benedictow, Anne-Marlene Blechschmidt, Juan Jose Dominguez, Richard Engelen, Henk Eskes, Johannes Flemming, Vincent Huijnen, Luke Jones, Zak Kipling, Sebastien Massart, Mark Parrington, Vincent-Henri Peuch, Miha Razinger, Samuel Remy, Michael Schulz, and Martin Suttie. "The CAMS reanalysis of atmospheric composition". In: *Atmospheric Chemistry and Physics* 19.6 (2019), pp. 3515–3556. DOI: 10.5194/acp-19-3515-2019.

[151] Sara M Maxwell, Elliott L Hazen, Steven J Bograd, Benjamin S Halpern, Greg A Breed, Barry Nickel, Nicole M Teutschel, Larry B Crowder, Scott Benson, Peter H Dutton, et al. "Cumulative human impacts on marine predators". In: *Nature communications* 4.1 (2013), p. 2688. DOI: 10.1038/nclimate2029.

[152] Benjamin S Halpern, Carrie V Kappel, Kimberly A Selkoe, Fiorenza Micheli, Colin M Ebert, Caitlin Kontgis, Caitlin M Crain, Rebecca G Martone, Christine Shearer, and Sarah J Teck. "Mapping cumulative human impacts to California Current marine ecosystems". In: *Conservation letters* 2.3 (2009), pp. 138–148. DOI: 10.1111/j.1755-263X.2009.00058.x.

[153] Elie Grinfeder, Christian Lorenzi, Yann Teytaut, Sylvain Haupert, and Jérôme Sueur. "Introducing evascape, a model-based soundscape assembler: impact of background sounds on biodiversity monitoring with ecoacoustic indices". In: *Ecological Indicators* 178 (2025), p. 113882. ISSN: 1470-160X. DOI: https://doi.org/10.1016/j.ecolind.2025.113882.

[154] Henrike Hultsch and Dietmar Todt. "Repertoire Sharing and Song-Post Distance in Nightingales". In: *Behavioral Ecology and Sociobiology* 8.3 (1981), pp. 183–88. DOI: https://doi.org/10.1007/BF00299828.

[155] Pauli Virtanen et al. "SciPy 1.0: Fundamental Algorithms for Scientific Computing in Python". In: *Nature Methods* 17 (2020), pp. 261–272. DOI: 10.1038/s41592-019-0686-2.

[156] Posit team. *RStudio: Integrated Development Environment for R*. Posit Software, PBC. Boston, MA, 2025. URL: http://www.posit.co/.

[157] Ramprasaath R Selvaraju, Michael Cogswell, Abhishek Das, Ramakrishna Vedantam, Devi Parikh, and Dhruv Batra. "Grad-cam: Visual explanations from deep networks via gradient-based localization". In: *Proceedings of the IEEE international conference on computer vision*. 2017, pp. 618–626. DOI: 10.1109/ICCV.2017.74.

[158] Paul Best, Marion Poupard, Ricard Marxer, Paul Spong, Helena Symonds, and Hervé Glotin. "Analysing vocal complexity in relation to sociality in orcas of British Columbia: An application of long-term computational passive acoustics". In: *Ecological Informatics* 90 (2025), p. 103211. ISSN: 1574-9541. DOI: https://doi.org/10.1016/j.ecoinf.2025.103211.

[159] Kevin R Coffey, Ruby E Marx, and John F Neumaier. "DeepSqueak: a deep learning-based system for detection and analysis of ultrasonic vocalizations". In: *Neuropsychopharmacology : official publication of the American College of Neuropsychopharmacology* 44.5 (2019), 859—868. ISSN: 0893-133X. DOI: 10.1038/s41386-018-0303-6.

[160] Christian Escobar-Amado, Mohsen Badiey, and Lin Wan. "Computer Vision for Bioacoustics: Detection of Bearded Seal Vocalizations in the Chukchi Shelf Using YOLOV5". In: *IEEE Journal of Oceanic Engineering* 49.1 (2024), pp. 133–144. DOI: 10.1109/JOE.2023.3307175.

[161] Clea Parcerisas, Elena Schall, Kees te Velde, Dick Botteldooren, Paul Devos, and Elisabeth Debusschere. "Machine learning for efficient segregation and labeling of potential biological sounds in long-term underwater recordings". In: *Frontiers in Remote Sensing* 5 (2024). ISSN: 2673-6187. DOI: 10.3389/frsen.2024.1390687.

[162] Edward Pandolfino and Lily Douglas. "Regional song dialects of the Ruby-crowned Kinglet". In: *Journal of Field Ornithology* 93 (June 2022). DOI: 10.5751/JFO-00120-930206.

[163] Gabriel B. Mindlin. "Nonlinear dynamics in the study of birdsong". In: *Chaos: An Interdisciplinary Journal of Nonlinear Science* 27.9 (Sept. 2017), p. 092101. ISSN: 1054-1500. DOI: 10.1063/1.4986932.

[164] Hans Slabbekoorn and Thomas B. Smith. "Bird song, ecology and speciation". In: *Philosophical Transactions of the Royal Society B: Biological Sciences* 357.1420 (Apr. 2002), pp. 493–503. ISSN: 0962-8436. DOI: 10.1098/rstb.2001.1056.

[165] Myron Charles Baker and Michael A. Cunningham. "The Biology of Bird-Song Dialects". In: *Behavioral and Brain Sciences* 8.1 (1985), 85–100. DOI: 10.1017/S0140525X00019750.

[166] David Funosas, Luc Barbaro, Laura Schillé, Arnaud Elger, Bastien Castagneyrol, and Maxime Cauchoix. "Assessing the potential of BirdNET to infer European bird communities from large-scale ecoacoustic data". In: *Ecological Indicators* 164 (2024), p. 112146. ISSN: 1470-160X. DOI: https://doi.org/10.1016/j.ecolind.2024.112146.

[167] Cristian Pérez-Granados. "BirdNET: applications, performance, pitfalls and future opportunities". In: *Ibis* 165.3 (2023), pp. 1068–1075. DOI: https://doi.org/10.1111/ibi.13193.

[168] Jerry S Cole, Nicole L Michel, Shane A Emerson, and Rodney B Siegel. "Automated bird sound classifications of long-duration recordings produce occupancy model outputs similar to manually annotated data". In: *Ornithological Applications* 124.2 (Apr. 2022), duac003. ISSN: 0010-5422. DOI: 10.1093/ornithapp/duac003.

[169] Cristian Pérez-Granados et al. "Optimization of passive acoustic bird surveys: a global assessment of BirdNET settings". In: *Ibis* n/a.n/a (2025). DOI: https://doi.org/10.1111/ibi.70013.

[170] Amanda K. Navine, Richard J. Camp, Matthew J. Weldy, Tom Denton, and Patrick J. Hart. "Counting the chorus: A bioacoustic indicator of population density". In: *Ecological Indicators* 169 (2024), p. 112930. ISSN: 1470-160X. DOI: https://doi.org/10.1016/j.ecolind.2024.112930.

[171] Eira Bermúdez-Cuamatzin, Alejandro Rios-Chelen, Diego Gil, and Constantino Garcia. "Experimental evidence for real-time song frequency shift in response to urban noise in a passerine bird". In: *Biology letters* 7 (July 2010), pp. 36–8. DOI: 10.1098/rsbl.2010.0437.

[172] Bryan C. Pijanowski, Luis J. Villanueva-Rivera, Sarah L. Dumyahn, Almo Farina, Bernie L. Krause, Brian M. Napoletano, Stuart H. Gage, and Nadia Pieretti. "Soundscape Ecology: The Science of Sound in the Landscape". In: *BioScience* 61.3 (Mar. 2011), pp. 203–216. ISSN: 0006-3568. DOI: 10.1525/bio.2011.61.3.6.

[173] Luciano Dalla Rosa, John K.B. Ford, and Andrew W. Trites. "Distribution and relative abundance of humpback whales in relation to environmental variables in coastal British Columbia and adjacent waters". In: *Continental Shelf Research* 36 (2012), pp. 89–104. ISSN: 0278-4343. DOI: https://doi.org/10.1016/j.csr.2012.01.017.

[174] Jolanda A Luksenburg. "The cetaceans of Aruba, southern Caribbean". In: *Journal of the Marine Biological Association of the United Kingdom* 94.6 (2014), pp. 1161–1174. DOI: doi:10.1017/S0025315413000337.

[175] Gregory S. Stone, Steven K. Katona, and Edward B. Tucker. "History, migration and present status of humpback whales *Megaptera novaeangliae* at Bermuda". In: *Biological Conservation* 42.2 (1987), pp. 133–145. ISSN: 0006-3207. DOI: https://doi.org/10.1016/0006-3207(87)90019-X.

[176] Thomas Grove, Ruth King, Andrew Stevenson, and Lea-Anne Henry. "A decade of humpback whale abundance estimates at Bermuda, an oceanic migratory stopover site". In: *Frontiers in Marine Science* 9 (2023). ISSN: 2296-7745. DOI: 10.3389/fmars.2022.971801.

[177] Travis Horton, Alexandre Zerbini, Artur Andriolo, Daniel Danilewicz, and Federico Sucunza. "Multi-Decadal Humpback Whale Migratory Route Fidelity Despite Oceanographic and Geomagnetic Change". In: *Frontiers in Marine Science* 7 (2020). DOI: 10.3389/fmars.2020.00414.

[178] A. R. Martin, S. K. Katona, D. Matilla, D. Hembree, and T. D. Waters. "Migration of Humpback Whales between the Caribbean and Iceland". In: *Journal of Mammalogy* 65.2 (May 1984), pp. 330–333. DOI: https://doi.org/10.2307/1381174.

[179] Peter Stevick, Laurent Bouveret, Nadege Gandilhon, Caroline Rinaldi, Renato Rinaldi, Fredrik Broms, Carole Carlson, Amy Kennedy, Nathalie Ward, and Frederick Wenzel. "Migratory destinations and timing of humpback whales in the southeastern Caribbean differ from those off the Dominican Republic". In: *Journal of Cetacean Research and Management* 18 (Jan. 2019), pp. 127–133. DOI: 10.47536/jcrm.v18i1.442.

[180] Amanda K Navine, Richard J Camp, Matthew J Weldy, Tom Denton, and Patrick J Hart. "Counting the chorus: A bioacoustic indicator of population density". In: *Ecological Indicators* 169 (2024), p. 112930. DOI: 10.1016/j.ecolind.2024.112930.

[181] Junior A Tremblay, Jacques Ibarzabal, and Jean-Pierre L Savard. "Foraging ecology of Black-backed Woodpeckers (Picoides arcticus) in unburned eastern boreal forest stands". In: *Canadian Journal of Forest Research* 40.5 (2010), pp. 991–999. DOI: https://doi.org/10.1139/X10-044.

[182] G. Chilton, M. C. Baker, C. D. Barrentine, and M. A. Cunningham. "White-crowned Sparrow (Zonotrichia leucophrys), version 1.0." In: *Birds of the World, Cornell Lab of Ornithology, Ithaca, NY, USA.* (2020). DOI: https://doi.org/10.2173/bow.whcspa.01.

[183] D. L. Swanson, J. L. Ingold, and G. E. Wallace. "Ruby-crowned Kinglet (Corthylio calendula), version 1.1". In: *Birds of the World, Cornell Lab of Ornithology, Ithaca, NY, USA.* (2021). DOI: https://doi.org/10.2173/bow.ruckin.01.1.

[184] Jay Carlisle, Sarah Stock, Gregory Kaltenecker, and David Swanson. "Habitat Associations, Relative Abundance, and Species Richness of Autumn Landbird Migrants in Southwestern Idaho". In: *The Condor* 106 (Aug. 2004), pp. 549–566. DOI: 10.1093/condor/106.3.549.

[185] Yan Boucher, Dominique Arseneault, Luc Sirois, and Louis Blais. "Logging pattern and landscape changes over the last century at the boreal and deciduous forest transition in Eastern Canada". In: *Landscape Ecology* 24.2 (2009), pp. 171–184. DOI: 10.1007/s10980-008-9293-2.

[186] P. Porneluzi, M. A. Van Horn, and T. M. Donovan. "Ovenbird (Seiurus aurocapilla), version 1.0". In: *Birds of the World, Cornell Lab of Ornithology, Ithaca, NY, USA.* (2020). DOI: https://doi.org/10.2173/bow.ovenbi1.01.

[187] MA Van Horn and Donovan TM Ovenbird. "Birds of North America/A. Poole and F. Gill (Eds.). №. 88". In: *Academy of Natural Sciences, Philadelphia, and American Ornithologists' Union, Washington, DC Population Status of Wood Thrush and Ovenbird in Great Smoky Mountains National Park/Ph. D. dissertation. North Carolina State University, Raleigh* (2003). URL: https://www.biodiversitylibrary.org/item/109266.

[188] Xinghao Lu, Yifei Jia, and Yuncai Wang. "The effect of landscape composition, complexity, and heterogeneity on bird richness: A systematic review and meta-analysis on a global scale". In: *Landscape Ecology* 39.8 (2024), p. 132. DOI: https://doi.org/10.1007/s10980-024-01933-w.

[189] Louis Imbeau, Jean-Pierre L Savard, and Réjean Gagnon. "Comparing bird assemblages in successional black spruce stands originating from fire and logging". In: *Canadian Journal of Zoology* 77.12 (2000), pp. 1850–1860. DOI: https://doi.org/10.1139/z99-172.

[190] Vincent Lostanlen, Aurora Cramer, Justin Salamon, Andrew Farnsworth, Benjamin M Van Doren, Steve Kelling, and Juan Pablo Bello. "BirdVoxDetect: Large-scale detection and classification of flight calls for bird migration monitoring". In: *IEEE/ACM Transactions on Audio, Speech, and Language Processing* 32 (2024), pp. 4134–4145. DOI: 10.1109/TASLP.2024.3444486.

[191] Ellen C Garland, Anne W Goldizen, Melinda L Rekdahl, Rochelle Constantine, Claire Garrigue, Nan Daeschler Hauser, M Michael Poole, Jooke Robbins, and Michael J Noad. "Dynamic horizontal cultural transmission of humpback whale song at the ocean basin scale". In: *Current biology* 21.8 (2011), pp. 687–691. DOI: https://doi.org/10.1016/j.cub.2011.03.019.

[192] Josephine N. Schulze, Judith Denkinger, Javier Oña, M. Michael Poole, and Ellen C. Garland. "Humpback whale song revolutions continue to spread from the central into the eastern South Pacific". In: *Royal Society Open Science* 9.8 (2022), p. 220158. DOI: 10.1098/rsos.220158.

[193] Eduardo Mercado, Louis M Herman, and Adam A Pack. "Stereotypical sound patterns in humpback whale songs: Usage and function". In: *Aquatic Mammals* 29.1 (2003), pp. 37–52. DOI: https://doi.org/10.1578/016754203101024068.

[194] April E Reside, Jeremy J VanDerWal, Alex S Kutt, and Genevieve C Perkins. "Weather, not climate, defines distributions of vagile bird species". In: *PloS one* 5.10 (2010), e13569. DOI: https://doi.org/10.1371/journal.pone.0013569.

[195] Walter MX Zimmer, John Harwood, Peter L Tyack, Mark P Johnson, and Peter T Madsen. "Passive acoustic detection of deep-diving beaked whales". In: *J. Acoustical Soc. of America* 124.5 (2008), pp. 2823–32. DOI: 10.1121/1.2988277.

[196] Mehdi Aïssi, Cristina Fiori, Jessica Alessi, et al. "Mediterranean submarine canyons as stepping stones for pelagic top predators: the case of sperm whale". In: *Mediterranean Submarine Canyons: Ecology and Governance. IUCN* (2012), pp. 99–103. URL: https://www.academia.edu/25150621/Mediterranean_submarine_canyons_as_stepping_stones_for_pelagic_top_predators_The_case_of_sperm_whale_Physeter_catodon_.

[197] Douglas C Biggs, Robert R Leben, and Joel G Ortega-Ortiz. "Ship and satellite studies of mesoscale circulation and sperm whale habitats in the northeast Gulf of Mexico during GulfCet II". In: *Gulf of Mexico Science* 18.1 (2000), p. 2. DOI: 10.18785/goms.1801.02.

[198] Caterina Lanfredi, Arianna Azzellino, et al. "Key Oceanographic Characteristics of Cuvier's Beaked Whale (Ziphius cavirostris) Habitat in the Gulf of Genoa (Ligurian Sea, NW Mediterranean)." In: *Journal of Oceanography and Marine Research* 4.145 (2016), pp. 1–12. DOI: 10.4172/2572-3103.1000145.

[199] Alexandre Gannier and Emilie Praca. "SST fronts and the summer sperm whale distribution in the north-west Mediterranean Sea". In: *Journal of the Marine Biological Association of the United Kingdom* 87.1 (2007), pp. 187–193. DOI: doi:10.1017/S0025315407054689.

[200] Tim Lewis, Oliver Boisseau, Magnus Danbolt, Claire Lacey, Russell Leaper, Justin Matthews, Richard McLanaghan, Anna Moscrop, et al. "Abundance estimates for sperm whales in the Mediterranean Sea from acoustic line-transect surveys". In: *J. Cetacean Res. Manage.* 18 (2018), pp. 103–117. DOI: https://doi.org/10.47536/jcrm.v18i1.437.

[201] Oliver Boisseau, Jonathan Reid, Conor Ryan, Anna Moscrop, Richard McLanaghan, and Simone Panigada. "Acoustic estimates of sperm whale abundance in the Mediterranean Sea as part of the ACCOBAMS Survey Initiative". In: *Frontiers in*

Marine Science 11 (2024), p. 1164026. DOI: https://doi.org/10.3389/fmars.2024.1164026.

[202] Guillemette Labadie, Yan Boulanger, Pierre Drapeau, Diana Stralberg, and Junior A Tremblay. "Projecting bird assemblage responses to climate-driven changes in managed boreal forest landscapes of Québec". In: *Biological Conservation* 302 (2025), p. 110956. DOI: https://doi.org/10.1016/j.biocon.2024.110956.

[203] Elizabeth A Gow, Lauren Burke, David W Winkler, Samantha M Knight, David W Bradley, Robert G Clark, Marc Belisle, Lisha L Berzins, Tricia Blake, Eli S Bridge, et al. "A range-wide domino effect and resetting of the annual cycle in a migratory songbird". In: *Proceedings of the Royal Society B: Biological Sciences* 286.1894 (2019), p. 20181916. DOI: https://doi.org/10.1098/rspb.2018.1916.

[204] Audrey Bourret, Marc Bélisle, Fanie Pelletier, and Dany Garant. "Multidimensional environmental influences on timing of breeding in a tree swallow population facing climate change". In: *Evolutionary Applications* 8.10 (2015), pp. 933–944. DOI: 10.1111/eva.12315.

[205] Lellouche Jean-Michel, Greiner Eric, Bourdallé-Badie Romain, Garric Gilles, Melet Angélique, Drévillon Marie, Bricaud Clément, Hamon Mathieu, Le Galloudec Olivier, Regnier Charly, et al. "The Copernicus global 1/12 oceanic and sea ice GLORYS12 reanalysis". In: *Frontiers in Earth Science* 9 (2021), p. 698876. DOI: https://doi.org/10.3389/feart.2021.698876.

[206] Pierre Cauchy, Karen J Heywood, Denise Risch, Nathan D Merchant, Bastien Y Queste, and Pierre Testor. "Sperm whale presence observed using passive acoustic monitoring from gliders of opportunity". In: *Endangered Species Research* 42 (2020), pp. 133–149. DOI: https://doi.org/10.3354/esr01044.

[207] Emily Hague et al. "AIS data underrepresents vessel traffic around coastal Scotland". In: *Marine Policy* 178 (2025), p. 106719. ISSN: 0308-597X. DOI: https://doi.org/10.1016/j.marpol.2025.106719.

[208] Richard Pace and Gregory Silber. *Vessel Speed and Ship Strikes. Poster San Diego 2005MMS*. Dec. 2005. URL: https://www.researchgate.net/publication/341001162_Pace_Silber_Vessel_Speed_and_Ship_Strikes_Poster_San_Diego_2005MMS.

[209] Nathalie Di-Meglio, Lea David, Pascal Monestiez, et al. "Sperm whale ship strikes in the Pelagos Sanctuary and adjacent waters: assessing and mapping collision risks in summer". In: *J. Cetacean Res. Manage.* 18 (2018), pp. 135–147. DOI: https://doi.org/10.47536/jcrm.v18i1.446.

[210] Jens J Currie, Jessica A McCordic, Grace L Olson, Abigail F Machernis, and Stephanie H Stack. "The impact of vessels on humpback whale behavior: the benefit of added whale watching guidelines". In: *Frontiers in Marine Science* 8 (2021), p. 601433. DOI: https://doi.org/10.3389/fmars.2021.601433.

[211] Lars Bejder, S Videsen, L Hermannsen, M Simon, D Hanf, and PT Madsen. "Low energy expenditure and resting behaviour of humpback whale mother-calf pairs highlights conservation importance of sheltered breeding areas". In: *Scientific Reports* 9.1 (2019), p. 771. DOI: https://doi.org/10.1038/s41598-018-36870-7.

[212] Renata S Sousa-Lima and Christopher W Clark. "Modeling the effect of boat traffic on the fluctuation of humpback whale singing activity in the Abrolhos National Marine Park, Brazil". In: *Canadian Acoustics* 36.1 (2008), pp. 174–181. URL: https://jcaa.caa-aca.ca/index.php/jcaa/article/view/2008.

[213] Cameron Albert Duquette, Scott R Loss, and Torre J Hovick. "A meta-analysis of the influence of anthropogenic noise on terrestrial wildlife communication strategies". In: *Journal of Applied Ecology* 58.6 (2021), pp. 1112–1121. DOI: https://doi.org/10.1111/1365-2664.13880.

DECLARATION

I hereby declare that this thesis is my original work and that all sources have been properly cited and acknowledged.

La Garde, France, September 2026

Stéphane CHAVIN